

# Quantifying Context Bias in Domain Adaptation

Hojun Son

Asma Almutairi

Arpan Kusari

University of Michigan Transportation Research Institute  
 2901 Baxter Road, Ann Arbor, MI - 48109  
 {hojunson, asmaalm, kusari}@umich.edu

## Abstract

*Domain adaptation for object detection (DAOD) seeks to transfer a trained model from a source to a target domain. Various DAOD methods exist, some of which aim to minimize context bias between foreground-background associations in various domains. However, no prior work has studied context bias in DAOD by analyzing changes in background features during adaptation and how context bias is represented in different domains. Our research experiment highlights the potential usability of context bias in DAOD. We address the problem by varying activation values over different layers of two different trained models, Detectron2 and YOLOv11, and by masking the background, both of which impact the number and quality of detections. We use two synthetic datasets, CARLA and Virtual KITTI, and two different versions of real open-source data, Cityscapes and KITTI semantic, as separate domains to represent and quantify context bias. We utilize different metrics such as Maximum Mean Discrepancy (MMD) and Maximum Variance Discrepancy (MVD) to find the layer-specific conditional probability estimates of foreground given manipulated background regions for separate domains. We further analyze foreground-background associations across various dataset combinations. We find that state-of-the-art domain adaptation methods exhibit some form of context bias and apply a potentially simple way to alleviate the context bias achieving improved accuracy (from 51.189 to 53.646 mAP on Cityscapes foggy validation with 63.207 mAP and 64.233 mAP on Cityscapes validation respectively). We demonstrate through detailed analysis that understanding of the context bias can affect DAOD approach and focusing solely on aligning foreground features is insufficient for effective DAOD.*

## 1. Introduction

Domain adaptation for object detection (DAOD) has been studied extensively to enable object detectors to perform well on datasets with distribution shifts from the training

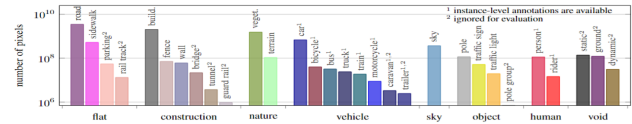


Figure 1. The proportion of background pixels in Cityscapes [11] are the highest of all classes. The image is from Cityscapes publication.

data [8, 12, 20, 24, 25, 27, 29]. It is well known that there's an entanglement between background and foreground features in object detection, leading to a phenomenon called context bias in DAOD [10, 13, 26, 42, 46, 54]. Here, significant differences in background features between the source and target domains can cause a notable decline in the quality and number of detections, even when the foreground features remain unchanged. Recent studies in image classification [28] and segmentation [9, 15, 59] have attempted to mitigate context bias by minimizing this association. Oliva & Torralba [33] demonstrated that context bias could result in the corruption of foreground objects by contextually correlated backgrounds, substantially degrading detection quality. However, there has been no prior work specifically analyzing the impact of context bias in DAOD. This work aims to address this gap.

In the realm of human cognition, the brain can accurately and instantly recognize foreground-background associations without extensive training [35]. Several studies, including [22, 35, 38, 52], have investigated the processes of background suppression and foreground representation to understand the scene and temporal dynamics of foreground and background modulation in the brain. These insights can be applied to the field of computer vision for DAOD through comprehensive analysis of the representation of foreground-background associations.

To motivate our problem, we first look at the proportion of background features in autonomous driving datasets, as an example. For Cityscapes dataset [11], the number of pixels from built-up features (such as "road" and "sidewalk") are much greater than the foreground object pixels (see Fig-

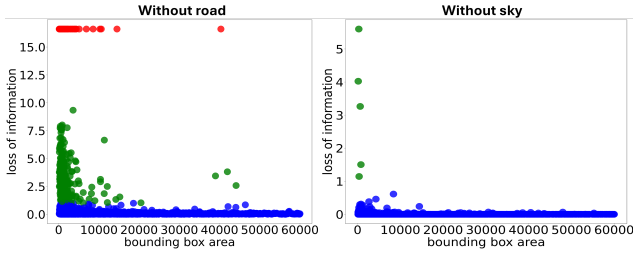


Figure 2. Loss of information as a function of the bounding box area of the object. Left side figure shows the suppression of “road” while right side figure shows the suppression of “sky”. The dots are grouped into three clusters - red dots have maximum loss of information, green dots have significant loss while blue dots indicate no change. We also find that the loss generally decreases with the bounding box area.

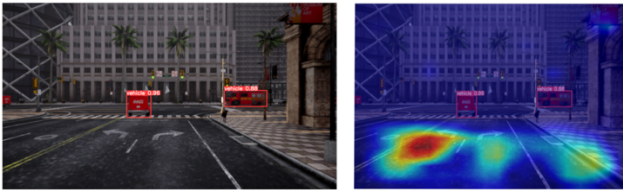


Figure 3. Left figure shows 2D inference of CARLA dataset using YOLOv4 model while right figure shows the CAM attention map of the inference.

ure. 1). As an image feature, “roads” are very simple and constant which leads them to be trained more rapidly than more complex objects such as vehicles. As a motivating experiment, we aim to quantify the change in performance as a function of the background masking for a real dataset. We define performance drop  $\Delta D$  as  $0 \leq \Delta D \leq 1$  and the amount of loss of information as the negative log of the complement of  $\Delta D$  ( $-\log(1 - \Delta D)$ ). Figure 2 shows the loss of information when activated features on “road” regions are zeroed out using semantic labels as a function of the ground truth bounding box area of the foreground objects. We used the second layer of backbone in the Detectron2 [49], trained on the Cityscapes dataset for object detection. We found that the loss of information is much higher with the “road” suppressed as compared to “sky”, which means that “road” has more contextual association with vehicles, particularly when the vehicle size is small.

Additionally, we trained a YOLOv4 detection model [3] on a sample CARLA [14] dataset collected under sunny conditions and provide inference on a separate CARLA dataset collected under cloudy conditions. We find that the model is focused on the road in front of the vehicles rather than the vehicles themselves (see Figure 3) using Class Activation Mapping (CAM). We also performed another analogous experiment where we transform the road pixels by masking them and found that the newer YOLOv8 model

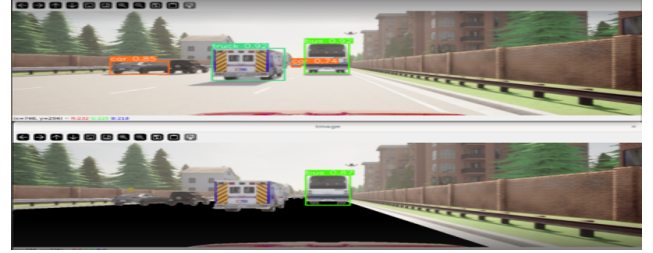


Figure 4. Masking road on CARLA output and getting inference using YOLOv8 model - top figure shows that 3 out of 4 vehicles get detected correctly while in the bottom figure with road masking, only one vehicle is detected.

was unable to detect most of the vehicles otherwise detected in the normal image (see Figure 4). This outcome suggests that the neural network model may have implicitly learned to associate vehicles with road environments, leading to poor performance in detecting vehicles when a different background is present.

Our fundamental questions are as follows: 1) *Why does the context bias occur during training?* 2) *Can we evaluate the context bias in different domains?* 3) *Can we quantify the context bias across different domains?*

Firstly, we investigate the underlying reasons for foreground-background associations. Then we set up hypotheses about how the association is represented in different domains and analysis it using feature embedding. Next, we quantify the discrepancy between foreground-background representations across multiple domains. This quantitative assessment aims to provide insights into the extent of context bias in object detection and its implications for DAOD.

Our main contributions are as follows:

- We examine the issue of DAOD in relation to context bias. Although context bias is a well-recognized challenge in computer vision, none of the current approaches investigate how context bias can manifest across various domains.
- We highlight a crucial gap, suggesting that considering context bias is essential for enhancing the generalization and robustness of models across various environments.
- We employ distance-based metrics to measure the association between foreground and background under domain shifts. Additionally, we calculate these metrics for each layer of the neural network and expand the background region across bins to assess the impact of background regions on object detection.

## 2. Related Work

### 2.1. Foreground-background associations and context bias

Background influence [2, 30, 39–41, 50, 53, 61] and context bias [10, 26, 42, 46] aim at improving performance in tasks such as classification, object recognition, and object localization. Xiao et al. [50] and Zhu et al. [61] studied background effect on accuracy of classification by modifying images with different combinations of foreground and background. [10] proposed a graphical model which modeled foreground-background associations using conditional probability which serves as a methodological inspiration for us. Several studies have addressed context bias using techniques, such as data augmentation to generate out-of-distributions samples into the background, combination of naturally unmatched background and foreground (e.g., an elephant in room), and applying background removal during training. Torralba [45] demonstrated that background effect can be factorized into object priming, focus of attention, and scale selection by modeling the foreground-background associations in a probabilistic model. Liang et al. [30] studied background influence using fashion dataset [23, 43]. These studies [48, 51] can localize foreground objects better than CAM-based algorithms without using bounding box information and with only classification labels. These prior works focus on context bias in the same domain and use datasets with smaller variations like centered objects or single objects. Thus, we find that there remains a gap in understanding how context bias affects DAOD.

### 2.2. Domain Adaptation for Object Detection

Different variations of DAOD methods have been proposed using feature alignment, synthetic images, and self-training or self-distillation. Feature alignment finds transformations between source and target domain to reduce distribution shift with adversarial training [9, 16, 19, 60]. It can be helpful to extract common latent features from different domains. Progressive Domain Adaptation for Object Detection [21] synthesized new dataset by using cycleGAN [58] which enables to bridge domain gaps and Self-Adversarial Disentangling for Specific Domain Adaptation [57] achieved 45.2 mAP on Cityscapes to Cityscapes foggy dataset using synthetic images. Gong et al. [17] utilized transformers to focus on aligning features across backbone and decoder networks. However, combining multiple sources into a single dataset and performing single-source domain adaptation for feature alignment does not guarantee better performance compared to using the best individual source domain [55].

Self-training uses a *teacher* model to predict pseudo labels on target domains to gradually understand domain shift

[5–8, 36]. MIC [20] employed masked images on teacher-student model and MRT [56] suggested modified masked based retraining approach on the teacher-student model. [25] performed an alignment and distillation to enforce invariance across domains to reduce discrepancy of features.

Finding common features from multiple domains is critical for DAOD. They have summarily demonstrated that the foreground features in latent space can be aligned using dimension reduction methods such as UMAP [32] and t-SNE [47]. These studies do not address how to manage context bias when adapting across different domains. Instead, they propose and validate their methods within DAOD framework using accuracy metrics. Thus, we focus on analyzing the root causes of domain discrepancy in object detection both qualitatively and quantitatively.

## 3. Methods

### 3.1. Why does the context bias occur during training?

Prior studies [10, 45] researched context bias for object classification. The studies pointed out that relying only on local features (foreground features in our case) has limitations, including degraded quality due to noise and ambiguity in the target search space. They extended the likelihood to incorporate context information surrounding the foreground, which enhances object classification by providing a stronger conditional probability. The conditional probability of the object ( $O$ ) given the features ( $f$ ) was given as:

$$P(O|f) = P(O|F, B) = \frac{P(F|O, B)P(O|B)}{P(F|B)} \quad (1)$$

where  $F$  and  $B$  are the foreground and background features. The modeling can also be interpreted as:

$$\begin{aligned} P(O|B) &= P(c|\sigma, Y, B)P(\sigma|Y, B)P(Y|B) \\ &= P(\sigma|Y, c, B)P(x|c, B)P(c|B) \end{aligned} \quad (2)$$

where the object is represented by scale ( $\sigma$ ), location ( $Y$ ), and category ( $c$ ).

The challenge with using a convolutional neural network (CNN) to estimate likelihood is the inability to explicitly teach the model to learn each factor in a specific order. In other words, it means that parameters of CNN can be different depending on how it can be trained. In CNNs, likelihood estimation is a process to find the mean of a distribution, which necessitates more samples to accurately estimate the true mean. This aligns with the principle that a more extensive and refined dataset, achieved through data augmentation, is crucial for better performance [44].

In the context of a graphical causal model ( $F \rightarrow Y \leftarrow B$ ), it represents the joint distribution  $P(Y, F, B)$ , which

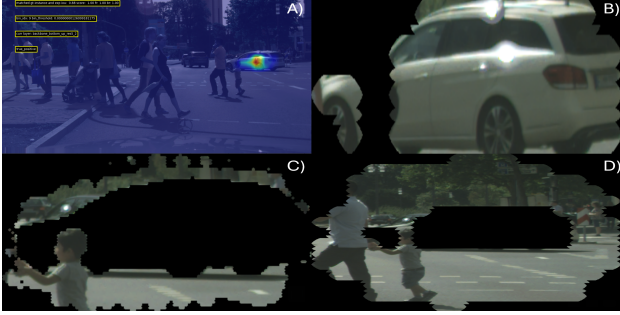


Figure 5. Each alphabet represent visualized foreground and background area in the image. “A” is a color image on which attention map is overlaid for the car object. “B” is the foreground region. It does not change depending on the bin. “C” and “D” are threshold background region. “C” has more narrow background region compared to “D”. “C” is the background region with bin threshold 4 and “D” is the background region when the bin is 9.

can be decomposed as either  $P(Y|F, B)P(F|B)P(B)$  or  $P(Y|F, B)P(B|F)P(F)$ . In the SUN 09 training set used by [10], the association between *roads* and *cars* is strong, and the number of *road* pixels surpasses object pixels (similar to Cityscapes: Fig. 1). Consequently, the CNN is more likely to learn  $P(F = \text{car}|B = \text{road})$  than  $P(B = \text{road}|F = \text{car})$ , leading to the induction of the equation  $P(Y|F, B)P(F|B)P(B)$  during training. Also, the factor  $P(B = \text{road})$  can be factorized as  $P(\text{Color}|X) * P(\text{shape}|X)$  and can be learned more easily and earlier than  $P(F = \text{car}) = P(\text{Color}|X) * P(\text{shape}|X)$ . It can cause the object detection model to fail to detect on different domain especially when the background (in this case, the *road*) changes.

Another reason is related to the receptive field of CNN architecture. As layers in a CNN go deeper, the receptive field increases, causing pooled information after convolution operations mixing foreground and background features [37]. This mixing can create ambiguity between foreground and background features. Given these considerations, we now delve into how we empirically provide results of context bias on different datasets.

### 3.2. Can we evaluate the context bias in different domains?

#### 3.2.1. Training

We utilized two DNN models, Detectron2 and YOLOv11, with multiple combinations of the following datasets with semantic and instance labels:

- Cityscapes and Cityscapes validation [11] -This dataset consists of 2,975 images and validation set contains 500 images. It has 8 different labels.
- Cityscapes foggy beta 0.01 and 0.02 - This dataset is used exclusively for experimental purposes. It contains synthetic foggy images with two levels of foggy density.

- CARLA [14] - This dataset consists of 19 synthetic driving scenarios and same number of images as Cityscapes training set. It has 3 labels.
- Virtual KITTI [4] - This dataset comprises 5 converted scenes from KITTI tracking dataset into synthetic images. Since it is based on object tracking, each image within a scene exhibits high correlation with the others. It has 6 labels.
- KITTI Semantic [1] - This dataset is based on KITTI flow. It includes 200 training images with instances masks. It has 8 labels such as Cityscapes.

Detectron2 model consists of a backbone network which extracts feature maps from the input image at five different scales, region proposal networks (RPN) extracting object regions from multi-scale features and box heads which aggregates the region proposals. To train the Detectron2 model, we employed a batch size of 8, a stepLR scheduler with iterations of {10,000, 20,000, 30,000, 35,000, and 37,500} (about 100 epochs). The initial learning rate was set to 0.015, and the image resolution was  $1024 \times 2048$  for Cityscapes and Carla and  $618 \times 2048$  for images based on the KITTI dataset with horizontal flip and brightness augmentation. We used the Adam optimizer, regression loss for bounding boxes, and cross-entropy loss for label classifications. The evaluation results on each training dataset are provided in Supplementary (see Supplementary Section 7). While the result on CARLA indicates overfitting, it provides useful insights into feature alignment between the two different domains.

We used Ultralytics framework to fine-tune YOLOv11 model on Cityscapes. We trained on pre-trained YOLOv11 weights for 100 epochs, 15 batch size, SGD optimizer, and we utilized cosine learning rate scheduler.

#### 3.2.2. Foreground and background feature extraction

To separate foreground and background related features per target object, we utilized a combination of activation hooks, semantic pixel labels, and instance masks. To obtain the overall activation region of each instance, we used Smooth Grad-CAM++[34], to extract spatial information for each instance from attention mechanisms by computing activation weights and applying instance masks to distinguish between foreground and background features. Following this separation, we saved feature maps as feature vectors per object across various layers. While the entire area of the activation was provided by Smooth Grad-CAM++, we manipulated what percentage of the background activation region is required for the foreground object detection. Therefore, we expanded the area thresholds in terms of bins (where bin 1 represents almost no background and bin 9 represents “all” activation). In other words, the region of interest from background is gradually extended as *bin* parameter increases. Figure 5 illustrates visualized example of foreground and

---

**Algorithm 1** algorithm to extract features

---

```

1: Input: activation maps per object, semantic labels,
   trained model.
2: Output:  $F$  and  $B$  per object, layers, and threshold
3: for  $1 \leq \text{bin} \leq 10$  do
4:    $THS \leftarrow (MAV * \text{POWER}(0.1, \text{bin}))$   $\triangleright MAV$  is
      maximum activation value
5:   if  $THS$  is zero then
6:     Return
7:   end if
8:   for  $Target_L$  in [ $res_2, res_3, res_4, res_5$ ] do
9:     if  $Target_L$  is in activation hooks then
10:       Separate foreground and background
11:       activation maps with  $THS$ 
12:       and semantic labels
13:     else
14:       Forward activation maps
15:     end if
16:     Compute average feature vectors ( $F$  and  $B$ )
17:     Save the feature vectors
18:   end for
19: end for

```

---

background extracted in from different layers and threshold on image from the Cityscapes and CARLA. The algorithm 1 outlines the feature extraction process. For further validation of gradient-based CAM methods, we provide a detailed analysis of the ratio of attention area from Smooth Grad-CAM++ on foreground and background regions in Supplementary (see Supplementary Section 9).

### 3.2.3. Computing associations between foreground and background

We quantified associations between foreground and background by leveraging semantic labels for specific background regions. After loading a trained model, we created a modified version by copying the original model. Both models were then used to infer outcomes on the same input images; however, in the modified model, a specific background region was removed during inference. We compared both outcomes to compute a *Droprate* which is defined as the ratio of number of changes in detection as a result of background modification to the number of ground truth detections. An example of *Droprate* computation is provided in Supplementary Section 10. After processing *Droprate* per each foreground-background pair, we constructed an association matrix (see Figure 6). From this matrix, we derived both the *Normalized droprate* and *Droprate*. The *Normalized droprate* highlights the strongest association between foreground and background (see Figure 7). It is important to consider both metrics because a high *Normalized Droprate* does not necessarily indicate

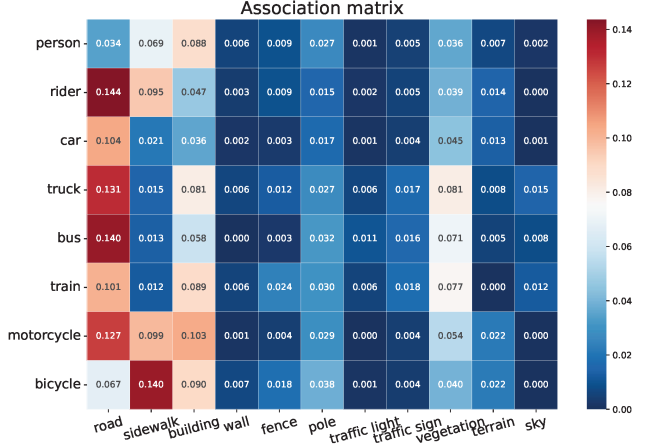


Figure 6. **Association matrix of Cityscapes.** Most foreground objects exhibit strong associations with “roads”. A larger visualization is provided in Supplementary Section 10.

a high *Droprate*. This means that while an object label may exhibit a strong relative association with a background class after normalization, its absolute *Droprate* may still be low implying weak dependence on any specific background. For example, in Virtual KITTI association graph, “car” label has 0.03 *Droprate* and other *Droprates* are less than the value. However, it exhibits the strong association with “building” after the normalization. Additional association graphs can be found in Supplementary Section 11).

### 3.3. Can we quantify the context bias across different domains?

MMD was proposed by [18] as a kernel-based statistical test to find the distance between two given distributions. MMD between two distributions  $X$  and  $Y$  can be mathematically defined as:

$$MMD^2(X, Y) = \|\mu_k(X) - \mu_k(Y)\|_b^2 \quad (3)$$

where  $x_i \in X, y_i \in Y$ . Alternatively, a variance based discrepancy has also been proposed by [31] as:

$$MVD^2(X, Y) = \|\Sigma_k(X) - \Sigma_k(Y)\|_b^2 \quad (4)$$

where  $b$  represents the unit ball of kernel Hilbert space  $\mathcal{H}_k$ . We computed MMD and MVD between foreground and background feature vectors from different datasets with separated scaled features. Since the MMD values were too small to comprehend, we scaled the values by 100. UMAP clustering depends on the hyper-parameters such as minimum distance to visualize and number of neighbors to compute weights among samples. To avoid bias, we kept all hyper parameters constant for all experiments.

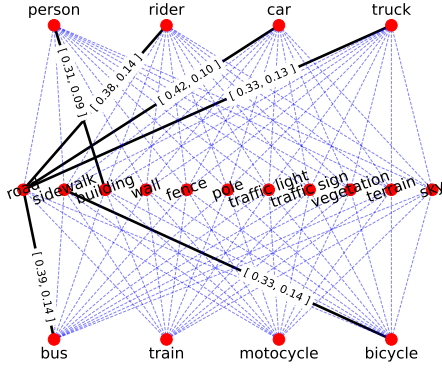


**Figure 7. Association graph of Cityscapes.** We visualized only associations where the normalized value exceeds 0.3, highlighting them in bold. Background nodes are in the middle and foreground nodes are deployed at the top and bottom. The first number is *Normalized droprate* and the second number is *Droprate*.

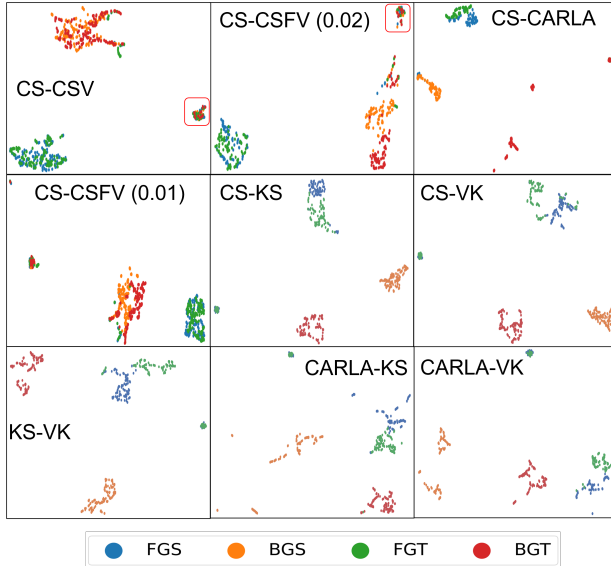


**Figure 8. UMAP feature embedding results.** “CS” is Cityscapes, “CSV” is Cityscapes validation, “CSFV (0.0X)” are Cityscapes foggy with different parameters for fogginess. “KS” means KITTI semantic, “VK” is Virtual KITTI clone. The red rectangles are empty images because of small object size. We used the “car” label, as it is the most common category across the datasets. “FGS” is foreground in source domain and “BGS” is background in source domain. “FGT” and “BGT” are foreground and background in target domain.

## 4. Experiments

### 4.1. UMAP visualization

We started our analysis by plotting the foreground and background feature distributions of different domains using UMAP. Figure 8 presents the visualization of the fore-

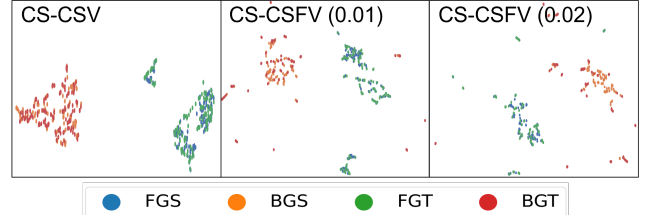


**Figure 9. UMAP feature embedding results with YOLOv11.** “Car” label was used for visualization. Embedding results for other labels are provided in Supplementary Section 17.

ground and background features from different domains in 2D. We used the features at the 5<sup>th</sup> ResNet layer from different data distributions. The interesting finding is the differences of background alignment across the comparisons. It is immediately apparent that as the target domain shifts away from the source domain, the background becomes more separable than the foreground. For the Cityscapes training (CS) and validation (CSV) dataset, foreground and background features were distinguishable from each other but appeared intermingled between the source and target domains. In the CS-CSFV panel, foreground features remained clustered together while the background features were separable but overlapping. We saw an extreme case in the CS-CARLA where the foreground features between Cityscape and CARLA were next to each other but were non-overlapping while the background features were very distant from each other. The similar patterns were observed in synthetic datasets such as Virtual KITTI and Carla. In supplementary, we visualized different labels embedding results and corresponding image patches for qualitative analysis in 3D for the CS-CARLA (see Supplementary Section 14 and 16). Figure 9 presents the embedding results of YOLOv11. It demonstrates aggregation of foreground-foreground and background-background, though the separation between background features is less distinct compared to Detectron2.

### 4.2. MMD and MVD comparison

Given the qualitative analysis, we derived quantitative estimates of difference in foreground and background feature distributions using MMD and MVD. Table 98 shows the MMD across different layers and bins respectively for car objects in different domains. Additional MMD with different labels are provided in the supplementary sections (see Supplementary Section 12 and 13). The highest discrepancies were observed between foreground-background (“f2b”) and background-foreground (“b2f”), with lower discrepancies between foreground-foreground (“f2f”) and background-background (“b2b”). No significant patterns were found in the MVD analysis (see Supplementary Section 12). Although Bin 1 shows no significant difference,

while Bin 9 exhibits notable differences across all label pairs.

### 4.3. Observations

The Detectron2 model trained on the Cityscapes dataset achieves 53.72 mAP with only three labels (Car, Truck, and Bus), with performance dropping to 41.06 mAP on the CARLA validation set and 37.77 mAP on the Cityscapes foggy beta 0.02 set. Despite the CARLA dataset being relatively easier, there is a significant drop of 47.56 mAP from 88.62 mAP, which implies that even when foreground features are well-aligned, the difference in background associations contributes to the significant drop. Similarly, considerable drops are shown with cross validation (see Supplementary Section 7). This indicates that using a trained model without proper alignment of background context can lead to severe degradation in performance. The minimal variance observed among features post-embedding suggests that the CNN model captures backgrounds across various domains. The challenge of DAOD may stem from insufficient understanding of the association between foreground and background elements.

YOLOv11 was used to analyze the impact of model architecture on context bias. We observed similar patterns in MMD and MVD with YOLOv11 trained on Cityscapes. The ‘‘f2f’’ shows the lowest MMD values across 3 selected layers ( $16^{th}$ ,  $19^{th}$ , and  $22^{th}$  layer). 2D embedding results demonstrate an analogous pattern to Detectron2, but the background embedding pattern is less explicit compared to Detectron2’s results. While no statistical analysis was performed on the correlation between dataset pixel distribution and context bias, strong associations are observed between foreground and background, with the background containing the most pixels. For example, *road*, which occupies the most pixels in Cityscapes, has the strongest associations with the foreground. In CARLA, *road* similarly dominates the pixel distribution and shows the most associations. In KITTI semantic, *vegetation* takes the place of *road*. Although *sky* and *building* are not dominant in Virtual KITTI but it shows associations with foreground. It might be because Virtual KITTI is based on tracking scenes which has strong correlations between images.

### 4.4. Ablation study

The method for overcoming context bias during training is uncertain, along with the process through which association can be represented through various domain adaptation techniques for object detection. We applied MIC data augmentation [20] which randomly removes input images and trains unchanged Detectron2 on Cityscapes for training. We discovered two interesting findings: 1) By applying the data augmentation, the mAP on Cityscape validation and Cityscapes foggy validation set improves from

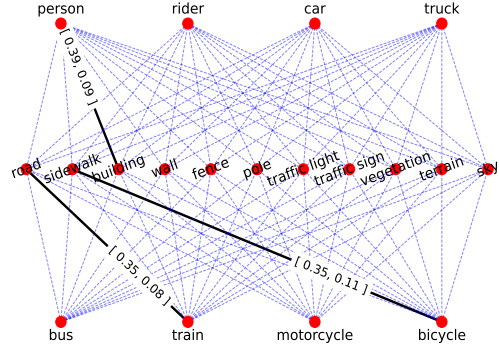


Figure 10. **Association graph of Cityscapes with MIC data augmentation.** The number of strong association decreases and the absolute *Droprate* is lower than in Figure 7 and 11. A larger image can be found in Supplementary Section 11.

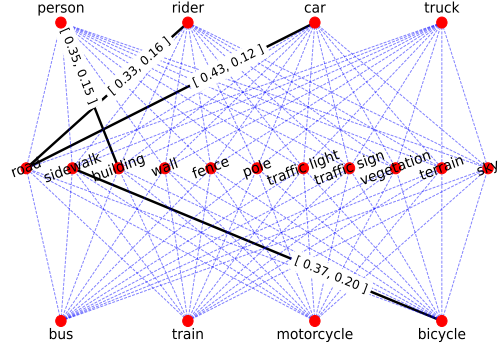


Figure 11. **Association graph of Cityscapes with ALDI++.** A larger image is provided in Supplementary Section 11.

(63.207, 51.189) mAP to (64.233, 53.646) mAP, achieving the best performance with the unchanged model. The best Cityscapes validation of Detectron2 without MIC is 65.544 mAP with 46.321 mAP on Cityscapes foggy validation. This suggests that while accuracy improvements are observed, they do not guarantee better performance across different domains due to context bias and 2) With the data augmentation, the associations weaken, leading to fewer strong associations and a reduced drop rate (see Figure 10). When we generate the association graph from state-of-the-art DAOD model [25], the associations get re-expressed with stronger association. It is because the method uses target information (Cityscapes foggy images) during training. The target dataset is corrupted to detect foreground features, and as a result, the model improves the performance by generating strong associations with background (see Figure 11).

### 4.5. Supplementary

Due to page limits, a detailed data analysis is provided in the supplementary material. The following outline summa-

Layer	MMD mean			
	f2f	f2b	b2f	b2b
res2_2	0.112268	4.881973	3.929306	<b>0.01152</b>
res3_3	0.101458	0.37918	0.741803	<b>0.002722</b>
res4_5	0.044441	0.810117	0.876053	<b>0.004992</b>
res5_2	0.243604	0.910576	0.394352	<b>0.009945</b>

Table 1. Dataset: CS-CSV, Label: car, Bin: 1

Layer	MMD mean			
	f2f	f2b	b2f	b2b
res2_2	0.706163	3.668221	6.906667	<b>0.00722</b>
res3_3	0.266325	0.624368	0.665097	<b>0.009918</b>
res4_5	0.193847	0.587321	0.445625	<b>0.009935</b>
res5_2	0.238423	0.609772	0.455897	<b>0.023235</b>

Table 3. Dataset: CS-CSFV(0.02), Label: car, Bin: 1

Layer	MMD mean			
	f2f	f2b	b2f	b2b
res2_2	1.474862	4.618558	9.167279	<b>0.04245</b>
res3_3	0.756124	0.714063	1.732928	<b>0.009051</b>
res4_5	1.948283	<b>0.605148</b>	3.242881	0.016089
res5_2	1.266142	<b>0.711531</b>	2.555629	0.013822

Table 5. Dataset: CS-CARLA, Label: car, Bin: 1

Layer	MMD mean			
	f2f	f2b	b2f	b2b
res2_2	1.316904	6.91777	9.976782	<b>0.121352</b>
res3_3	0.383061	0.659464	1.136501	<b>0.006596</b>
res4_5	1.301864	0.801997	2.831493	<b>0.011471</b>
res5_2	2.354437	0.642958	3.765359	<b>0.02679</b>

Table 7. Dataset: CS-KS, Label: car, Bin: 1

Layer	MMD mean			
	f2f	f2b	b2f	b2b
res2_2	0.394442	6.340317	4.72146	<b>0.057999</b>
res3_3	0.340322	0.723728	0.936803	<b>0.007423</b>
res4_5	0.922104	1.309442	1.98693	<b>0.039161</b>
res5_2	0.444258	0.723626	0.995179	<b>0.012534</b>

Table 9. Dataset: CS-VK, Label: car, Bin: 1

Table 11. MMD mean for each layer with different bins across multiple datasets. We highlight the lowest MMD mean in each table.

rizes the content: 1) evaluation of training results (Sec. 7), 2) number of instances of each dataset (Sec. 8), 3) heat ratio of foreground and background (Sec. 9), 4) association matrix (Sec. 10), 5) association graph (Sec. 11), 6) MMD and MVD tables with various labels (Sec. 12), 7) MMD with different labels (Sec. 13), 8) pixel distribution of each dataset (Sec. 15), 9) UMAP embedding results in different layers (Sec. 14), 10) 3D embedding CS-CARLA with image patches (Sec. 16), and 11) Quantification results with YOLOv11 (Sec. 17).

Layer	MMD mean			
	f2f	f2b	b2f	b2b
res2_2	1.805033	30.8593	50.86228	<b>1.452292</b>
res3_3	<b>0.065135</b>	5.822784	6.834551	0.370164
res4_5	<b>0.17106</b>	7.135566	7.30036	0.893516
res5_2	<b>0.177859</b>	12.35796	10.96273	0.794648

Table 2. Dataset: CS-CSV, Label: car, Bin: 9

Layer	MMD mean			
	f2f	f2b	b2f	b2b
res2_2	<b>1.777187</b>	49.25025	58.34242	5.902651
res3_3	<b>1.211607</b>	11.16027	8.95446	7.724574
res4_5	<b>1.296171</b>	10.59698	10.02815	7.319046
res5_2	<b>1.188299</b>	14.29075	16.87545	10.05994

Table 4. Dataset: CS-CSFV(0.02), Label: car, Bin: 9

Layer	MMD mean			
	f2f	f2b	b2f	b2b
res2_2	<b>4.706366</b>	81.14032	33.57919	18.7133
res3_3	<b>2.958311</b>	24.68571	6.973638	15.17487
res4_5	<b>4.136291</b>	30.6901	9.366244	21.64019
res5_2	<b>3.269869</b>	43.7039	16.25924	32.42696

Table 6. Dataset: CS-CARLA, Label: car, Bin: 9

Layer	MMD mean			
	f2f	f2b	b2f	b2b
res2_2	<b>8.462852</b>	77.83188	46.50161	12.42845
res3_3	<b>4.789057</b>	21.42746	5.870001	11.30017
res4_5	<b>3.258732</b>	15.73727	7.743903	9.583368
res5_2	<b>3.861421</b>	25.83357	14.01313	15.18826

Table 8. Dataset: CS-KS, Label: car, Bin: 9

Layer	MMD mean			
	f2f	f2b	b2f	b2b
res2_2	<b>2.08684</b>	32.95272	42.70539	8.973137
res3_3	<b>3.184757</b>	16.73043	4.830855	7.803452
res4_5	<b>3.900409</b>	19.50111	7.2131	11.52038
res5_2	<b>2.395806</b>	13.3933	14.83892	9.781686

Table 10. Dataset: CS-VK, Label: car, Bin: 9

## 5. Conclusion and limitations

We present a detailed analysis of occurrence of context bias in DAOD applications. Even though we demonstrate how the background and foreground features are aligned and separable, extracting the features separately and using them is tremendously computationally expensive. Therefore, using any contextual cue in the object detection model needs to be computationally efficient to make it useful. We explain data augmentation on image space by spatial random removal can help reduce the context

bias. DAOD methods using target dataset might lead to another context bias again. We believe the experimental study to provide different perspective to DAODs.

## References

- [1] Hassan Abu Alhaija, Siva Karthik Mustikovela, Lars Mescheder, Andreas Geiger, and Carsten Rother. Augmented reality meets computer vision: Efficient data generation for urban driving scenes. *International Journal of Computer Vision*, 126:961–972, 2018. [4](#)
- [2] Andrei Barbu, David Mayo, Julian Alverio, William Luo, Christopher Wang, Dan Gutfreund, Josh Tenenbaum, and Boris Katz. Objectnet: A large-scale bias-controlled dataset for pushing the limits of object recognition models. *Advances in neural information processing systems*, 32, 2019. [3](#)
- [3] Alexey Bochkovskiy, Chien-Yao Wang, and Hong-Yuan Mark Liao. Yolov4: Optimal speed and accuracy of object detection. *arXiv preprint arXiv:2004.10934*, 2020. [2](#)
- [4] Yohann Cabon, Naila Murray, and Martin Humenberger. Virtual kitti 2. *arXiv preprint arXiv:2001.10773*, 2020. [4](#)
- [5] Qi Cai, Yingwei Pan, Chong-Wah Ngo, Xinmei Tian, Lingyu Duan, and Ting Yao. Exploring object relation in mean teacher for cross-domain detection. In *Proceedings of the IEEE/CVF Conference on Computer Vision and Pattern Recognition*, pages 11457–11466, 2019. [3](#)
- [6] Shengcao Cao, Dhiraj Joshi, Liang-Yan Gui, and Yu-Xiong Wang. Contrastive mean teacher for domain adaptive object detectors. In *Proceedings of the IEEE/CVF conference on computer vision and pattern recognition*, pages 23839–23848, 2023.
- [7] Mathilde Caron, Hugo Touvron, Ishan Misra, Hervé Jégou, Julien Mairal, Piotr Bojanowski, and Armand Joulin. Emerging properties in self-supervised vision transformers. In *Proceedings of the IEEE/CVF international conference on computer vision*, pages 9650–9660, 2021.
- [8] Meilin Chen, Weijie Chen, Shicai Yang, Jie Song, Xinchao Wang, Lei Zhang, Yunfeng Yan, Donglian Qi, Yueting Zhuang, Di Xie, et al. Learning domain adaptive object detection with probabilistic teacher. *arXiv preprint arXiv:2206.06293*, 2022. [1, 3](#)
- [9] Yuhua Chen, Haoran Wang, Wen Li, Christos Sakaridis, Dengxin Dai, and Luc Van Gool. Scale-aware domain adaptive faster r-cnn. *International Journal of Computer Vision*, 129(7):2223–2243, 2021. [1, 3](#)
- [10] Myung Jin Choi, Antonio Torralba, and Alan S Willsky. Context models and out-of-context objects. *Pattern Recognition Letters*, 33(7):853–862, 2012. [1, 3, 4](#)
- [11] Marius Cordts, Mohamed Omran, Sebastian Ramos, Timo Rehfeld, Markus Enzweiler, Rodrigo Benenson, Uwe Franke, Stefan Roth, and Bernt Schiele. The cityscapes dataset for semantic urban scene understanding. In *Proceedings of the IEEE conference on computer vision and pattern recognition*, pages 3213–3223, 2016. [1, 4](#)
- [12] Jinhong Deng, Wen Li, Yuhua Chen, and Lixin Duan. Unbiased mean teacher for cross-domain object detection. In *Proceedings of the IEEE/CVF Conference on Computer Vision and Pattern Recognition*, pages 4091–4101, 2021. [1](#)
- [13] Santosh K Divvala, Derek Hoiem, James H Hays, Alexei A Efros, and Martial Hebert. An empirical study of context in object detection. In *2009 IEEE Conference on computer vision and Pattern Recognition*, pages 1271–1278. IEEE, 2009. [1](#)
- [14] Alexey Dosovitskiy, German Ros, Felipe Codevilla, Antonio Lopez, and Vladlen Koltun. Carla: An open urban driving simulator. In *Conference on robot learning*, pages 1–16. PMLR, 2017. [2, 4](#)
- [15] Maximilian Dreyer, Reduan Achitbat, Thomas Wiegand, Wojciech Samek, and Sebastian Lapuschkin. Revealing hidden context bias in segmentation and object detection through concept-specific explanations. 2023 ieee. In *CVF Conference on Computer Vision and Pattern Recognition Workshops (CVPRW)*, pages 3829–3839, 2023. [1](#)
- [16] Yaroslav Ganin, Evgeniya Ustinova, Hana Ajakan, Pascal Germain, Hugo Larochelle, François Laviolette, Mario March, and Victor Lempitsky. Domain-adversarial training of neural networks. *Journal of machine learning research*, 17(59):1–35, 2016. [3](#)
- [17] Kaixiong Gong, Shuang Li, Shugang Li, Rui Zhang, Chi Harold Liu, and Qiang Chen. Improving transferability for domain adaptive detection transformers. In *Proceedings of the 30th ACM International Conference on Multimedia*, pages 1543–1551, 2022. [3](#)
- [18] Arthur Gretton, Karsten M Borgwardt, Malte J Rasch, Bernhard Schölkopf, and Alexander Smola. A kernel two-sample test. *The Journal of Machine Learning Research*, 13(1):723–773, 2012. [5](#)
- [19] Zhenwei He and Lei Zhang. Multi-adversarial faster-rcnn for unrestricted object detection. In *Proceedings of the IEEE/CVF international conference on computer vision*, pages 6668–6677, 2019. [3](#)
- [20] Lukas Hoyer, Dengxin Dai, Haoran Wang, and Luc Van Gool. Mic: Masked image consistency for context-enhanced domain adaptation. In *Proceedings of the IEEE/CVF conference on computer vision and pattern recognition*, pages 11721–11732, 2023. [1, 3, 7](#)
- [21] Han-Kai Hsu, Chun-Han Yao, Yi-Hsuan Tsai, Wei-Chih Hung, Hung-Yu Tseng, Maneesh Singh, and Ming-Hsuan Yang. Progressive domain adaptation for object detection. In *Proceedings of the IEEE/CVF winter conference on applications of computer vision*, pages 749–757, 2020. [3](#)
- [22] Ling Huang, Lijuan Wang, Wangming Shen, Mengsha Li, Shiyu Wang, Xiaotong Wang, Leslie G Ungerleider, and Xilin Zhang. A source for awareness-dependent figure-ground segregation in human prefrontal cortex. *Proceedings of the National Academy of Sciences*, 117(48):30836–30847, 2020. [1](#)
- [23] Menglin Jia, Mengyun Shi, Mikhail Sirotenko, Yin Cui, Claire Cardie, Bharath Hariharan, Hartwig Adam, and Serge Belongie. Fashionpedia: Ontology, segmentation, and an attribute localization dataset. In *Computer Vision–ECCV 2020: 16th European Conference, Glasgow, UK, August 23–28, 2020, Proceedings, Part I 16*, pages 316–332. Springer, 2020. [3](#)

- [24] Tarun Kalluri, Wangdong Xu, and Manmohan Chandraker. Geonet: Benchmarking unsupervised adaptation across geographies. In *Proceedings of the IEEE/CVF Conference on Computer Vision and Pattern Recognition*, pages 15368–15379, 2023. 1
- [25] Justin Kay, Timm Haucke, Suzanne Stathatos, Siqi Deng, Erik Young, Pietro Perona, Sara Beery, and Grant Van Horn. Align and distill: Unifying and improving domain adaptive object detection. *arXiv preprint arXiv:2403.12029*, 2024. 1, 3, 7
- [26] Aditya Khosla, Tinghui Zhou, Tomasz Malisiewicz, Alexei A Efros, and Antonio Torralba. Undoing the damage of dataset bias. In *Computer Vision–ECCV 2012: 12th European Conference on Computer Vision, Florence, Italy, October 7–13, 2012, Proceedings, Part I 12*, pages 158–171. Springer, 2012. 1, 3
- [27] Pang Wei Koh, Shiori Sagawa, Henrik Marklund, Sang Michael Xie, Marvin Zhang, Akshay Balsubramani, Weihua Hu, Michihiro Yasunaga, Richard Lanas Phillips, Irena Gao, et al. Wilds: A benchmark of in-the-wild distribution shifts. In *International conference on machine learning*, pages 5637–5664. PMLR, 2021. 1
- [28] Wuyang Li, Jie Liu, Bo Han, and Yixuan Yuan. Adjustment and alignment for unbiased open set domain adaptation (supplementary material). 1
- [29] Yu-Jhe Li, Xiaoliang Dai, Chih-Yao Ma, Yen-Cheng Liu, Kan Chen, Bichen Wu, Zijian He, Kris Kitani, and Peter Vajda. Cross-domain adaptive teacher for object detection. In *Proceedings of the IEEE/CVF Conference on Computer Vision and Pattern Recognition*, pages 7581–7590, 2022. 1
- [30] Junhui Liang, Ying Liu, and Vladimir Vlassov. The impact of background removal on performance of neural networks for fashion image classification and segmentation. In *2023 Congress in Computer Science, Computer Engineering, & Applied Computing (CSCE)*, pages 1960–1968. IEEE, 2023. 3
- [31] Natsumi Makigusa. Two-sample test based on maximum variance discrepancy. *Communications in Statistics-Theory and Methods*, pages 1–18, 2023. 5
- [32] Leland McInnes, John Healy, and James Melville. Umap: Uniform manifold approximation and projection for dimension reduction. *arXiv preprint arXiv:1802.03426*, 2018. 3
- [33] Aude Oliva and Antonio Torralba. The role of context in object recognition. *Trends in cognitive sciences*, 11(12):520–527, 2007. 1
- [34] Daniel Omeiza, Skyler Speakman, Celia Cintas, and Komminist Weldermariam. Smooth grad-cam++: An enhanced inference level visualization technique for deep convolutional neural network models. *arXiv preprint arXiv:1908.01224*, 2019. 4
- [35] Paolo Papale, Andrea Leo, Luca Cecchetti, Giacomo Handjara, Kendrick N Kay, Pietro Pietrini, and Emiliano Ricciardi. Foreground-background segmentation revealed during natural image viewing. *eneuro*, 5(3), 2018. 1
- [36] Minh Pham, Minsu Cho, Ameya Joshi, and Chinmay Hegde. Revisiting self-distillation. *arXiv preprint arXiv:2206.08491*, 2022. 3
- [37] Huy Phan, Philipp Koch, Lars Hertel, Marco Maass, Radoslaw Mazur, and Alfred Mertins. Cnn-lte: a class of 1-x pooling convolutional neural networks on label tree embeddings for audio scene classification. In *2017 IEEE International Conference on Acoustics, Speech and Signal Processing (ICASSP)*, pages 136–140. IEEE, 2017. 4
- [38] Jasper Poort, Matthew W Self, Bram Van Vugt, Hemmi Malkki, and Pieter R Roelfsema. Texture segregation causes early figure enhancement and later ground suppression in areas v1 and v4 of visual cortex. *Cerebral cortex*, 26(10):3964–3976, 2016. 1
- [39] Marco Tulio Ribeiro, Sameer Singh, and Carlos Guestrin. “why should i trust you?” explaining the predictions of any classifier. In *Proceedings of the 22nd ACM SIGKDD international conference on knowledge discovery and data mining*, pages 1135–1144, 2016. 3
- [40] Amir Rosenfeld, Richard Zemel, and John K Tsotsos. The elephant in the room. *arXiv preprint arXiv:1808.03305*, 2018.
- [41] Shiori Sagawa, Pang Wei Koh, Tatsunori B Hashimoto, and Percy Liang. Distributionally robust neural networks for group shifts: On the importance of regularization for worst-case generalization. *arXiv preprint arXiv:1911.08731*, 2019. 3
- [42] Rakshith Shetty, Bernt Schiele, and Mario Fritz. Not using the car to see the sidewalk—quantifying and controlling the effects of context in classification and segmentation. In *Proceedings of the IEEE/CVF conference on computer vision and pattern recognition*, pages 8218–8226, 2019. 1, 3
- [43] Moeko Takagi, Edgar Simo-Serra, Satoshi Iizuka, and Hiroshi Ishikawa. What makes a style: Experimental analysis of fashion prediction. In *Proceedings of the IEEE International Conference on Computer Vision Workshops*, pages 2247–2253, 2017. 3
- [44] Luke Taylor and Geoff Nitschke. Improving deep learning with generic data augmentation. In *2018 IEEE symposium series on computational intelligence (SSCI)*, pages 1542–1547. IEEE, 2018. 3
- [45] Antonio Torralba. Contextual priming for object detection. *International journal of computer vision*, 53:169–191, 2003. 3
- [46] Antonio Torralba and Alexei A Efros. Unbiased look at dataset bias. In *CVPR 2011*, pages 1521–1528. IEEE, 2011. 1, 3
- [47] Laurens Van der Maaten and Geoffrey Hinton. Visualizing data using t-sne. *Journal of machine learning research*, 9(11), 2008. 3
- [48] Pingyu Wu, Wei Zhai, and Yang Cao. Background activation suppression for weakly supervised object localization. In *2022 IEEE/CVF Conference on Computer Vision and Pattern Recognition (CVPR)*, pages 14228–14237. IEEE, 2022. 3
- [49] Yuxin Wu, Alexander Kirillov, Francisco Massa, Wan-Yen Lo, and Ross Girshick. Detectron2. <https://github.com/facebookresearch/detectron2>, 2019. 2
- [50] Kai Xiao, Logan Engstrom, Andrew Ilyas, and Aleksander Madry. Noise or signal: The role of image backgrounds in

object recognition. *arXiv preprint arXiv:2006.09994*, 2020.

3

- [51] Wei Zhai, Pingyu Wu, Kai Zhu, Yang Cao, Feng Wu, and Zheng-Jun Zha. Background activation suppression for weakly supervised object localization and semantic segmentation. *International Journal of Computer Vision*, 132(3):750–775, 2024. 3
- [52] Baoqiang Zhang, Saisai Hu, Tingkang Zhang, Min Hai, Yongchun Wang, Ya Li, and Yonghui Wang. Different patterns of foreground and background processing contribute to texture segregation in humans: an electrophysiological study. *PeerJ*, 11:e16139, 2023. 1
- [53] Jianguo Zhang, Marcin Marszałek, Svetlana Lazebnik, and Cordelia Schmid. Local features and kernels for classification of texture and object categories: A comprehensive study. *International journal of computer vision*, 73:213–238, 2007. 3
- [54] Kexuan Zhang, Qiyu Sun, Chaoqiang Zhao, and Yang Tang. Causal reasoning in typical computer vision tasks. *Science China Technological Sciences*, 67(1):105–120, 2024. 1
- [55] Sicheng Zhao, Bo Li, Pengfei Xu, and Kurt Keutzer. Multi-source domain adaptation in the deep learning era: A systematic survey. *arXiv preprint arXiv:2002.12169*, 2020. 3
- [56] Zijing Zhao, Sitong Wei, Qingchao Chen, Dehui Li, Yifan Yang, Yuxin Peng, and Yang Liu. Masked retraining teacher-student framework for domain adaptive object detection. In *Proceedings of the IEEE/CVF International Conference on Computer Vision*, pages 19039–19049, 2023. 3
- [57] Qianyu Zhou, Qiqi Gu, Jiangmiao Pang, Xuequan Lu, and Lizhuang Ma. Self-adversarial disentangling for specific domain adaptation. *IEEE Transactions on Pattern Analysis and Machine Intelligence*, 45(7):8954–8968, 2023. 3
- [58] Jun-Yan Zhu, Taesung Park, Phillip Isola, and Alexei A Efros. Unpaired image-to-image translation using cycle-consistent adversarial networks. In *Proceedings of the IEEE international conference on computer vision*, pages 2223–2232, 2017. 3
- [59] Lanyun Zhu, Tianrun Chen, Jianxiong Yin, Simon See, and Jun Liu. Addressing background context bias in few-shot segmentation through iterative modulation. In *Proceedings of the IEEE/CVF Conference on Computer Vision and Pattern Recognition*, pages 3370–3379, 2024. 1
- [60] Xinge Zhu, Jiangmiao Pang, Ceyuan Yang, Jianping Shi, and Dahua Lin. Adapting object detectors via selective cross-domain alignment. In *Proceedings of the IEEE/CVF Conference on Computer Vision and Pattern Recognition*, pages 687–696, 2019. 3
- [61] Zhuotun Zhu, Lingxi Xie, and Alan L Yuille. Object recognition with and without objects. *arXiv preprint arXiv:1611.06596*, 2016. 3

# Quantifying Context Bias in Domain Adaptation

## Supplementary Material

### 6. Description

This supplementary includes the outcomes of experiments because of page limits:

1) evaluation of training results (Sec. 7), 2) number of instances of each dataset (Sec. 8), 3) heat ratio of foreground and background (Sec. 9), 4) association matrix (Sec. 10), 5) association graph (Sec. 11), 6) MMD and MVD tables with various labels (Sec. 12), 7) MMD with different labels (Sec. 13), 8) pixel distribution of each dataset (Sec. 15), 9) UMAP embedding results in different layers (Sec. 14), 10) 3D embedding CS-CARLA with image patches (Sec. 16), and 11) Quantification results with YOLOv11 (Sec. 17).

### 7. Evaluation results

This section presents the evaluation results across different datasets.

Category	AP50	AP
person	-	40.126
truck	-	30.376
motorcycle	-	25.225
rider	-	43.699
bus	-	50.767
bicycle	-	34.554
car	-	56.398
train	-	25.914
<b>total</b>	<b>65.544</b>	38.382

Table 12. Training: Cityscapes. Validation: Cityscapes validation.

Category	AP50	AP
person	-	35.398
truck	-	18.712
motorcycle	-	14.679
rider	-	39.455
bus	-	33.538
bicycle	-	29.297
car	-	44.165
train	-	9.193
<b>total</b>	<b>46.321</b>	28.055

Table 13. Training: Cityscapes. Validation: Cityscapes foggy validation all.

Category	AP50	AP
person	-	28.942
truck	-	8.051
motorcycle	-	16.606
rider	-	18.490
bus	-	20.403
bicycle	-	18.701
car	-	46.856
train	-	13.346
<b>total</b>	<b>36.084</b>	21.424

Table 14. Training: Cityscapes. Validation: KITTI semantic train

Category	AP50	AP
person	-	58.013
truck	-	59.062
motorcycle	-	35.752
rider	-	46.421
bus	-	58.673
bicycle	-	51.926
car	-	66.548
train	-	65.054
<b>total</b>	<b>86.660</b>	55.181

Table 15. Training: KITTI semantic train. Validation: KITTI semantic train

Category	AP50	AP
person	-	24.072
truck	-	13.642
motorcycle	-	9.964
rider	-	22.429
bus	-	22.164
bicycle	-	17.779
car	-	39.317
train	-	7.411
<b>total</b>	<b>36.223</b>	19.597

Table 16. Training: KITTI semantic train. Validation: Cityscapes validation

Category	AP50	AP
person	-	15.646
truck	-	3.935
motorcycle	-	5.199
rider	-	17.623
bus	-	8.977
bicycle	-	13.425
car	-	25.612
train	-	2.341
<b>total</b>	<b>20.706</b>	11.595

Table 17. Training: KITTI semantic train. Validation: Cityscapes foggy validation all.

Val	car	van	truck	total(AP)	AP50
1	54.746	67.053	89.046	70.282	<b>81.568</b>
2	15.031	13.233	6.877	11.714	<b>15.101</b>
3	38.852	37.775	45.143	40.590	<b>50.430</b>
4	53.072	63.894	85.589	67.518	<b>80.428</b>
5	47.008	60.719	78.962	62.230	<b>77.144</b>
6	48.063	54.348	77.718	60.043	<b>73.081</b>
7	46.037	55.620	76.348	59.335	<b>71.923</b>
8	51.730	63.583	82.532	65.948	<b>79.119</b>
9	51.382	63.180	83.475	66.012	<b>79.303</b>
10	45.979	50.295	80.961	59.078	<b>73.782</b>

Table 18. Training: Virtual KITTI clone. Validation (Val): 1 - Virtual KITTI clone, 2 - Virtual KITTI fog, 3 - Virtual KITTI rain, 4 - Virtual KITTI 15 degree left, 5 - Virtual KITTI morning, 6 - Virtual KITTI overcast, 7 - Virtual KITTI sunset, 8 - Virtual KITTI 30 degree left, 9 - Virtual KITTI 15 degree left, 10 - Virtual KITTI 30 degree right

Val	car	truck	bus	total	AP50
1	64.968	67.053	68.883	66.926	<b>88.220</b>

Table 19. Training: CARLA train. Validation: CARLA validation

## 8. Instances statistics

This section provides statistics on the instances of the datasets used for training and feature extraction.

Category	# Instances
person	3394
rider	543
car	4652
truck	93
bus	98
train	23
motorcycle	149
bicycle	1165
total	10117

Table 20. Instances statistics of Cityscapes validation

Category	# Instances
person	10182
rider	1629
car	13956
truck	279
bus	294
train	69
motorcycle	447
bicycle	3495
total	30351

Table 21. Instances statistics of Cityscapes foggy validation all.

Category	# Instances
person	100
rider	29
car	1678
truck	101
bus	19
train	18
motorcycle	8
bicycle	47
total	2000

Table 22. Instances statistics of KITTI semantic train.

Category	# Instances
Car	24603
Van	2054
Truck	461
total	27118

Table 23. Instances statistics of Virtual KITTI clone. Different weather conditions have the same statistics.

Category	# Instances
Car	24614
Van	1948
Truck	369
total	26931

Table 24. Instances statistics of Virtual KITTI 30 degree left.

Category	# Instances
car	6962
truck	2887
bus	789
total	10638

Table 25. Instances statistics of CARLA train.

Category	# Instances
car	1156
truck	421
bus	0
total	1577

Table 26. Instances statistics of CARLA validation

Category	# Instances
Car	24916
Van	2000
Truck	447
total	27363

Table 27. Instances statistics of Virtual KITTI 15 degree left.

Category	# Instances
Car	20165
Van	1443
Truck	389
total	21997

Table 28. Instances statistics of Virtual KITTI 30 degree right.

Category	# Instances
Car	23680
Van	1922
Truck	434
total	26036

Table 29. Instances statistics of Virtual KITTI 15 degree right.

## 9. Heat ratio

This section shows Smooth Grad-CAM++ correspondences with foreground region using instance masks. For all activated pixels via Smooth Grad-CAM++,  $A_c$ , of a particular foreground object, we can divide  $A_c$  into activated foreground pixels  $f_c$  and activated background pixels  $b_c$ . The foreground heat ratio is then given by the activated foreground pixels over the total foreground pixels  $f_c/f$  while the background heat ratio is the activated background pixels over the total foreground pixels  $b_c/f$  where  $f$  represents the total foreground pixels. The foreground and background heat ratios provide the amount of contextual information and validity of use of Smooth Grad-CAM++. Overall, the entire foreground region was activated and background region was various depending on threshold during our experiments.

Layer	Heat ratio			
	FG mean	FG std	BG mean	BG std
res2_2	0.81	0.24	1.81	2.80
res3_3	0.80	0.24	1.85	3.23
res4_5	0.80	0.25	1.75	2.75
res5_2	0.77	0.27	0.76	1.12

Table 30. Dataset: Cityscapes, Label: Car, Bin: 1

Layer	Heat ratio			
	FG mean	FG std	BG mean	BG std
res2_2	0.79	0.24	1.29	2.01
res3_3	0.79	0.24	1.30	2.04
res4_5	0.79	0.25	1.39	2.57
res5_2	0.76	0.27	0.81	0.27

Table 32. Dataset: Cityscapes foggy 0.01, Label: Person, Bin: 1

Layer	Heat ratio			
	FG mean	FG std	BG mean	BG std
res2_2	0.74	0.24	1.0	5.7
res3_3	0.74	0.24	0.82	1.79
res4_5	0.74	0.25	0.89	1.98
res5_2	0.72	0.26	0.61	1.11

Table 34. Dataset: Cityscapes foggy 0.02, Label: Car, Bin: 1

Layer	Heat ratio			
	FG mean	FG std	BG mean	BG std
res2_2	0.85	0.2	5.28	17.76
res3_3	0.85	0.2	3.30	5.36
res4_5	0.84	0.21	2.58	3.89
res5_2	0.82	0.24	0.82	1.04

Table 36. Dataset: CARLA, Label: Car, Bin: 1

Layer	Heat ratio			
	FG mean	FG std	BG mean	BG std
res2_2	0.81	0.19	2.35	3.67
res3_3	0.81	0.19	2.37	3.85
res4_5	0.79	0.21	1.68	2.28
res5_2	0.79	0.27	0.73	1.05

Table 38. Dataset: KITTI semantic, Label: Car, Bin: 1

Layer	Heat ratio			
	FG mean	FG std	BG mean	BG std
res2_2	0.77	0.22	3.81	10.28
res3_3	0.77	0.22	3.40	6.88
res4_5	0.75	0.24	1.79	2.52
res5_2	0.71	0.29	0.70	0.98

Table 40. Dataset: Virtual KITTI, Label: Car, Bin: 1

Table 42. Heat ratio of Cityscapes. Label: Car

Layer	Heat ratio			
	FG mean	FG std	BG mean	BG std
res2_2	1.0	0.03	44.43	67.04
res3_3	1.0	0.03	45.25	73.18
res4_5	1.0	0.03	44.76	64.97
res5_2	1.0	0.03	26.81	25.96

Table 31. Dataset: Cityscapes, Label: Car, Bin: 9

Layer	Heat ratio			
	FG mean	FG std	BG mean	BG std
res2_2	1.0	0.0	32.76	47.70
res3_3	1.0	0.0	32.99	48.89
res4_5	1.0	0.0	35.47	58.04
res5_2	1.0	0.0	26.07	28.41

Table 33. Dataset: Cityscapes foggy 0.01, Label: Car, Bin: 9

Layer	Heat ratio			
	FG mean	FG std	BG mean	BG std
res2_2	1.0	0.0	24.56	86.45
res3_3	1.0	0.0	22.11	35.97
res4_5	1.0	0.0	23.37	39.77
res5_2	1.0	0.0	20.66	25.86

Table 35. Dataset: Cityscapes foggy 0.02, Label: Car, Bin: 9

Layer	Heat ratio			
	FG mean	FG std	BG mean	BG std
res2_2	1.0	0.0	78.77	228.56
res3_3	1.0	0.0	53.06	73.71
res4_5	1.0	0.0	44.59	51.49
res5_2	1.0	0.0	22.95	18.59

Table 37. Dataset: CARLA, Label: Car, Bin: 9

Layer	Heat ratio			
	FG mean	FG std	BG mean	BG std
res2_2	1.0	0.0	74.43	119.17
res3_3	1.0	0.0	76.10	129.94
res4_5	1.0	0.0	63.38	86.72
res5_2	1.0	0.0	32.84	29.50

Table 39. Dataset: KITTI semantic, Label: Car, Bin: 9

Layer	Heat ratio			
	FG mean	FG std	BG mean	BG std
res2_2	1.0	0.0	63.59	176.25
res3_3	1.0	0.0	56.10	116.33
res4_5	1.0	0.0	32.25	40.88
res5_2	1.0	0.0	18.96	15.74

Table 41. Dataset: Virtual KITTI, Label: Car, Bin: 9

Layer	Heat ratio			
	FG mean	FG std	BG mean	BG std
res2_2	0.92	0.16	2.92	3.31
res3_3	0.92	0.16	2.92	3.34
res4_5	0.92	0.17	2.59	3.12
res5_2	0.9	0.20	1.12	1.47

Table 43. Dataset: Cityscapes, Label: Person, Bin: 1

Layer	Heat ratio			
	FG mean	FG std	BG mean	BG std
res2_2	0.93	0.14	25.53	44.49
res3_3	0.93	0.14	25.30	43.94
res4_5	0.93	0.15	27.31	51.37
res5_2	0.92	0.17	18.70	27.04

Table 45. Dataset: Cityscapes, Label: Bicycle, Bin: 1

Layer	Heat ratio			
	FG mean	FG std	BG mean	BG std
res2_2	0.8	0.21	2.37	3.03
res3_3	0.8	0.21	2.37	2.97
res4_5	0.8	0.23	2.53	3.34
res5_2	0.73	0.29	1.17	1.21

Table 47. Dataset: Cityscapes, Label: Rider, Bin: 1

Table 49. Heat ratio of non-car labels of Cityscapes

Layer	Heat ratio			
	FG mean	FG std	BG mean	BG std
res2_2	0.92	0.16	2.92	3.31
res3_3	0.92	0.16	2.92	3.34
res4_5	0.92	0.17	2.59	3.12
res5_2	0.9	0.20	1.12	1.47

Table 50. Dataset: Cityscapes foggy 0.01, Label: Person, Bin: 1

Layer	Heat ratio			
	FG mean	FG std	BG mean	BG std
res2_2	0.82	0.2	1.7	1.62
res3_3	0.83	0.2	1.71	1.67
res4_5	0.83	0.21	1.69	1.68
res5_2	0.80	0.24	1.31	1.53

Table 52. Dataset: Cityscapes foggy 0.01, Label: Bicycle, Bin: 1

Layer	Heat ratio			
	FG mean	FG std	BG mean	BG std
res2_2	0.74	0.24	1.77	2.35
res3_3	0.74	0.24	1.86	3.06
res4_5	0.73	0.26	1.86	2.42
res5_2	0.72	0.29	1.21	1.39

Table 54. Dataset: Cityscapes foggy 0.01, Label: Rider, Bin: 1

Table 56. Heat ratio of non-car labels of Cityscapes foggy 0.01

Layer	Heat ratio			
	FG mean	FG std	BG mean	BG std
res2_2	1.0	0.0	73.94	93.65
res3_3	1.0	0.0	74.06	95.34
res4_5	1.0	0.0	68.99	84.17
res5_2	1.0	0.0	37.37	28.80

Table 44. Dataset: Cityscapes, Label: Person, Bin: 9

Layer	Heat ratio			
	FG mean	FG std	BG mean	BG std
res2_2	1.0	0.0	48.96	53.44
res3_3	1.0	0.0	48.52	52.69
res4_5	1.0	0.0	52.36	63.36
res5_2	1.0	0.0	36.15	29.18

Table 46. Dataset: Cityscapes, Label: Bicycle, Bin: 9

Layer	Heat ratio			
	FG mean	FG std	BG mean	BG std
res2_2	1.0	0.0	59.26	78.25
res3_3	1.0	0.0	59.90	78.95
res4_5	1.0	0.0	63.75	84.67
res5_2	1.0	0.0	37.69	28.27

Table 48. Dataset: Cityscapes, Label: Rider, Bin: 9

Layer	Heat ratio			
	FG mean	FG std	BG mean	BG std
res2_2	1.0	0.0	52.96	64.47
res3_3	1.0	0.0	54.65	78.83
res4_5	1.0	0.0	55.07	70.81
res5_2	1.0	0.0	36.18	29.91

Table 51. Dataset: Cityscapes foggy 0.01, Label: Person, Bin: 9

Layer	Heat ratio			
	FG mean	FG std	BG mean	BG std
res2_2	0.99	0.07	39.15	37.81
res3_3	0.99	0.07	39.45	39.84
res4_5	0.99	0.07	38.18	33.54
res5_2	0.99	0.08	35.53	31.37

Table 53. Dataset: Cityscapes foggy 0.01, Label: Bicycle, Bin: 9

Layer	Heat ratio			
	FG mean	FG std	BG mean	BG std
res2_2	1.0	0.0	46.40	59.50
res3_3	1.0	0.0	49.66	84.49
res4_5	1.0	0.0	46.22	51.15
res5_2	1.0	0.0	39.93	33.55

Table 55. Dataset: Cityscapes foggy 0.01, Label: Rider, Bin: 9

Layer	Heat ratio			
	FG mean	FG std	BG mean	BG std
res2_2	0.9	0.17	2.13	7.57
res3_3	0.9	0.18	2.03	4.30
res4_5	0.89	0.18	1.94	2.41
res5_2	0.88	0.20	1.15	1.5

Table 57. Dataset: Cityscapes foggy 0.02, Label: Person, Bin: 1

Layer	Heat ratio			
	FG mean	FG std	BG mean	BG std
res2_2	0.81	0.18	1.3	1.16
res3_3	0.82	0.18	1.32	1.39
res4_5	0.81	0.19	1.33	1.65
res5_2	0.81	0.23	1.36	1.69

Table 59. Dataset: Cityscapes foggy 0.02, Label: Bicycle, Bin: 1

Layer	Heat ratio			
	FG mean	FG std	BG mean	BG std
res2_2	1.0	0.0	49.19	89.27
res3_3	1.0	0.0	48.66	65.85
res4_5	1.0	0.0	49.06	58.13
res5_2	1.0	0.0	36.40	31.73

Table 58. Dataset: Cityscapes foggy 0.02, Label: Person, Bin: 9

Layer	Heat ratio			
	FG mean	FG std	BG mean	BG std
res2_2	1.0	0.0	29.02	26.75
res3_3	1.0	0.0	29.90	34.22
res4_5	1.0	0.0	30.75	42.19
res5_2	1.0	0.0	32.01	30.92

Table 60. Dataset: Cityscapes foggy 0.02, Label: Bicycle, Bin: 9

Table 61. Heat ratio of non-car labels of Cityscapes foggy 0.02

Layer	Heat ratio			
	FG mean	FG std	BG mean	BG std
res2_2	0.85	0.18	1.76	1.93
res3_3	0.85	0.18	1.77	2.02
res4_5	0.84	0.19	1.88	2.39
res5_2	0.83	0.22	1.18	1.33

Table 62. Dataset: Cityscapes validation, Label: Car, Bin: 1

Layer	Heat ratio			
	FG mean	FG std	BG mean	BG std
res2_2	0.91	0.17	2.48	2.75
res3_3	0.91	0.17	2.62	3.56
res4_5	0.90	0.17	2.38	2.86
res5_2	0.89	0.20	1.09	1.39

Table 64. Dataset: Cityscapes validation, Label: Person, Bin: 1

Layer	Heat ratio			
	FG mean	FG std	BG mean	BG std
res2_2	0.79	0.24	1.63	2.48
res3_3	0.79	0.24	1.65	2.54
res4_5	0.79	0.25	1.60	2.49
res5_2	0.75	0.27	0.81	1.23

Table 66. Dataset: Cityscapes validation, Label: Bicycle, Bin: 1

Layer	Heat ratio			
	FG mean	FG std	BG mean	BG std
res2_2	0.77	0.23	1.73	1.83
res3_3	0.77	0.23	1.73	1.96
res4_5	0.78	0.24	1.87	2.27
res5_2	0.74	0.29	1.08	1.09

Table 68. Dataset: Cityscapes validation, Label: Rider, Bin: 1

Layer	Heat ratio			
	FG mean	FG std	BG mean	BG std
res2_2	1.0	0.02	39.38	58.87
res3_3	1.0	0.02	39.65	59.53
res4_5	1.0	0.02	40.22	60.05
res5_2	1.0	0.02	25.74	25.51

Table 63. Dataset: Cityscapes validation, Label: Car, Bin: 9

Layer	Heat ratio			
	FG mean	FG std	BG mean	BG std
res2_2	1.0	0.0	60.62	76.07
res3_3	1.0	0.0	64.18	94.67
res4_5	1.0	0.0	60.31	74.19
res5_2	1.0	0.0	35.33	27.09

Table 65. Dataset: Cityscapes validation, Label: Person, Bin: 9

Layer	Heat ratio			
	FG mean	FG std	BG mean	BG std
res2_2	1.0	0.0	39.94	41.21
res3_3	1.0	0.0	40.03	41.78
res4_5	1.0	0.0	43.01	51.92
res5_2	1.0	0.0	33.66	27.41

Table 67. Dataset: Cityscapes validation, Label: Bicycle, Bin: 9

Layer	Heat ratio			
	FG mean	FG std	BG mean	BG std
res2_2	1.0	0.0	45.55	53.82
res3_3	1.0	0.0	46.10	58.77
res4_5	1.0	0.0	48.52	60.15
res5_2	1.0	0.0	37.29	27.85

Table 69. Dataset: Cityscapes validation, Label: Rider, Bin: 9

Table 70. Heat ratio of non-car labels of Cityscapes validation

## 10. Association Matrix

This section shows association matrix of Cityscapes, KITTI semantic, CARLA, and Virtual KITTI.

Figure 12 illustrates an example of *Droprate* computation.

$DET1$  = number of original detections / the number of ground truth detections

$DET2$  = the number of no loss with background modification / the number of ground truth detections.

*Droprate* is defined as subtraction of  $DET1$  and  $DET2$ .

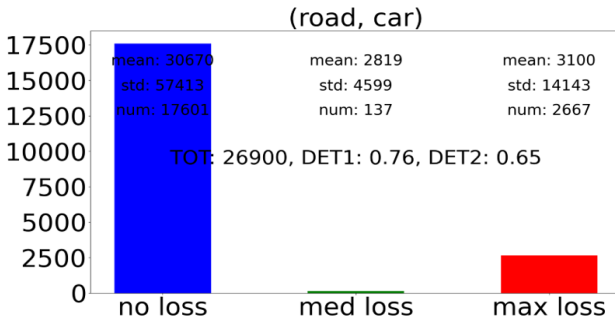


Figure 12. “TOT” means the total number of cars in Cityscapes dataset. Without modification road regions, the trained model could detect 76% of car objects and with the modification, it dropped 65%. *Droprate* is 0.11 for the (road, car) pair.

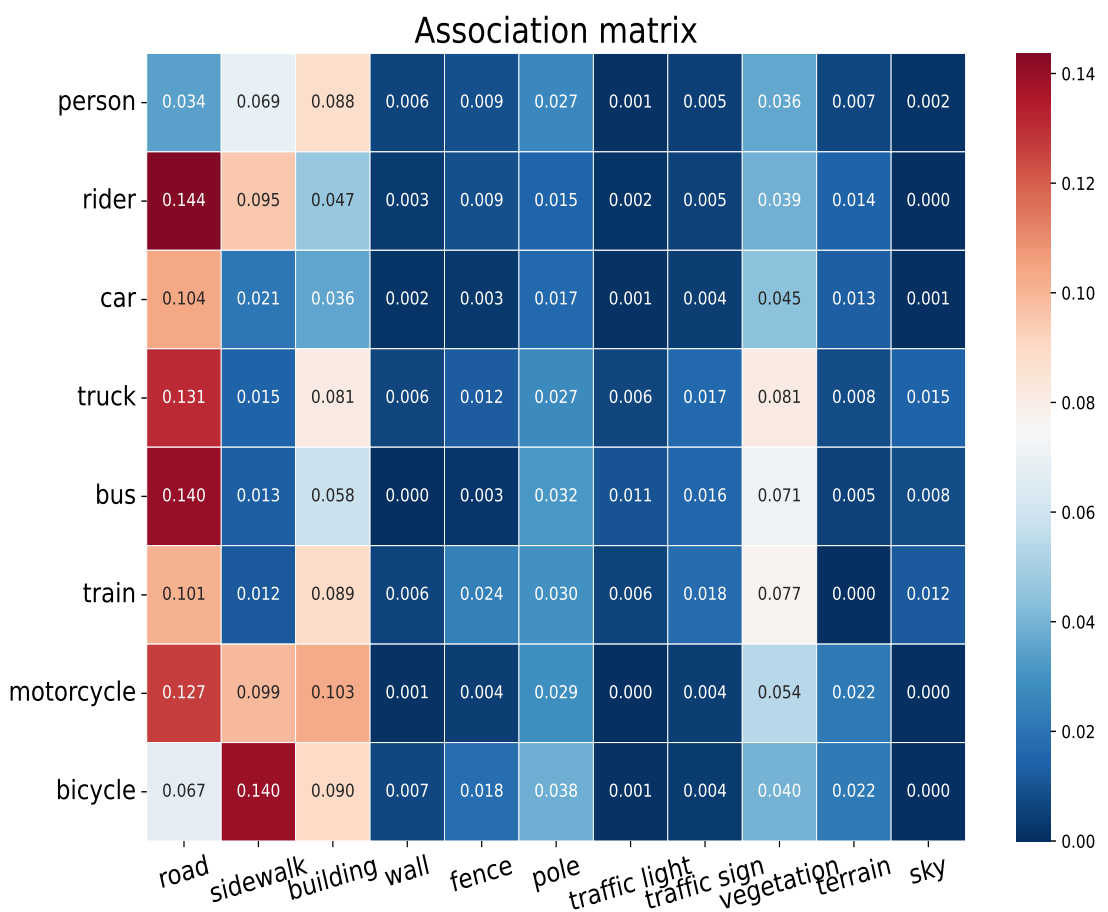


Figure 13. **Association matrix Cityscapes.**

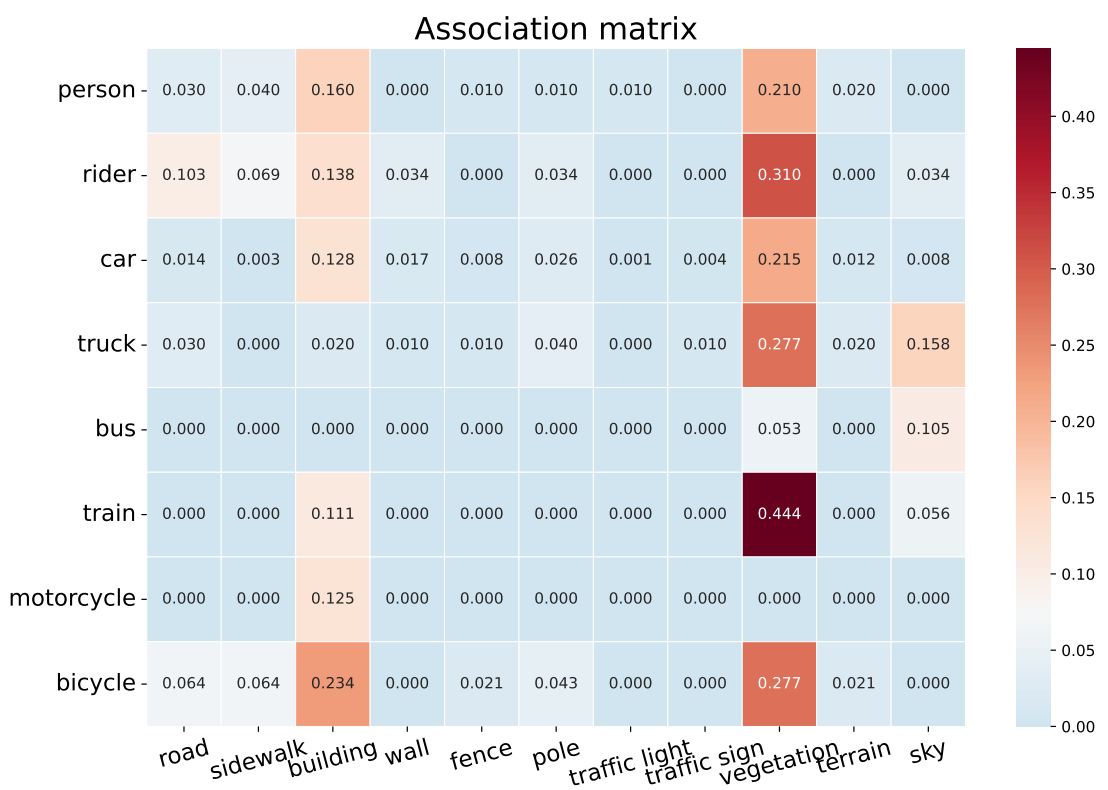


Figure 14. Association matrix KITTI semantic.

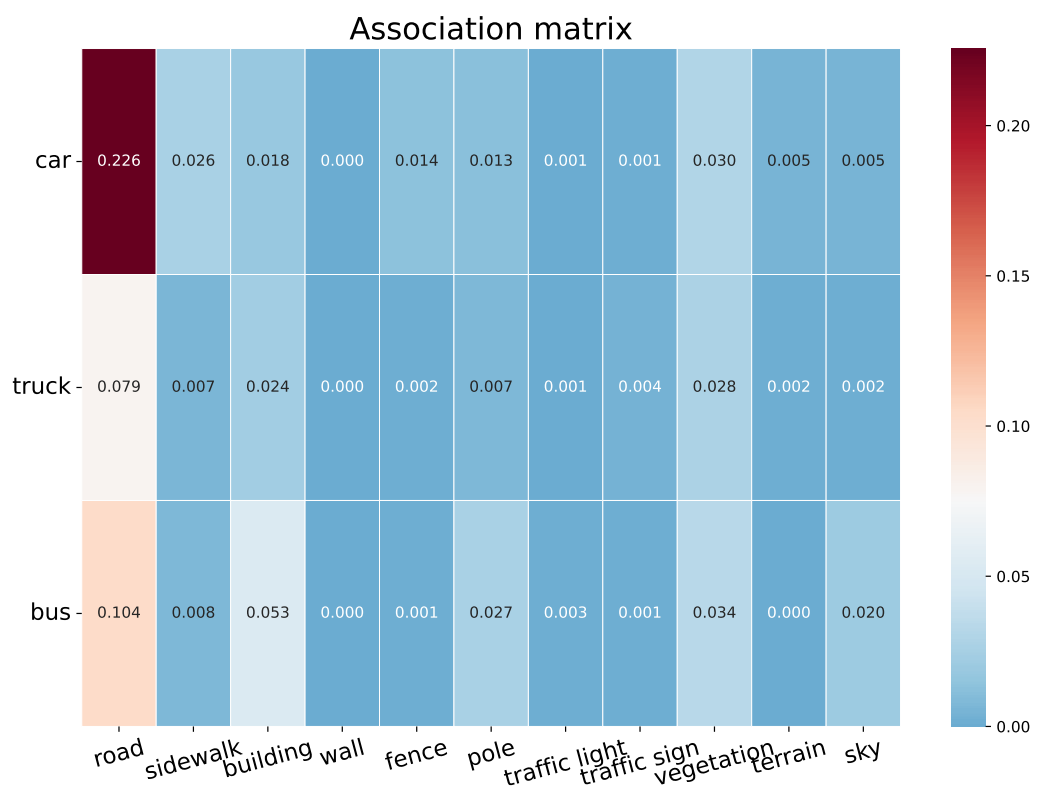


Figure 15. **Association matrix CARLA.**

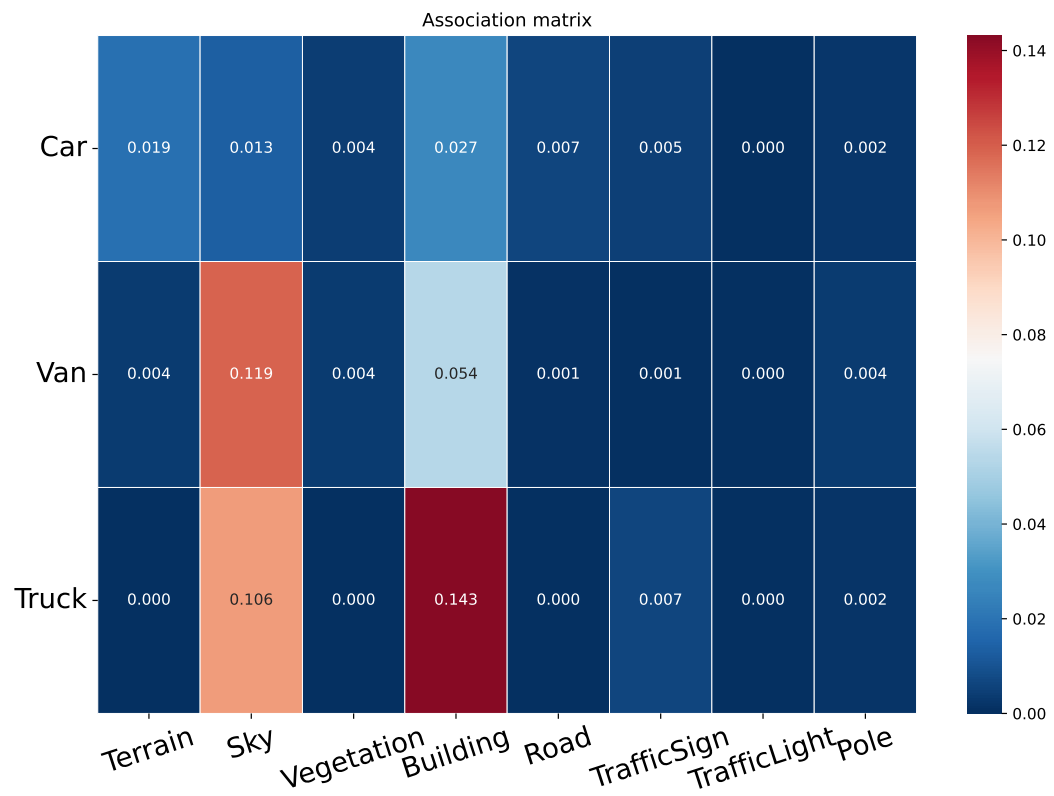


Figure 16. Association matrix **Virtual KITTI**.

## 11. Association Graph

This section presents the association graph of Cityscapes, KITTI semantic, CARLA, and Virtual KITTI.

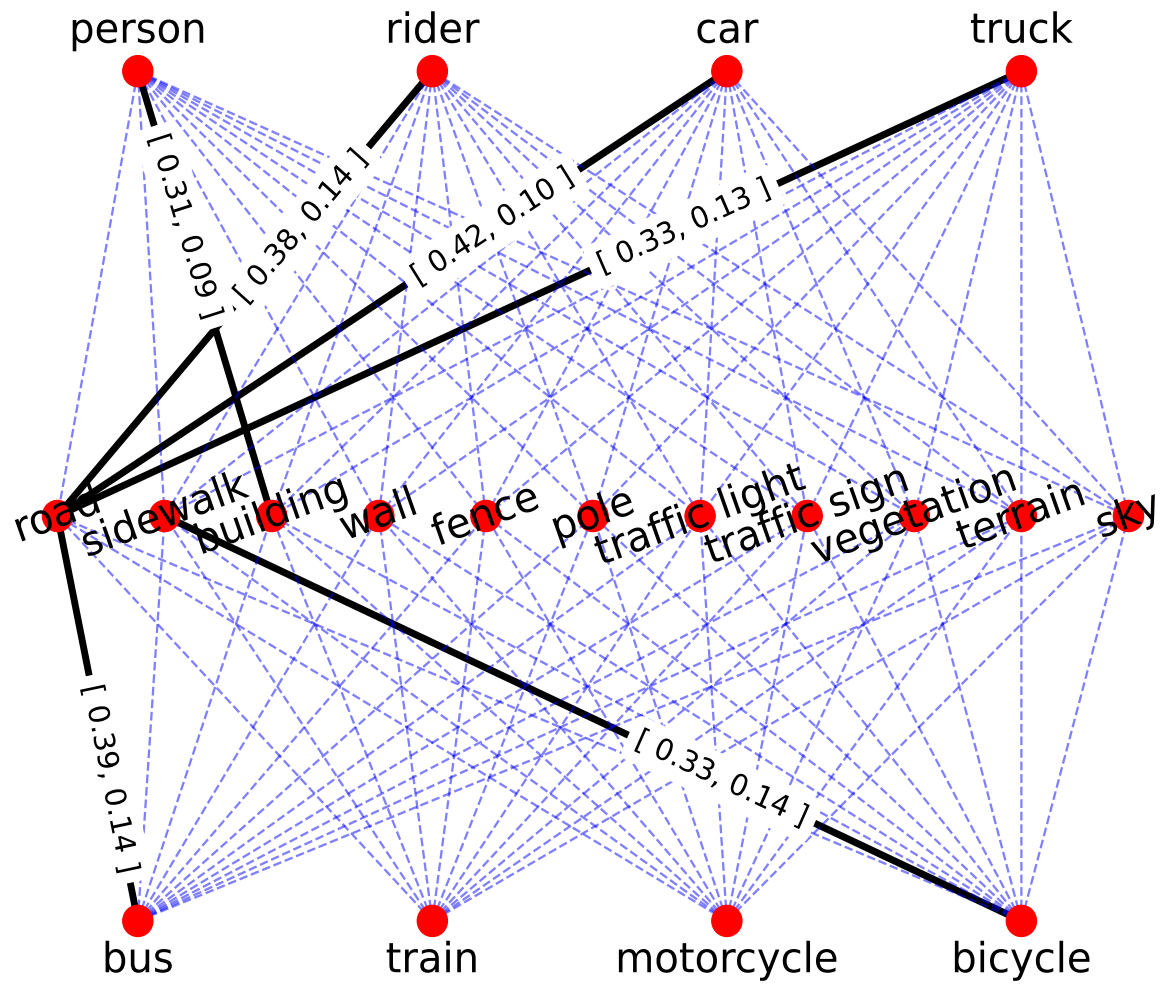


Figure 17. Association graph Cityscapes.

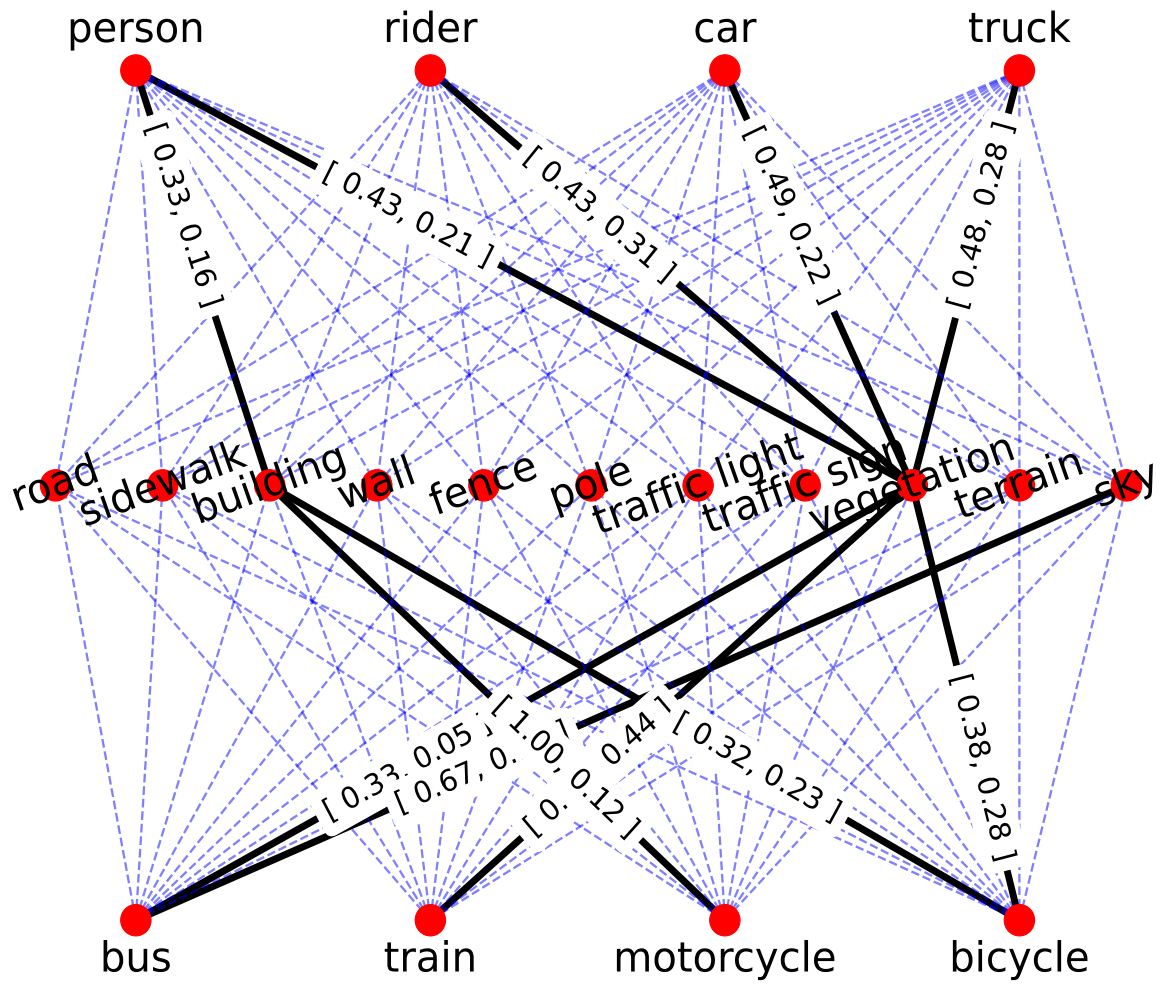


Figure 18. Association graph KITTI semantic. (bus,vegetation): [0.33, 0.05], (bus,sky): [0.67,0.11], (train,vegetation): [0.73,0.44]

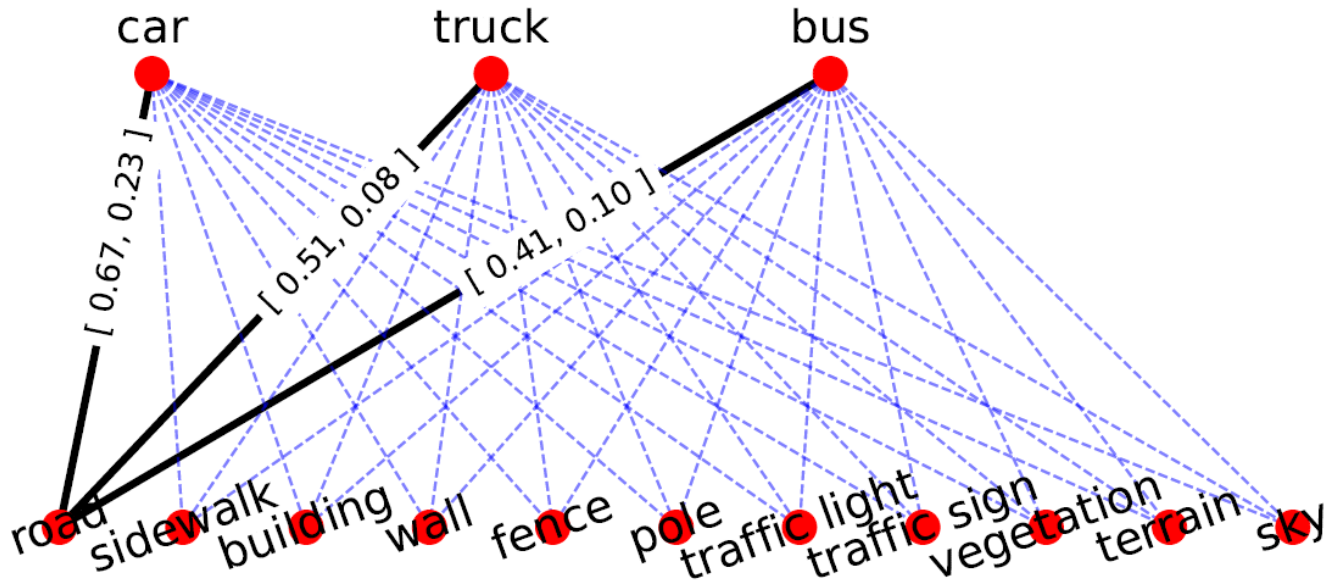


Figure 19. Association graph CARLA

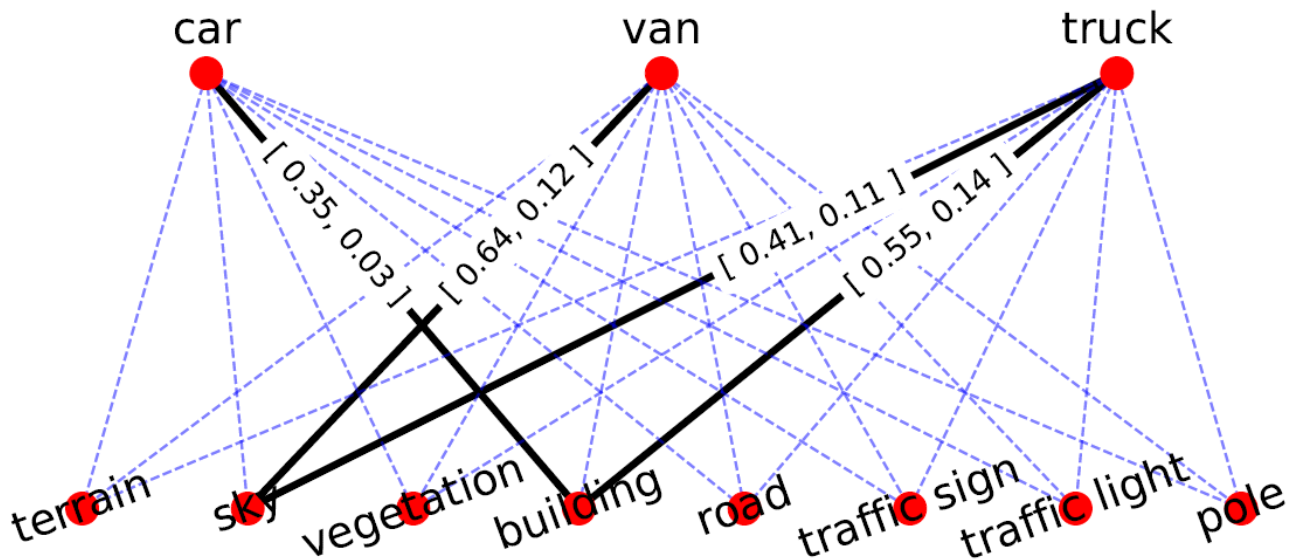


Figure 20. Association graph Virtual KITTI.

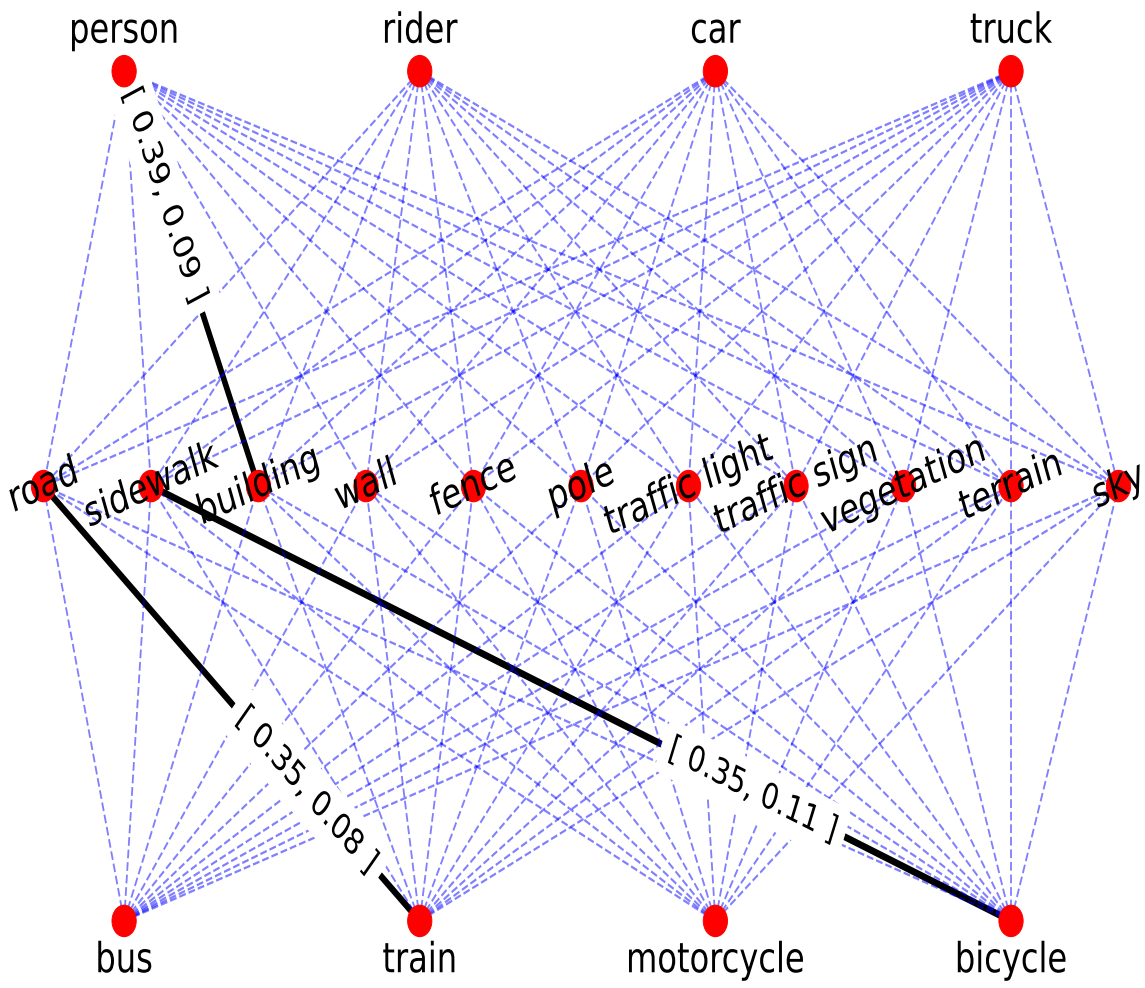


Figure 21. Association graph Cityscapes with MIC.

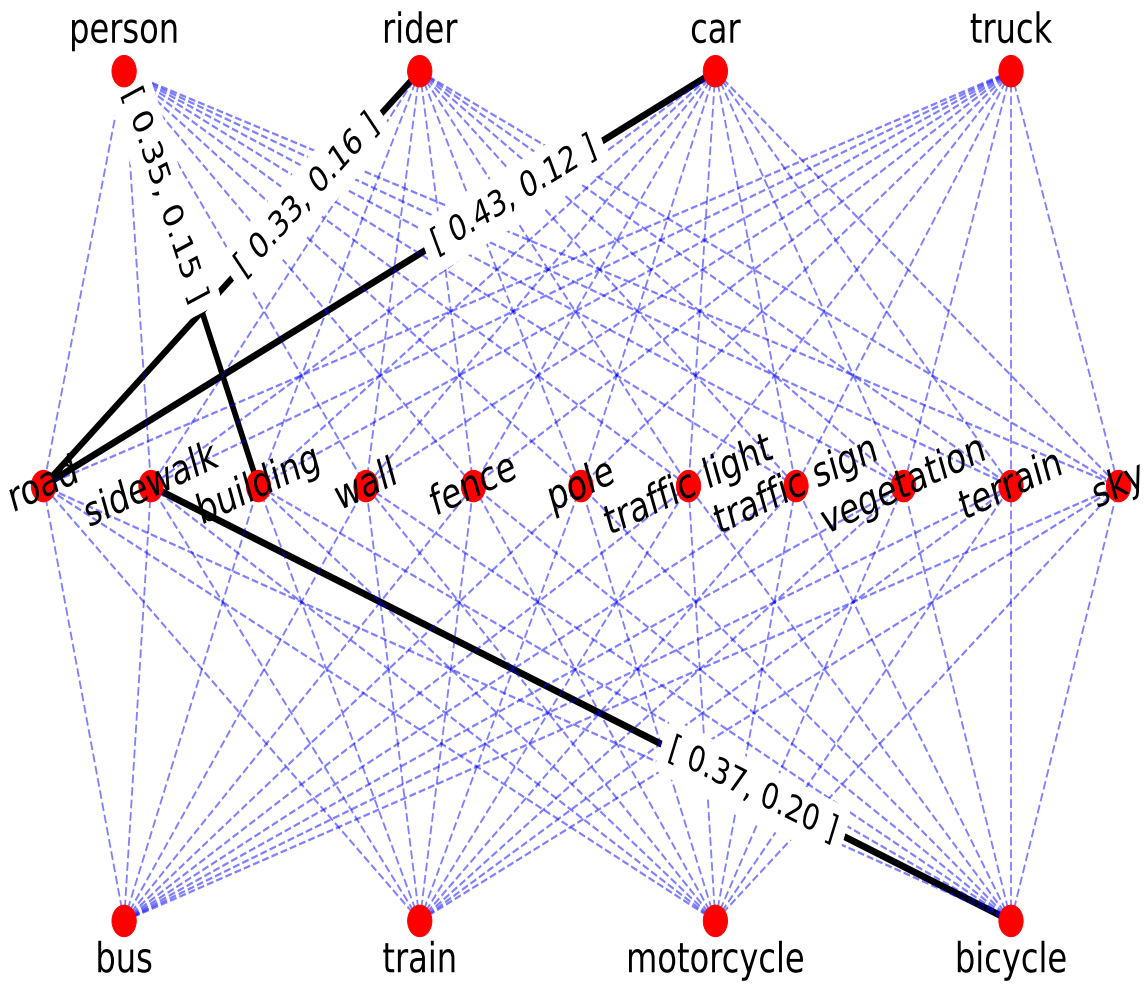


Figure 22. Association graph Cityscapes with ALDI++.

## **12. MMD and MVD Table**

This section contains the MMD and MVD across different domains.

Layer	MMD mean			
	f2f	f2b	b2f	b2b
res2_2	0.48597	7.520155	3.976121	<b>0.034143</b>
res3_3	0.279831	0.784058	0.49827	<b>0.008149</b>
res4_5	0.219191	0.714354	0.558228	<b>0.009553</b>
res5_2	0.465037	1.025705	0.411115	<b>0.012313</b>

Table 71. Dataset: CS-CSFV(0.01), Label: car, Bin: 1

Layer	MMD mean			
	f2f	f2b	b2f	b2b
res2_2	0.837967	9.278673	5.501331	<b>0.022671</b>
res3_3	0.545075	1.579772	1.34774	<b>0.006316</b>
res4_5	1.048955	2.660388	1.979247	<b>0.010752</b>
res5_2	1.213613	3.251228	1.754225	<b>0.018963</b>

Table 73. Dataset: KS-VK, Label: car, Bin: 1

Layer	MMD mean			
	f2f	f2b	b2f	b2b
res2_2	1.360337	13.39255	8.77936	<b>0.012672</b>
res3_3	1.006295	1.659392	2.757476	<b>0.007218</b>
res4_5	1.657877	3.228704	2.850062	<b>0.023023</b>
res5_2	1.084457	2.052765	2.509785	<b>0.014955</b>

Table 75. Dataset: CARLA-KS, Label: car, Bin: 1

Layer	MMD mean			
	f2f	f2b	b2f	b2b
res2_2	0.627815	9.902885	5.965082	<b>0.003665</b>
res3_3	0.615928	1.481266	1.443983	<b>0.002998</b>
res4_5	1.160176	2.663172	1.76238	<b>0.020648</b>
res5_2	0.878996	2.366584	1.085149	<b>0.012676</b>

Table 77. Dataset: CARLA-VK, Label: car, Bin: 1

Layer	MMD mean			
	f2f	f2b	b2f	b2b
res2_2	<b>1.929408</b>	75.95716	39.86969	5.954215
res3_3	<b>0.784393</b>	9.541647	12.91833	7.142425
res4_5	<b>0.931707</b>	9.65685	10.33697	5.973624
res5_2	<b>1.354234</b>	11.40708	16.86537	9.518532

Table 72. Dataset: CS-CSFV(0.01), Label: car, Bin: 9

Layer	MMD mean			
	f2f	f2b	b2f	b2b
res2_2	<b>1.701219</b>	30.11269	61.23091	20.14374
res3_3	<b>2.898878</b>	9.565176	17.82692	9.921293
res4_5	<b>3.847768</b>	18.5432	15.08211	10.13089
res5_2	<b>3.891656</b>	17.04114	27.30131	16.7562

Table 74. Dataset: KS-VK, Label: car, Bin: 9

Layer	MMD mean			
	f2f	f2b	b2f	b2b
res2_2	<b>3.183262</b>	69.27134	44.71856	18.60363
res3_3	<b>3.062511</b>	16.40809	23.81949	16.98051
res4_5	<b>3.930751</b>	18.59529	25.63895	22.29927
res5_2	<b>3.950112</b>	30.34706	42.61812	33.30783

Table 76. Dataset: CARLA-KS, Label: car, Bin: 9

Layer	MMD mean			
	f2f	f2b	b2f	b2b
res2_2	<b>4.07898</b>	38.00771	44.54776	14.14914
res3_3	<b>3.656437</b>	9.317527	25.74601	18.75477
res4_5	<b>4.998009</b>	18.28671	33.85126	29.11955
res5_2	<b>5.166857</b>	18.48426	54.46207	41.99809

Table 78. Dataset: CARLA-VK, Label: car, Bin: 9

Table 79. “Car” label MMD across other datasets. The lowest values are highlighted in bold.

Layer	MMD mean			
	f2f	f2b	b2f	b2b
res2_2	<b>0.002588</b>	0.005147	0.010467	0.012556
res3_3	0.000992	0.005338	0.006035	<b>0.000693</b>
res4_5	<b>0.008631</b>	0.012306	0.025341	0.008826
res5_2	<b>0.004781</b>	0.01386	0.016515	0.004828

Table 80. Dataset: CS-CSV, Label: Person, Bin: 1

Layer	MMD mean			
	f2f	f2b	b2f	b2b
res2_2	<b>0.007112</b>	43.16728	33.35849	1.326029
res3_3	<b>0.015106</b>	5.815366	3.460745	0.492159
res4_5	<b>0.004296</b>	3.961384	3.551943	0.224099
res5_2	<b>0.012289</b>	4.934453	5.327017	0.322196

Table 81. Dataset: CS-CSV, Label: Person, Bin: 9

Layer	MMD mean			
	f2f	f2b	b2f	b2b
res2_2	0.020487	0.006696	0.027399	<b>0.004261</b>
res3_3	0.001779	0.003611	0.006618	<b>0.001257</b>
res4_5	0.005283	0.017598	0.016919	<b>0.002194</b>
res5_2	0.008838	0.016117	0.015965	<b>0.004058</b>

Table 82. Dataset: CS-CSV, Label: Bicycle, Bin: 1

Layer	MMD mean			
	f2f	f2b	b2f	b2b
res2_2	<b>0.034208</b>	37.02699	27.83576	0.850653
res3_3	<b>0.012528</b>	4.389391	3.770594	0.149715
res4_5	<b>0.004156</b>	3.142533	3.765164	0.219377
res5_2	<b>0.005631</b>	3.758185	4.059784	0.164122

Table 83. Dataset: CS-CSV, Label: Bicycle, Bin: 9

Layer	MMD mean			
	f2f	f2b	b2f	b2b
res2_2	0.002653	0.002351	0.001569	<b>0.00188</b>
res3_3	<b>0.000731</b>	0.001856	0.001826	0.000775
res4_5	<b>0.002486</b>	0.008231	0.007975	0.004156
res5_2	0.003608	0.006807	0.007905	<b>0.00264</b>

Table 84. Dataset: CS-CSV, Label: Rider, Bin: 1

Layer	MMD mean			
	f2f	f2b	b2f	b2b
res2_2	<b>0.012084</b>	31.35223	32.10123	0.232441
res3_3	<b>0.001812</b>	3.521889	3.420648	0.106992
res4_5	<b>0.003306</b>	4.706572	2.788121	0.587758
res5_2	<b>0.003795</b>	3.965521	3.294167	0.305498

Table 85. Dataset: CS-CSV, Label: Rider, Bin: 9

Table 86. MMD for non-car labels between Cityscapes and Cityscapes validation.

Layer	MMD mean			
	f2f	f2b	b2f	b2b
res2_2	0.012706	0.02892	0.011056	<b>0.002405</b>
res3_3	0.009049	0.011817	0.01295	<b>0.004601</b>
res4_5	0.008535	0.01387	0.015293	<b>0.00595</b>
res5_2	0.033776	0.018467	0.050713	<b>0.009092</b>

Table 87. Dataset: CS-CSFV(0.01), Label: Person, Bin: 1

Layer	MMD mean			
	f2f	f2b	b2f	b2b
res2_2	<b>0.022442</b>	43.01485	37.45594	1.370968
res3_3	<b>0.020119</b>	4.622701	3.734675	1.755346
res4_5	<b>0.011593</b>	3.842468	3.364573	1.326394
res5_2	<b>0.024133</b>	6.014653	5.61746	2.983906

Table 88. Dataset: CS-CSFV(0.01), Label: Person, Bin: 9

Layer	MMD mean			
	f2f	f2b	b2f	b2b
res2_2	0.013605	0.009774	0.031494	<b>0.001712</b>
res3_3	0.010488	0.013481	0.008212	<b>0.004548</b>
res4_5	0.008836	0.015643	0.014073	<b>0.005412</b>
res5_2	0.018766	0.016117	0.025891	<b>0.007225</b>

Table 89. Dataset: CS-CSFV(0.01), Label: Bicycle, Bin: 1

Layer	MMD mean			
	f2f	f2b	b2f	b2b
res2_2	<b>0.079213</b>	47.07988	41.98639	1.40932
res3_3	<b>0.006467</b>	4.824563	4.173671	1.93347
res4_5	<b>0.01469</b>	3.879474	3.593062	1.470991
res5_2	<b>0.048684</b>	5.987271	4.586958	2.817607

Table 90. Dataset: CS-CSFV(0.01), Label: Bicycle, Bin: 9

Layer	MMD mean			
	f2f	f2b	b2f	b2b
res2_2	<b>0.001002</b>	29.86252	18.17271	2.760283
res3_3	<b>0.000388</b>	2.548376	2.227595	1.074819
res4_5	<b>0.000858</b>	3.606037	2.066544	1.463306
res5_2	<b>0.000741</b>	6.765415	3.495808	2.904991

Table 91. Dataset: CS-CSFV(0.01), Label: Rider, Bin: 1

Table 92. Dataset: CS-CSFV(0.01), Label: Rider, Bin: 9

Table 93. MMD for non-car labels between Cityscapes and Cityscapes foggy 0.01.

Layer	MMD mean			
	f2f	f2b	b2f	b2b
res2_2	0.041437	0.012486	0.066193	<b>0.007482</b>
res3_3	0.014406	0.011046	0.021534	<b>0.008058</b>
res4_5	0.014034	0.022386	0.027688	<b>0.008207</b>
res5_2	0.021939	0.027792	0.020891	<b>0.006338</b>

Table 94. Dataset: CS-CSFV(0.02), Label: Person, Bin: 1

Layer	MMD mean			
	f2f	f2b	b2f	b2b
res2_2	<b>0.028824</b>	57.38695	36.7982	4.730632
res3_3	<b>0.016363</b>	5.833781	4.020378	2.590734
res4_5	<b>0.010052</b>	4.37115	3.505711	1.842766
res5_2	<b>0.030776</b>	8.124074	4.471739	3.923804

Table 95. Dataset: CS-CSFV(0.02), Label: Person, Bin: 9

Layer	MMD mean			
	f2f	f2b	b2f	b2b
res2_2	0.069257	0.018532	0.080604	<b>0.011693</b>
res3_3	0.008585	0.008696	0.008337	<b>0.004168</b>
res4_5	0.017052	0.02381	0.03436	<b>0.007328</b>
res5_2	0.02084	0.01877	0.028686	<b>0.008349</b>

Table 96. Dataset: CS-CSFV(0.02), Label: Bicycle, Bin: 1

Layer	MMD mean			
	f2f	f2b	b2f	b2b
res2_2	<b>0.217501</b>	57.61874	30.51592	7.320393
res3_3	<b>0.036501</b>	5.757158	5.640691	3.037142
res4_5	<b>0.023576</b>	4.001144	3.928058	1.982261
res5_2	<b>0.032258</b>	6.698612	3.487616	3.109783

Table 97. Dataset: CS-CSFV(0.02), Label: Bicycle, Bin: 9

Table 98. **MMD for non-car labels between Cityscapes and Cityscapes foggy 0.02.**

Layer	MVD mean			
	f2f	f2b	b2f	b2b
res2_2	1.859608	1.942252	2.138036	1.954259
res3_3	1.940999	2.190022	2.181403	2.125913
res4_5	1.866465	2.523028	2.373373	1.999623
res5_2	1.952171	2.624203	2.58357	2.456547

Table 99. Dataset: CS-CSV, Label: car, Bin: 1

Layer	MVD mean			
	f2f	f2b	b2f	b2b
res2_2	2.15856	2.190183	2.074836	2.034821
res3_3	2.367371	2.450545	2.27529	2.351622
res4_5	2.653691	3.03468	2.548423	2.859754
res5_2	3.130844	3.103544	3.366491	2.490507

Table 101. Dataset: CS-CSFV(0.01), Label: car, Bin: 1

Layer	MVD mean			
	f2f	f2b	b2f	b2b
es2_2	2.632104	2.661585	2.611281	2.612724
res3_3	2.485537	2.654727	2.224296	2.383249
res4_5	2.727908	3.146172	2.648995	2.978889
res5_2	2.966326	2.762088	3.055754	2.363898

Table 103. Dataset: CS-CSFV(0.02), Label: car, Bin: 1

Layer	MVD mean			
	f2f	f2b	b2f	b2b
res2_2	2.026214	1.97831	1.888203	1.8471
res3_3	1.879495	1.93231	2.005498	2.038926
res4_5	1.913738	1.942838	1.984738	2.007567
res5_2	2.088159	2.181628	2.237213	2.166204

Table 105. Dataset: CS-CARLA, Label: car, Bin: 1

Layer	MVD mean			
	f2f	f2b	b2f	b2b
res2_2	2.841894	2.900838	2.803968	2.854438
res3_3	3.040334	3.084505	2.79029	2.832282
res4_5	3.783452	3.467538	3.489805	3.159332
res5_2	3.562711	3.679759	3.615911	3.658813

Table 107. Dataset: CS-KS, Label: car, Bin: 1

Layer	MVD mean			
	f2f	f2b	b2f	b2b
res2_2	3.12196	3.124747	2.963401	2.971671
res3_3	2.71388	3.25211	2.601027	3.130624
res4_5	3.036489	3.443498	3.249636	3.613924
res5_2	3.365768	3.809035	3.905568	3.924799

Table 109. Dataset: CS-VK, Label: car, Bin: 1

Layer	MVD mean			
	f2f	f2b	b2f	b2b
res2_2	1.779225	2.391159	2.297817	2.017024
res3_3	2.069057	2.331817	2.625383	2.074096
res4_5	2.216897	2.763882	2.686462	2.42473
res5_2	2.212517	2.989791	2.954901	2.349637

Table 100. Dataset: CS-CSV, Label: car, Bin: 9

Layer	MVD mean			
	f2f	f2b	b2f	b2b
res2_2	2.494561	2.705416	2.8487	2.833095
res3_3	2.941381	2.967594	2.98456	2.996845
res4_5	3.145998	3.242336	2.898611	3.033752
res5_2	3.00029	3.085102	2.819701	2.865075

Table 102. Dataset: CS-CSFV(0.01), Label: car, Bin: 9

Layer	MVD mean			
	f2f	f2b	b2f	b2b
res2_2	2.766881	2.750633	2.912888	2.896767
res3_3	3.341002	3.230562	3.30493	3.205884
res4_5	3.158577	2.907029	3.130123	2.861851
res5_2	2.849365	2.883997	3.069528	3.121087

Table 104. Dataset: CS-CSFV(0.02), Label: car, Bin: 9

Layer	MVD mean			
	f2f	f2b	b2f	b2b
res2_2	1.782944	1.760427	1.861272	1.814212
res3_3	2.124609	2.195519	2.001021	2.080952
res4_5	2.143426	2.191577	1.978246	2.034965
res5_2	2.253145	2.219374	2.140828	2.091627

Table 106. Dataset: CS-CARLA, Label: car, Bin: 9

Layer	MVD mean			
	f2f	f2b	b2f	b2b
res2_2	3.141126	3.132896	3.053914	3.047343
res3_3	3.047711	3.138398	3.051047	3.146816
res4_5	3.405747	3.560306	3.312046	3.446573
res5_2	3.899754	3.783358	3.548343	3.419083

Table 108. Dataset: CS-KS, Label: car, Bin: 9

Layer	MVD mean			
	f2f	f2b	b2f	b2b
res2_2	3.134635	3.170769	3.511757	3.559752
res3_3	3.487185	3.640578	3.473435	3.643497
res4_5	3.454606	3.59765	3.163142	3.313437
res5_2	4.074189	3.814336	3.960457	3.723863

Table 110. Dataset: CS-VK, Label: car, Bin: 9

Table 111. MVD for the “Car” label .

Layer	MVD mean			
	f2f	f2b	b2f	b2b
res2_2	3.0403	3.257182	2.966835	3.200019
res3_3	3.487007	3.659496	3.198339	3.365955
res4_5	3.461587	3.589998	3.44037	3.523223
res5_2	3.668298	4.402051	3.661002	3.658707

Table 112. Dataset: KS-VK, Label: car, Bin: 1

Layer	MVD mean			
	f2f	f2b	b2f	b2b
res2_2	3.507414	3.514249	3.520947	3.533183
res3_3	3.522346	3.425131	3.500015	3.398116
res4_5	3.134606	3.721532	3.046122	3.623823
res5_2	3.868461	3.875345	3.962465	3.89308

Table 114. Dataset: CARLA-KS, Label: car, Bin: 1

Layer	MVD mean			
	f2f	f2b	b2f	b2b
res2_2	3.454729	3.781761	3.236546	3.556824
res3_3	3.621748	3.465997	3.199012	3.197285
res4_5	3.920673	3.812993	3.799213	3.693012
res5_2	4.192141	4.380007	3.829396	3.916404

Table 116. Dataset: CARLA-VK, Label: car, Bin: 1

Layer	MVD mean			
	f2f	f2b	b2f	b2b
res2_2	3.461544	3.649635	3.48551	3.650191
res3_3	3.389041	3.510327	3.432087	3.544008
res4_5	3.686021	3.632678	3.58373	3.671303
res5_2	3.698969	3.541205	3.814748	3.669518

Table 113. Dataset: KS-VK, Label: car, Bin: 9

Layer	MVD mean			
	f2f	f2b	b2f	b2b
res2_2	3.555406	3.300934	3.764535	3.515109
res3_3	3.664688	4.024245	3.658104	4.019631
res4_5	3.814338	3.796126	3.644634	3.64071
res5_2	3.8482	3.789979	3.928309	3.856924

Table 115. Dataset: CARLA-KS, Label: car, Bin: 9

Layer	MVD mean			
	f2f	f2b	b2f	b2b
res2_2	3.539233	3.843425	3.823467	4.128982
res3_3	3.808752	3.700677	3.808876	3.707256
res4_5	3.67969	3.95423	3.824463	4.085565
res5_2	3.787977	3.547388	3.901427	3.631283

Table 117. Dataset: CARLA-VK, Label: car, Bin: 9

Layer	MVD mean			
	f2f	f2b	b2f	b2b
res2_2	1.90107	2.017769	2.194028	1.817359
res3_3	1.963989	2.232561	2.4385	1.997064
res4_5	2.151321	2.526028	2.610607	2.247859
res5_2	2.091379	2.417881	2.283058	1.922043

Table 119. Dataset: CS-CSV, Label: Person, Bin: 1

Layer	MVD mean			
	f2f	f2b	b2f	b2b
res2_2	2.196452	2.178004	2.406967	2.082812
res3_3	1.893176	2.151503	2.024893	1.804592
res4_5	2.522766	2.745728	2.502865	2.455195
res5_2	2.345473	2.538796	2.222222	2.148248

Table 121. Dataset: CS-CSV, Label: Bicycle, Bin: 1

Layer	MVD mean			
	f2f	f2b	b2f	b2b
res2_2	1.91087	2.360122	2.232521	2.203551
res3_3	2.466574	2.746785	2.682585	2.485354
res4_5	2.488866	2.824601	2.959751	2.64936
res5_2	2.159035	2.543545	2.623156	2.330251

Table 123. Dataset: CS-CSV, Label: Rider, Bin: 1

Layer	MVD mean			
	f2f	f2b	b2f	b2b
res2_2	2.186056	2.693957	2.535597	2.215452
res3_3	1.895071	2.485922	2.530775	2.090305
res4_5	2.130127	2.679075	2.804662	2.191113
res5_2	1.789653	2.642629	2.288085	2.042702

Table 122. Dataset: CS-CSV, Label: Bicycle, Bin: 9

Layer	MVD mean			
	f2f	f2b	b2f	b2b
res2_2	2.271712	2.855109	2.647117	2.247345
res3_3	2.502144	3.067891	3.095785	2.708157
res4_5	2.64991	2.99534	3.198842	2.948378
res5_2	2.650348	3.1807	3.208098	2.338952

Table 124. Dataset: CS-CSV, Label: Rider, Bin: 9

Table 125. MVD for non-car labels between Cityscapes and Cityscapes validation.

Layer	MVD mean			
	f2f	f2b	b2f	b2b
res2_2	2.533566	2.73321	2.390703	2.426263
res3_3	2.696752	2.698772	2.712317	2.722163
res4_5	2.622294	3.097147	2.268134	2.748999
res5_2	2.933978	2.900677	2.922567	2.68859

Table 126. Dataset: CS-CSFV(0.01), Label: Person, Bin: 1

Layer	MVD mean			
	f2f	f2b	b2f	b2b
res2_2	3.098768	2.959295	3.241907	3.012505
res3_3	2.878011	2.760813	2.803681	2.695595
res4_5	2.756639	2.868533	2.652746	2.728764
res5_2	2.983025	3.306338	3.109515	3.413838

Table 127. Dataset: CS-CSFV(0.01), Label: Person, Bin: 9

Layer	MVD mean			
	f2f	f2b	b2f	b2b
res2_2	2.727781	2.83114	2.52992	2.583405
res3_3	2.818721	2.756196	2.70085	2.6399
res4_5	2.5642	2.581732	2.259545	2.277248
res5_2	2.791654	2.624161	2.699361	2.453502

Table 128. Dataset: CS-CSFV(0.01), Label: Bicycle, Bin: 1

Layer	MVD mean			
	f2f	f2b	b2f	b2b
res2_2	2.882556	3.179741	3.197818	3.255915
res3_3	3.502498	3.495217	3.572915	3.527167
res4_5	3.392894	3.32361	3.329141	3.244925
res5_2	3.50345	3.782023	3.214624	3.504451

Table 129. Dataset: CS-CSFV(0.01), Label: Bicycle, Bin: 9

Layer	MVD mean			
	f2f	f2b	b2f	b2b
res2_2	3.00926	3.040015	3.064935	3.075195
res3_3	3.429043	3.47356	3.312546	3.365296
res4_5	3.005324	2.852956	3.2668	3.05431
res5_2	3.071791	3.246479	2.947047	3.006498

Table 130. Dataset: CS-CSFV(0.01), Label: Rider, Bin: 1

Layer	MVD mean			
	f2f	f2b	b2f	b2b
res2_2	3.3968	3.370571	3.59658	3.52491
res3_3	3.799668	4.047476	3.664054	3.885016
res4_5	3.304043	3.338629	3.423527	3.376016
res5_2	3.6104	3.774592	3.534143	3.568252

Table 131. Dataset: CS-CSFV(0.01), Label: Rider, Bin: 9

Table 132. **MVD for non-car labels between Cityscapes and Cityscapes foggy 0.01.**

Layer	MVD mean			
	f2f	f2b	b2f	b2b
res2_2	2.533566	2.73321	2.390703	2.426263
res3_3	2.696752	2.698772	2.712317	2.722163
res4_5	2.622294	3.097147	2.268134	2.748999
res5_2	2.933978	2.900677	2.922567	2.68859

Table 133. Dataset: CS-CSFV(0.02), Label: Person, Bin: 1

Layer	MVD mean			
	f2f	f2b	b2f	b2b
res2_2	2.837323	2.867575	2.98062	2.93537
res3_3	2.714125	2.893832	2.753119	2.937033
res4_5	3.117603	2.891447	2.947588	2.694934
res5_2	2.615213	2.597655	2.865389	2.793837

Table 134. Dataset: CS-CSFV(0.02), Label: Person, Bin: 9

Layer	MVD mean			
	f2f	f2b	b2f	b2b
res2_2	2.98205	3.045294	2.924633	2.981337
res3_3	3.266259	3.12661	3.140121	3.005347
res4_5	3.256986	3.103132	2.919774	2.744937
res5_2	2.599247	2.876435	2.602573	2.849469

Table 135. Dataset: CS-CSFV(0.02), Label: Bicycle, Bin: 1

Layer	MVD mean			
	f2f	f2b	b2f	b2b
res2_2	3.746639	3.715122	3.566788	3.546999
res3_3	3.404148	3.572299	3.375922	3.587521
res4_5	3.656142	3.349588	3.527766	3.152176
res5_2	3.141516	3.470738	3.360997	3.626434

Table 136. Dataset: CS-CSFV(0.02), Label: Bicycle, Bin: 9

Table 137. **MVD for non-car labels between Cityscapes and Cityscapes foggy 0.02.**

### 13. MMD Plot

This section presents the MMD plot, highlighting the discrepancy between bins 1 and 9. “small”, “medium”, and “large” means objects size.

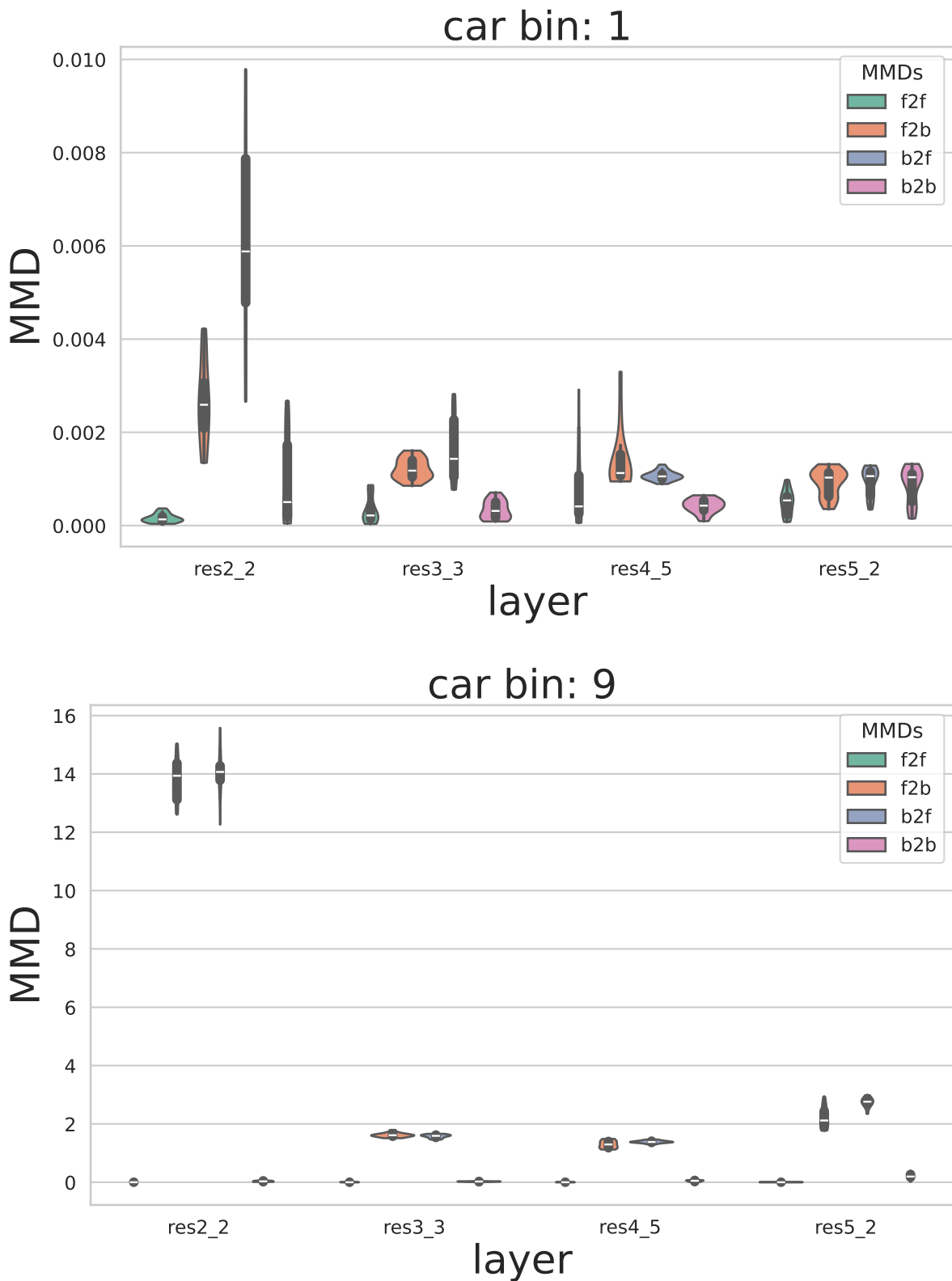


Figure 23. CS-CSV small MMD plots. Label: Car.

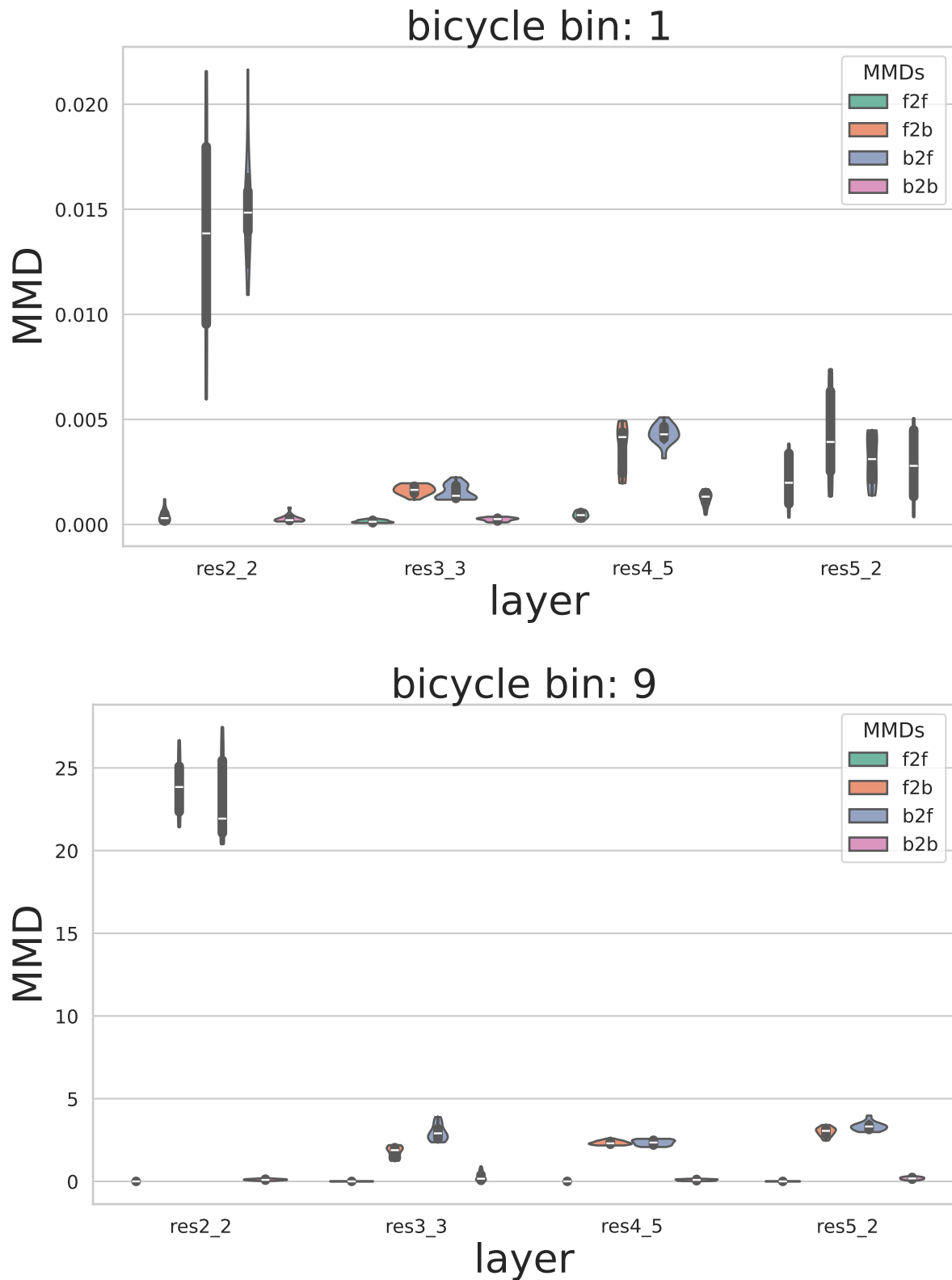


Figure 24. CS-CSV small MMD plots. Label: Bicycle.

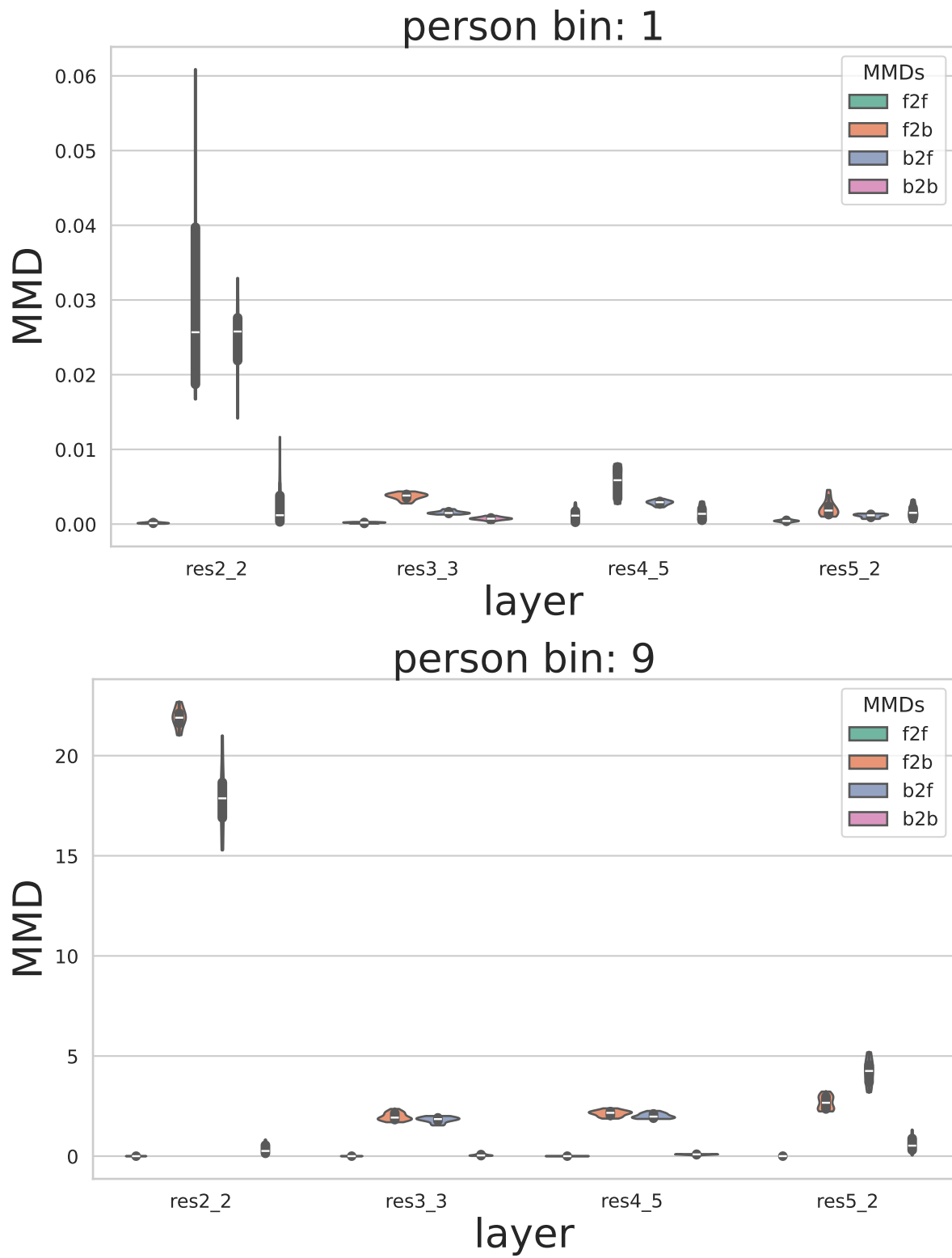


Figure 25. CS-CSV small MMD plots. Label: Person.

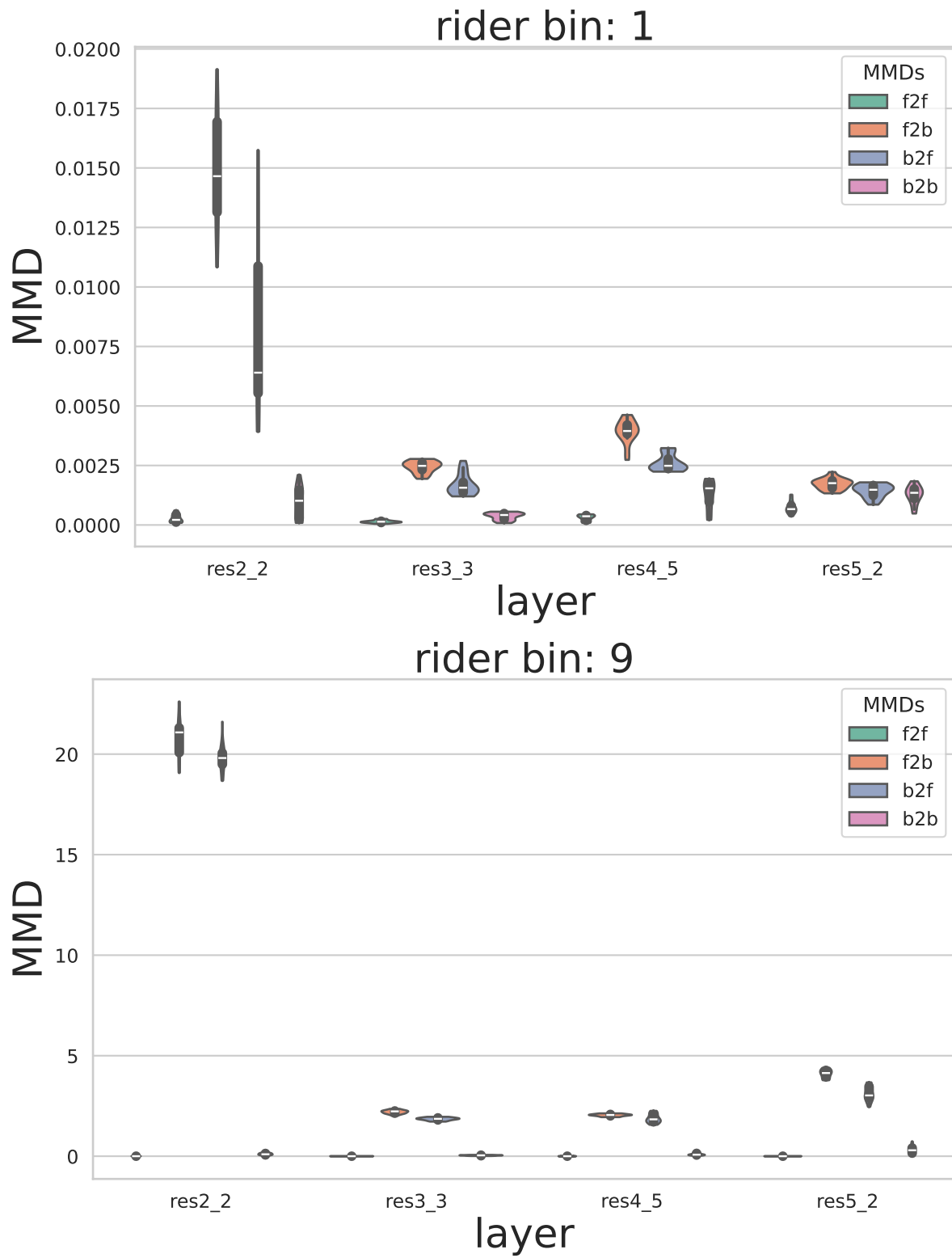


Figure 26. CS-CSV small MMD plots. Label: Rider.

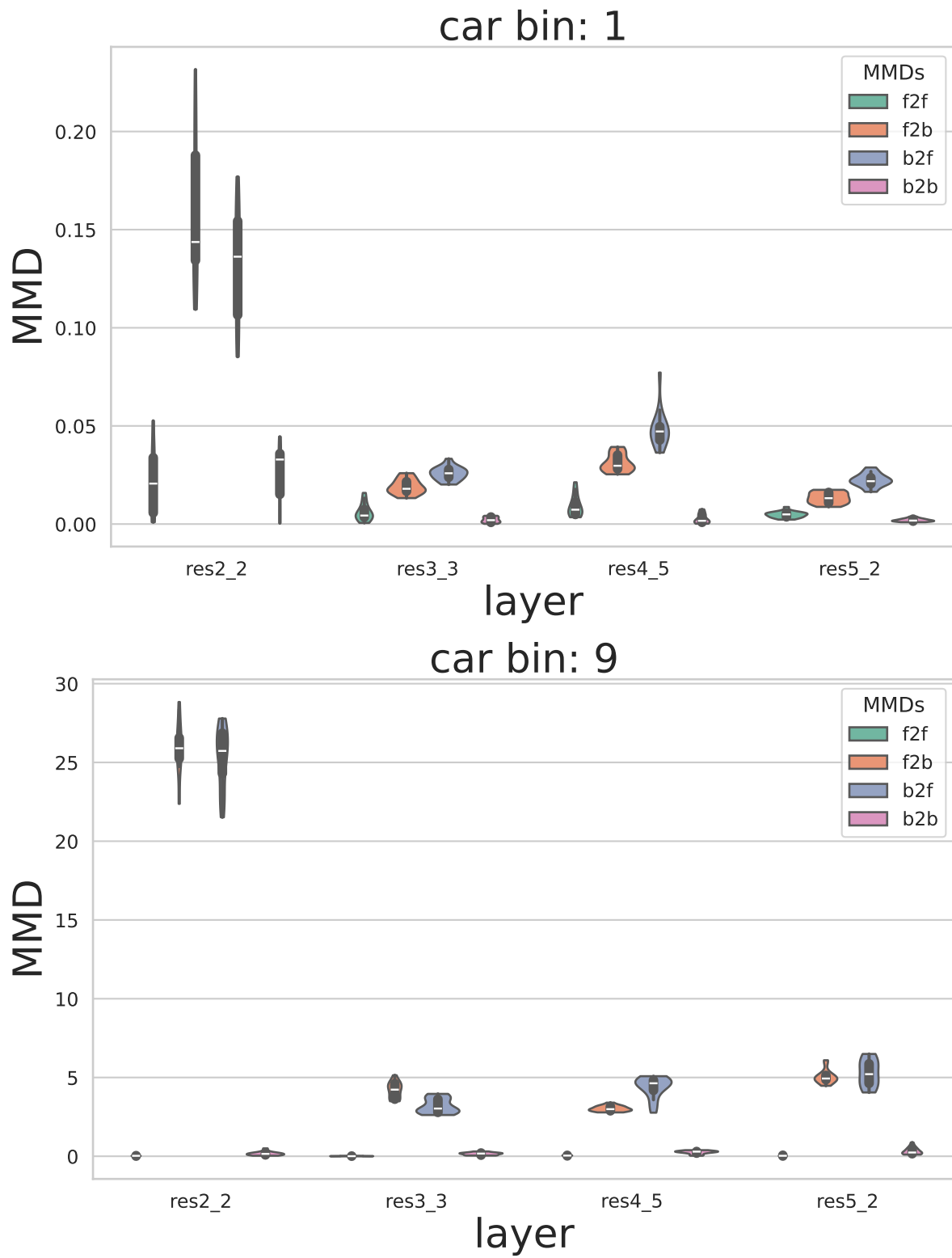


Figure 27. CS-CSV medium MMD plots. Label: Car.

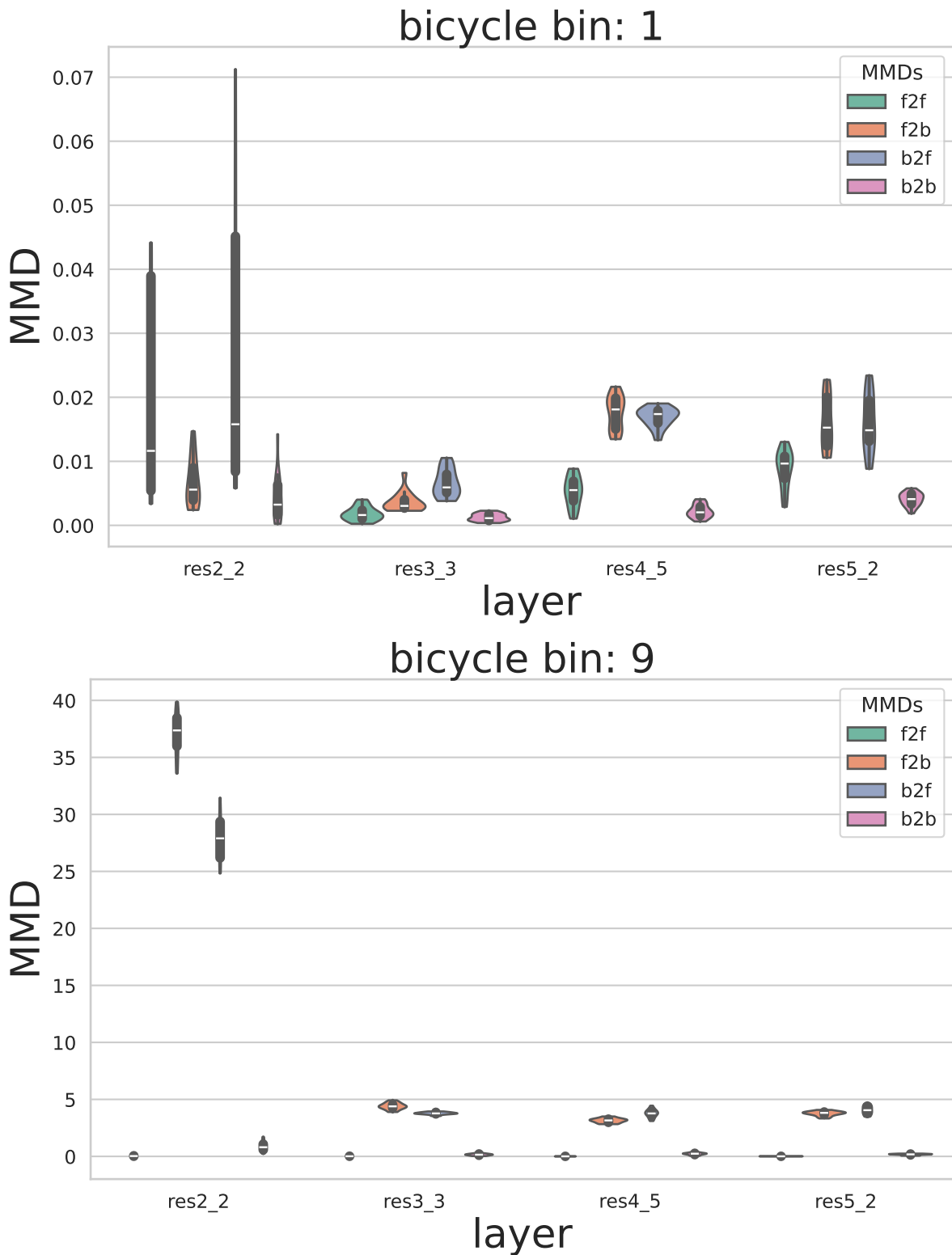


Figure 28. CS-CSV medium MMD plots. Label: Bicycle.

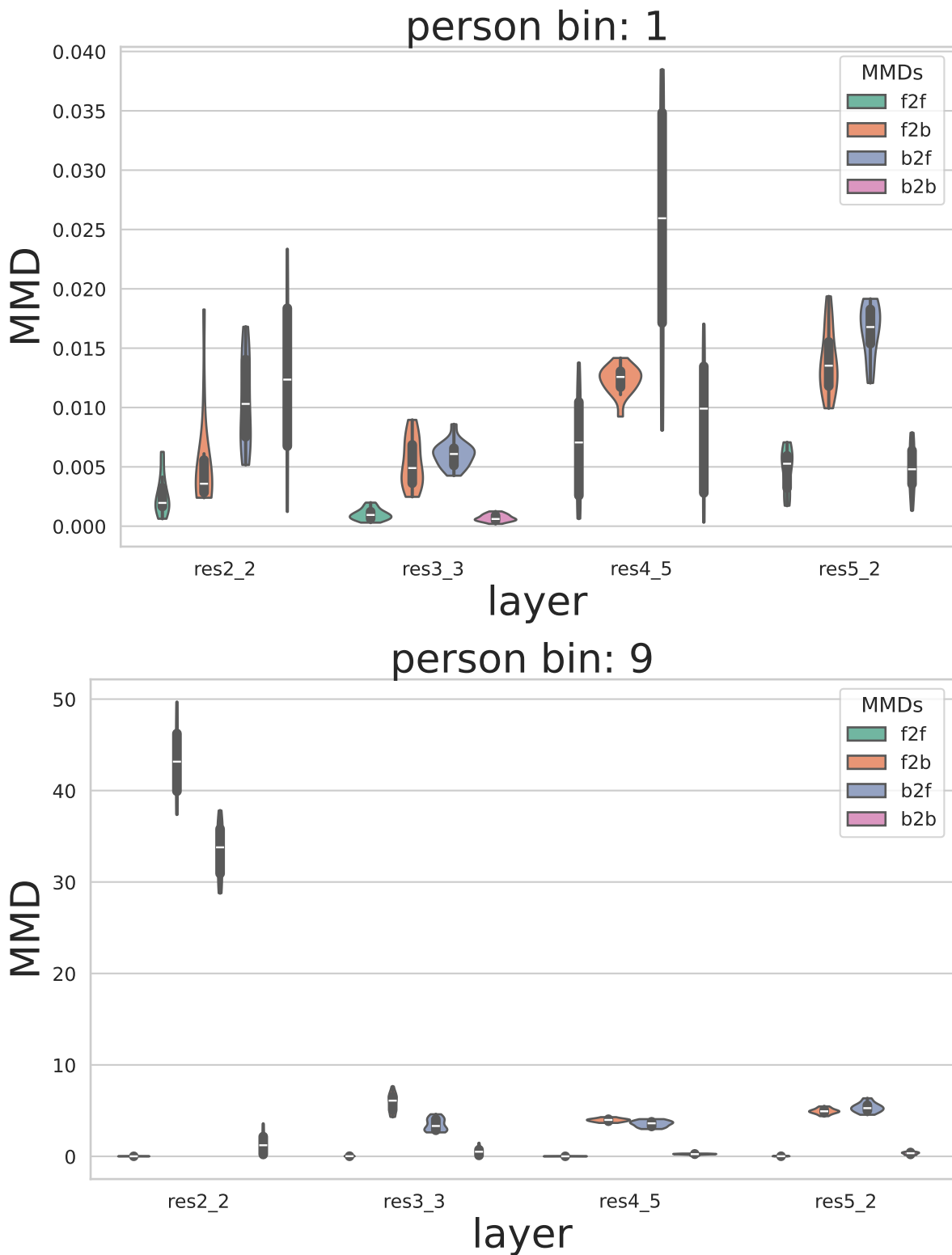


Figure 29. CS-CSV medium MMD plots. Label: Person.

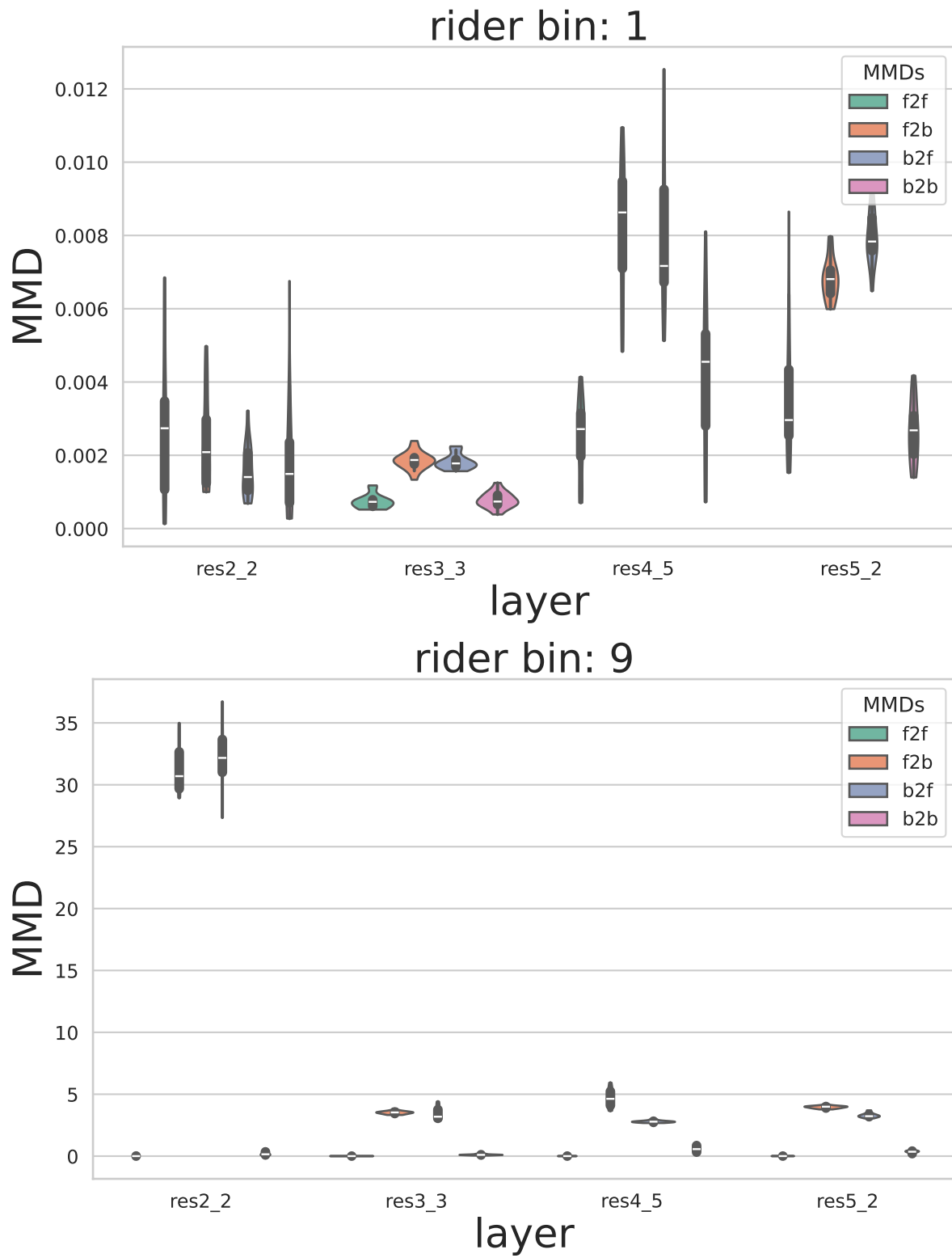


Figure 30. CS-CSV medium MMD plots. Label: Rider.

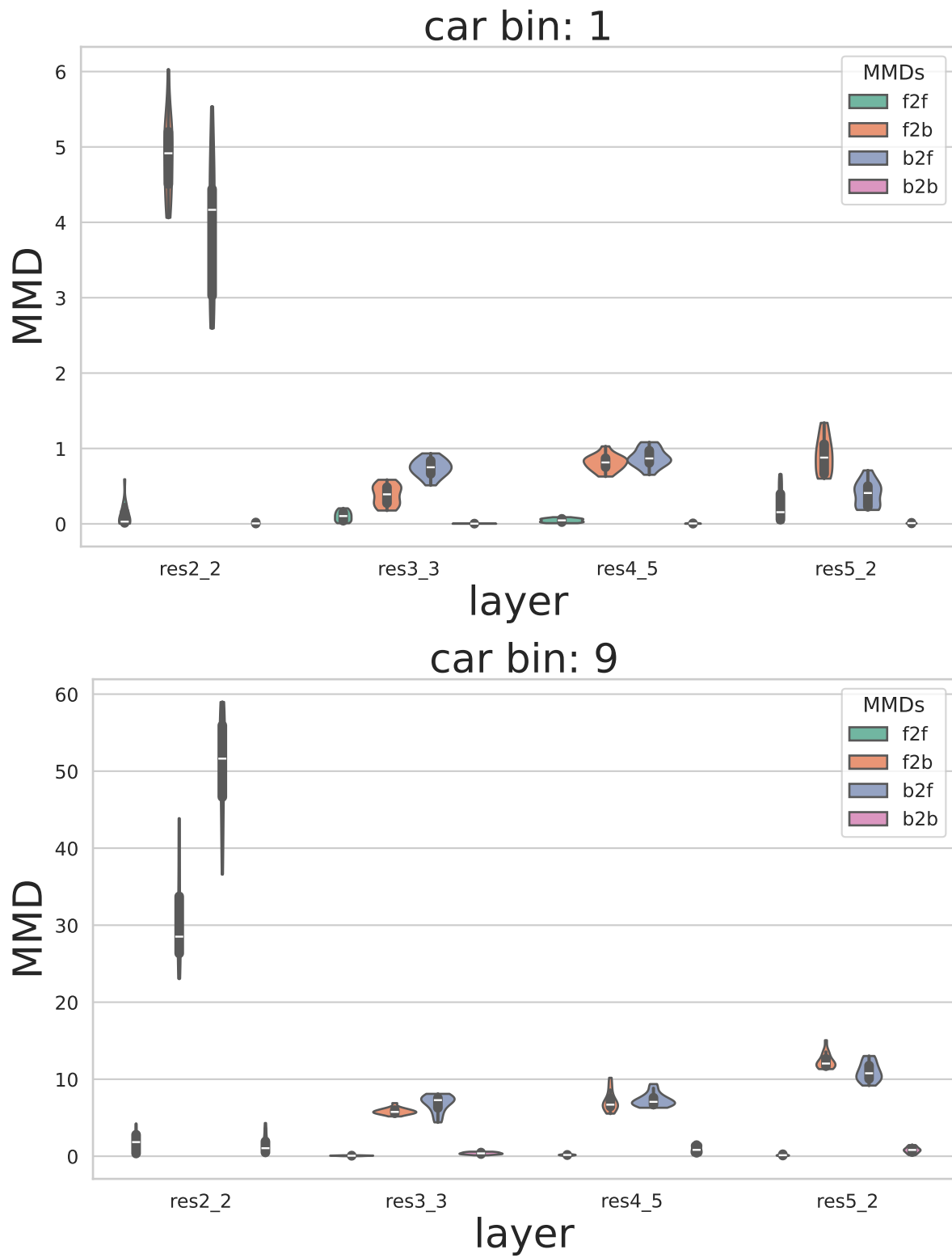


Figure 31. CS-CSV large MMD plots. Label: Car.

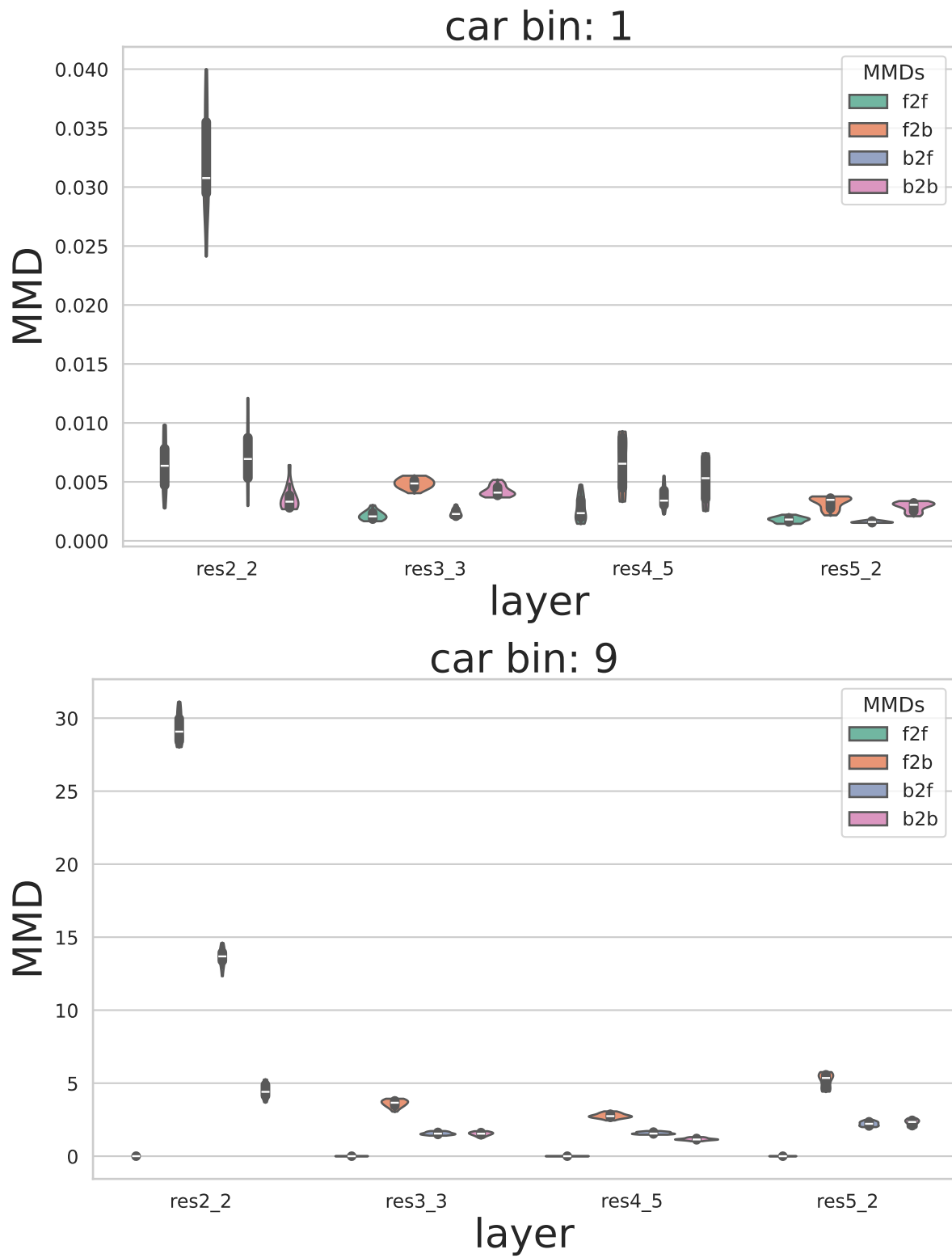


Figure 32. CS-CSFV(0.01) small MMD plots. Label: Car.

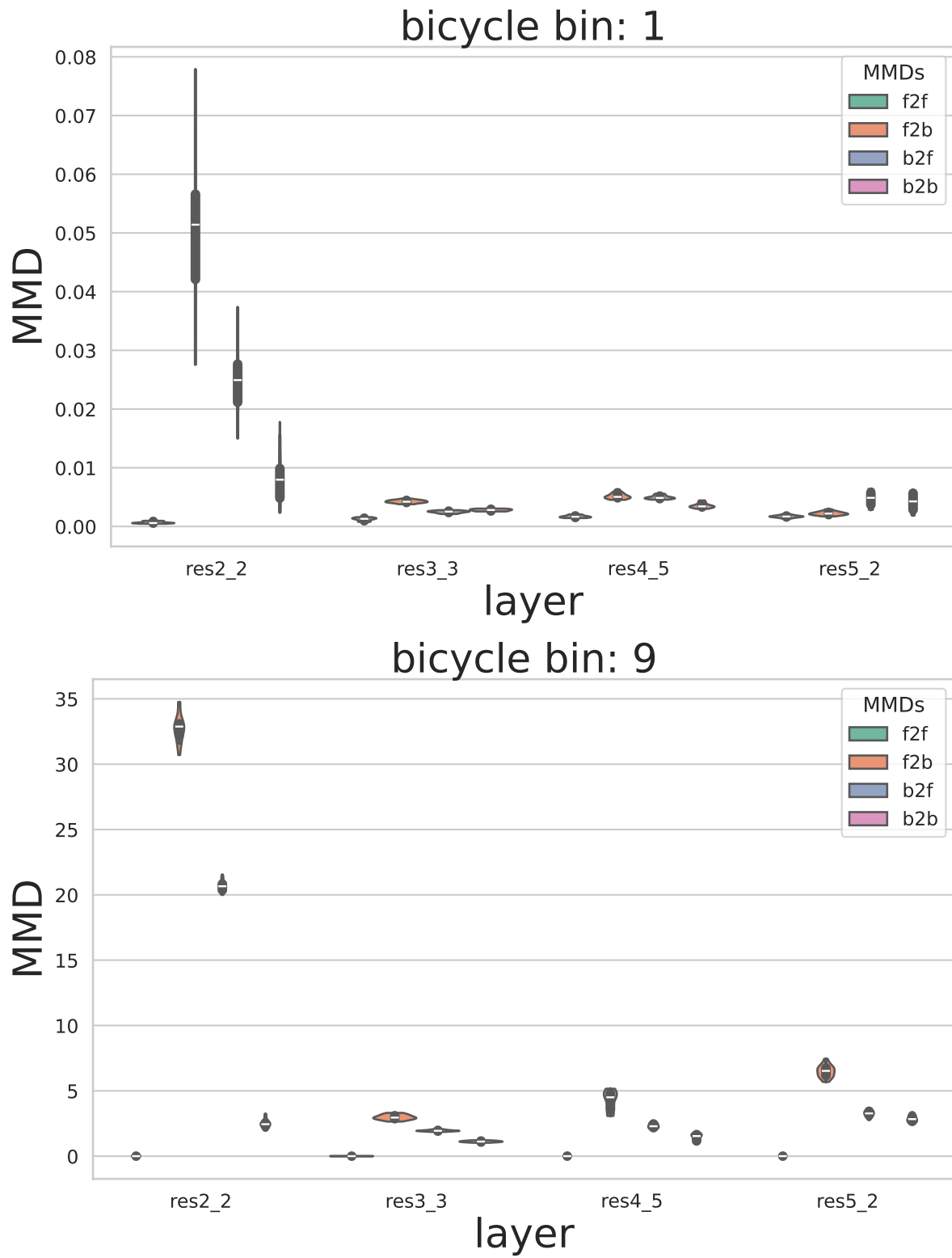


Figure 33. CS-CSFV(0.01) small MMD plots. Label: Bicycle.

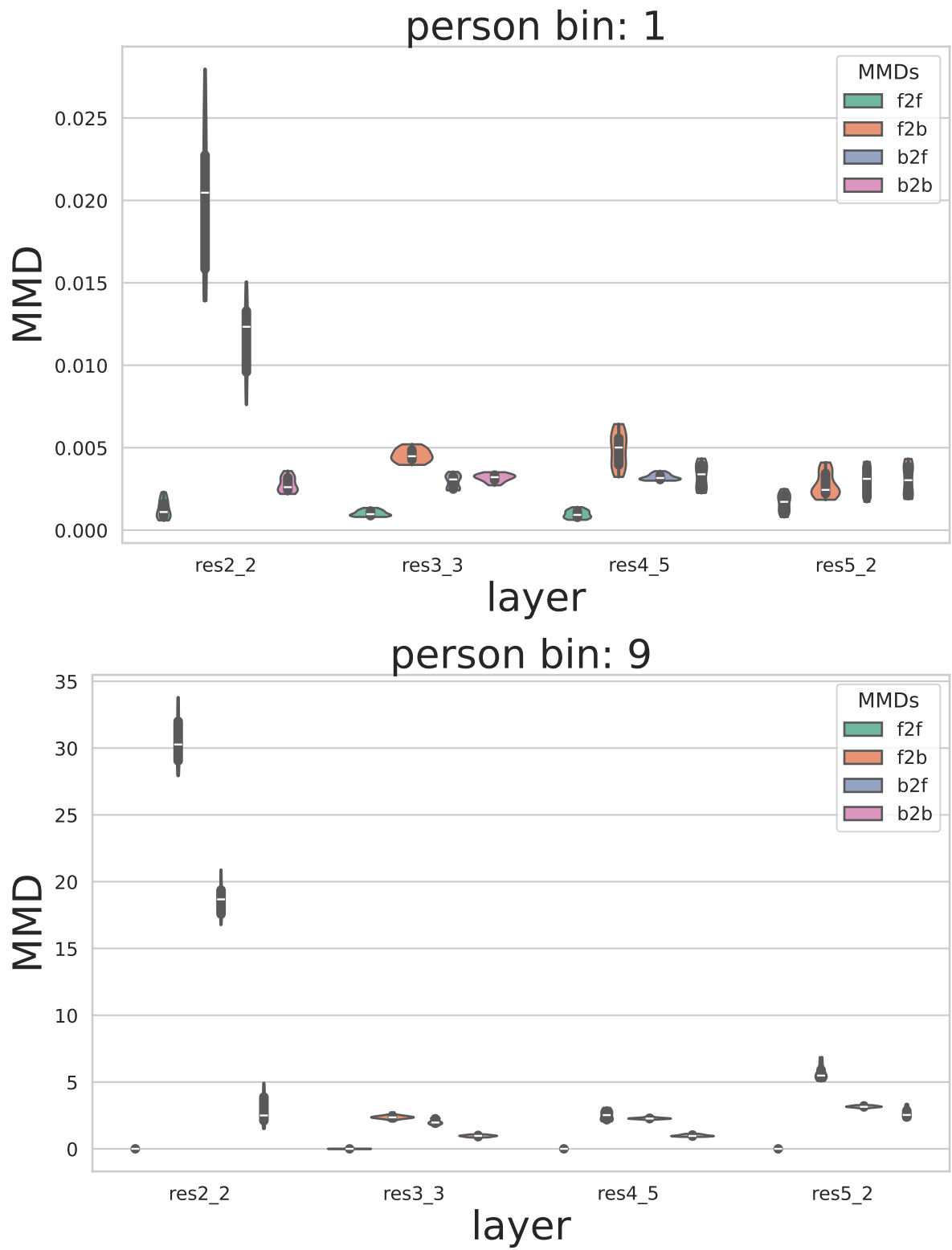


Figure 34. CS-CSFV(0.01) small MMD plots. Label: Person.

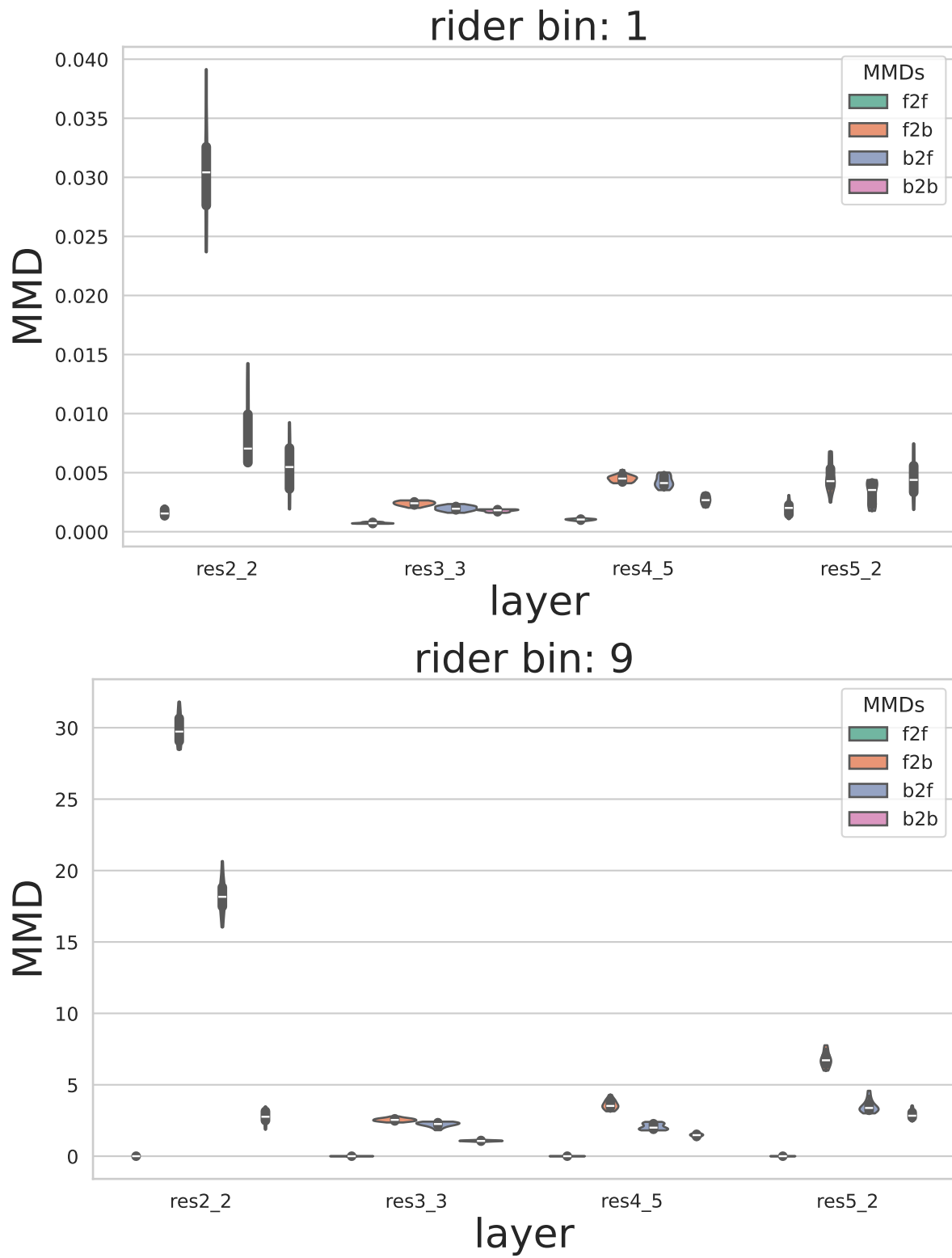


Figure 35. CS-CSFV(0.01) small MMD plots. Label: Rider.

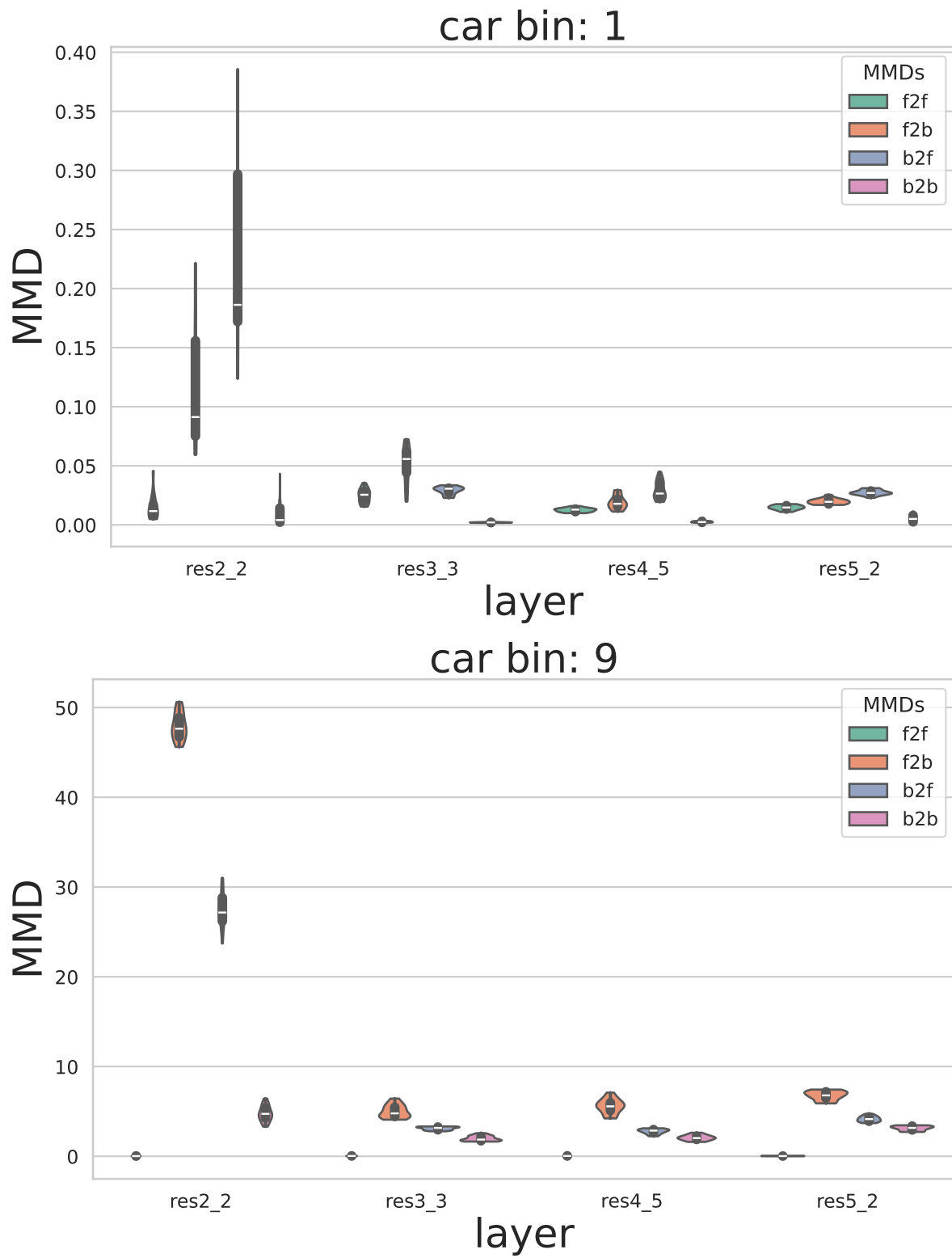


Figure 36. CS-CSFV(0.01) small MMD plots. Label: Car.

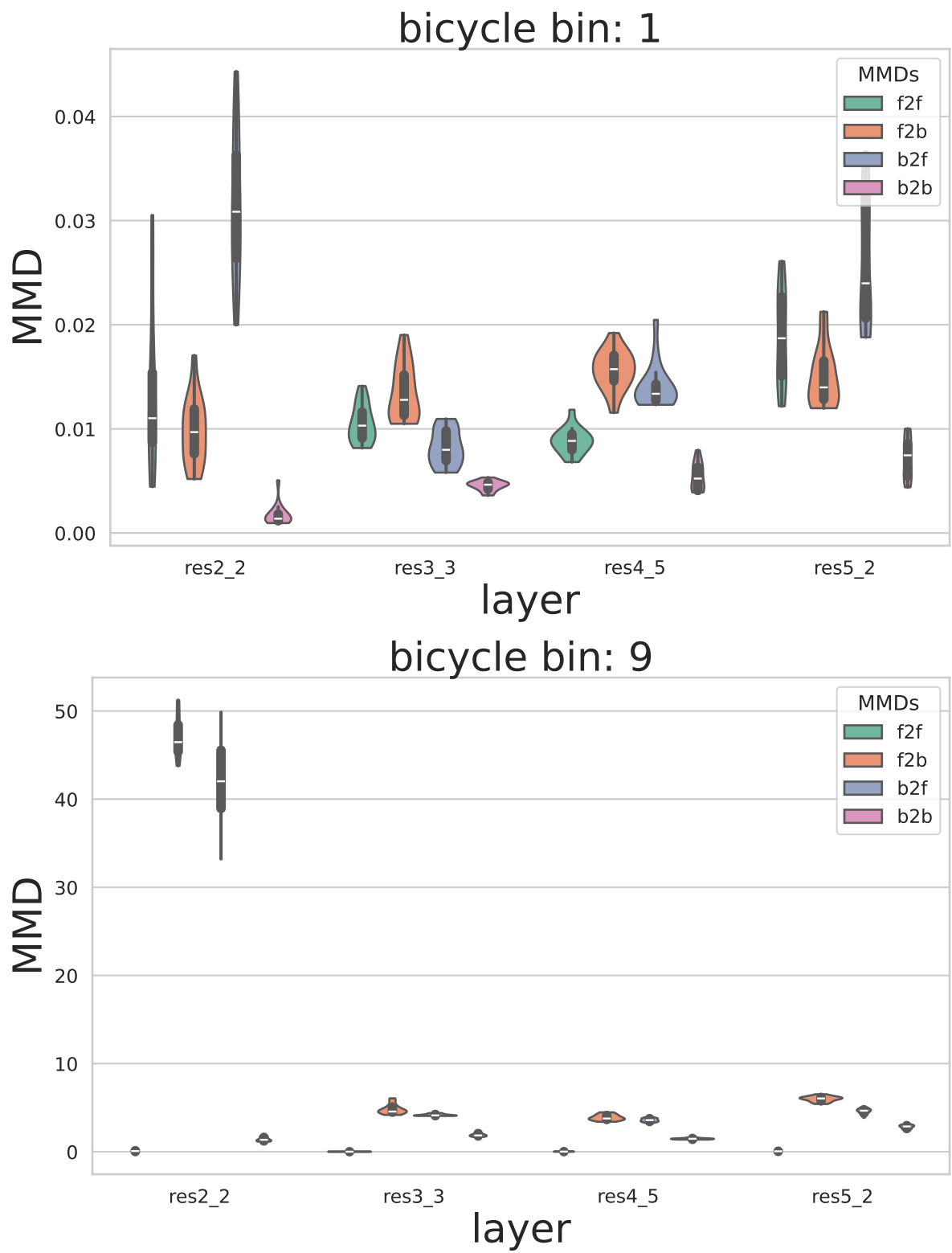


Figure 37. CS-CSFV(0.01) medium MMD plots. Label: Bicycle.

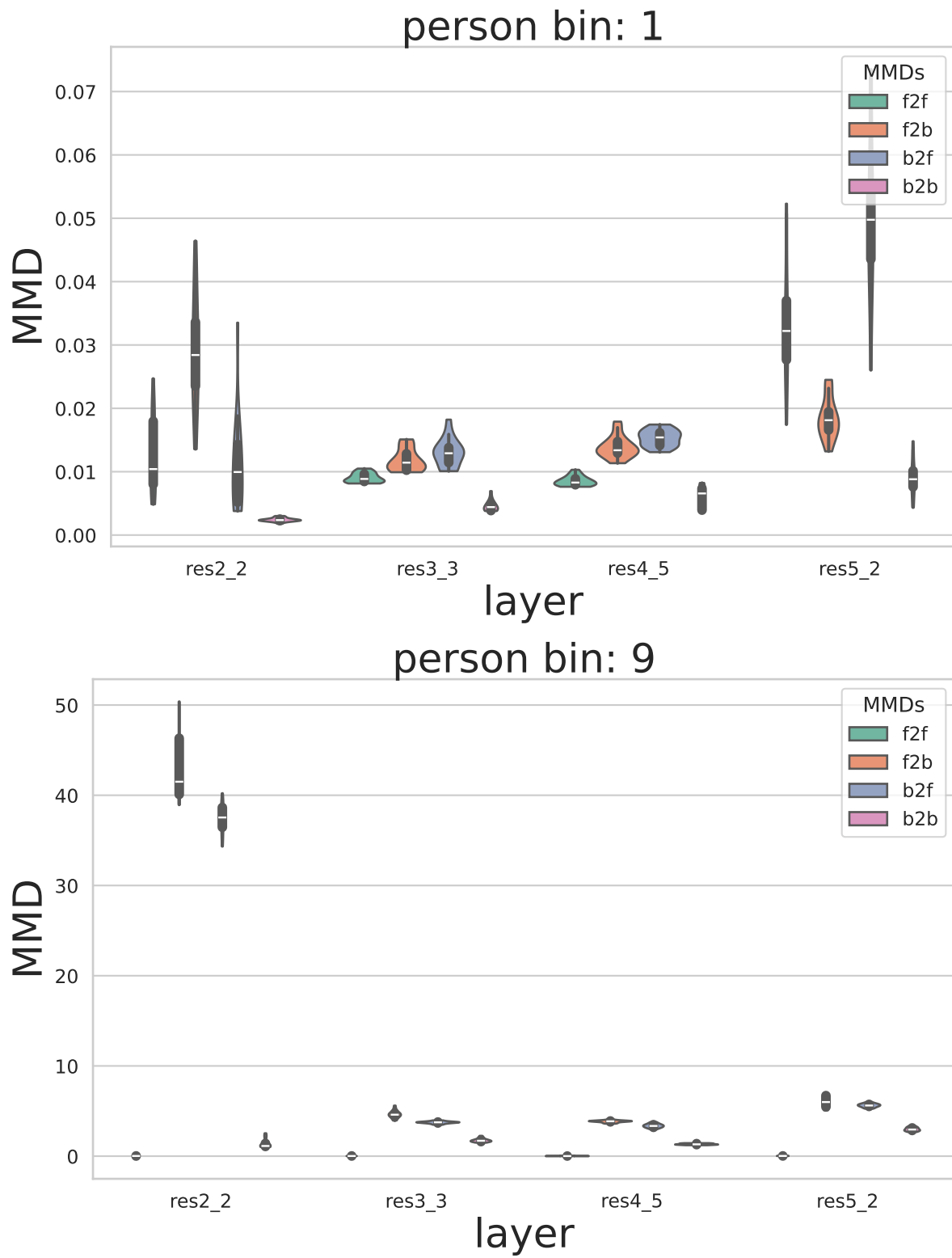
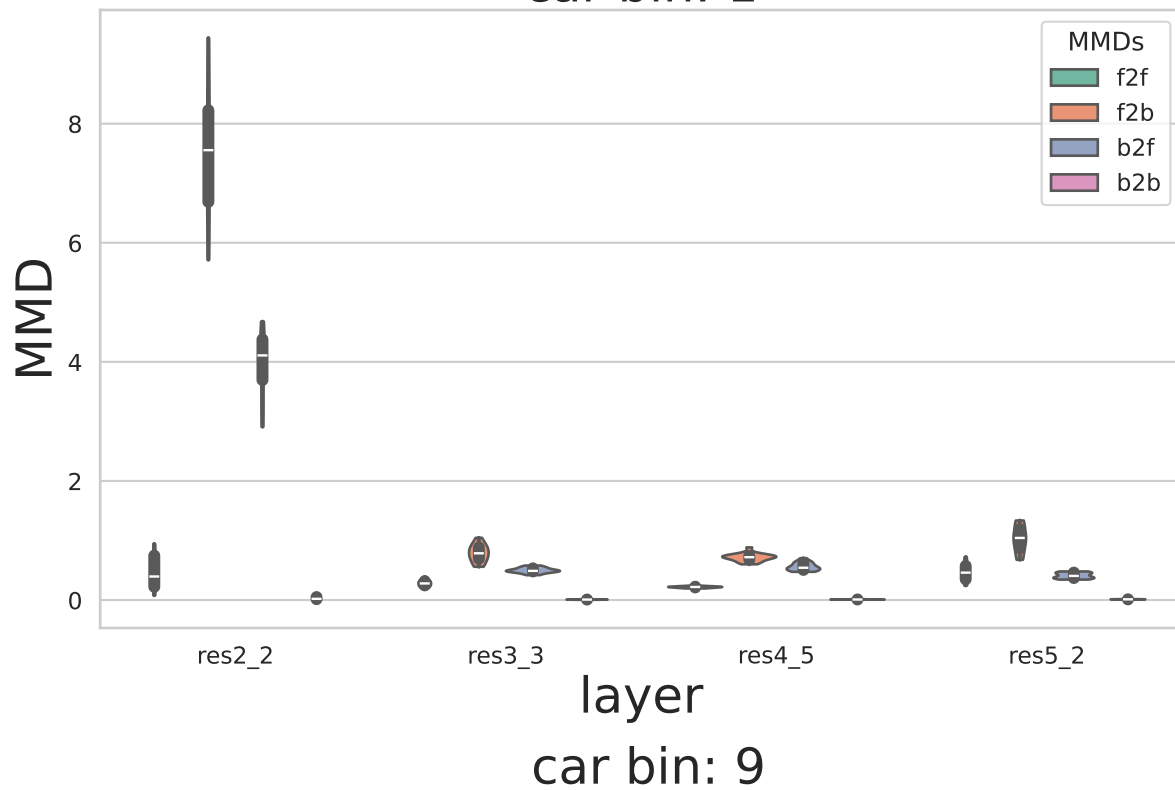


Figure 38. CS-CSFV(0.01) medium MMD plots. Label: Person.

car bin: 1



layer  
car bin: 9

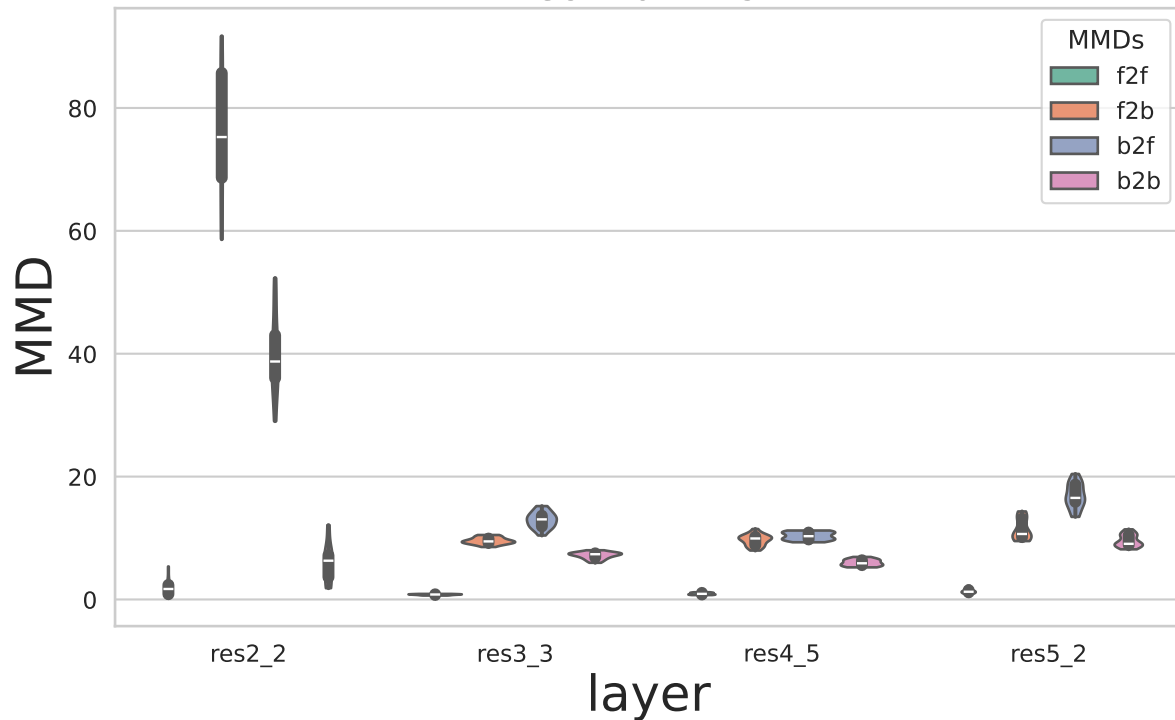


Figure 39. CS-CSFV(0.01) large MMD plots. Label: Car.

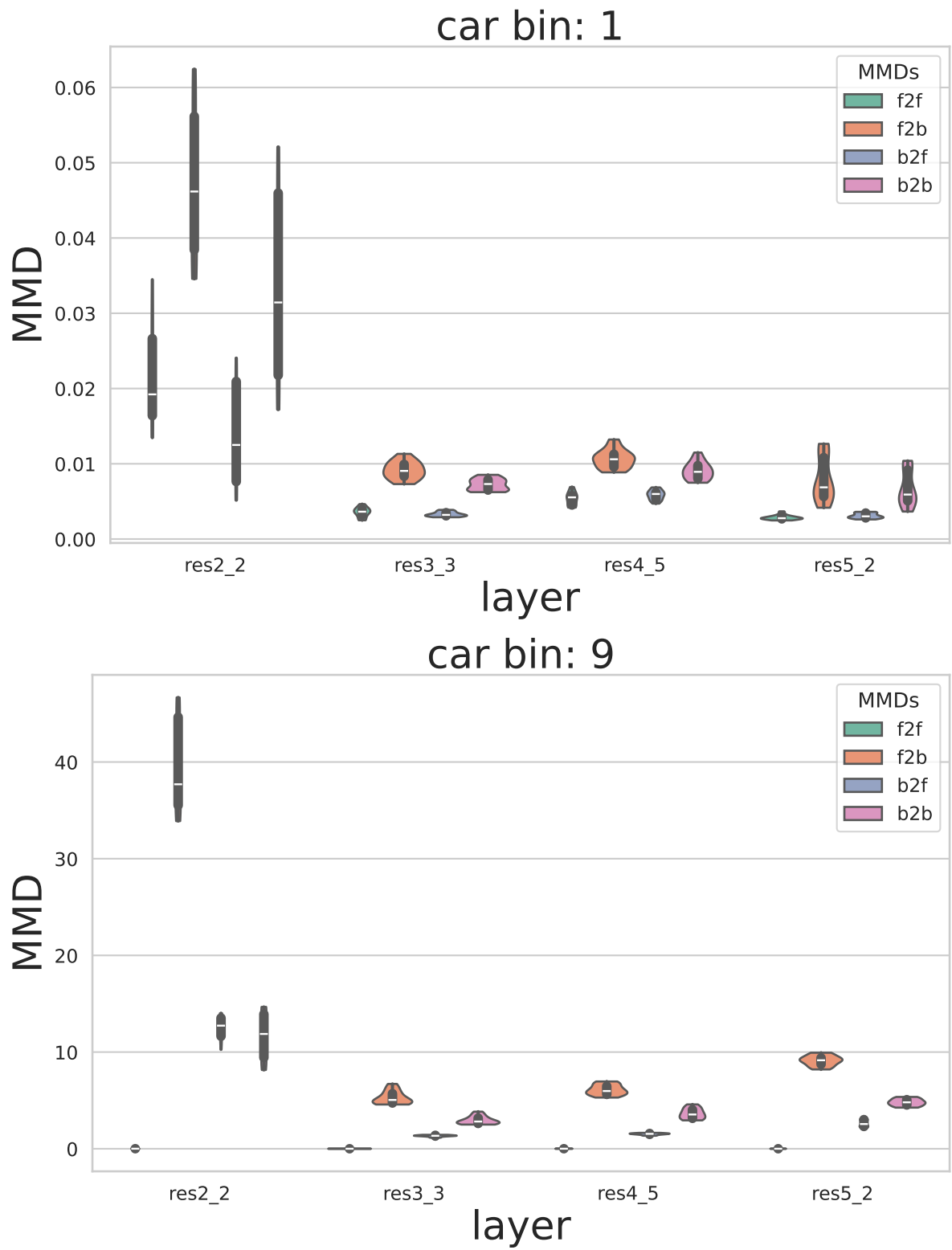


Figure 40. CS-CSFV(0.02) small MMD plots. Label: Car.

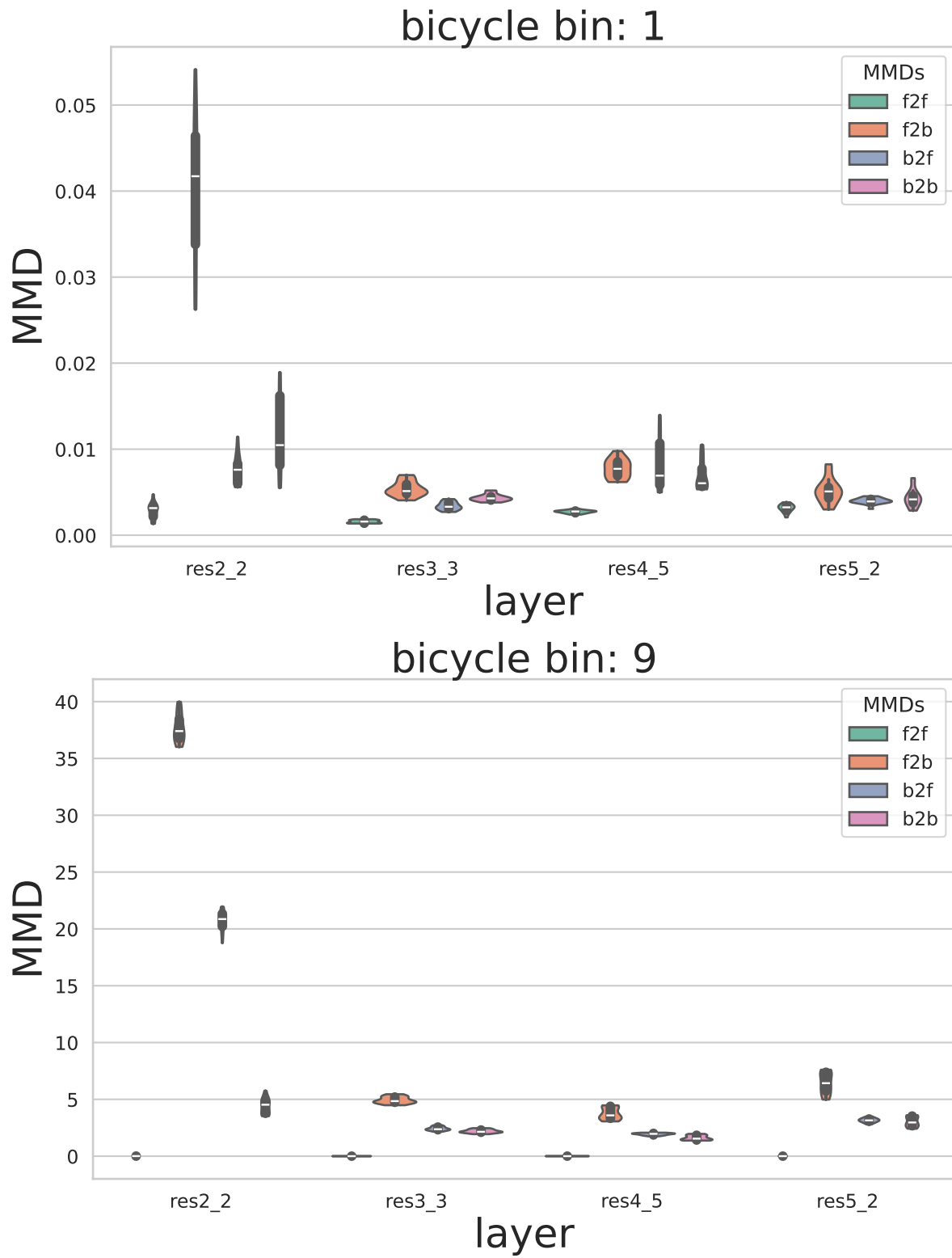


Figure 41. CS-CSFV(0.02) small MMD plots. Label: Bicycle.

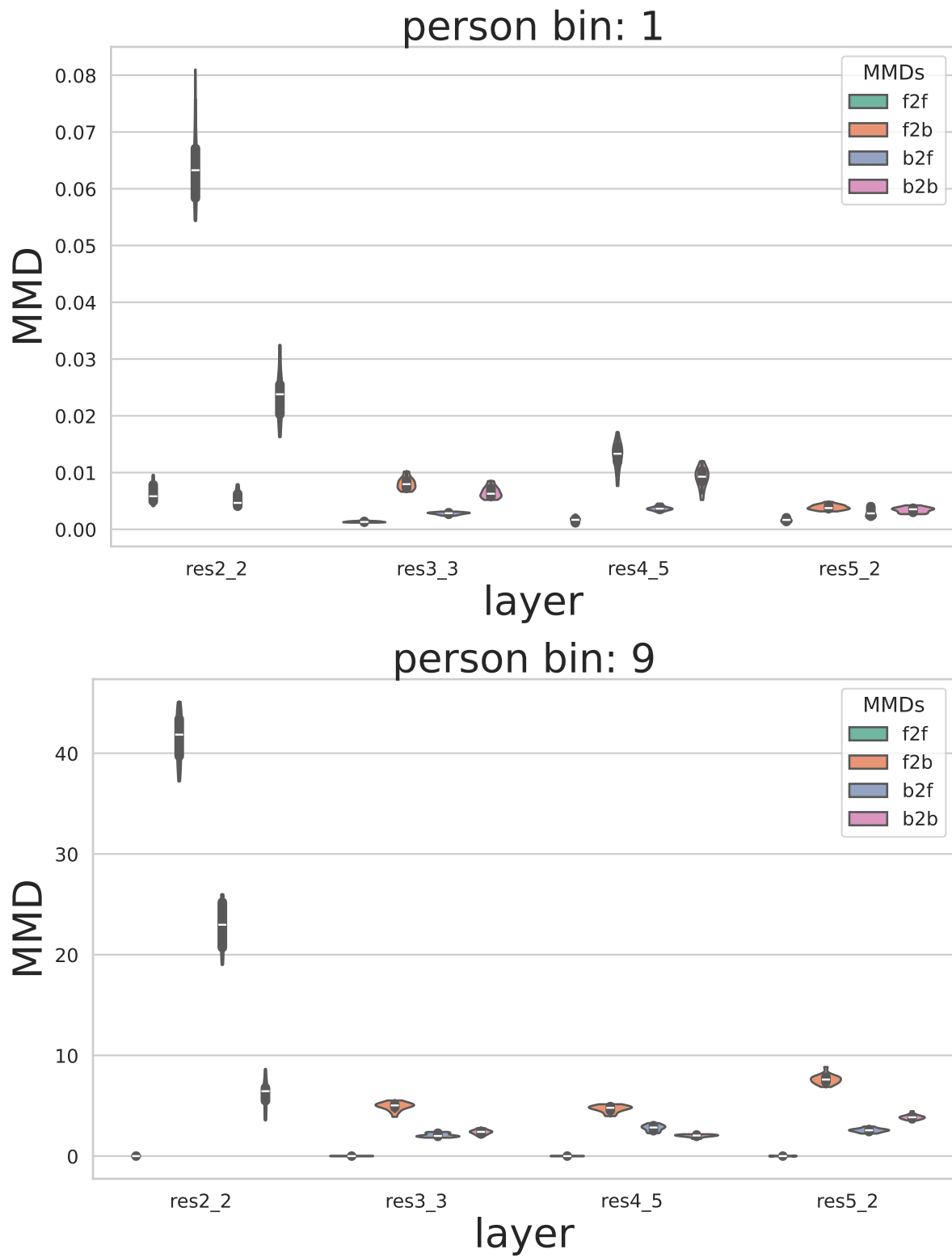


Figure 42. CS-CSFV(0.02) small MMD plots. Label: Person.

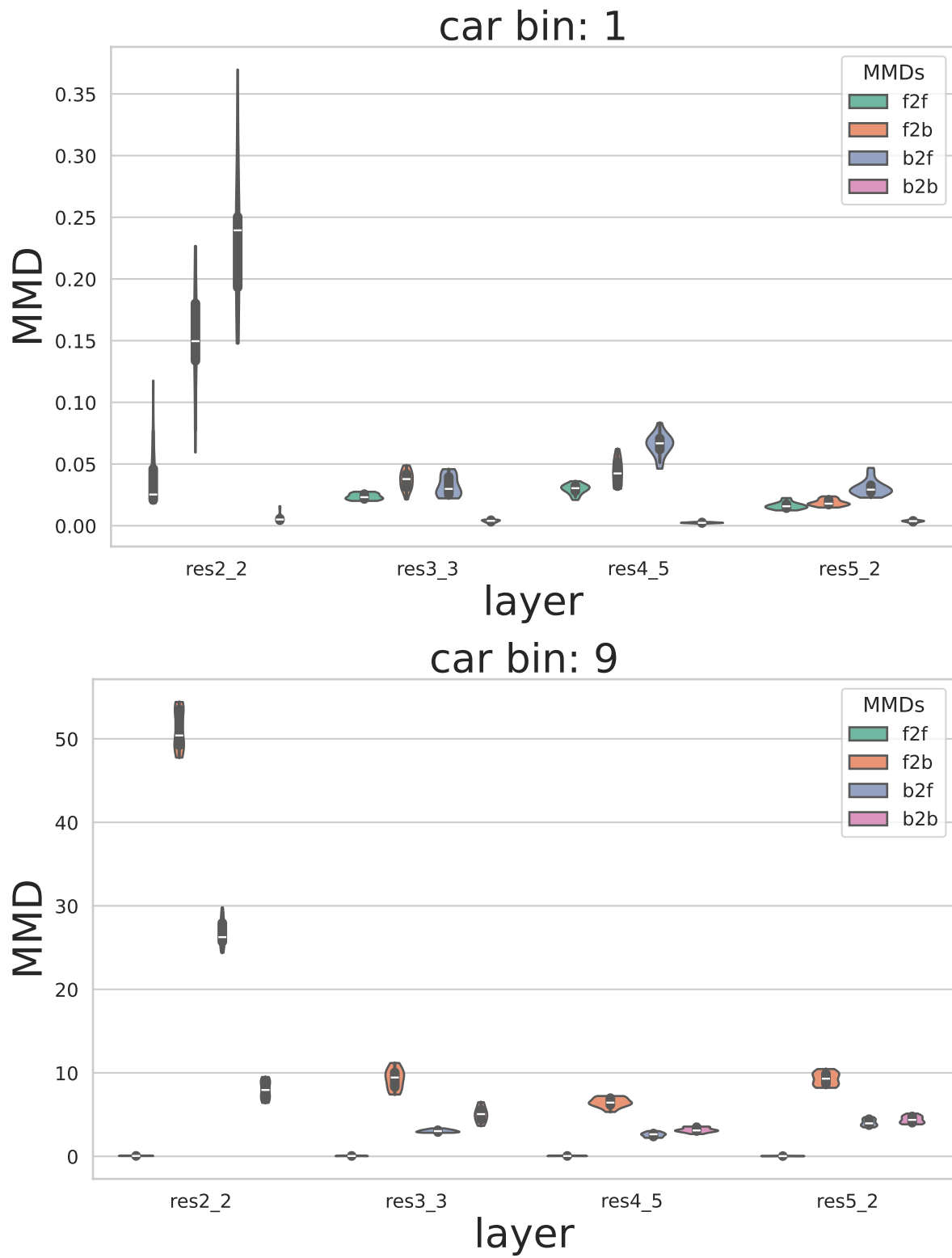


Figure 43. CS-CSFV(0.02) small MMD plots. Label: Car.

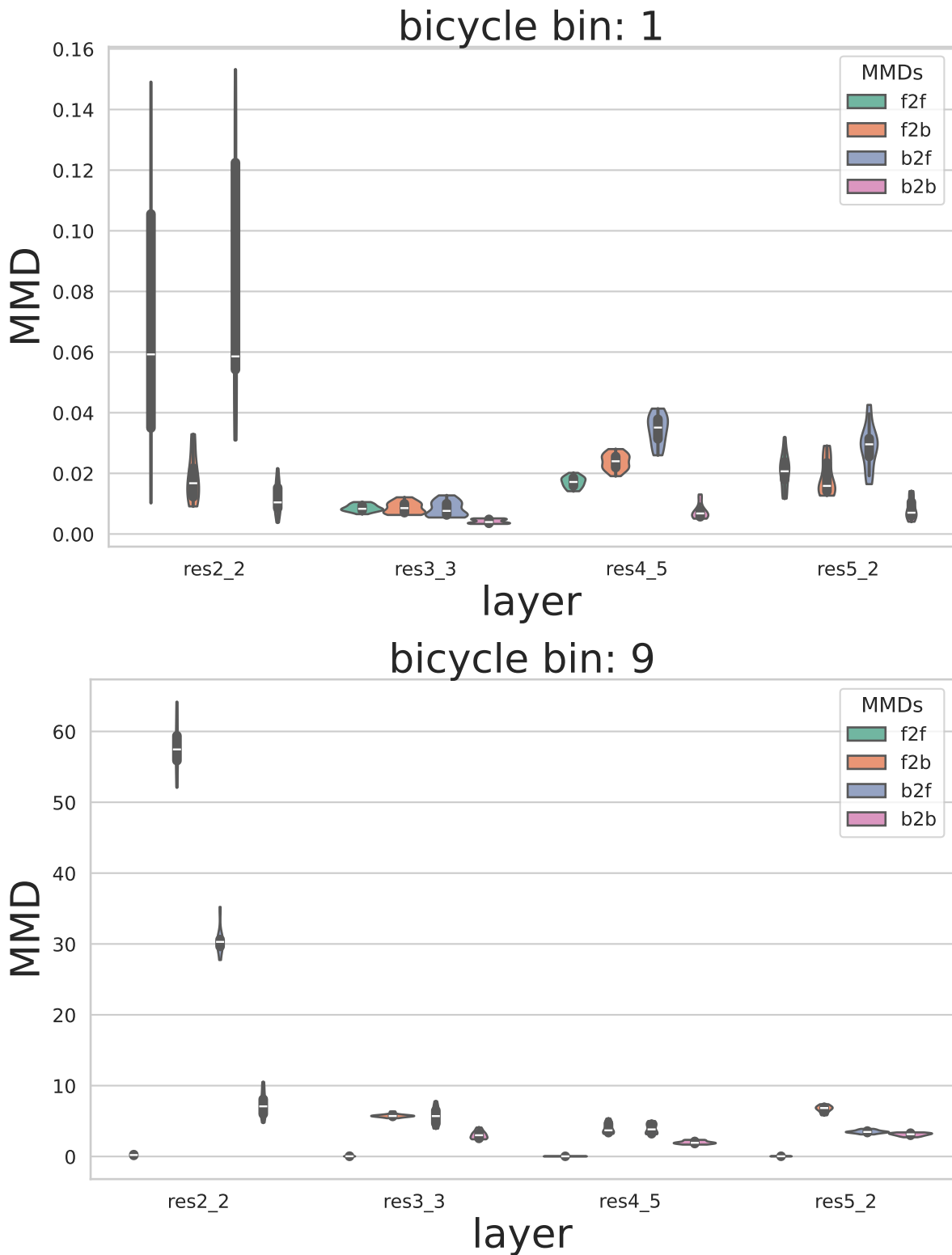


Figure 44. CS-CSFV(0.02) medium MMD plots. Label: Bicycle.

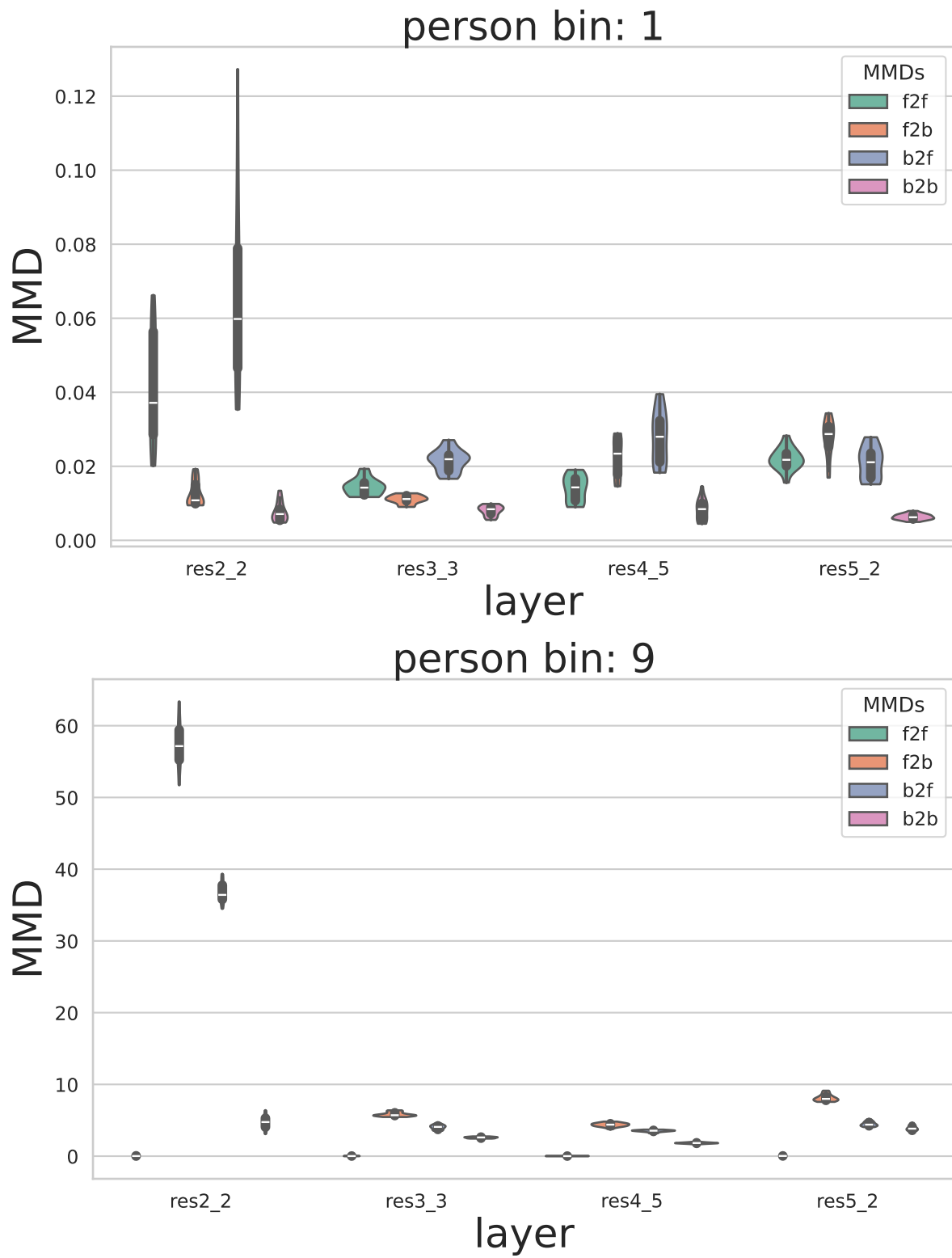


Figure 45. CS-CSFV(0.02) medium MMD plots. Label: Person.

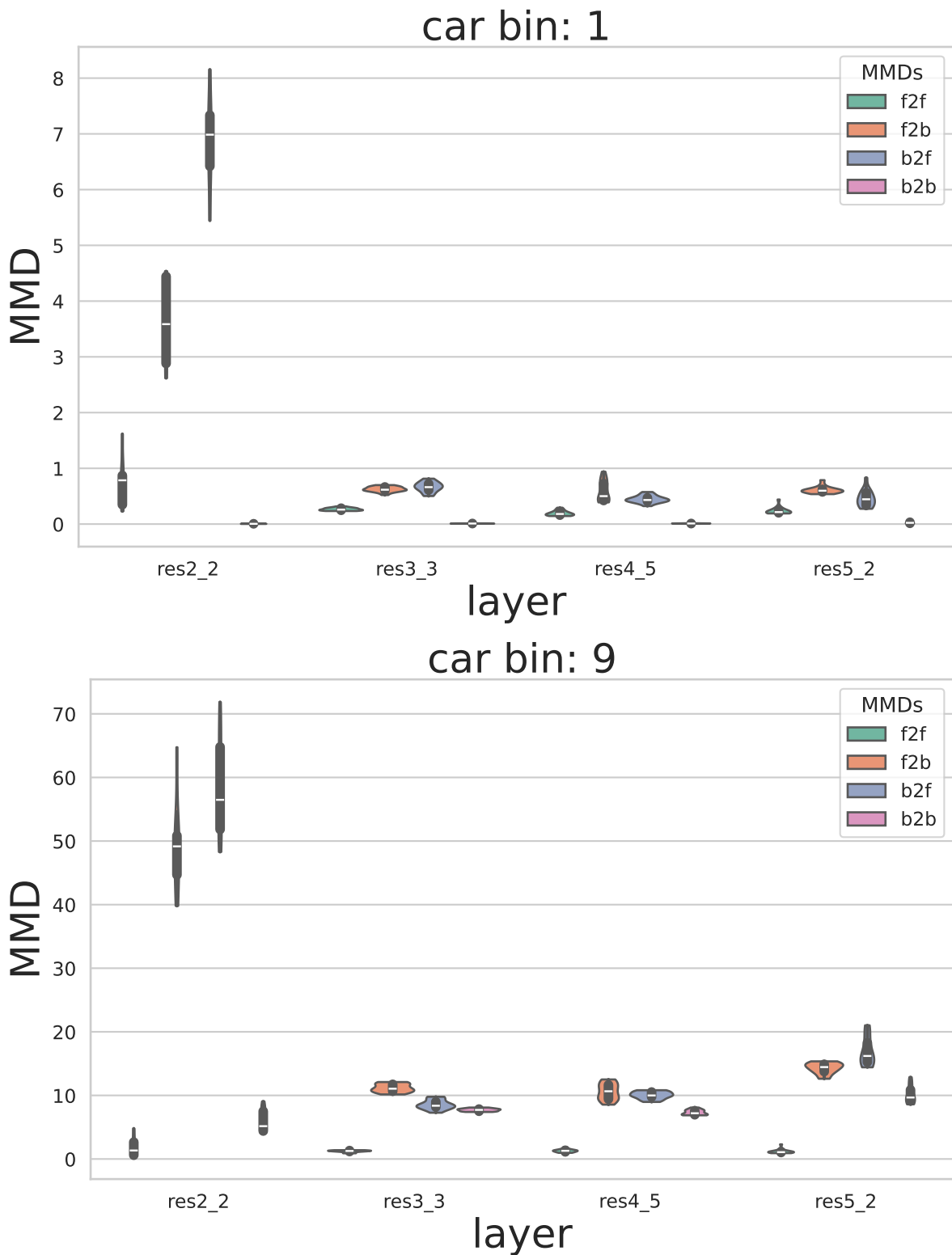


Figure 46. CS-CSFV(0.02) large MMD plots. Label: Car.

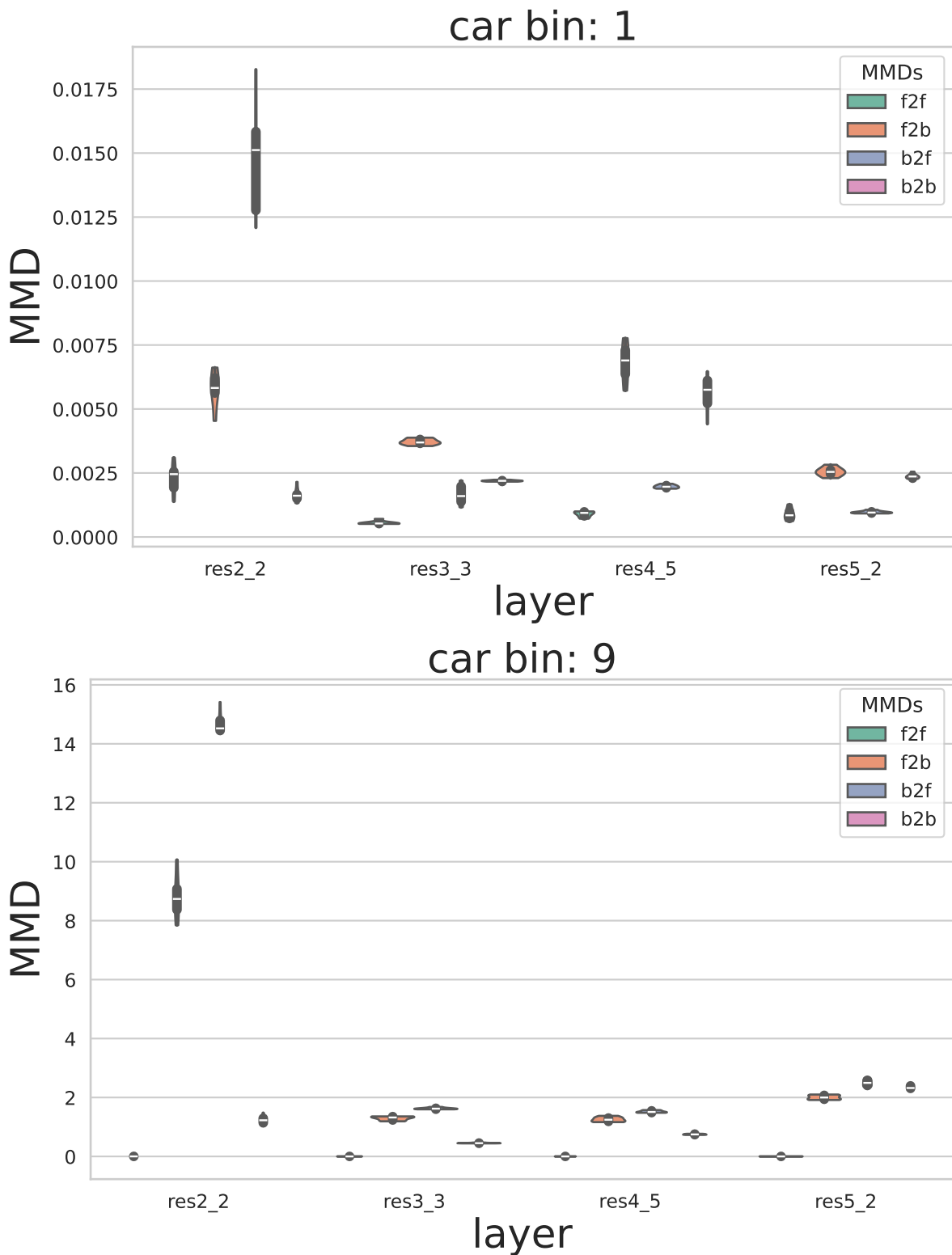


Figure 47. CS-CARLA small MMD plots. Label: Car.

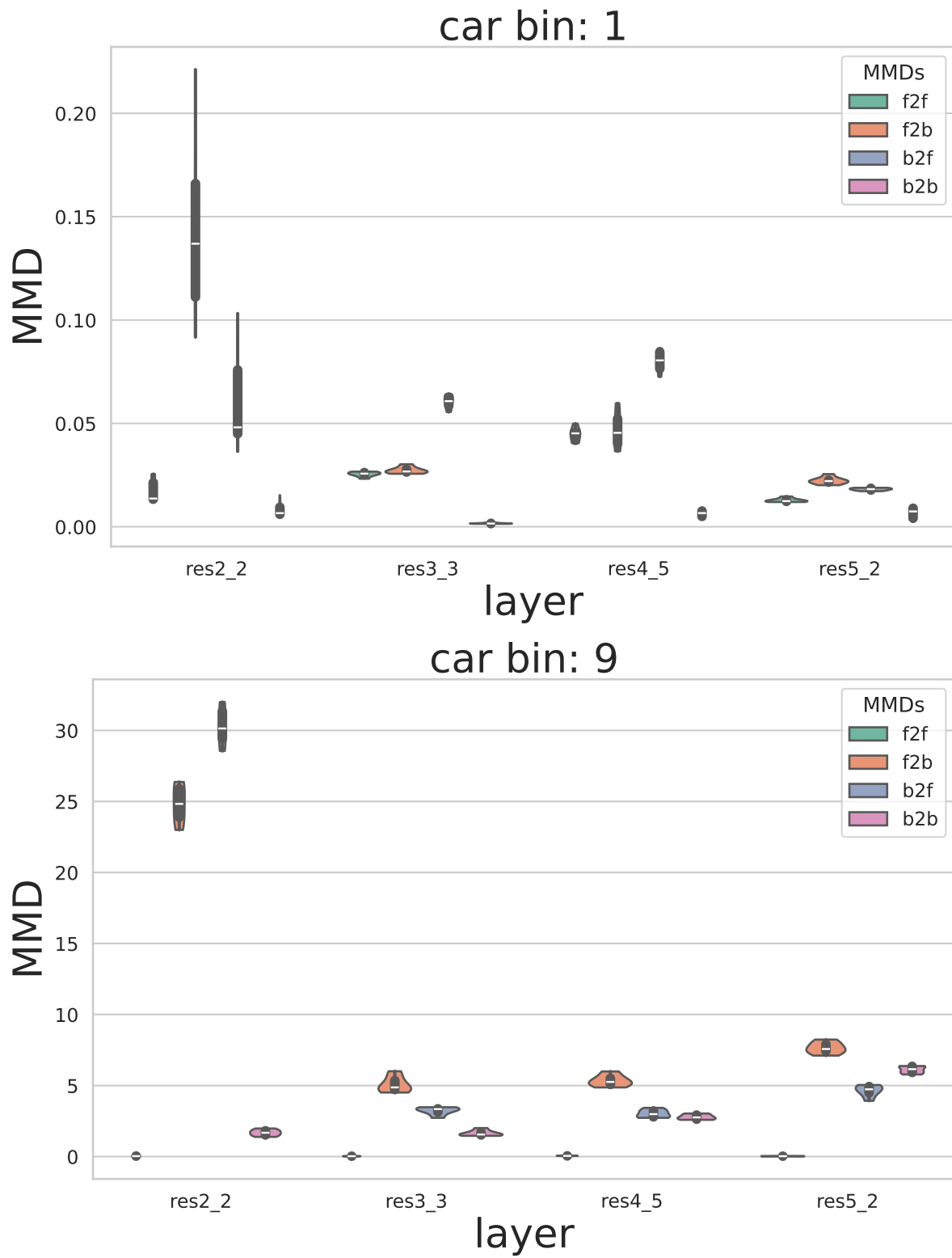


Figure 48. CS-CARLA medium MMD plots. Label: Car.

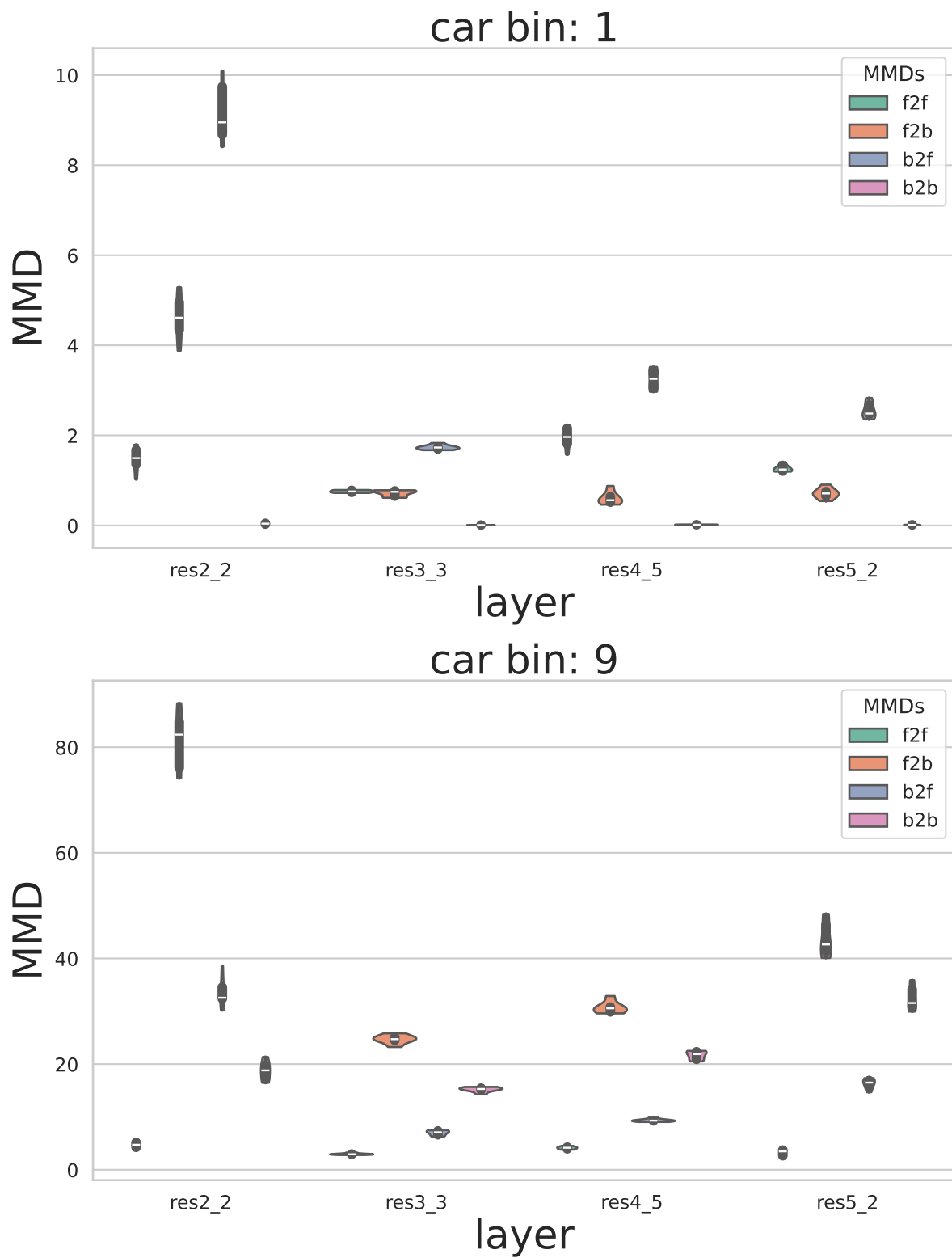


Figure 49. CS-CARLA large MMD plots. Label: Car.

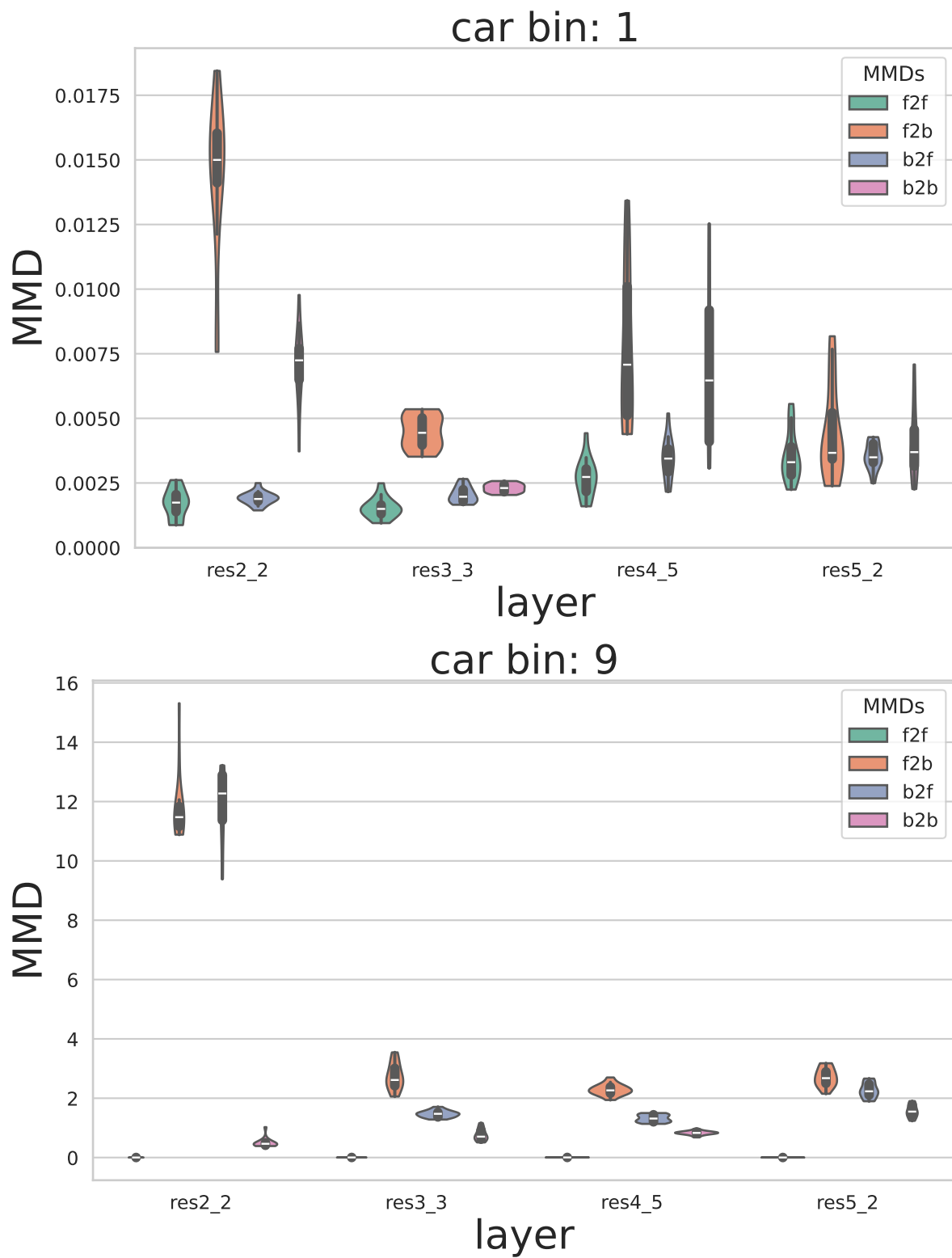


Figure 50. CS-VK small MMD plots. Label: Car.

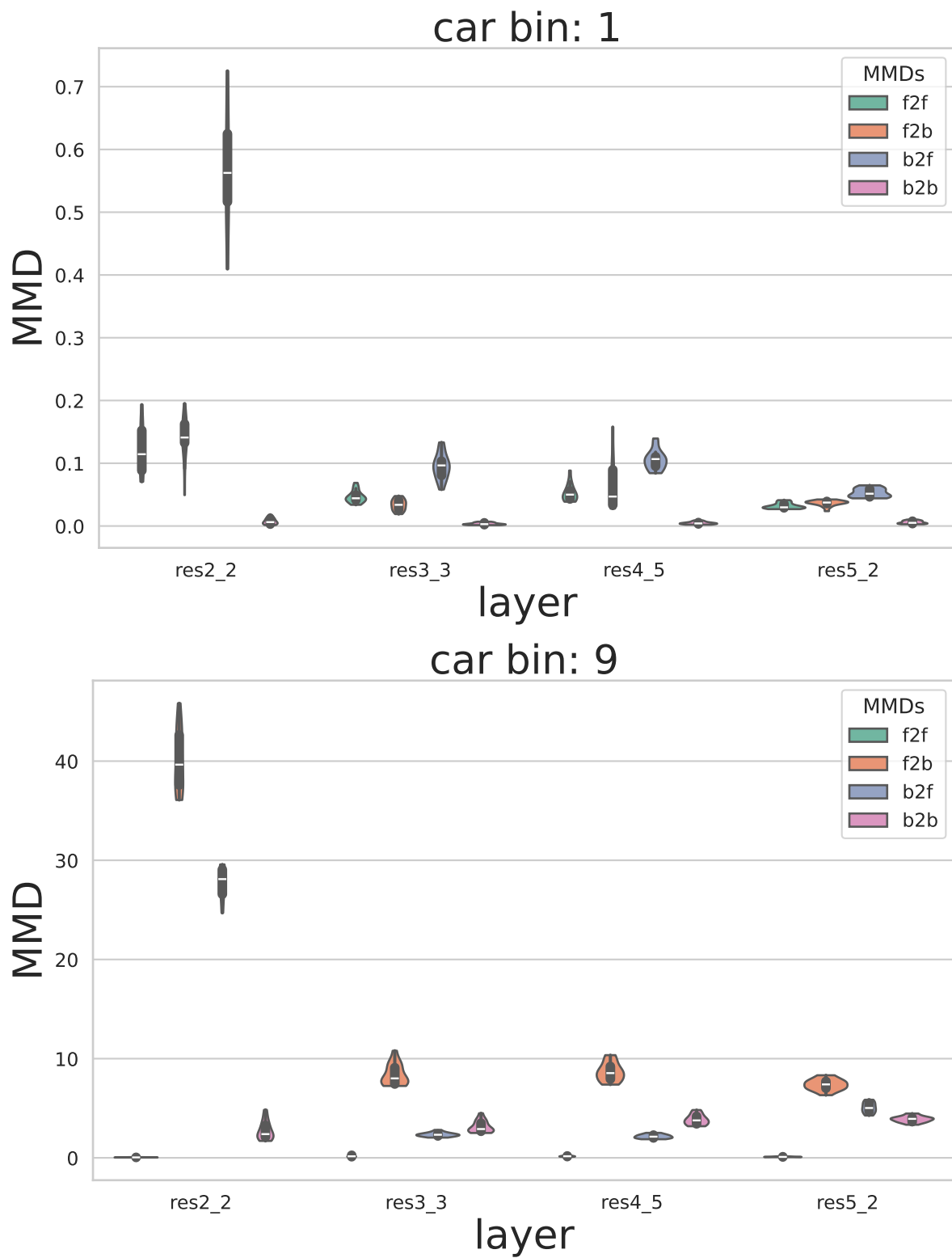


Figure 51. CS-VK medium MMD plots. Label: Car.

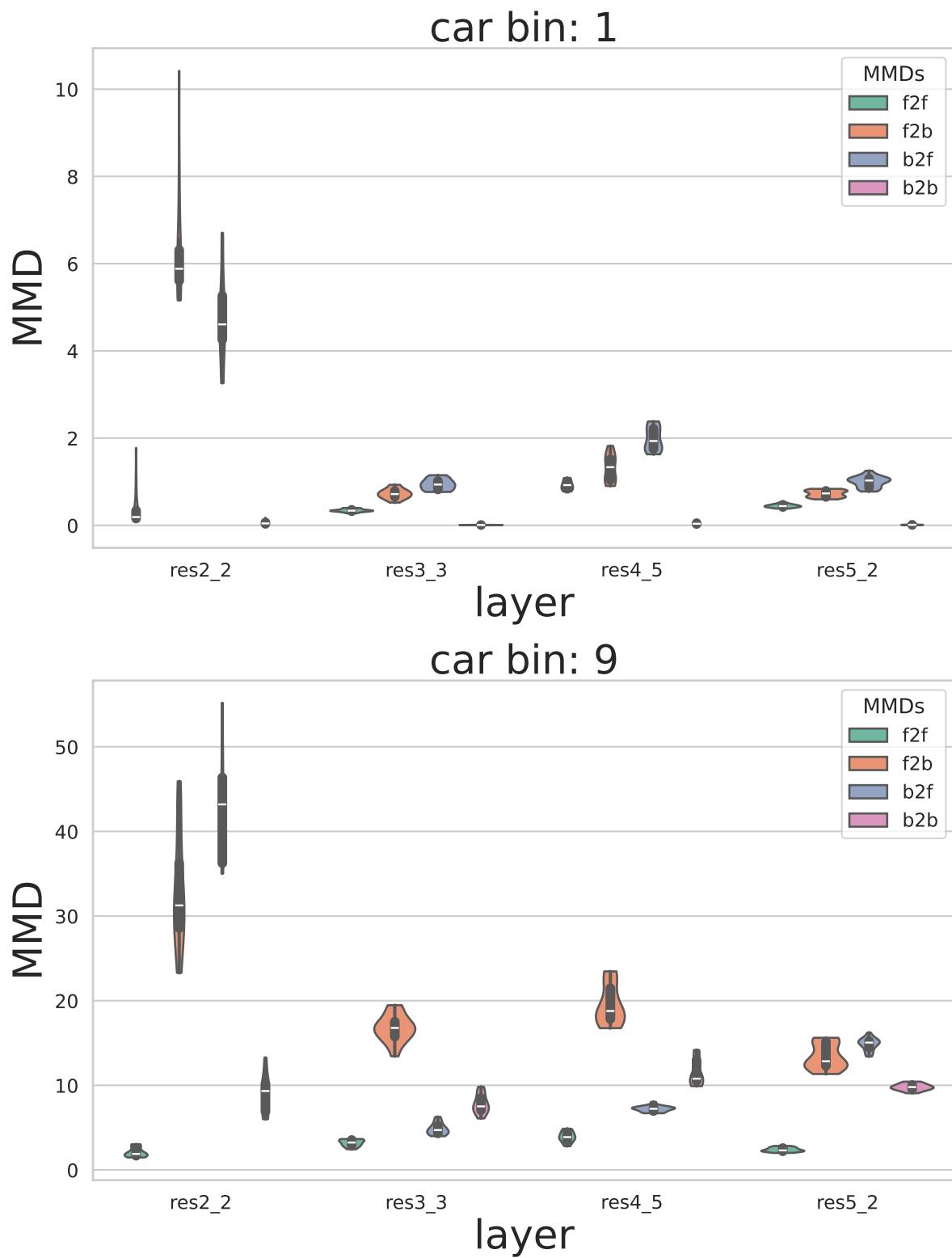


Figure 52. CS-VK large MMD plots. Label: Car.

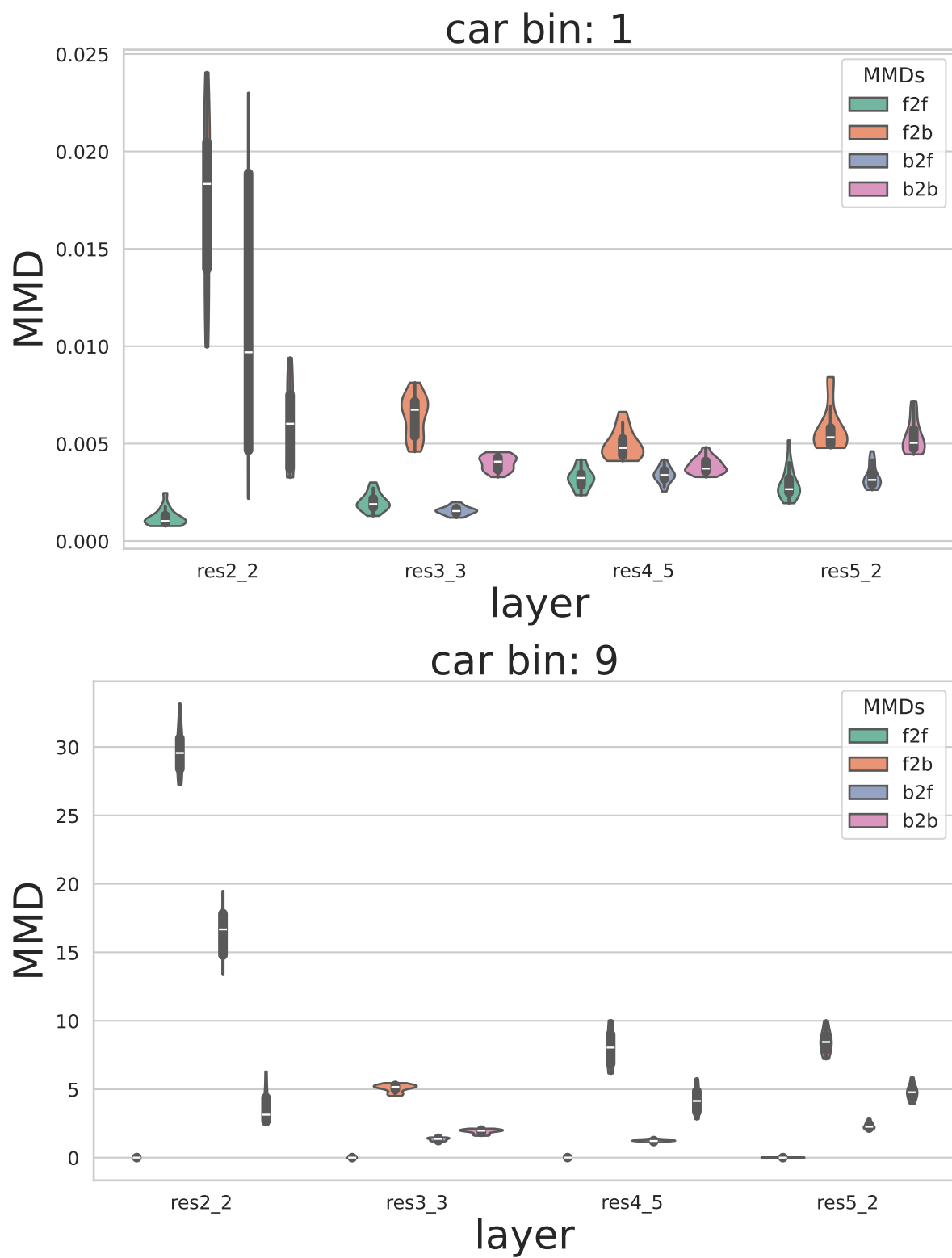


Figure 53. CS-KS small MMD plots. Label: Car.

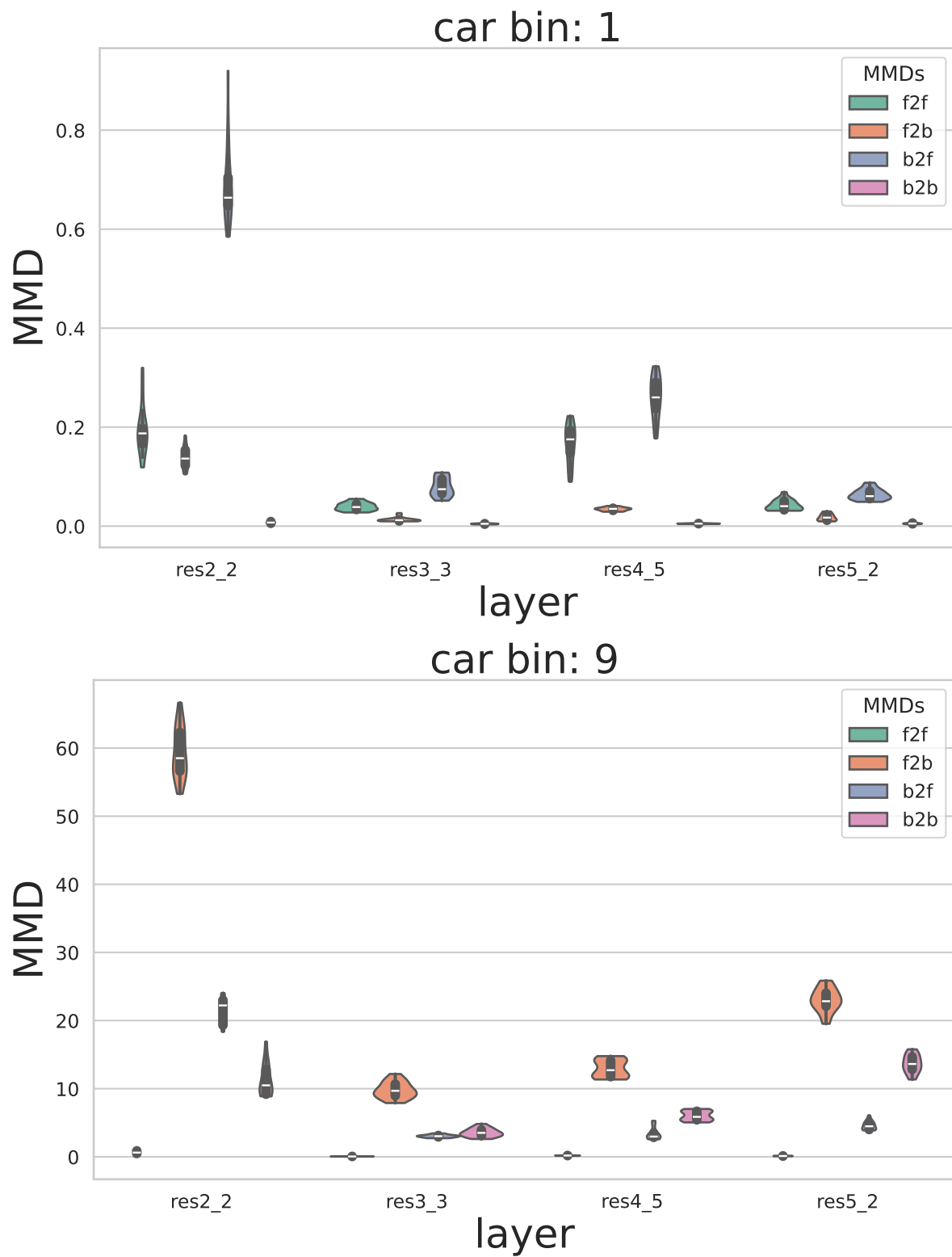


Figure 54. CS-KS medium MMD plots. Label: Car.

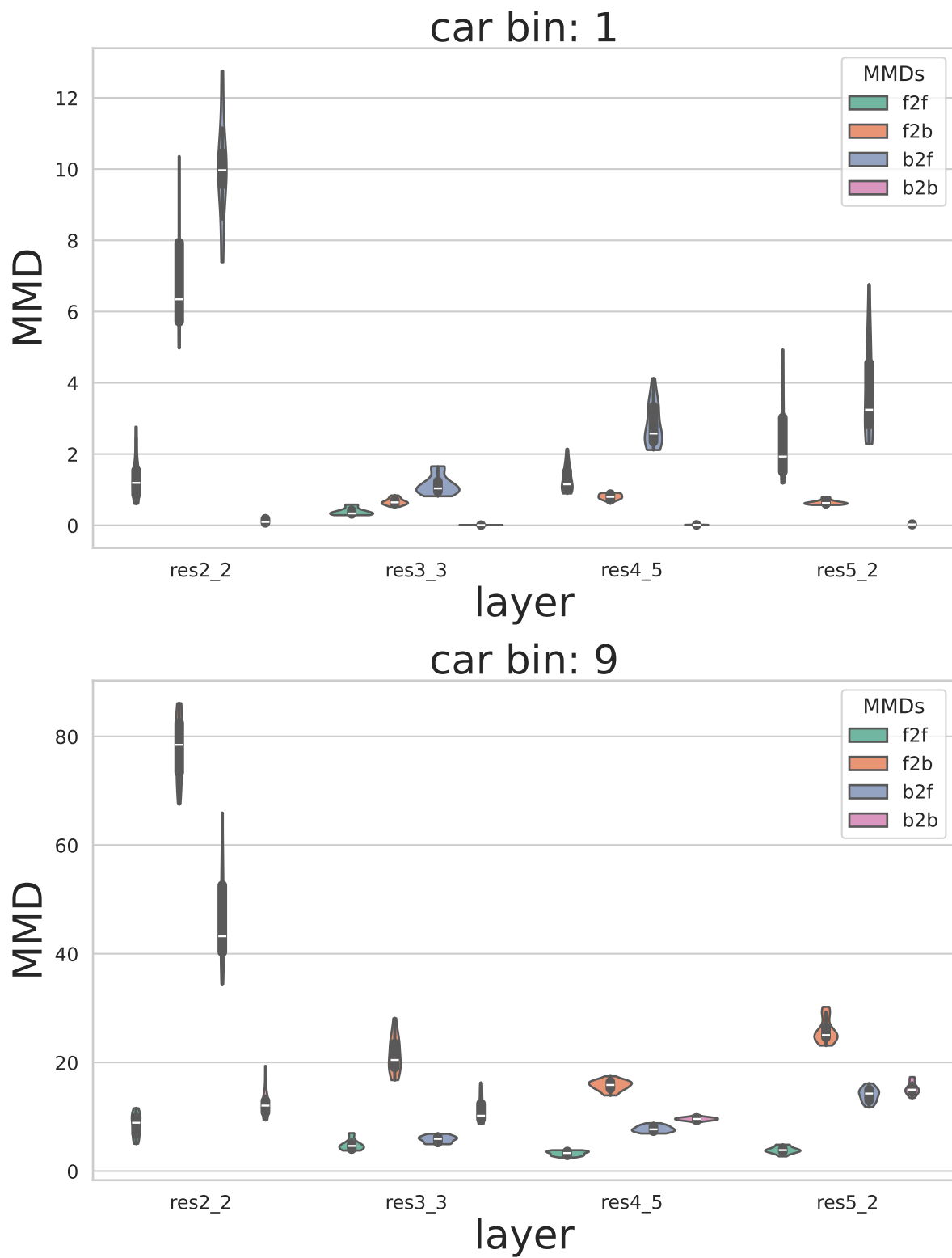


Figure 55. CS-KS large MMD plots. Label: Car.

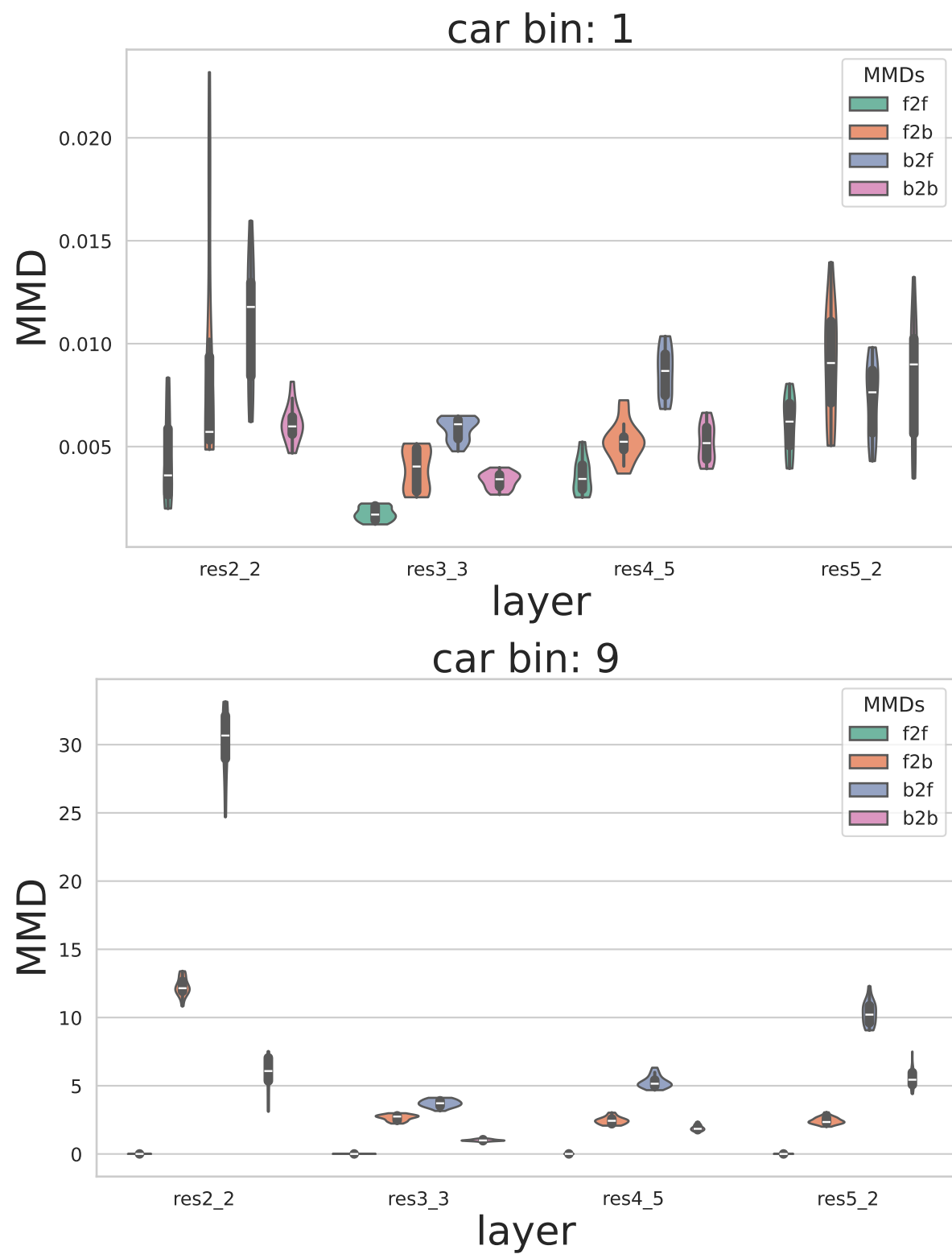


Figure 56. KS-VK small MMD plots. Label: Car.

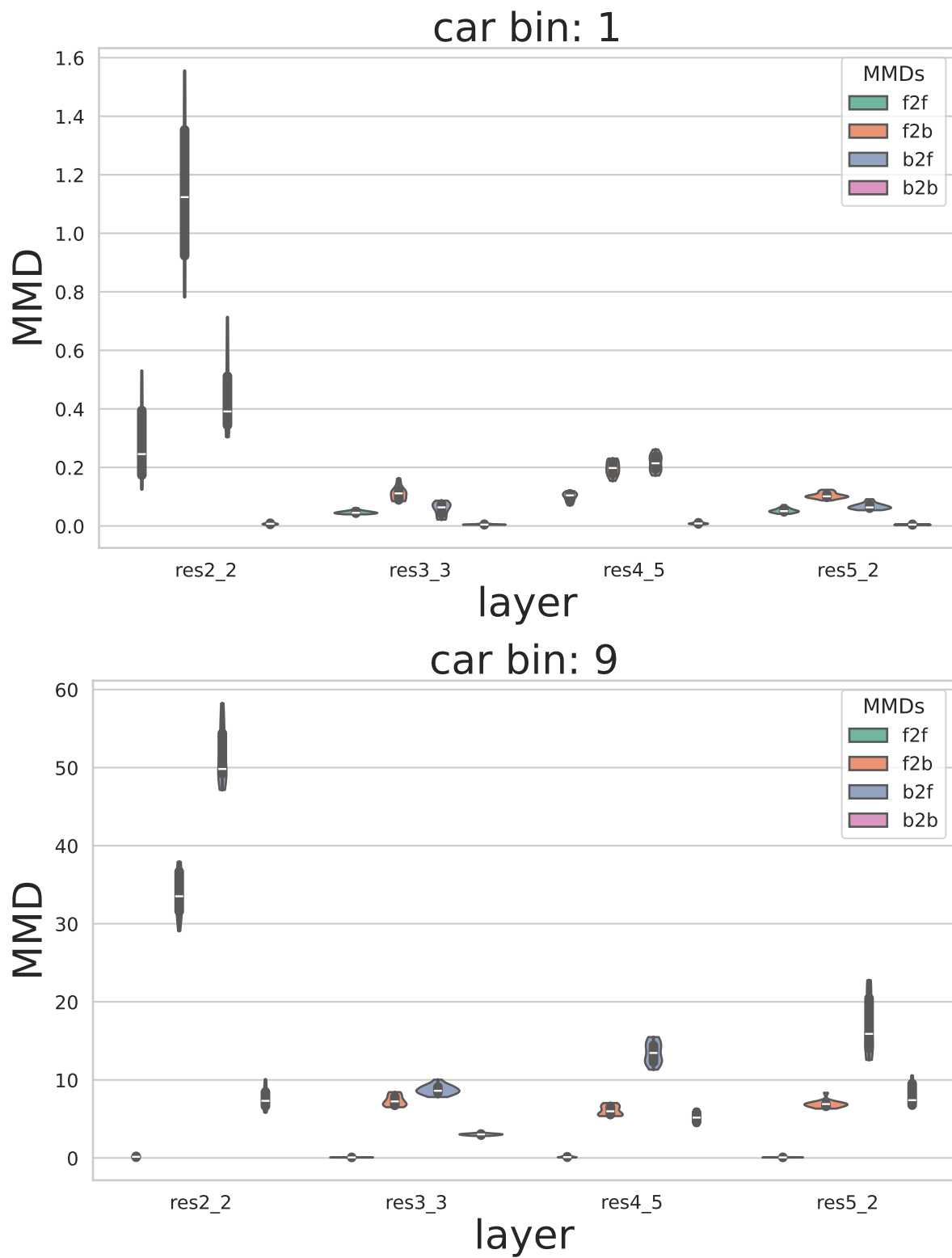


Figure 57. KS-VK medium MMD plots. Label: Car.

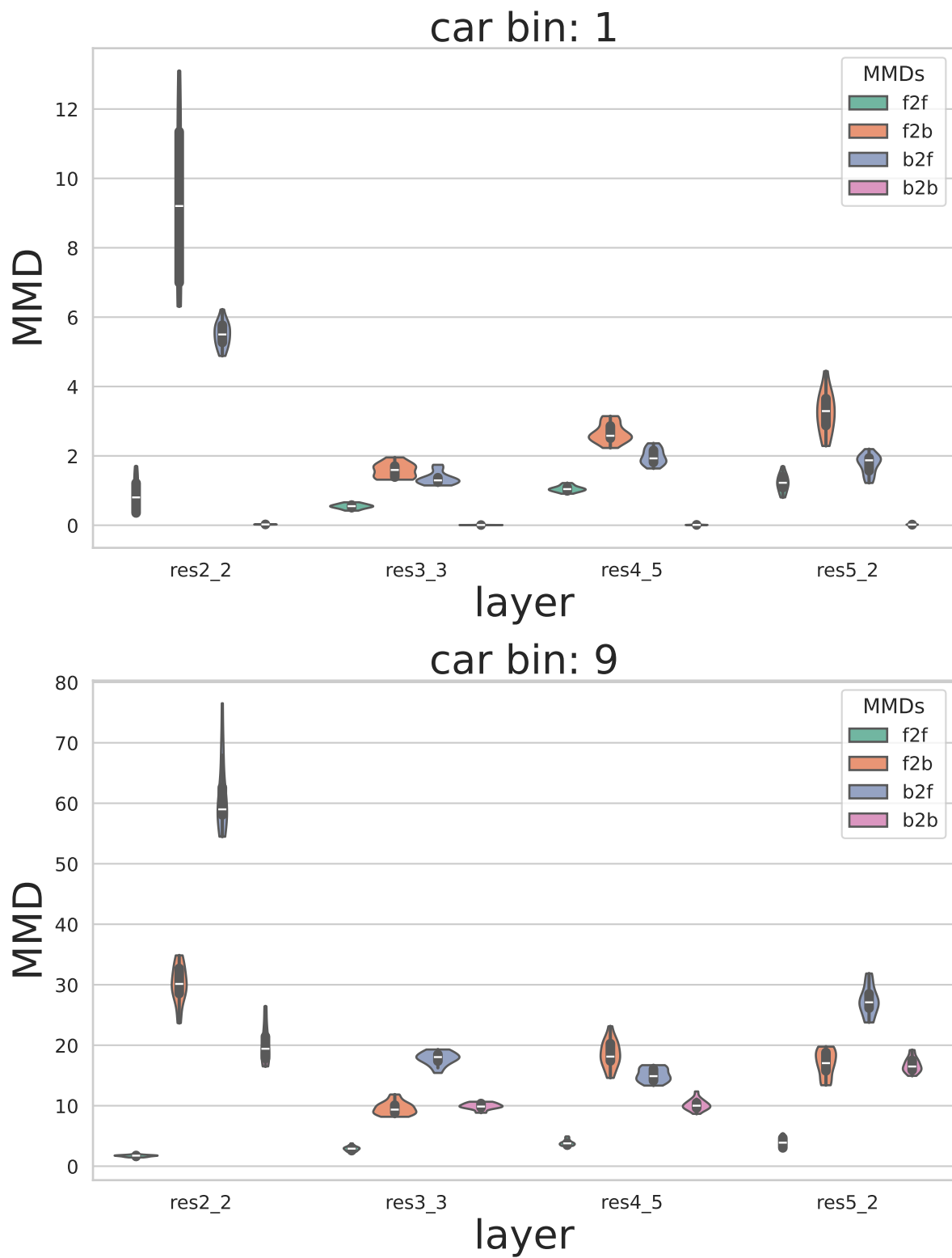


Figure 58. KS-VK large MMD plots. Label: Car.

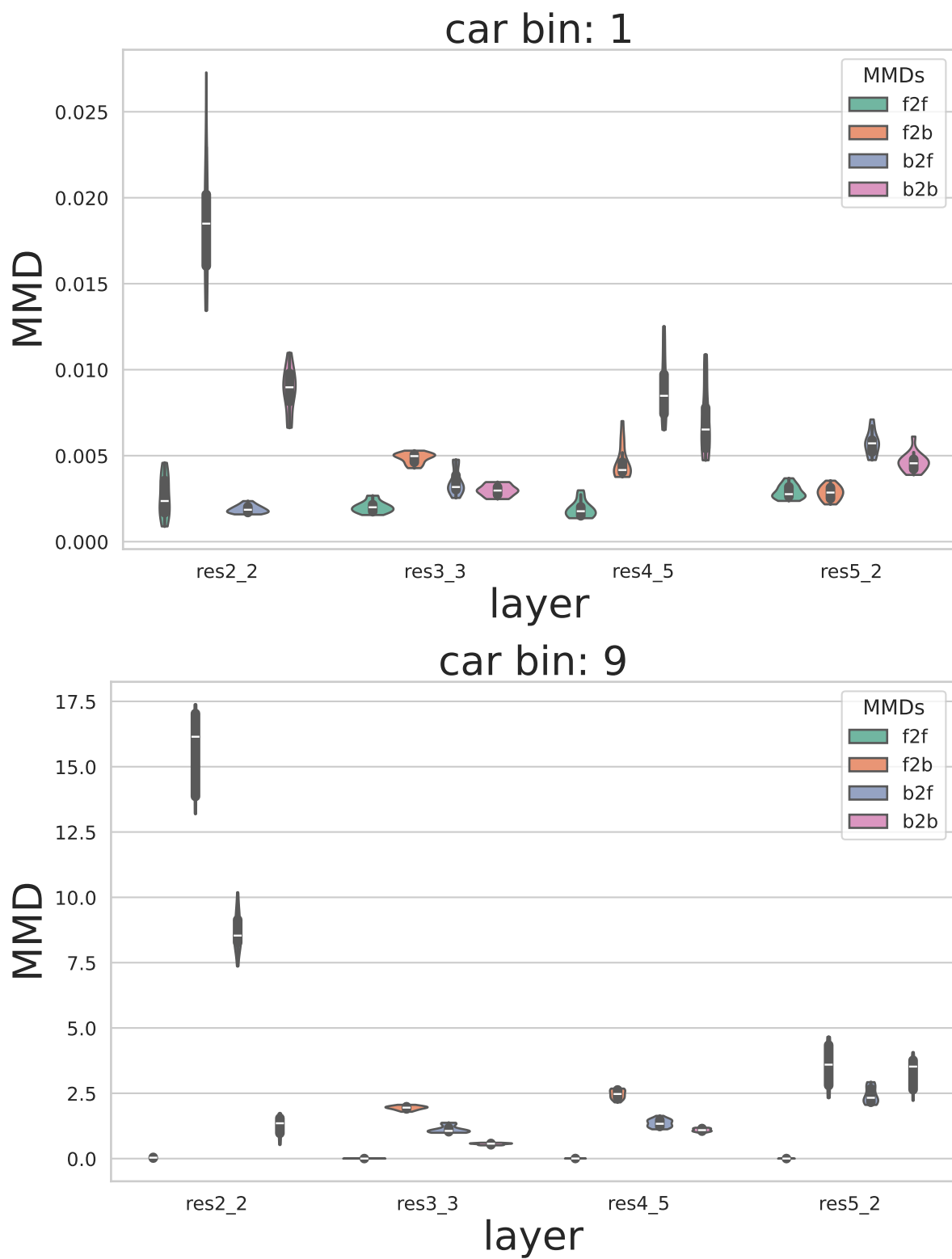


Figure 59. CARLA-VK small MMD plots. Label: Car.

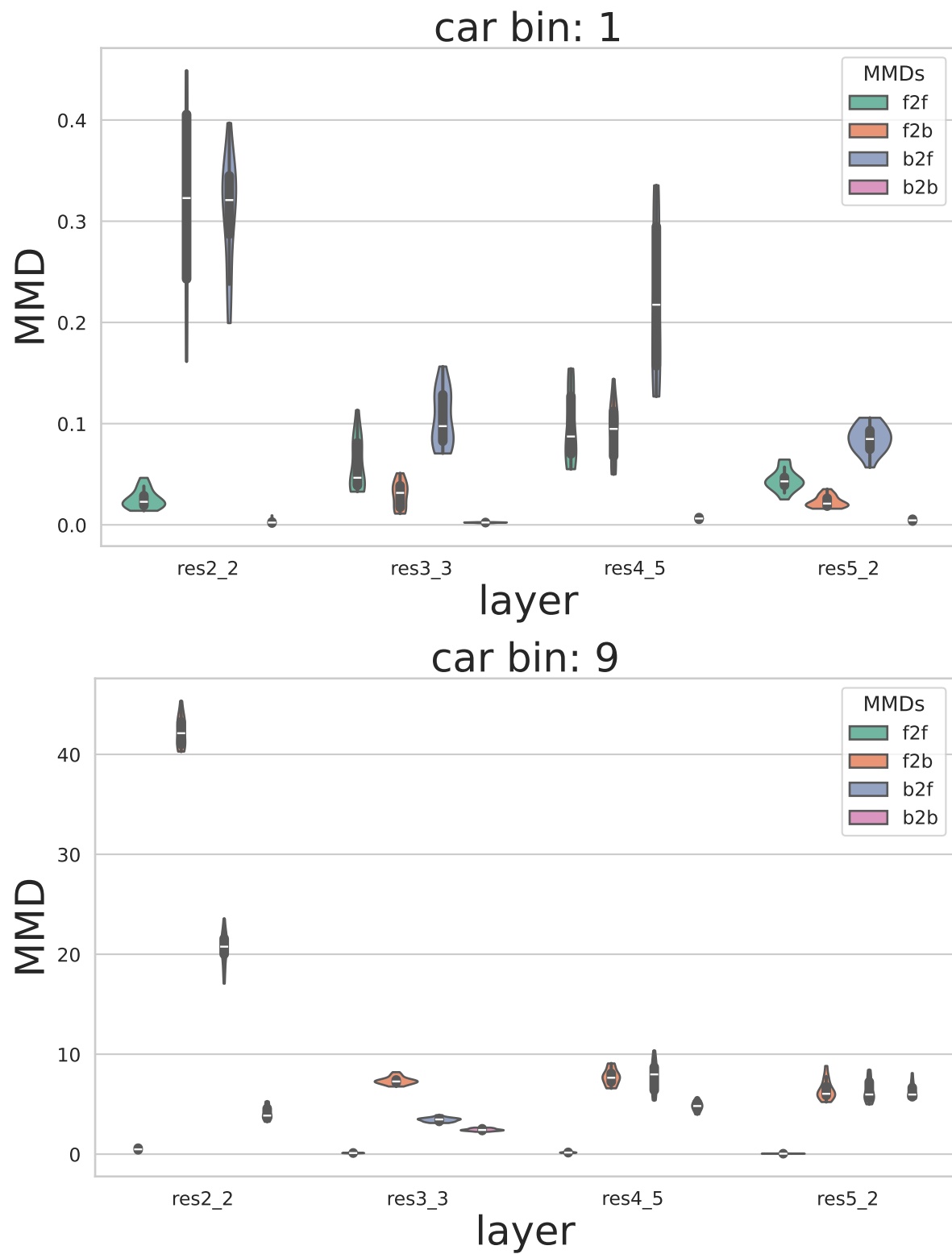


Figure 60. CARLA-VK medium MMD plots. Label: Car.

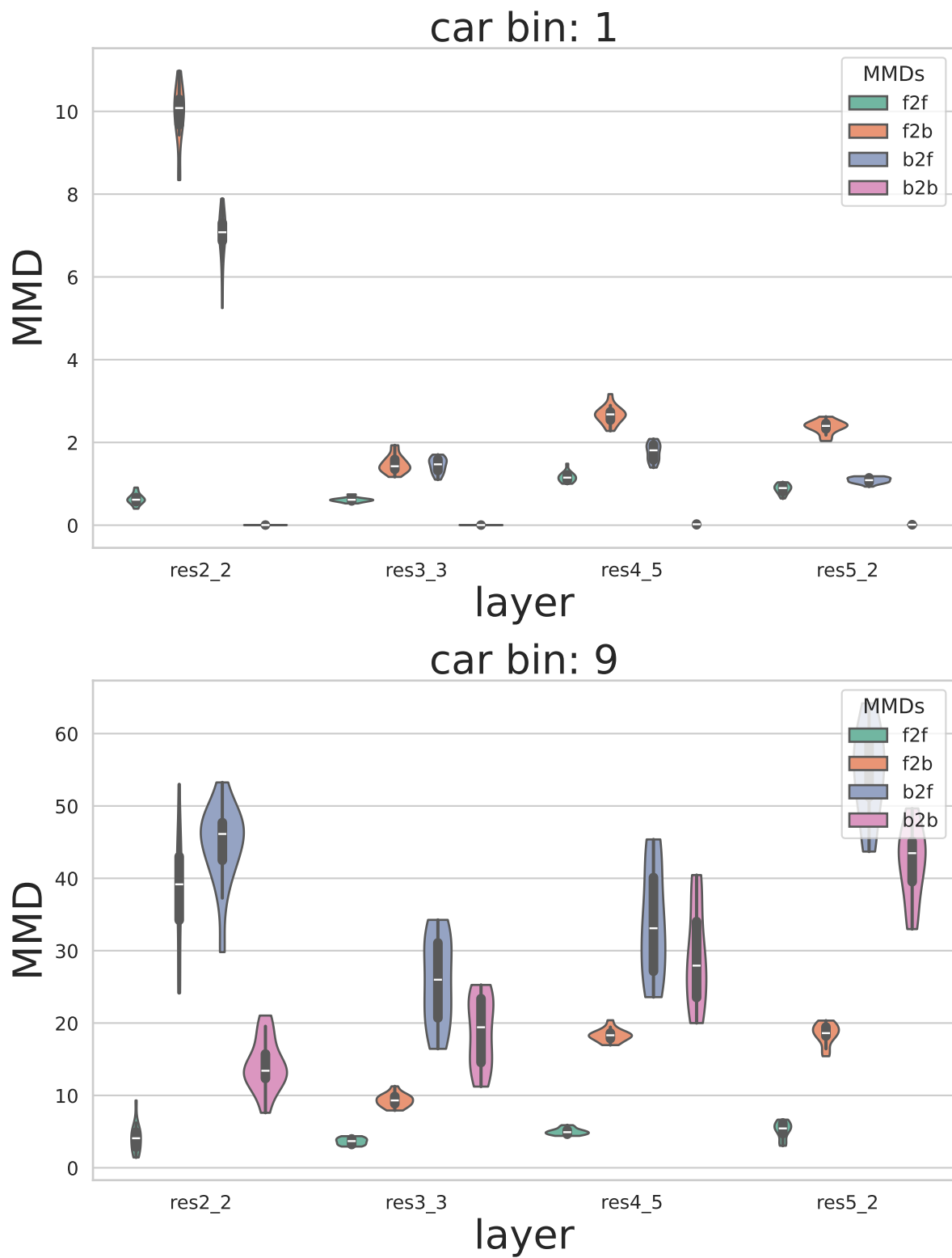


Figure 61. CARLA-VK large MMD plots. Label: Car.

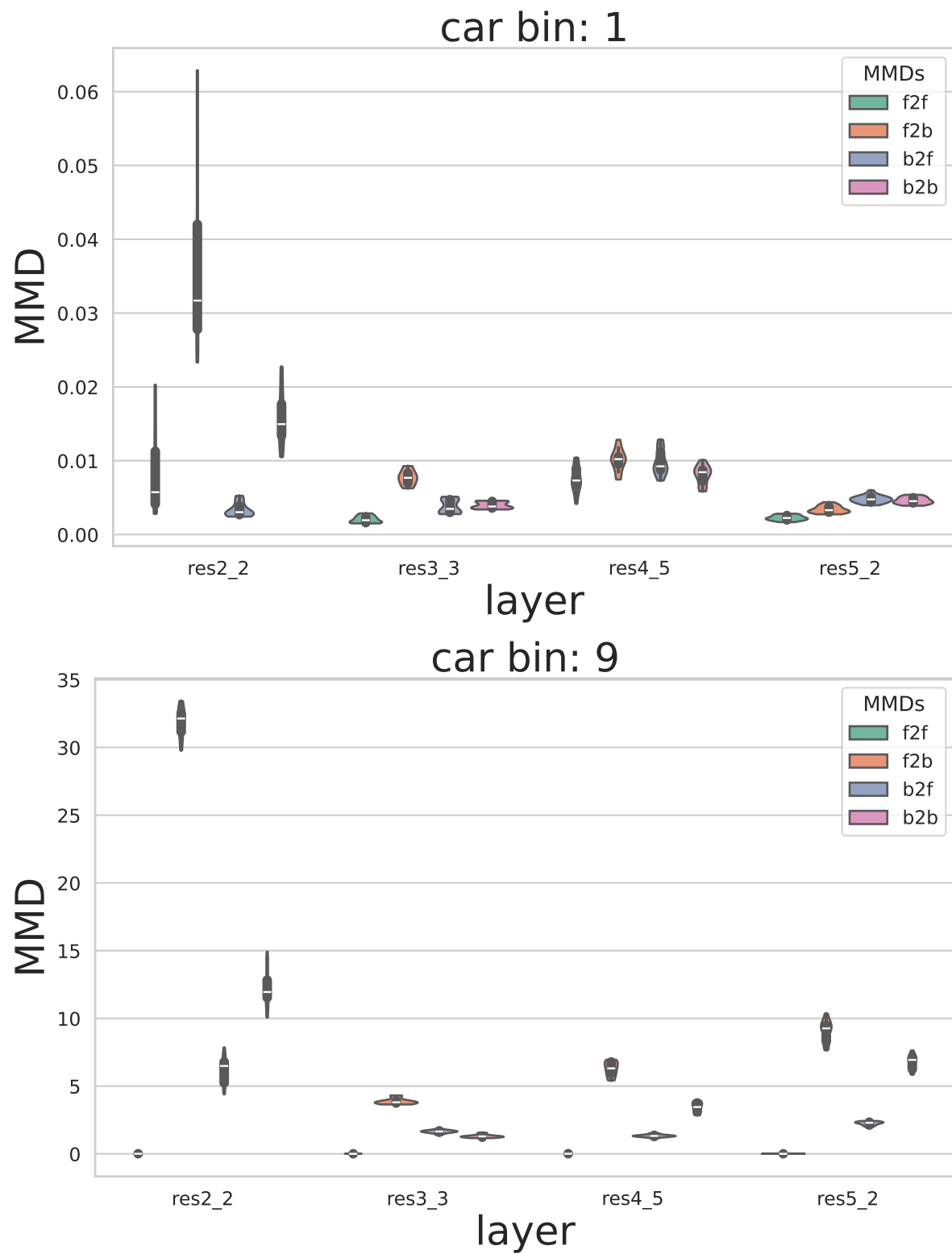


Figure 62. CARLA-KS small MMD plots. Label: Car.

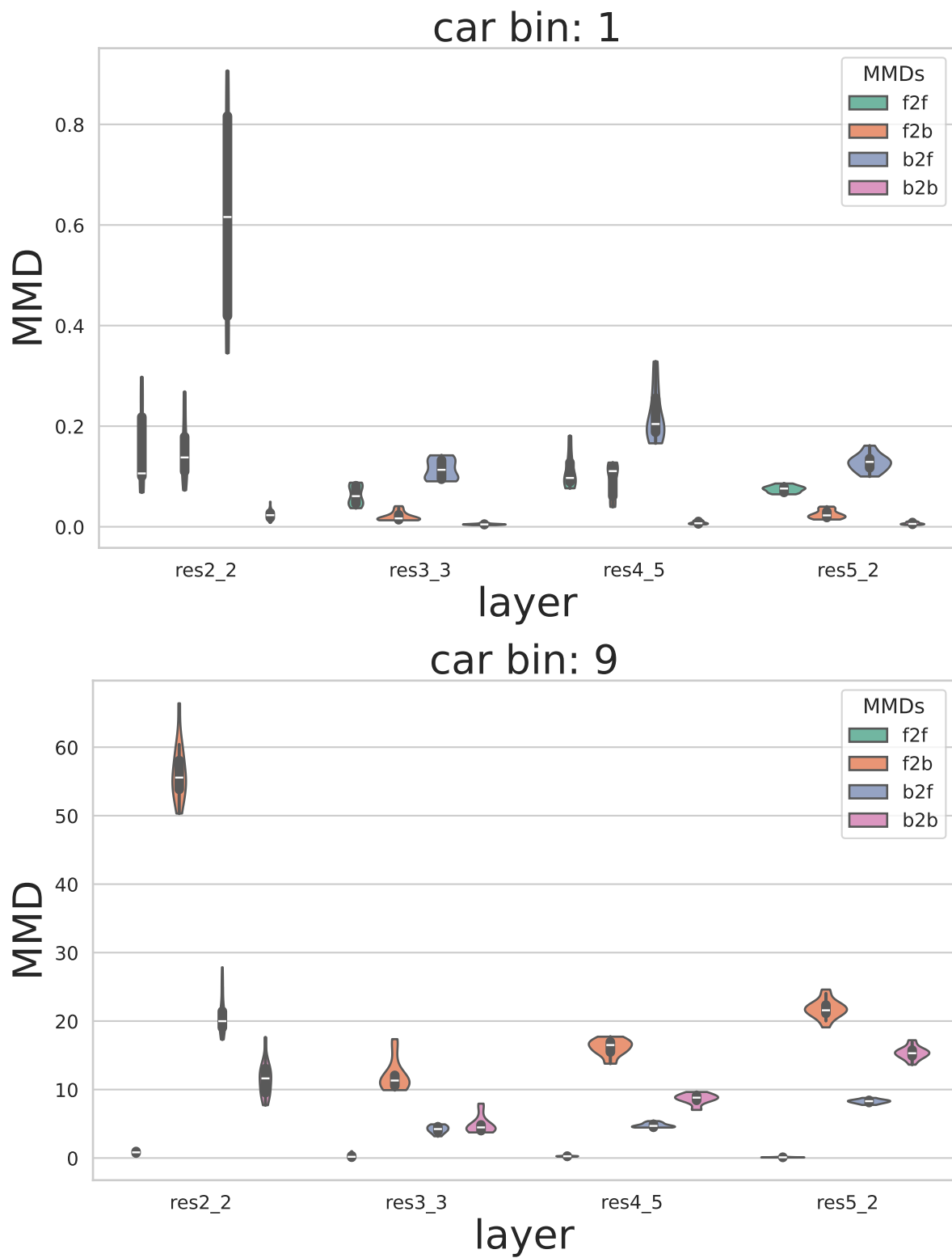


Figure 63. CARLA-ks medium MMD plots. Label: Car.

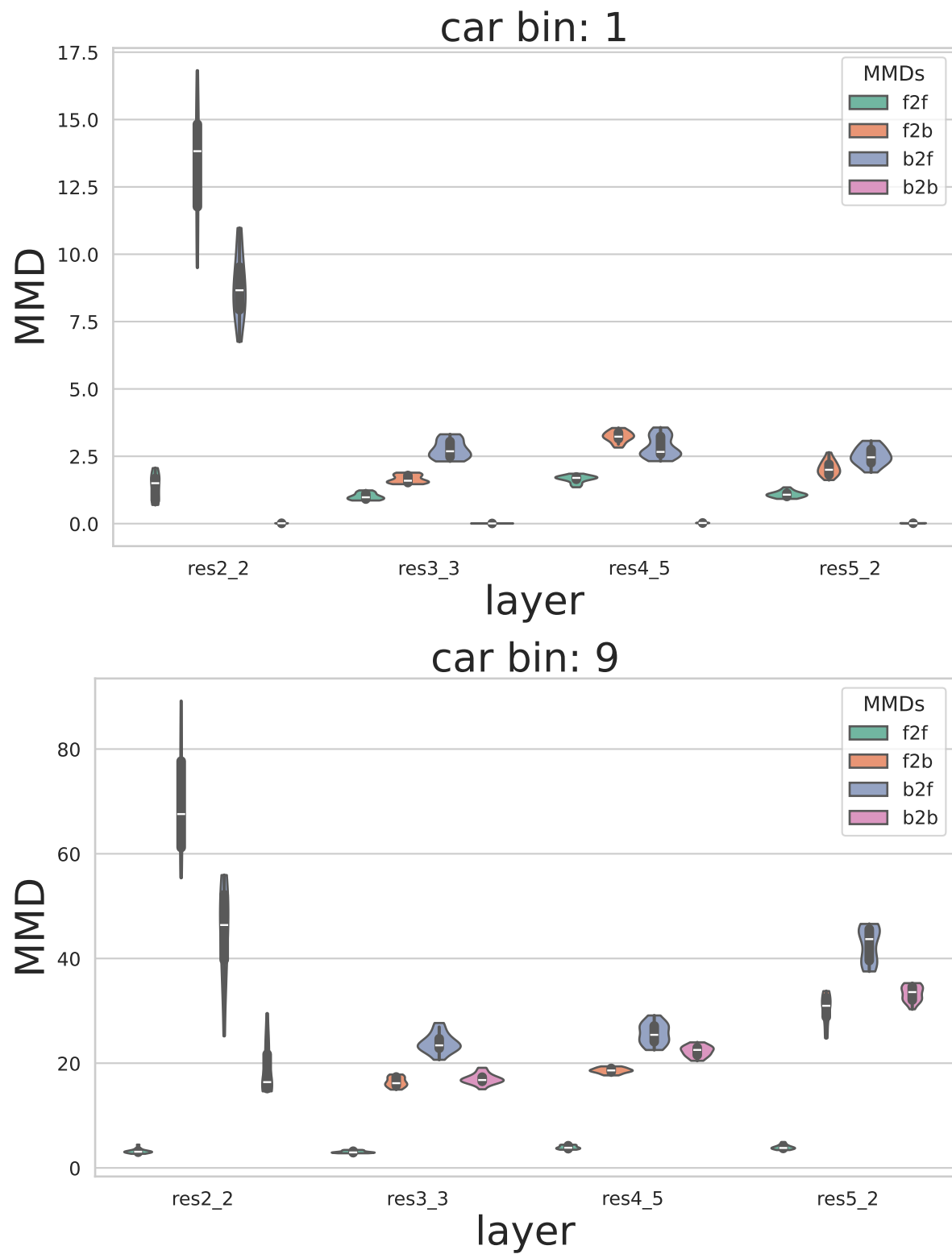
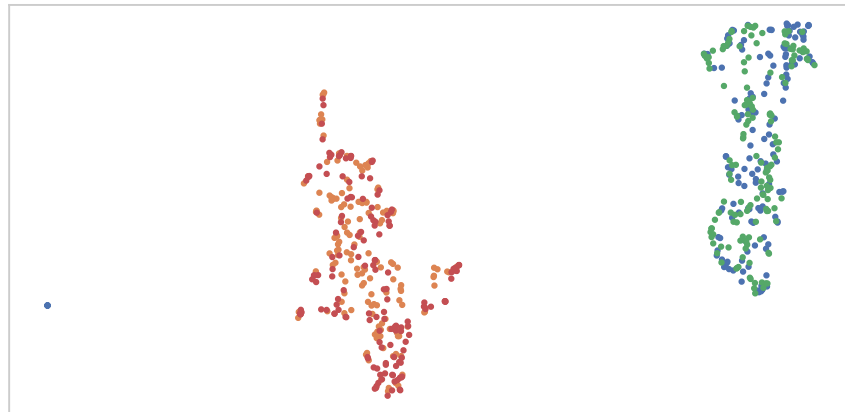


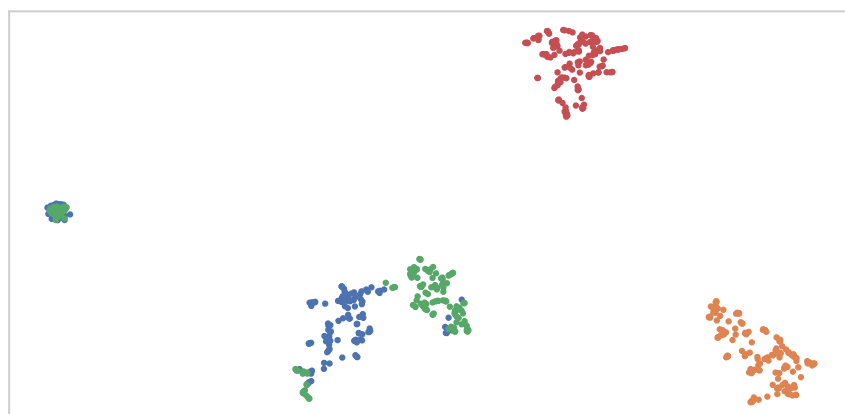
Figure 64. CARLA-KS large MMD plots. Label: Car.

## **14. UMAP embedding**

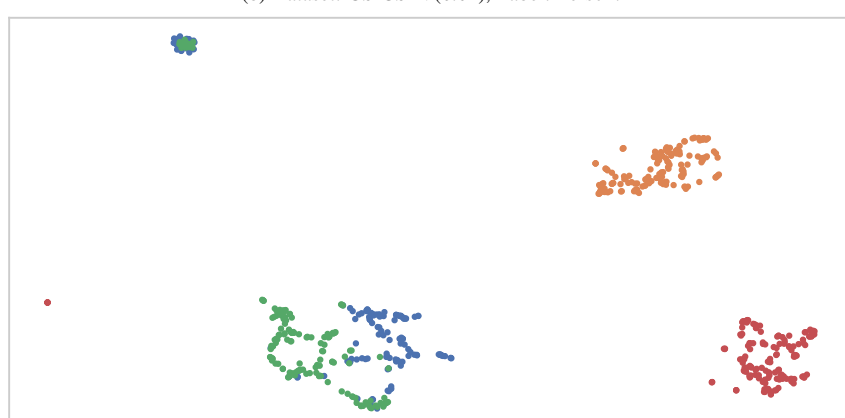
This section provides 2D embedding results of non-car labels.



(a) Dataset: CS-CSV, Label: Person.

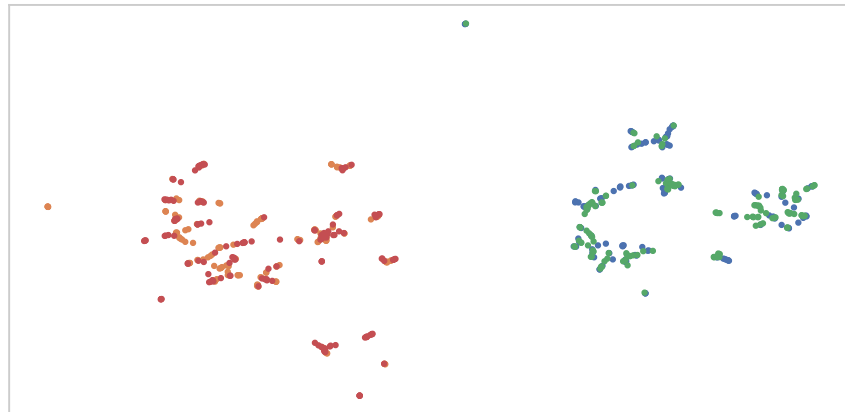


(b) Dataset: CS-CSFV(0.01), Label: Person.

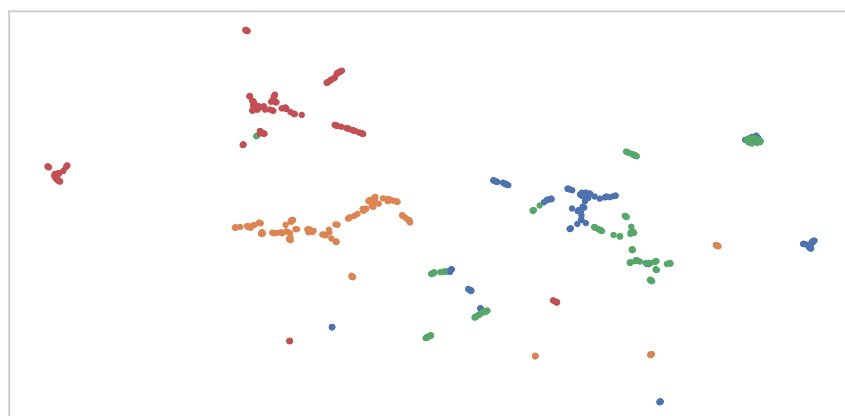


(c) Dataset: CS-CSFV(0.02), Label: Person.

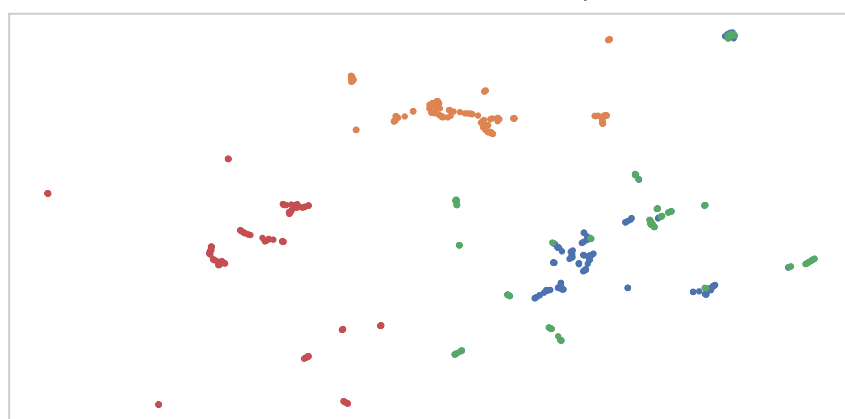
Figure 65. **Person 2D embedding using features extracted by Detectron2.**



(a) Dataset: CS-CSV, Label: Bicycle.

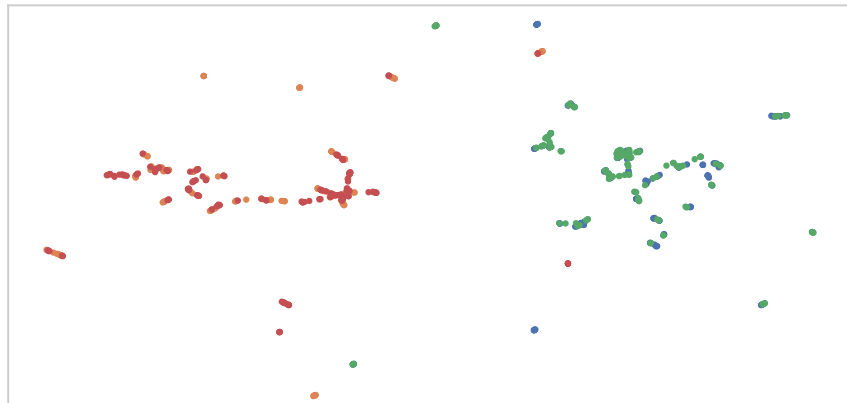


(b) Dataset: CS-CSFV(0.01), Label: Bicycle.

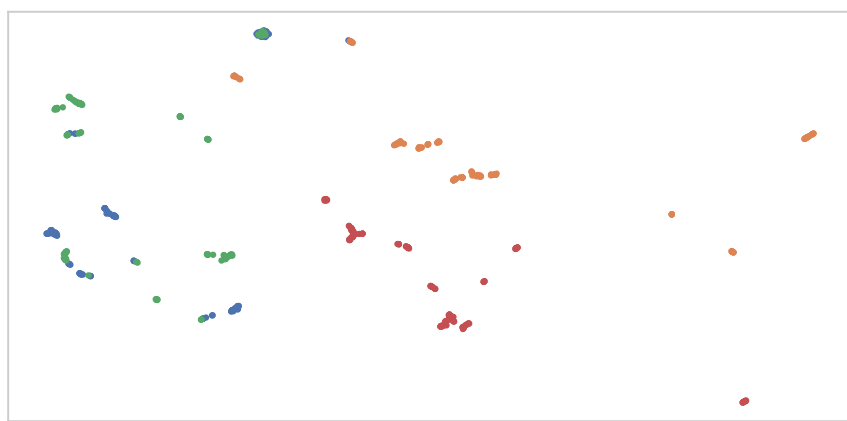


(c) Dataset: CS-CSFV(0.02), Label: Bicycle

Figure 66. **Bicycle 2d embedding using features extracted by Detectron2.**



(a) Dataset: CS-CSV, Label: Rider.



(b) Dataset: CS-CSFV(0.01), Label: Rider.

Figure 67. **Rider 2d embedding using features extracted by Detectron2.**

## **15. Pixel distribution of dataset**

This section presents the pixel distribution for each dataset.

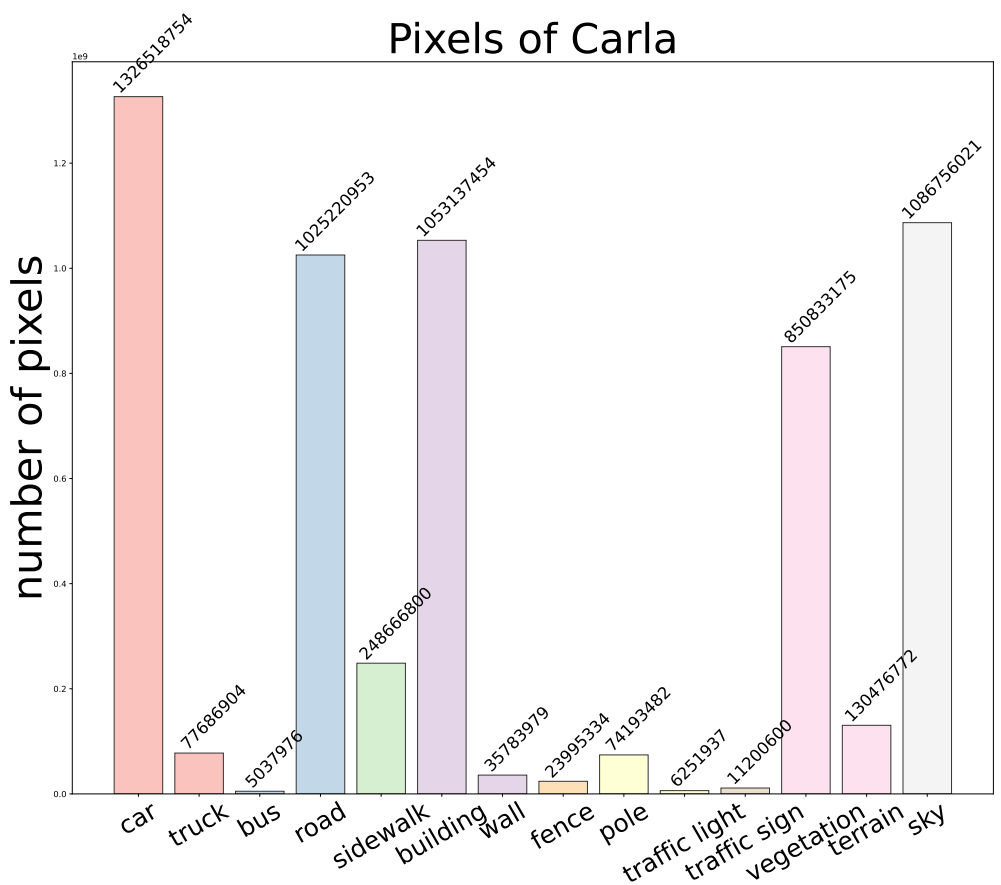


Figure 68. Pixel distribution of CARLA.

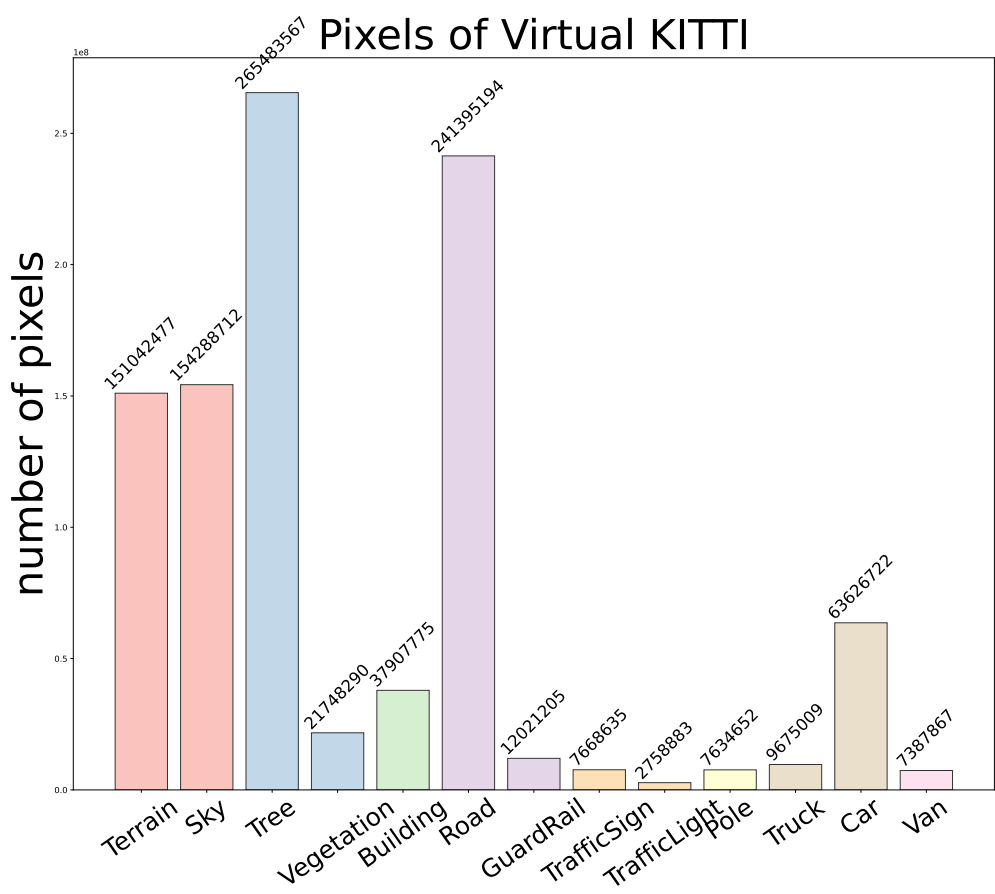


Figure 69. Pixel distribution of Virtual KITTI.

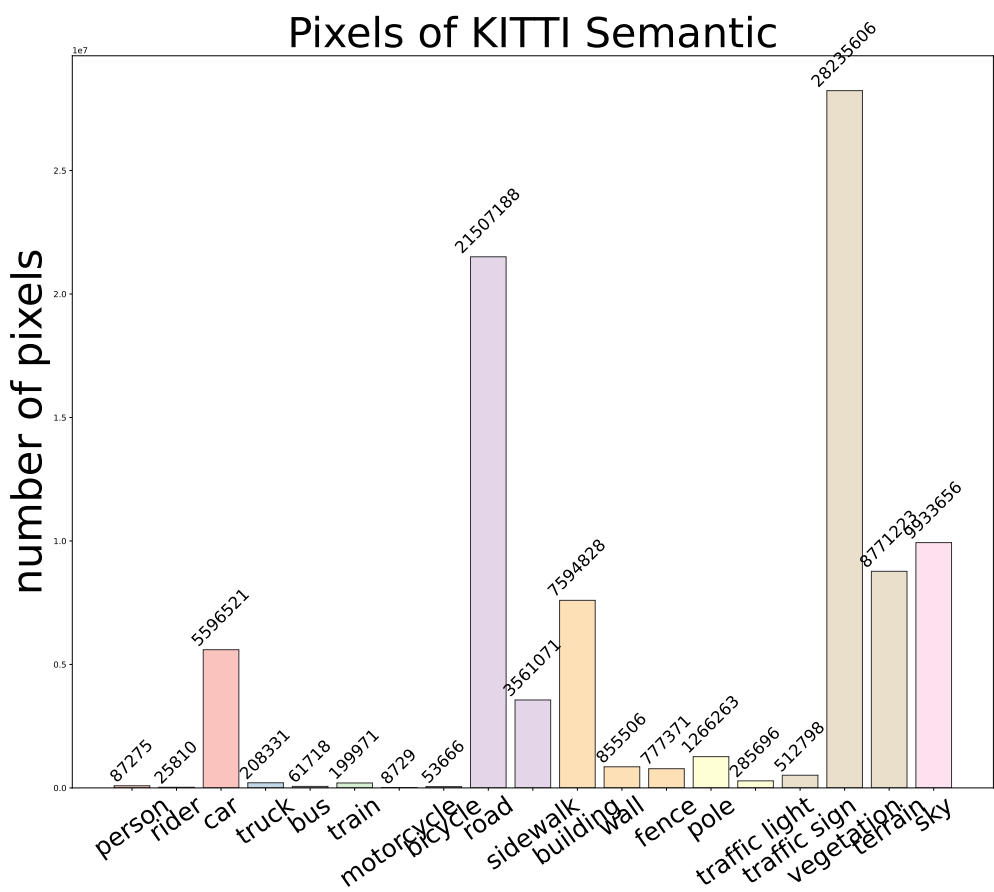


Figure 70. Pixel distribution of KITTI semantic.

## **16. 3D embedding with image patch**

This section contains 3D embedding result of CS-CARLA with image patches at each aggregated location.

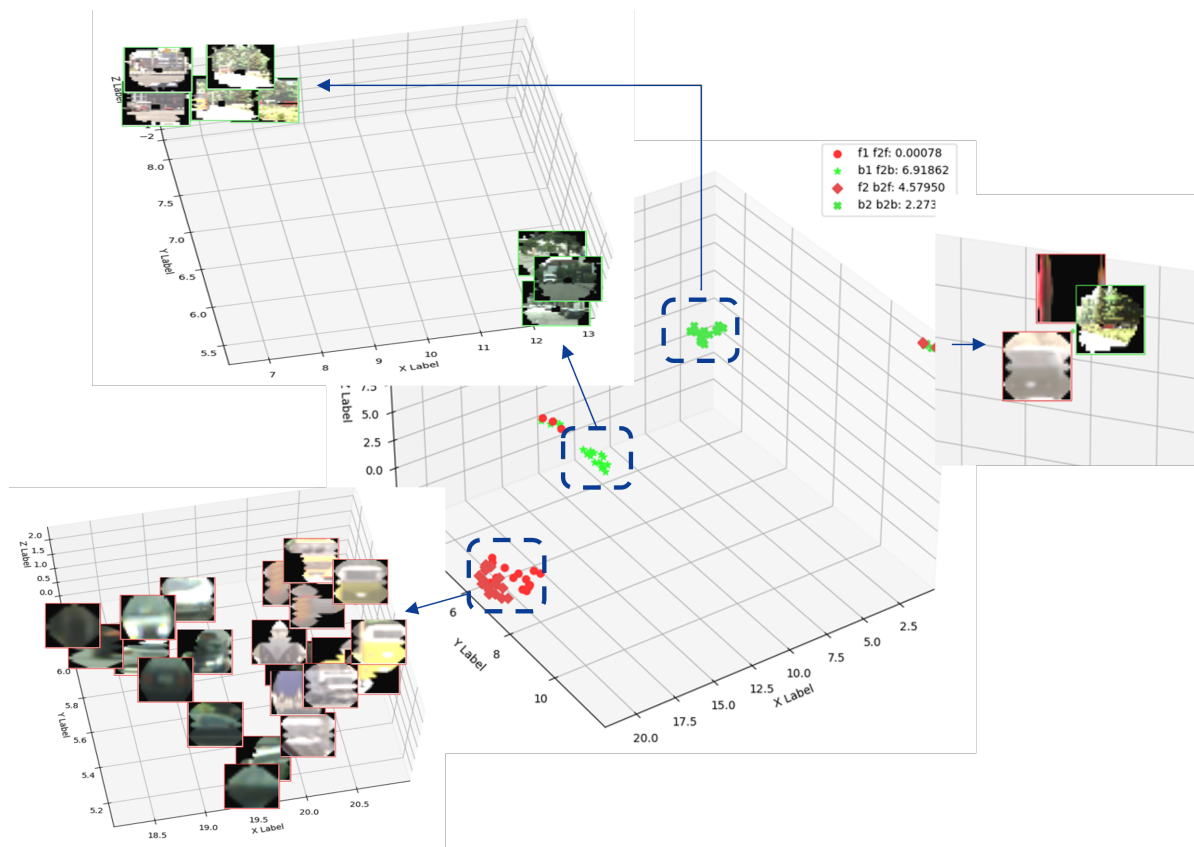


Figure 71. The 3D feature embedding results for CS-CARLA with image patches

## 17. Quantification results with YOLOv11

This section includes analysis results using YOLOv11.

Category	AP50	AP
person	-	39.136
truck	-	37.566
motorcycle	-	23.498
rider	-	39.701
bus	-	56.698
bicycle	-	28.720
car	-	60.100
train	-	27.338
<b>total</b>	<b>59.467</b>	39.095

Table 138. Training: Cityscapes. Validation: Cityscapes validation.

Category	AP50	AP
person	-	36.297
truck	-	26.304
motorcycle	-	19.945
rider	-	39.297
bus	-	43.760
bicycle	-	26.299
car	-	53.323
train	-	17.353
<b>total</b>	<b>49.502</b>	32.83

Table 139. Training: Cityscapes. Validation: Cityscapes Foggy validation all.

Layer	MMD mean			
	f2f	f2b	b2f	b2b
16	<b>0.062982</b>	46.527572	44.755515	0.739028
19	<b>0.021485</b>	33.528399	34.313704	0.385100
22	<b>0.063939</b>	49.361399	48.647746	1.886446

Table 140. Dataset: CS-CSV, Label: Car, Bin: 9

Layer	MVD mean			
	f2f	f2b	b2f	b2b
16	2.082891	2.768664	2.600703	2.235739
19	2.023870	2.480386	2.500061	2.051497
22	1.991999	2.581061	2.531971	1.971515

Table 141. Dataset: CS-CSV, Label: Car, Bin: 9

Layer	MMD mean			
	f2f	f2b	b2f	b2b
16	<b>0.001082</b>	48.304126	47.271472	0.316746
19	<b>0.000422</b>	43.704660	41.628886	1.214850
22	<b>0.006436</b>	55.798843	52.155659	2.215627

Table 142. Dataset: CS-CSV, Label: Person, Bin: 9

Layer	MVD mean			
	f2f	f2b	b2f	b2b
16	1.960343	2.573416	2.491306	2.023483
19	1.592186	2.651211	2.217081	2.216614
22	1.492126	3.311943	3.513309	1.975400

Table 143. Dataset: CS-CSV, Label: Person, Bin: 9

Layer	MMD mean			
	f2f	f2b	b2f	b2b
16	<b>0.003022</b>	49.215211	48.900521	0.359209
19	<b>0.001321</b>	40.103845	39.512206	0.694770
22	<b>0.039864</b>	56.192046	54.442013	1.584969

Table 144. Dataset: CS-CSV, Label: Bicycle, Bin: 9

Layer	MVD mean			
	f2f	f2b	b2f	b2b
16	2.230733	2.766177	2.818898	2.372704
19	2.171476	2.606431	2.676396	2.305838
22	3.153666	3.673676	3.407658	2.721582

Table 145. Dataset: CS-CSV, Label: Bicycle, Bin: 9

Layer	MMD mean			
	f2f	f2b	b2f	b2b
16	<b>0.000341</b>	48.350617	48.650631	0.234731
19	<b>0.006494</b>	39.833535	41.351455	0.646978
22	<b>0.002645</b>	55.750656	53.629656	1.461994

Table 146. Dataset: CS-CSV, Label: Rider, Bin: 9

Table 147. Dataset: CS-CSV, Label: Rider, Bin: 9

Table 148. MMD and MVD between Cityscapes and Cityscapes validation with YOLOv11.

Layer	MMD mean			
	f2f	f2b	b2f	b2b
16	<b>0.052369</b>	44.463880	44.449926	0.496768
19	<b>0.034595</b>	35.741977	34.263380	0.524899
22	<b>0.070419</b>	52.808069	47.863179	2.858149

Table 149. Dataset: CS-CSFV(0.01), Label: Car, Bin: 9

Layer	MVD mean			
	f2f	f2b	b2f	b2b
16	2.065351	2.728877	2.837551	2.233894
19	2.258033	2.975489	2.913789	2.448860
22	2.160244	3.065206	2.820929	2.627436

Table 150. Dataset: CS-CSFV(0.01), Label: Car, Bin: 9

Layer	MMD mean			
	f2f	f2b	b2f	b2b
16	<b>0.003848</b>	48.176220	48.276418	1.381587
19	<b>0.001514</b>	37.780063	43.631943	3.893865
22	<b>0.017657</b>	51.606834	55.297625	2.041304

Table 151. Dataset: CS-CSFV(0.01), Label: Person, Bin: 9

Layer	MVD mean			
	f2f	f2b	b2f	b2b
16	2.441030	3.065571	2.879739	2.834703
19	2.221090	2.844073	2.893038	2.923079
22	3.137492	3.757901	3.885831	2.926269

Table 152. Dataset: CS-CSFV(0.01), Label: Person, Bin: 9

Table 153. MMD and MVD between Cityscapes and Cityscapes foggy 0.01 with YOLOv11.

Layer	MMD mean			
	f2f	f2b	b2f	b2b
16	<b>0.002802</b>	48.780400	47.002906	1.857787
19	<b>0.006408</b>	38.230902	38.861622	2.255664
22	<b>0.017192</b>	55.024863	54.564572	2.540956

Table 154. Dataset: CS-CSFV(0.02), Label: Car, Bin: 9

Layer	MVD mean			
	f2f	f2b	b2f	b2b
16	2.138397	3.275905	2.848661	3.096649
19	2.196083	3.340245	2.868632	3.118983
22	3.123307	3.920284	3.048506	3.102361

Table 155. Dataset: CS-CSFV(0.02), Label: Car, Bin: 9

Layer	MMD mean			
	f2f	f2b	b2f	b2b
16	<b>0.000121</b>	49.264899	48.531709	1.154784
19	<b>0.000268</b>	38.410784	41.683570	4.211147
22	<b>0.001235</b>	57.679659	56.073639	6.379770

Table 156. Dataset: CS-CSFV(0.02), Label: Person, Bin: 9

Layer	MVD mean			
	f2f	f2b	b2f	b2b
16	2.350183	3.540801	2.983840	3.531022
19	3.238921	4.310045	3.734321	3.406865
22	0.442293	2.938622	2.451624	3.720328

Table 157. Dataset: CS-CSFV(0.02), Label: Person, Bin: 9

Table 158. **MMD and MVD between Cityscapes and Cityscapes foggy 0.02 with YOLOv11.**

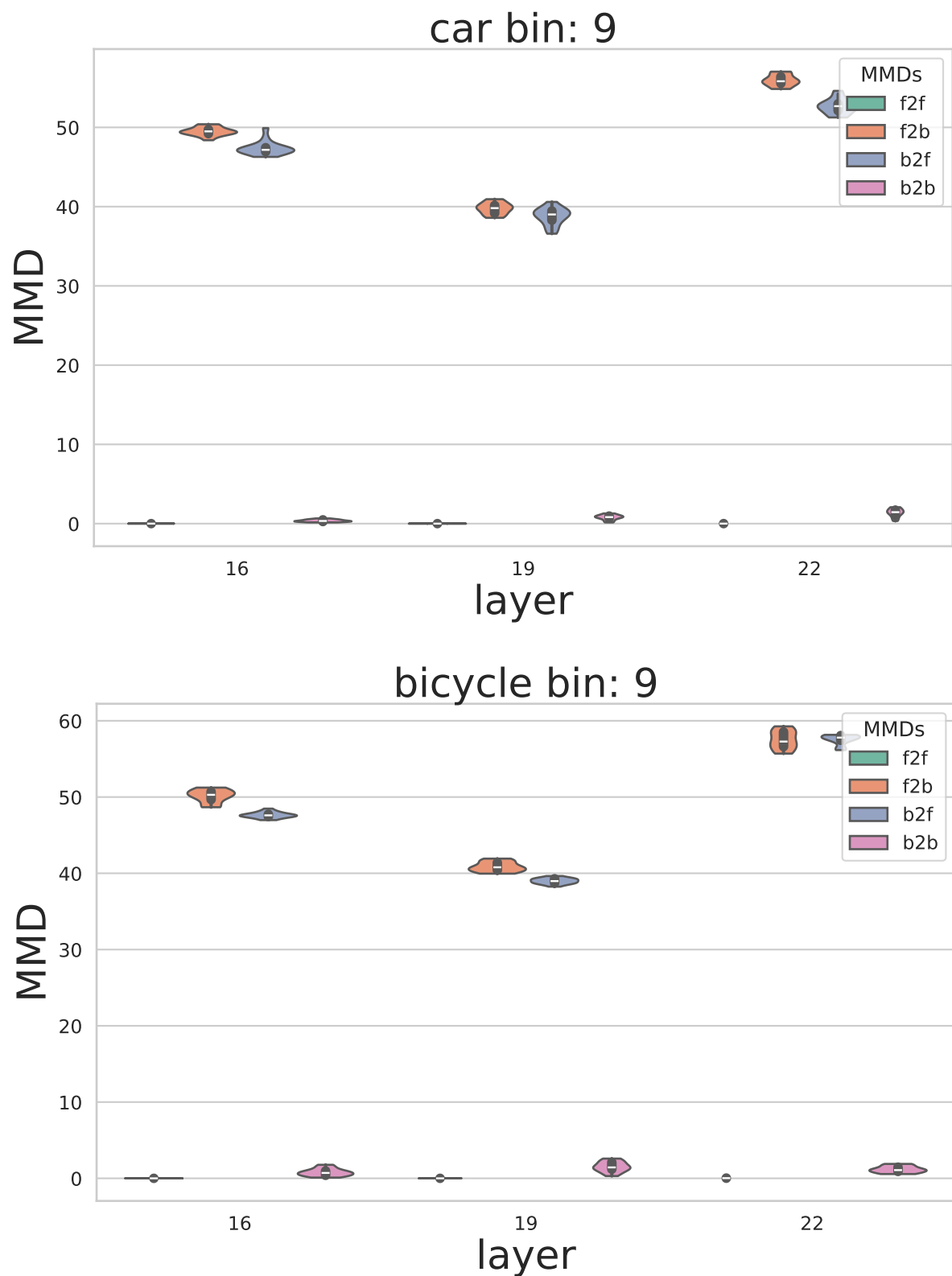


Figure 72. CS-CSV MMD plots YOLOv11.

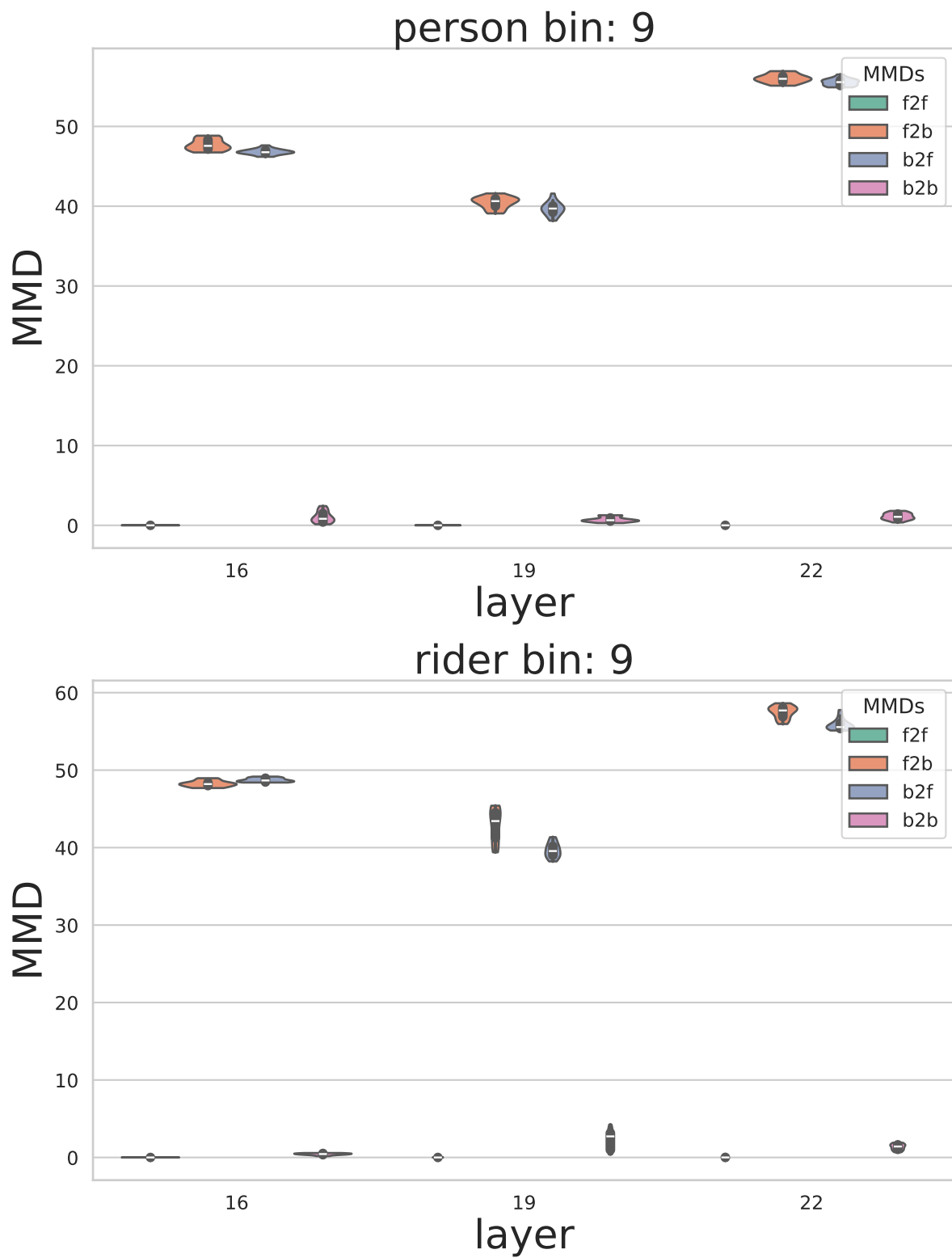


Figure 73. CS-CSV MMD plots YOLOv11.

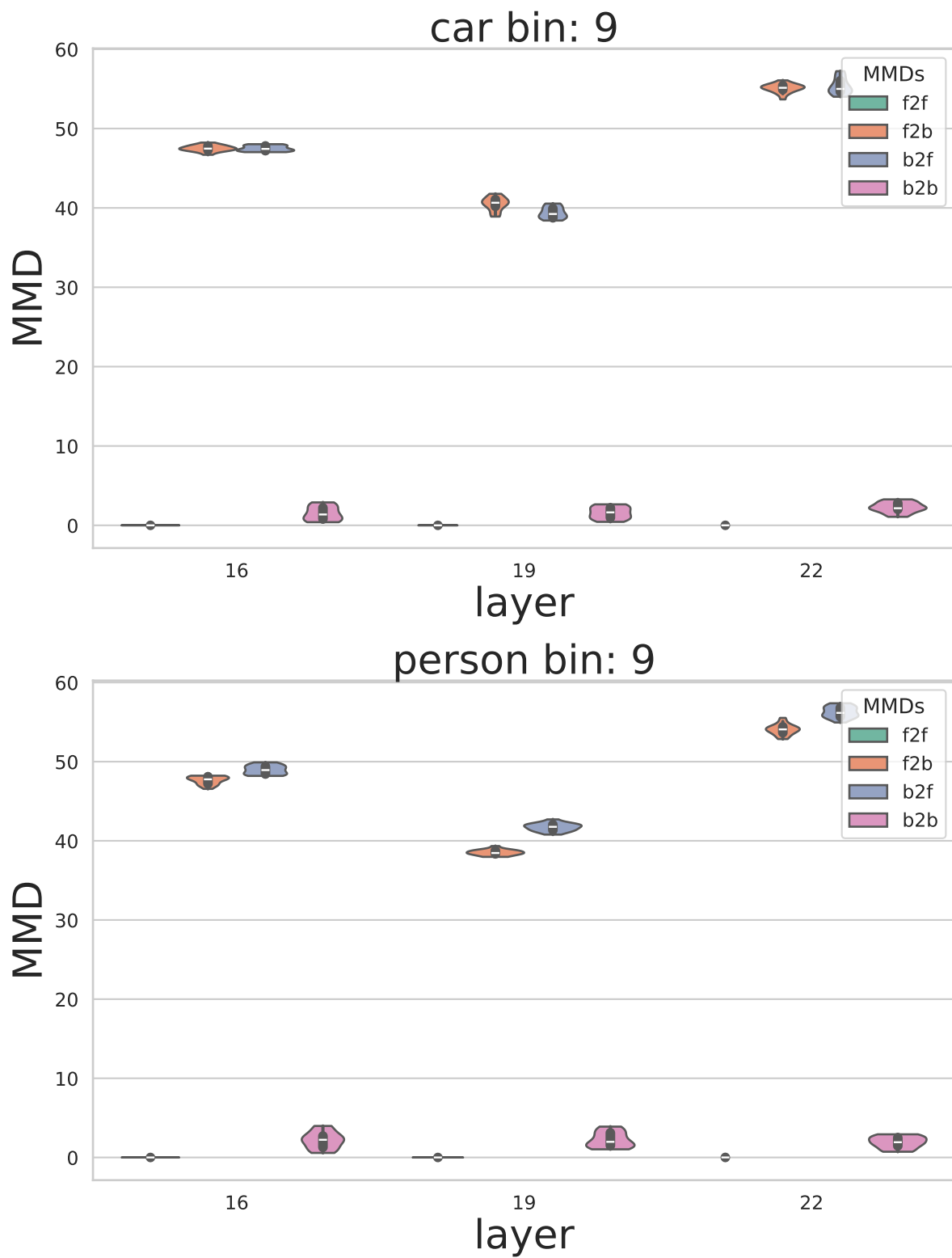


Figure 74. CS-CSFV(0.01) MMD plots YOLOv11.

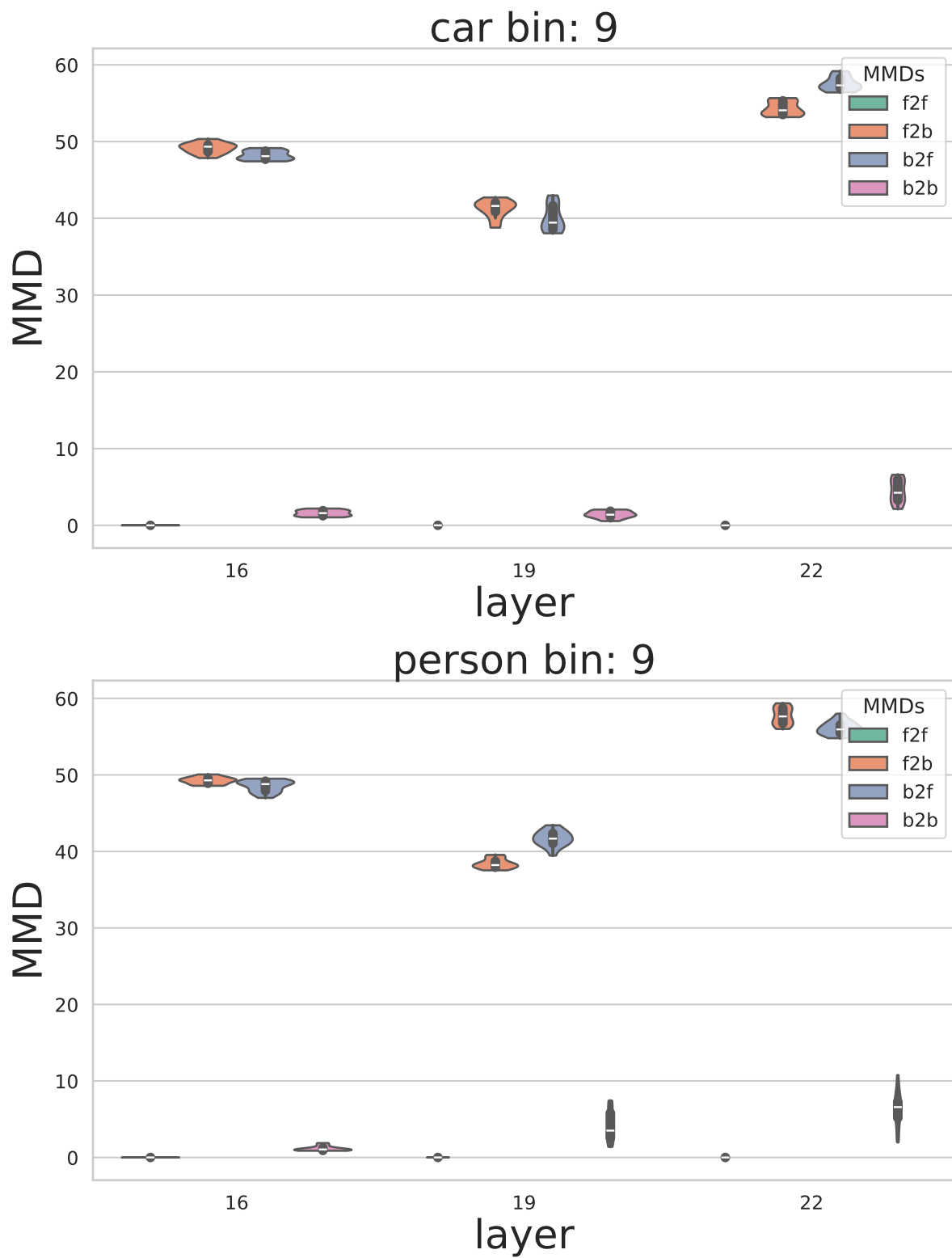
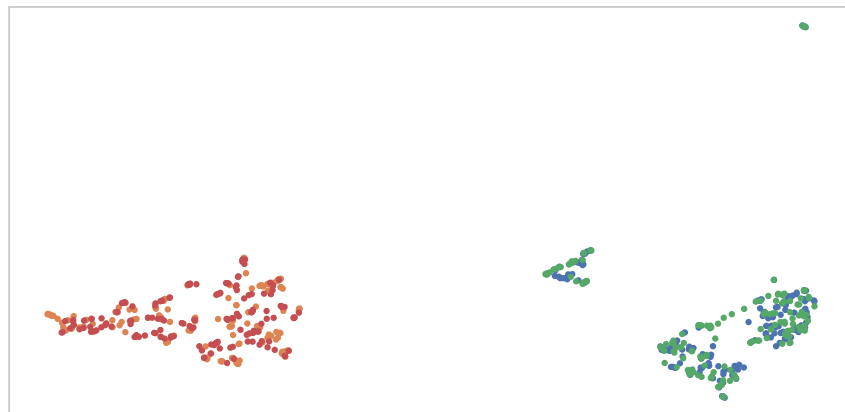


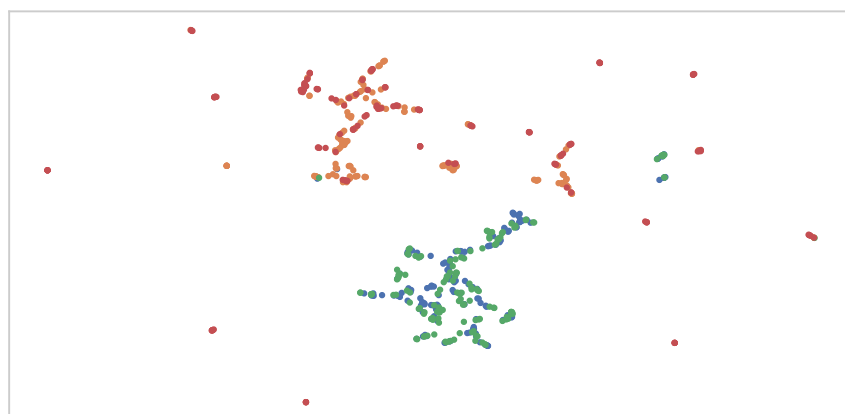
Figure 75. CS-CSFV(0.01) MMD plots YOLOv11.

c



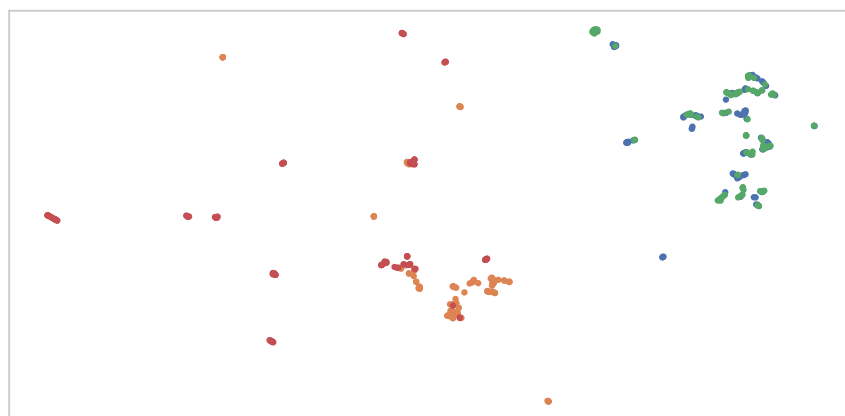
● FGS   ● BGS   ● FGT   ● BGT

(a) Dataset: CS-CSV, Label: Car



● FGS   ● BGS   ● FGT   ● BGT

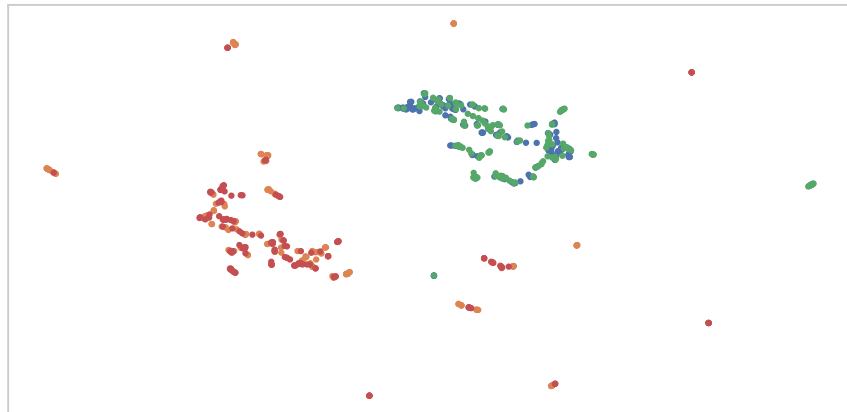
(b) Dataset: CS-CSFV(0.01), Label: Car



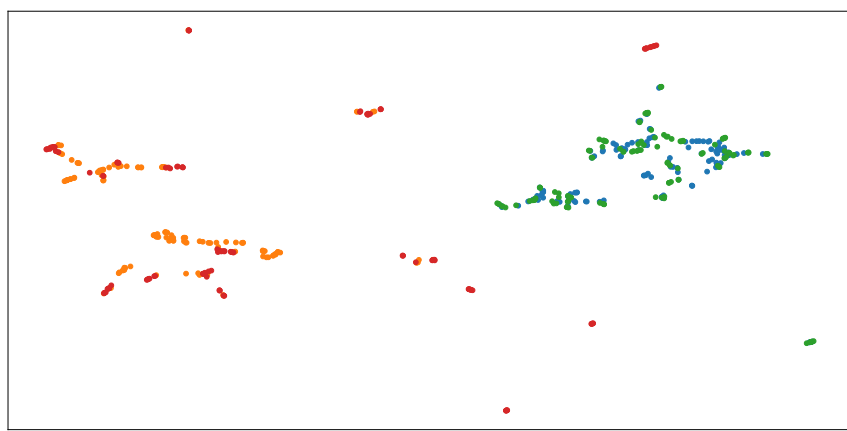
● FGS   ● BGS   ● FGT   ● BGT

(c) Dataset: CS-CSFV(0.02), Label: Car

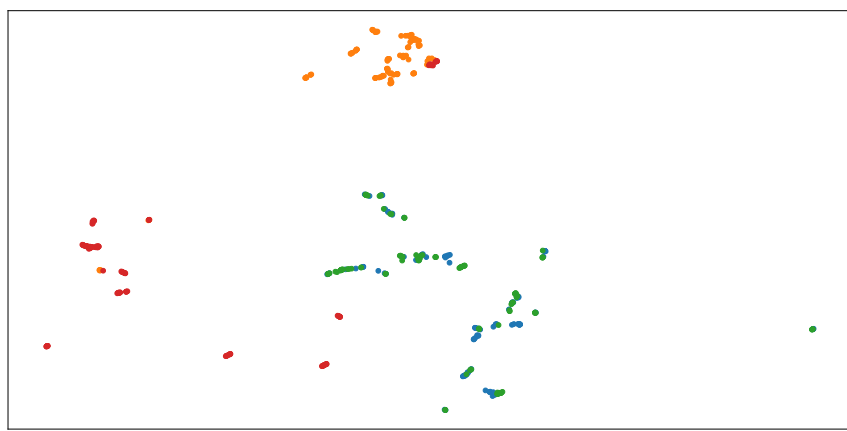
Figure 76. **Car 2D embedding YOLOv11.**



(a) Dataset: CS-CSV, Label: Person

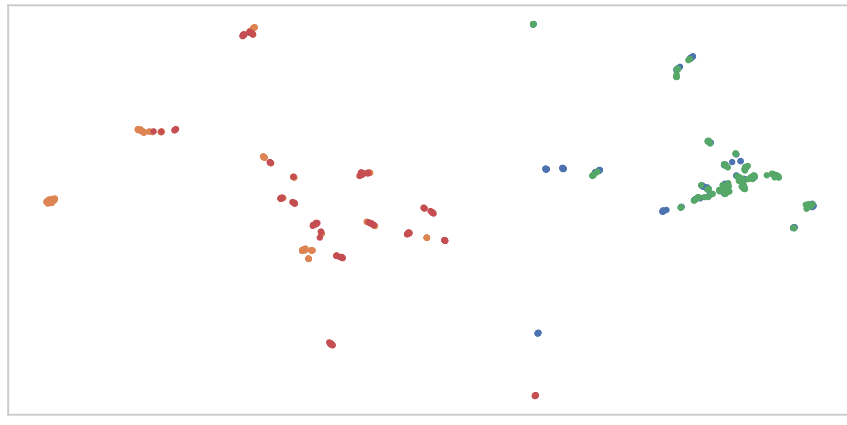


(b) Dataset: CS-CSFV(0.01), Label: Person

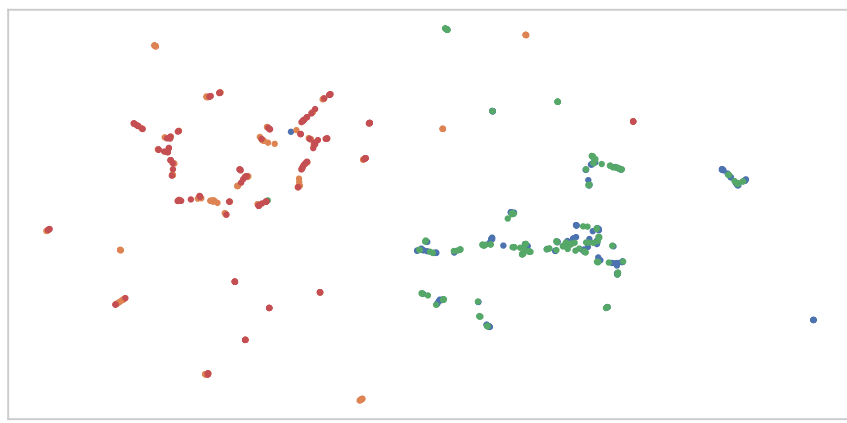


(c) Dataset: CS-CSFV(0.02), Label: Person

Figure 77. **Person 2D embedding YOLOv11.**



(a) Dataset: CS-CSV, Label: Rider



(b) Dataset: CS-CSV, Label: Bicycle

Figure 78. **Rider and Bicycle CS-CSV 2D embedding YOLOv11**

## Quantifying Context Bias in Domain Adaptation - Supplementary

Anonymous ICCV submission

Paper ID 14656

# Quantifying Context Bias in Domain Adaptation - Supplementary

## Supplementary Material

001

### 1. Description

002 This supplementary includes the outcomes of experiments  
 003 because of page limits:

004 1) evaluation of training results (Sec. 2), 2) number of instances of each dataset (Sec. 3), 3) heat ratio of foreground  
 005 and background (Sec. 4), 4) association matrix (Sec. 5), 5)  
 006 association graph (Sec. 6), 6) MMD and MVD tables with  
 007 various labels (Sec. 7), 7) MMD with different labels (Sec.  
 008 8), 8) pixel distribution of each dataset (Sec. 10), 9) UMAP  
 009 embedding results in different layers (Sec. 9), 10) 3D em-  
 010 bedding CS-CARLA with image patches (Sec. 11), and 11)  
 011 Quantification results with YOLOv11 (Sec. 12).

012

### 2. Evaluation results

014 This section presents the evaluation results across different  
 015 datasets.

Category	AP50	AP
person	-	40.126
truck	-	30.376
motorcycle	-	25.225
rider	-	43.699
bus	-	50.767
bicycle	-	34.554
car	-	56.398
train	-	25.914
<b>total</b>	<b>65.544</b>	38.382

Table 1. Training: Cityscapes. Validation: Cityscapes validation.

Category	AP50	AP
person	-	28.942
truck	-	8.051
motorcycle	-	16.606
rider	-	18.490
bus	-	20.403
bicycle	-	18.701
car	-	46.856
train	-	13.346
<b>total</b>	<b>36.084</b>	21.424

Table 3. Training: Cityscapes. Validation: KITTI semantic train

Category	AP50	AP
person	-	58.013
truck	-	59.062
motorcycle	-	35.752
rider	-	46.421
bus	-	58.673
bicycle	-	51.926
car	-	66.548
train	-	65.054
<b>total</b>	<b>86.660</b>	55.181

Table 4. Training: KITTI semantic train. Validation: KITTI semantic train

Category	AP50	AP
person	-	35.398
truck	-	18.712
motorcycle	-	14.679
rider	-	39.455
bus	-	33.538
bicycle	-	29.297
car	-	44.165
train	-	9.193
<b>total</b>	<b>46.321</b>	28.055

Table 2. Training: Cityscapes. Validation: Cityscapes foggy validation all.

Category	AP50	AP
person	-	24.072
truck	-	13.642
motorcycle	-	9.964
rider	-	22.429
bus	-	22.164
bicycle	-	17.779
car	-	39.317
train	-	7.411
<b>total</b>	<b>36.223</b>	19.597

Table 5. Training: KITTI semantic train. Validation: Cityscapes validation

Category	AP50	AP
person	-	15.646
truck	-	3.935
motorcycle	-	5.199
rider	-	17.623
bus	-	8.977
bicycle	-	13.425
car	-	25.612
train	-	2.341
<b>total</b>	<b>20.706</b>	11.595

Table 6. Training: KITTI semantic train. Validation: Cityscapes foggy validation all.

Val	car	van	truck	total(AP)	AP50
1	54.746	67.053	89.046	70.282	<b>81.568</b>
2	15.031	13.233	6.877	11.714	<b>15.101</b>
3	38.852	37.775	45.143	40.590	<b>50.430</b>
4	53.072	63.894	85.589	67.518	<b>80.428</b>
5	47.008	60.719	78.962	62.230	<b>77.144</b>
6	48.063	54.348	77.718	60.043	<b>73.081</b>
7	46.037	55.620	76.348	59.335	<b>71.923</b>
8	51.730	63.583	82.532	65.948	<b>79.119</b>
9	51.382	63.180	83.475	66.012	<b>79.303</b>
10	45.979	50.295	80.961	59.078	<b>73.782</b>

Table 7. Training: Virtual KITTI clone. Validation (Val): 1 - Virtual KITTI clone, 2 - Virtual KITTI fog, 3 - Virtual KITTI rain, 4 - Virtual KITTI 15 degree left, 5 - Virtual KITTI morning, 6 - Virtual KITTI overcast, 7 - Virtual KITTI sunset, 8 - Virtual KITTI 30 degree left, 9 - Virtual KITTI 15 degree left, 10 - Virtual KITTI 30 degree right

Val	car	truck	bus	total	AP50
1	64.968	67.053	68.883	66.926	<b>88.220</b>

Table 8. Training: CARLA train. Validation: CARLA validation

016 **3. Instances statistics**

017 This section provides statistics on the instances of the  
 018 datasets used for training and feature extraction.

Category	# Instances
person	3394
rider	543
car	4652
truck	93
bus	98
train	23
motorcycle	149
bicycle	1165
total	10117

Table 9. Instances statistics of Cityscapes validation

Category	# Instances
person	10182
rider	1629
car	13956
truck	279
bus	294
train	69
motorcycle	447
bicycle	3495
total	30351

Table 10. Instances statistics of Cityscapes foggy validation all.

Category	# Instances
person	100
rider	29
car	1678
truck	101
bus	19
train	18
motorcycle	8
bicycle	47
total	2000

Table 11. Instances statistics of KITTI semantic train.

Category	# Instances
Car	24603
Van	2054
Truck	461
total	27118

Table 12. Instances statistics of Virtual KITTI clone. Different weather conditions have the same statistics.

Category	# Instances
Car	24614
Van	1948
Truck	369
total	26931

Table 13. Instances statistics of Virtual KITTI 30 degree left.

Category	# Instances
car	6962
truck	2887
bus	789
total	10638

Table 14. Instances statistics of CARLA train.

Category	# Instances
car	1156
truck	421
bus	0
total	1577

Table 15. Instances statistics of CARLA validation

Category	# Instances
Car	24916
Van	2000
Truck	447
total	27363

Table 16. Instances statistics of Virtual KITTI 15 degree left.

Category	# Instances
Car	20165
Van	1443
Truck	389
total	21997

Table 17. Instances statistics of Virtual KITTI 30 degree right.

Category	# Instances
Car	23680
Van	1922
Truck	434
total	26036

Table 18. Instances statistics of Virtual KITTI 15 degree right.

019 **4. Heat ratio**

020 This section shows Smooth Grad-CAM++ correspondences  
021 with foreground region using instance masks. For all ac-  
022 tivated pixels via Smooth Grad-CAM++,  $A_c$ , of a particu-  
023 lar foreground object, we can divide  $A_c$  into activated fore-  
024 ground pixels  $f_c$  and activated background pixels  $b_c$ . The  
025 foreground heat ratio is then given by the activated fore-  
026 ground pixels over the total foreground pixels  $f_c/f$  while  
027 the background heat ratio is the activated background pix-  
028 els over the total foreground pixels  $b_c/f$  where  $f$  represents  
029 the total foreground pixels. The foreground and background  
030 heat ratios provide the amount of contextual information  
031 and validity of use of Smooth Grad-CAM++. Overall, the  
032 entire foreground region was activated and background re-  
033 gion was various depending on threshold during our exper-  
034 iments.

Layer	Heat ratio			
	FG mean	FG std	BG mean	BG std
res2_2	0.81	0.24	1.81	2.80
res3_3	0.80	0.24	1.85	3.23
res4_5	0.80	0.25	1.75	2.75
res5_2	0.77	0.27	0.76	1.12

Table 19. Dataset: Cityscapes, Label: Car, Bin: 1

Layer	Heat ratio			
	FG mean	FG std	BG mean	BG std
res2_2	0.79	0.24	1.29	2.01
res3_3	0.79	0.24	1.30	2.04
res4_5	0.79	0.25	1.39	2.57
res5_2	0.76	0.27	0.81	0.27

Table 21. Dataset: Cityscapes foggy 0.01, Label: Person, Bin: 1

Layer	Heat ratio			
	FG mean	FG std	BG mean	BG std
res2_2	0.74	0.24	1.0	5.7
res3_3	0.74	0.24	0.82	1.79
res4_5	0.74	0.25	0.89	1.98
res5_2	0.72	0.26	0.61	1.11

Table 23. Dataset: Cityscapes foggy 0.02, Label: Car, Bin: 1

Layer	Heat ratio			
	FG mean	FG std	BG mean	BG std
res2_2	0.85	0.2	5.28	17.76
res3_3	0.85	0.2	3.30	5.36
res4_5	0.84	0.21	2.58	3.89
res5_2	0.82	0.24	0.82	1.04

Table 25. Dataset: CARLA, Label: Car, Bin: 1

Layer	Heat ratio			
	FG mean	FG std	BG mean	BG std
res2_2	0.81	0.19	2.35	3.67
res3_3	0.81	0.19	2.37	3.85
res4_5	0.79	0.21	1.68	2.28
res5_2	0.79	0.27	0.73	1.05

Table 27. Dataset: KITTI semantic, Label: Car, Bin: 1

Layer	Heat ratio			
	FG mean	FG std	BG mean	BG std
res2_2	0.77	0.22	3.81	10.28
res3_3	0.77	0.22	3.40	6.88
res4_5	0.75	0.24	1.79	2.52
res5_2	0.71	0.29	0.70	0.98

Table 29. Dataset: Virtual KITTI, Label: Car, Bin: 1

Table 31. Heat ratio of Cityscapes. Label: Car

Layer	Heat ratio			
	FG mean	FG std	BG mean	BG std
res2_2	1.0	0.03	44.43	67.04
res3_3	1.0	0.03	45.25	73.18
res4_5	1.0	0.03	44.76	64.97
res5_2	1.0	0.03	26.81	25.96

Table 20. Dataset: Cityscapes, Label: Car, Bin: 9

Layer	Heat ratio			
	FG mean	FG std	BG mean	BG std
res2_2	1.0	0.0	32.76	47.70
res3_3	1.0	0.0	32.99	48.89
res4_5	1.0	0.0	35.47	58.04
res5_2	1.0	0.0	26.07	28.41

Table 22. Dataset: Cityscapes foggy 0.01, Label: Car, Bin: 9

Layer	Heat ratio			
	FG mean	FG std	BG mean	BG std
res2_2	1.0	0.0	24.56	86.45
res3_3	1.0	0.0	22.11	35.97
res4_5	1.0	0.0	23.37	39.77
res5_2	1.0	0.0	20.66	25.86

Table 24. Dataset: Cityscapes foggy 0.02, Label: Car, Bin: 9

Layer	Heat ratio			
	FG mean	FG std	BG mean	BG std
res2_2	1.0	0.0	78.77	228.56
res3_3	1.0	0.0	53.06	73.71
res4_5	1.0	0.0	44.59	51.49
res5_2	1.0	0.0	22.95	18.59

Table 26. Dataset: CARLA, Label: Car, Bin: 9

Layer	Heat ratio			
	FG mean	FG std	BG mean	BG std
res2_2	1.0	0.0	74.43	119.17
res3_3	1.0	0.0	76.10	129.94
res4_5	1.0	0.0	63.38	86.72
res5_2	1.0	0.0	32.84	29.50

Table 28. Dataset: KITTI semantic, Label: Car, Bin: 9

Layer	Heat ratio			
	FG mean	FG std	BG mean	BG std
res2_2	1.0	0.0	63.59	176.25
res3_3	1.0	0.0	56.10	116.33
res4_5	1.0	0.0	32.25	40.88
res5_2	1.0	0.0	18.96	15.74

Table 30. Dataset: Virtual KITTI, Label: Car, Bin: 9

Layer	Heat ratio			
	FG mean	FG std	BG mean	BG std
res2_2	0.92	0.16	2.92	3.31
res3_3	0.92	0.16	2.92	3.34
res4_5	0.92	0.17	2.59	3.12
res5_2	0.9	0.20	1.12	1.47

Table 32. Dataset: Cityscapes, Label: Person, Bin: 1

Layer	Heat ratio			
	FG mean	FG std	BG mean	BG std
res2_2	0.93	0.14	25.53	44.49
res3_3	0.93	0.14	25.30	43.94
res4_5	0.93	0.15	27.31	51.37
res5_2	0.92	0.17	18.70	27.04

Table 34. Dataset: Cityscapes, Label: Bicycle, Bin: 1

Layer	Heat ratio			
	FG mean	FG std	BG mean	BG std
res2_2	0.8	0.21	2.37	3.03
res3_3	0.8	0.21	2.37	2.97
res4_5	0.8	0.23	2.53	3.34
res5_2	0.73	0.29	1.17	1.21

Table 36. Dataset: Cityscapes, Label: Rider, Bin: 1

Table 38. Heat ratio of non-car labels of Cityscapes

Layer	Heat ratio			
	FG mean	FG std	BG mean	BG std
res2_2	0.92	0.16	2.92	3.31
res3_3	0.92	0.16	2.92	3.34
res4_5	0.92	0.17	2.59	3.12
res5_2	0.9	0.20	1.12	1.47

Table 39. Dataset: Cityscapes foggy 0.01, Label: Person, Bin: 1

Layer	Heat ratio			
	FG mean	FG std	BG mean	BG std
res2_2	0.82	0.2	1.7	1.62
res3_3	0.83	0.2	1.71	1.67
res4_5	0.83	0.21	1.69	1.68
res5_2	0.80	0.24	1.31	1.53

Table 41. Dataset: Cityscapes foggy 0.01, Label: Bicycle, Bin: 1

Layer	Heat ratio			
	FG mean	FG std	BG mean	BG std
res2_2	0.74	0.24	1.77	2.35
res3_3	0.74	0.24	1.86	3.06
res4_5	0.73	0.26	1.86	2.42
res5_2	0.72	0.29	1.21	1.39

Table 43. Dataset: Cityscapes foggy 0.01, Label: Rider, Bin: 1

Layer	Heat ratio			
	FG mean	FG std	BG mean	BG std
res2_2	1.0	0.0	73.94	93.65
res3_3	1.0	0.0	74.06	95.34
res4_5	1.0	0.0	68.99	84.17
res5_2	1.0	0.0	37.37	28.80

Table 33. Dataset: Cityscapes, Label: Person, Bin: 9

Layer	Heat ratio			
	FG mean	FG std	BG mean	BG std
res2_2	1.0	0.0	48.96	53.44
res3_3	1.0	0.0	48.52	52.69
res4_5	1.0	0.0	52.36	63.36
res5_2	1.0	0.0	36.15	29.18

Table 35. Dataset: Cityscapes, Label: Bicycle, Bin: 9

Layer	Heat ratio			
	FG mean	FG std	BG mean	BG std
res2_2	1.0	0.0	59.26	78.25
res3_3	1.0	0.0	59.90	78.95
res4_5	1.0	0.0	63.75	84.67
res5_2	1.0	0.0	37.69	28.27

Table 37. Dataset: Cityscapes, Label: Rider, Bin: 9

Layer	Heat ratio			
	FG mean	FG std	BG mean	BG std
res2_2	1.0	0.0	52.96	64.47
res3_3	1.0	0.0	54.65	78.83
res4_5	1.0	0.0	55.07	70.81
res5_2	1.0	0.0	36.18	29.91

Table 40. Dataset: Cityscapes foggy 0.01, Label: Person, Bin: 9

Layer	Heat ratio			
	FG mean	FG std	BG mean	BG std
res2_2	0.99	0.07	39.15	37.81
res3_3	0.99	0.07	39.45	39.84
res4_5	0.99	0.07	38.18	33.54
res5_2	0.99	0.08	35.53	31.37

Table 42. Dataset: Cityscapes foggy 0.01, Label: Bicycle, Bin: 9

Layer	Heat ratio			
	FG mean	FG std	BG mean	BG std
res2_2	1.0	0.0	46.40	59.50
res3_3	1.0	0.0	49.66	84.49
res4_5	1.0	0.0	46.22	51.15
res5_2	1.0	0.0	39.93	33.55

Table 44. Dataset: Cityscapes foggy 0.01, Label: Rider, Bin: 9

Table 45. Heat ratio of non-car labels of Cityscapes foggy 0.01

Layer	Heat ratio			
	FG mean	FG std	BG mean	BG std
res2_2	0.9	0.17	2.13	7.57
res3_3	0.9	0.18	2.03	4.30
res4_5	0.89	0.18	1.94	2.41
res5_2	0.88	0.20	1.15	1.5

Table 46. Dataset: Cityscapes foggy 0.02, Label: Person, Bin: 1

Layer	Heat ratio			
	FG mean	FG std	BG mean	BG std
res2_2	0.81	0.18	1.3	1.16
res3_3	0.82	0.18	1.32	1.39
res4_5	0.81	0.19	1.33	1.65
res5_2	0.81	0.23	1.36	1.69

Table 48. Dataset: Cityscapes foggy 0.02, Label: Bicycle, Bin: 1

Layer	Heat ratio			
	FG mean	FG std	BG mean	BG std
res2_2	1.0	0.0	49.19	89.27
res3_3	1.0	0.0	48.66	65.85
res4_5	1.0	0.0	49.06	58.13
res5_2	1.0	0.0	36.40	31.73

Table 47. Dataset: Cityscapes foggy 0.02, Label: Person, Bin: 9

Layer	Heat ratio			
	FG mean	FG std	BG mean	BG std
res2_2	1.0	0.0	29.02	26.75
res3_3	1.0	0.0	29.90	34.22
res4_5	1.0	0.0	30.75	42.19
res5_2	1.0	0.0	32.01	30.92

Table 49. Dataset: Cityscapes foggy 0.02, Label: Bicycle, Bin: 9

Table 50. Heat ratio of non-car labels of Cityscapes foggy 0.02

Layer	Heat ratio			
	FG mean	FG std	BG mean	BG std
res2_2	0.85	0.18	1.76	1.93
res3_3	0.85	0.18	1.77	2.02
res4_5	0.84	0.19	1.88	2.39
res5_2	0.83	0.22	1.18	1.33

Table 51. Dataset: Cityscapes validation, Label: Car, Bin: 1

Layer	Heat ratio			
	FG mean	FG std	BG mean	BG std
res2_2	0.91	0.17	2.48	2.75
res3_3	0.91	0.17	2.62	3.56
res4_5	0.90	0.17	2.38	2.86
res5_2	0.89	0.20	1.09	1.39

Table 53. Dataset: Cityscapes validation, Label: Person, Bin: 1

Layer	Heat ratio			
	FG mean	FG std	BG mean	BG std
res2_2	0.79	0.24	1.63	2.48
res3_3	0.79	0.24	1.65	2.54
res4_5	0.79	0.25	1.60	2.49
res5_2	0.75	0.27	0.81	1.23

Table 55. Dataset: Cityscapes validation, Label: Bicycle, Bin: 1

Layer	Heat ratio			
	FG mean	FG std	BG mean	BG std
res2_2	0.77	0.23	1.73	1.83
res3_3	0.77	0.23	1.73	1.96
res4_5	0.78	0.24	1.87	2.27
res5_2	0.74	0.29	1.08	1.09

Table 57. Dataset: Cityscapes validation, Label: Rider, Bin: 1

Layer	Heat ratio			
	FG mean	FG std	BG mean	BG std
res2_2	1.0	0.02	39.38	58.87
res3_3	1.0	0.02	39.65	59.53
res4_5	1.0	0.02	40.22	60.05
res5_2	1.0	0.02	25.74	25.51

Table 52. Dataset: Cityscapes validation, Label: Car, Bin: 9

Layer	Heat ratio			
	FG mean	FG std	BG mean	BG std
res2_2	1.0	0.0	60.62	76.07
res3_3	1.0	0.0	64.18	94.67
res4_5	1.0	0.0	60.31	74.19
res5_2	1.0	0.0	35.33	27.09

Table 54. Dataset: Cityscapes validation, Label: Person, Bin: 9

Layer	Heat ratio			
	FG mean	FG std	BG mean	BG std
res2_2	1.0	0.0	39.94	41.21
res3_3	1.0	0.0	40.03	41.78
res4_5	1.0	0.0	43.01	51.92
res5_2	1.0	0.0	33.66	27.41

Table 56. Dataset: Cityscapes validation, Label: Bicycle, Bin: 9

Layer	Heat ratio			
	FG mean	FG std	BG mean	BG std
res2_2	1.0	0.0	45.55	53.82
res3_3	1.0	0.0	46.10	58.77
res4_5	1.0	0.0	48.52	60.15
res5_2	1.0	0.0	37.29	27.85

Table 58. Dataset: Cityscapes validation, Label: Rider, Bin: 9

Table 59. Heat ratio of non-car labels of Cityscapes validation

035 **5. Association Matrix**

036 This section shows association matrix of Cityscapes, KITTI  
037 semantic, CARLA, and Virtual KITTI.

038 Figure 1 illustrates an example of *Droprate* computa-  
039 tion.

040  $DET1$  = number of original detections / the number of  
041 ground truth detections

042  $DET2$  = the number of no loss with background modi-  
043 fication / the number of ground truth detections.

044 *Droprate* is defined as subtraction of  $DET1$  and  
045  $DET2$ .

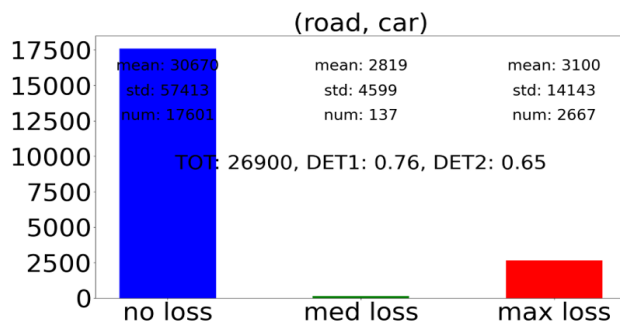


Figure 1. “TOT” means the total number of cars in Cityscapes dataset. Without modification road regions, the trained model could detect 76% of car objects and with the modification, it dropped 65%. *Droprate* is 0.11 for the (road, car) pair.

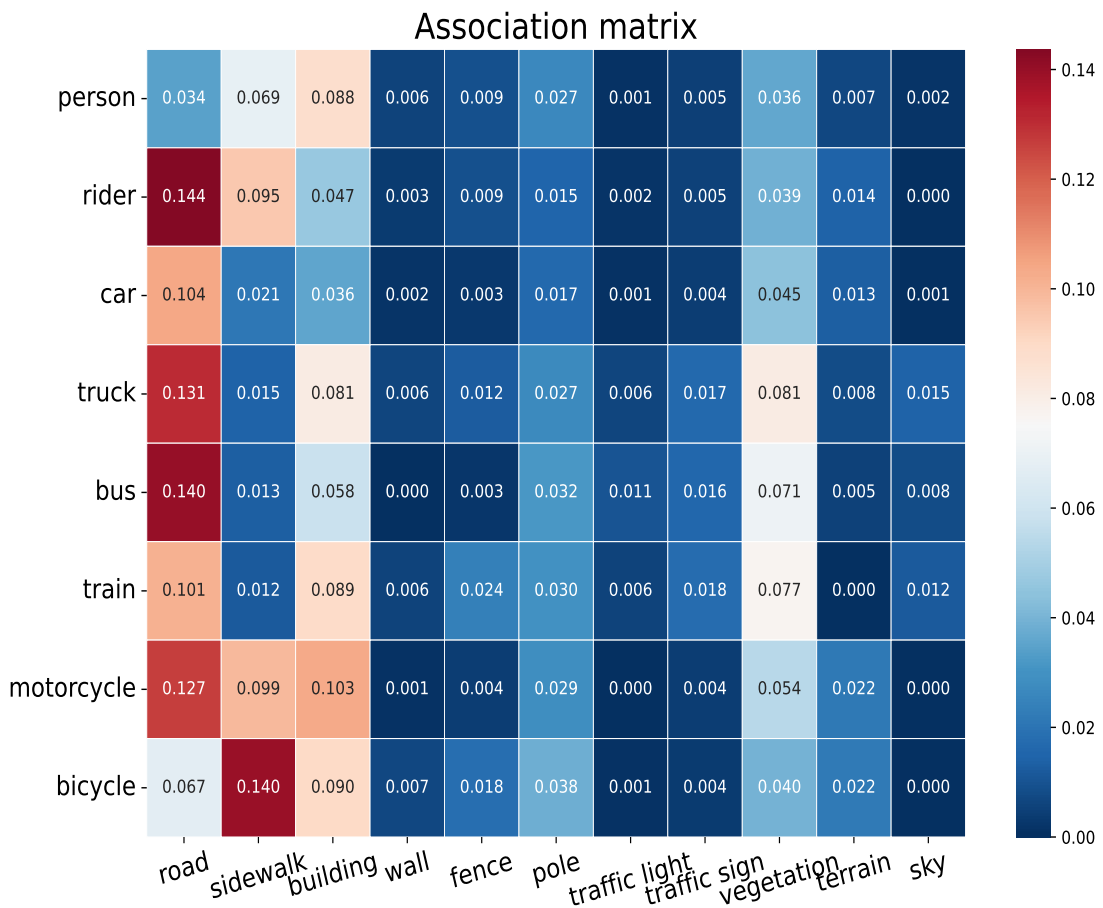


Figure 2. Association matrix Cityscapes.

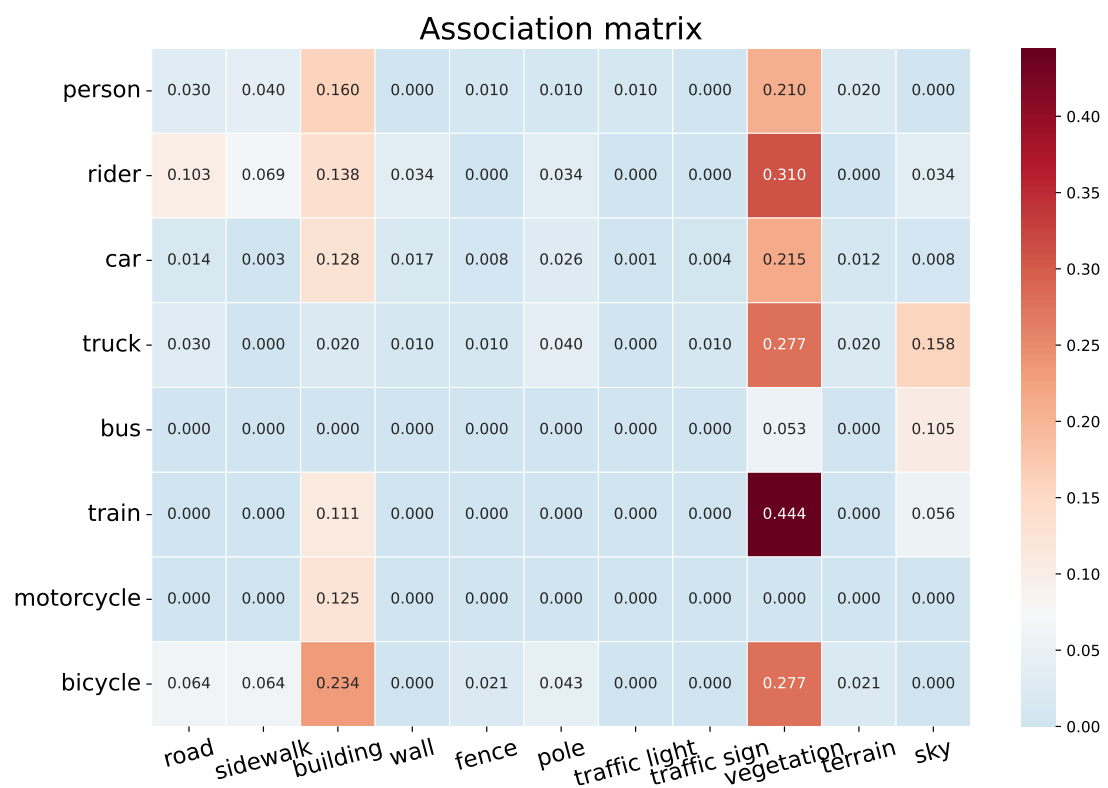
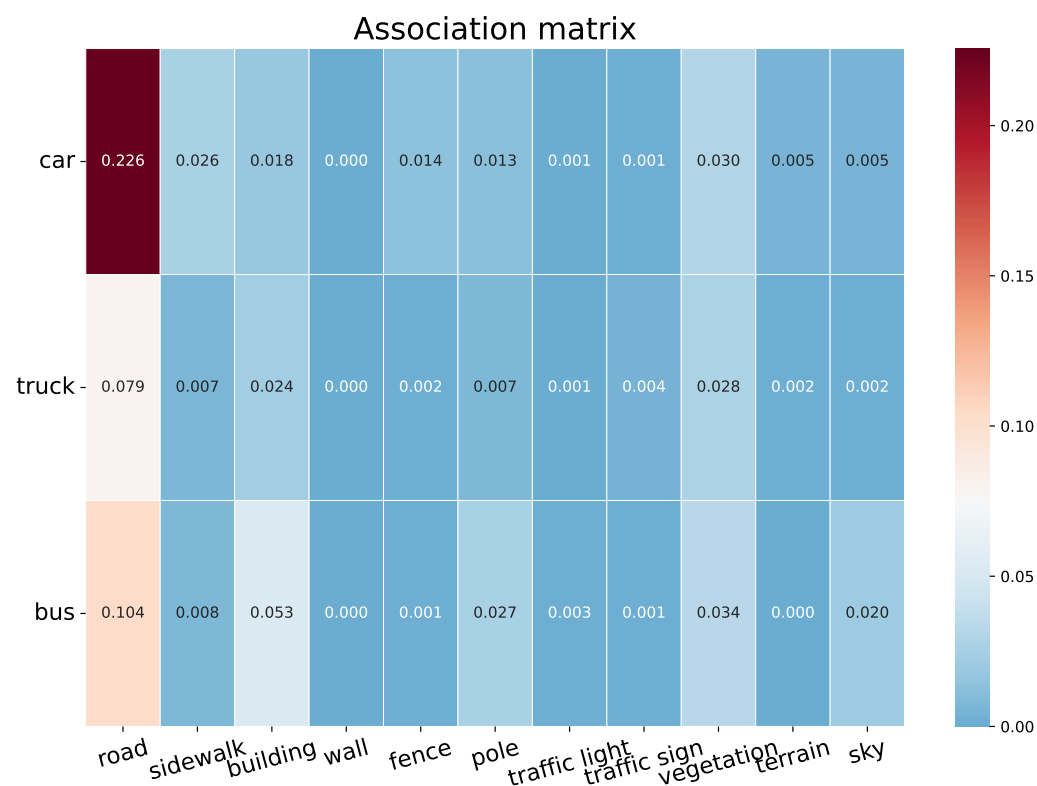


Figure 3. Association matrix KITTI semantic.

Figure 4. **Association matrix CARLA.**

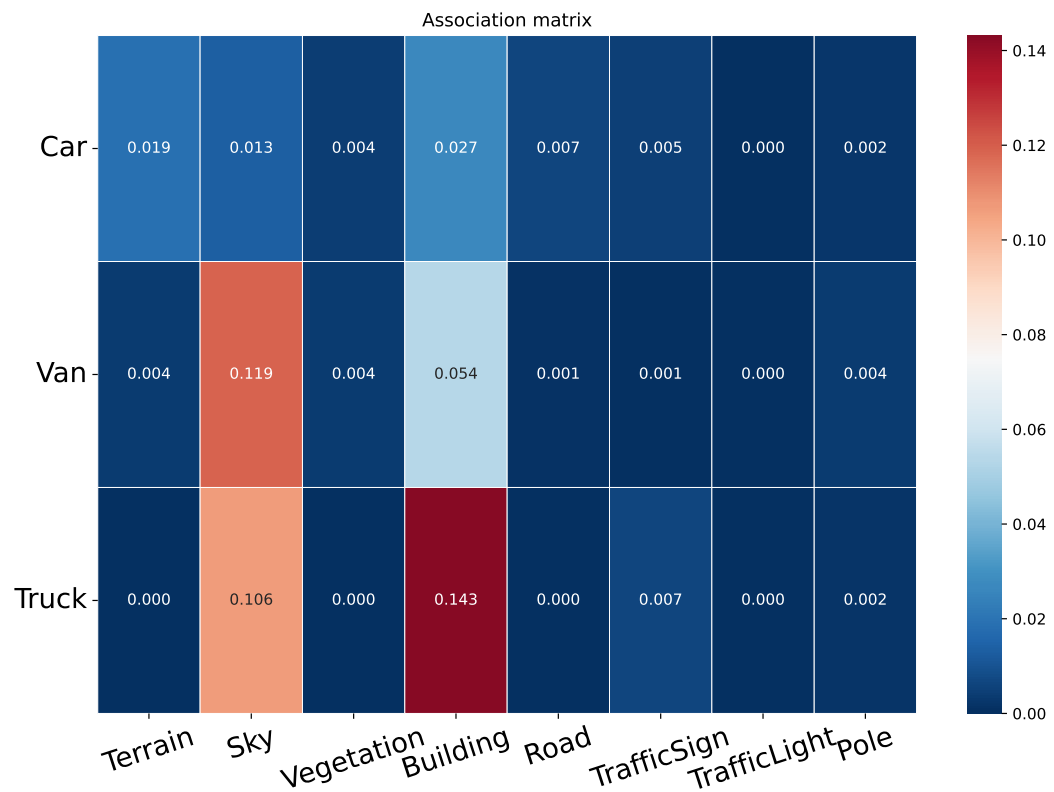


Figure 5. Association matrix Virtual KITTI.

046    **6. Association Graph**

047    This section presents the association graph of Cityscapes,  
048    KITTI semantic, CARLA, and Virtual KITTI.

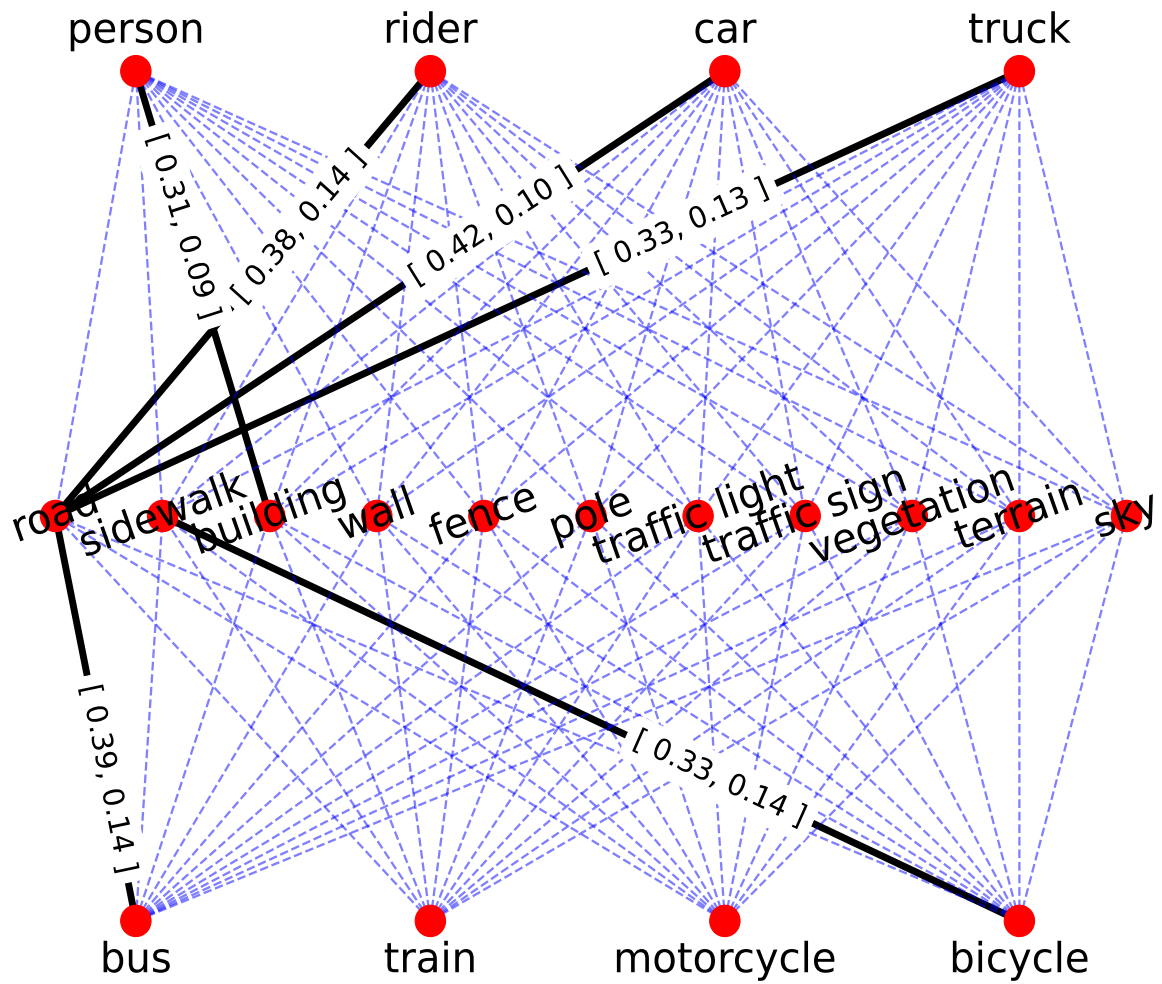


Figure 6. Association graph Cityscapes.

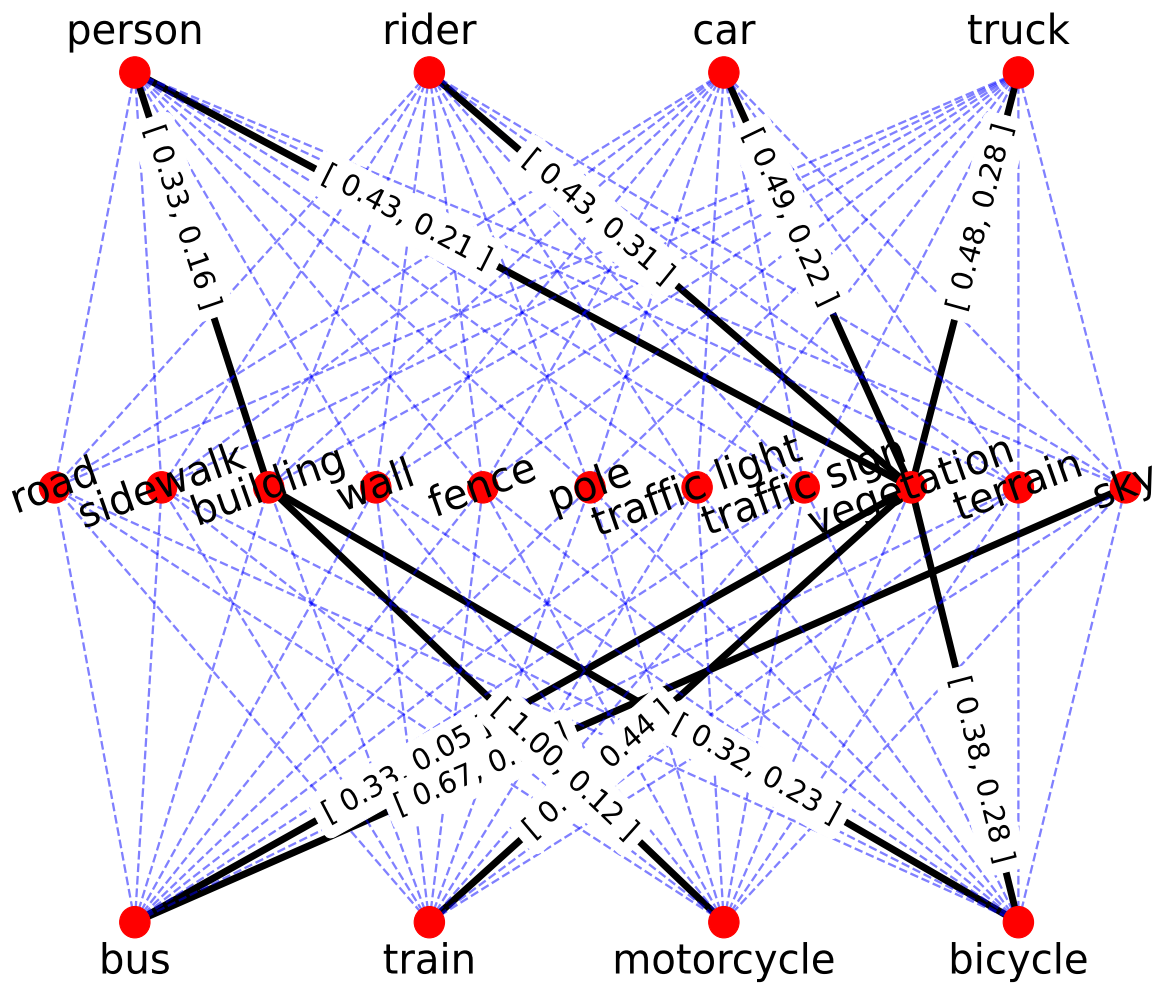


Figure 7. **Association graph KITTI semantic.** (bus,vegetation): [0.33, 0.05], (bus,sky): [0.67,0.11], (train,vegetation): [0.73,0.44]

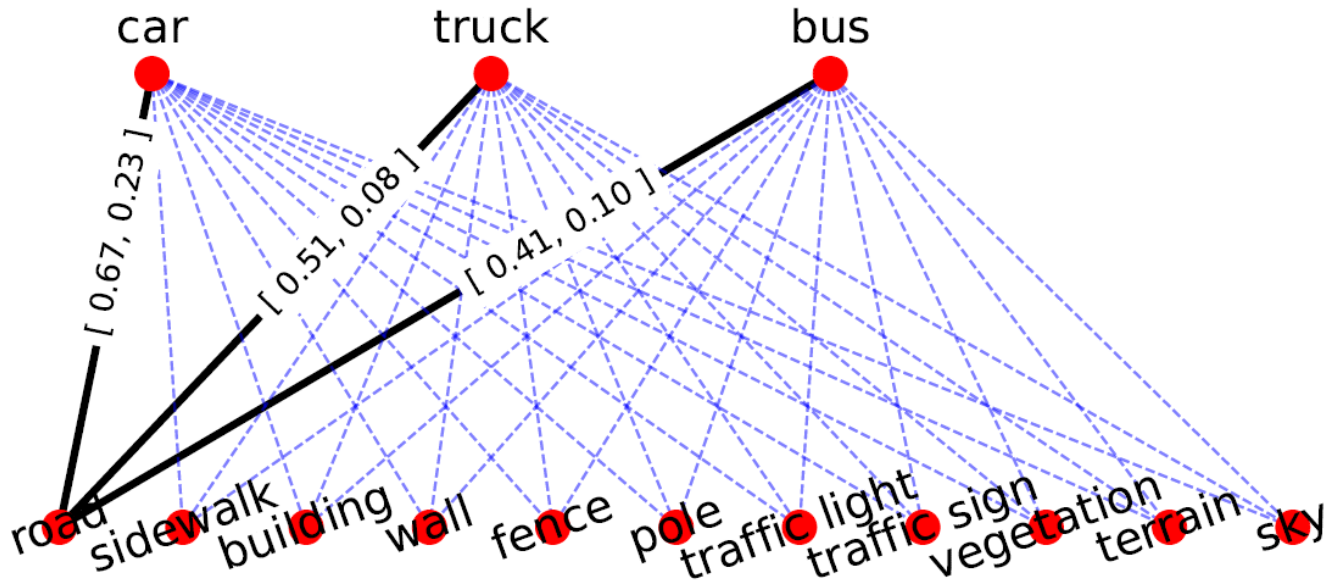


Figure 8. Association graph CARLA

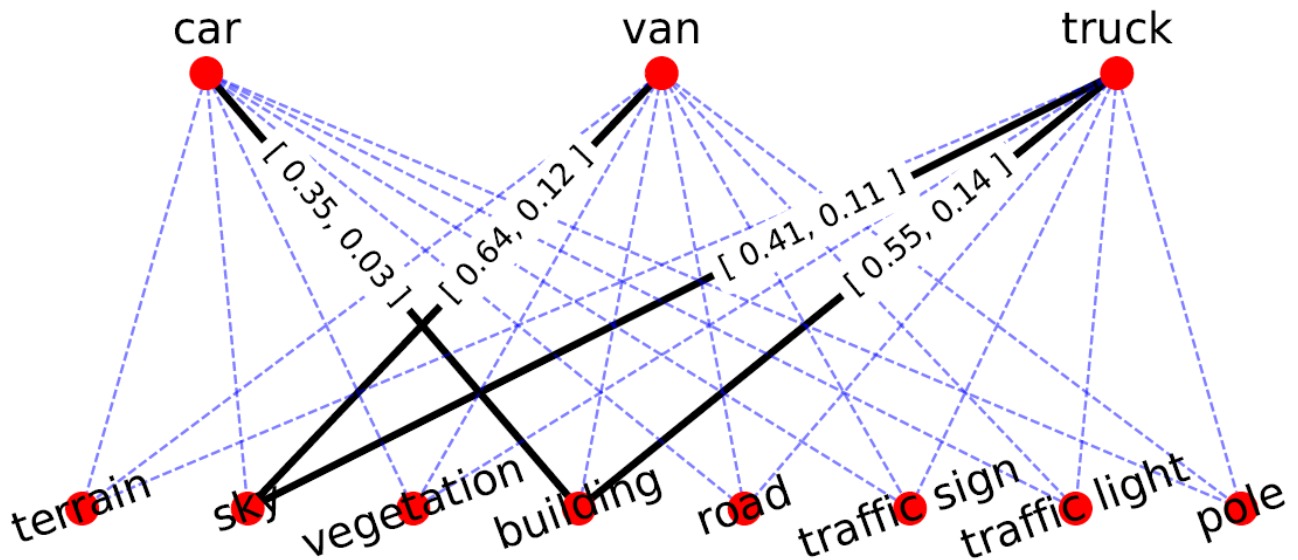


Figure 9. Association graph Virtual KITTI.

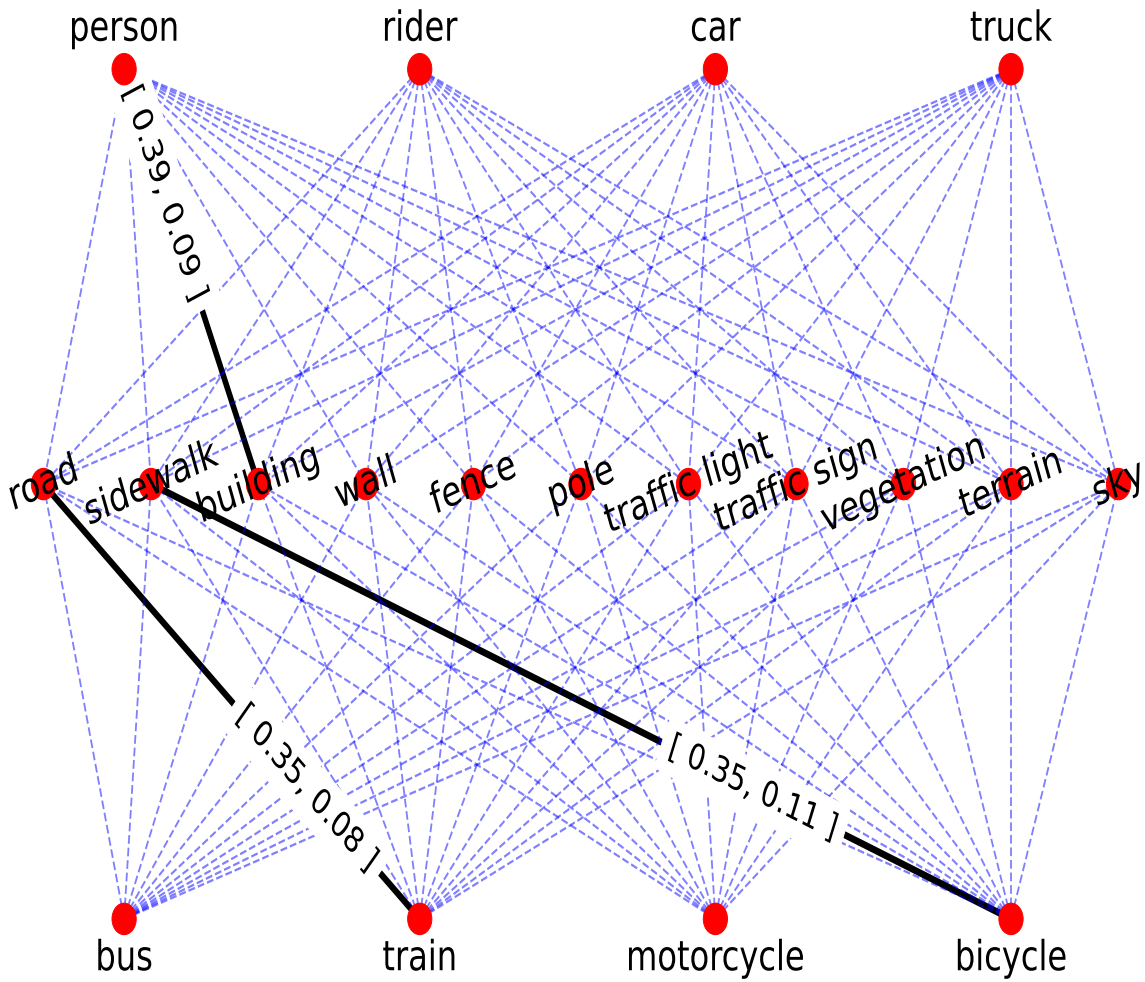


Figure 10. Association graph Cityscapes with MIC.

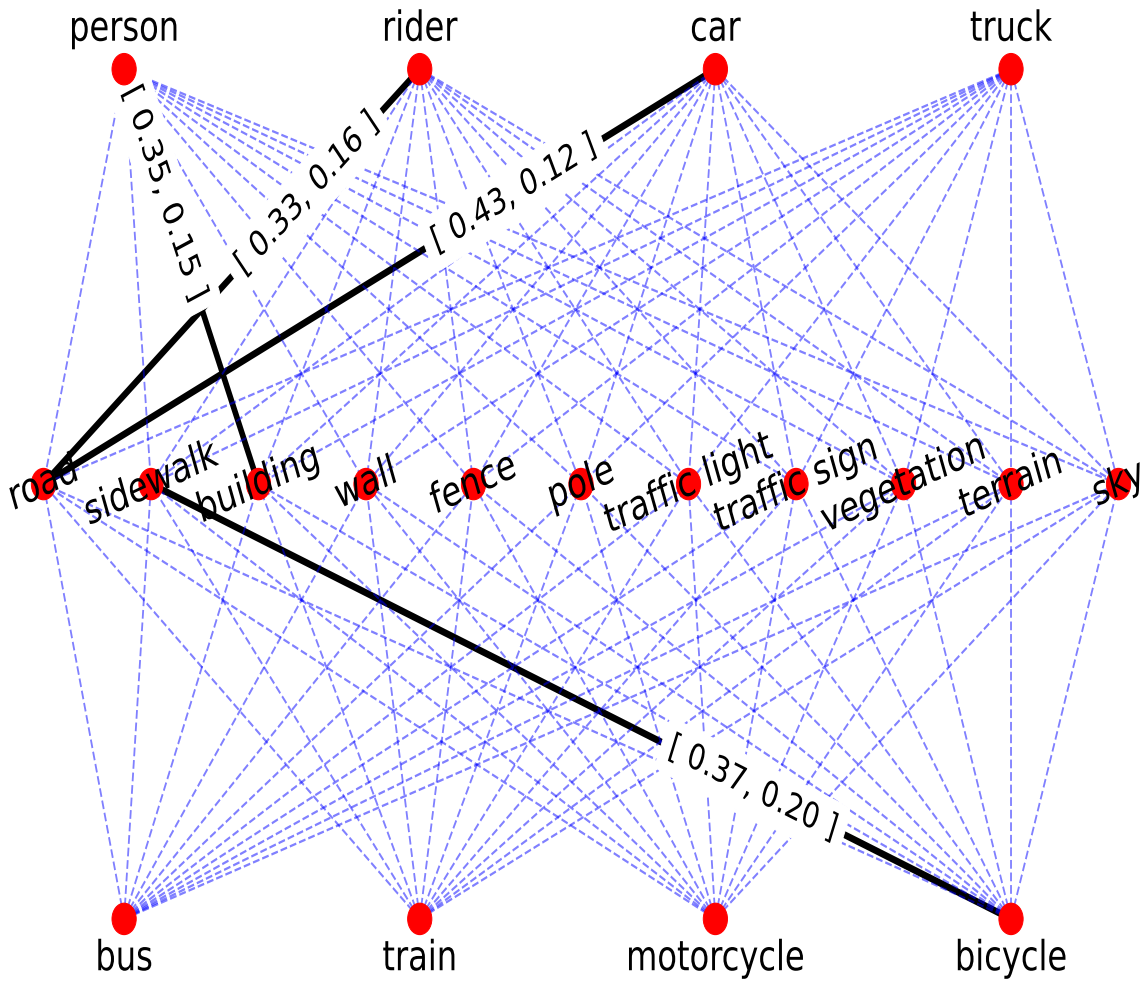


Figure 11. Association graph Cityscapes with ALDI++.

049    **7. MMD and MVD Table**

050    This section contains the MMD and MVD across different  
051    domains.

Layer	MMD mean			
	f2f	f2b	b2f	b2b
res2_2	0.48597	7.520155	3.976121	<b>0.034143</b>
res3_3	0.279831	0.784058	0.49827	<b>0.008149</b>
res4_5	0.219191	0.714354	0.558228	<b>0.009553</b>
res5_2	0.465037	1.025705	0.411115	<b>0.012313</b>

Table 60. Dataset: CS-CSFV(0.01), Label: car, Bin: 1

Layer	MMD mean			
	f2f	f2b	b2f	b2b
res2_2	0.837967	9.278673	5.501331	<b>0.022671</b>
res3_3	0.545075	1.579772	1.34774	<b>0.006316</b>
res4_5	1.048955	2.660388	1.979247	<b>0.010752</b>
res5_2	1.213613	3.251228	1.754225	<b>0.018963</b>

Table 62. Dataset: KS-VK, Label: car, Bin: 1

Layer	MMD mean			
	f2f	f2b	b2f	b2b
res2_2	1.360337	13.39255	8.77936	<b>0.012672</b>
res3_3	1.006295	1.659392	2.757476	<b>0.007218</b>
res4_5	1.657877	3.228704	2.850062	<b>0.023023</b>
res5_2	1.084457	2.052765	2.509785	<b>0.014955</b>

Table 64. Dataset: CARLA-KS, Label: car, Bin: 1

Layer	MMD mean			
	f2f	f2b	b2f	b2b
res2_2	0.627815	9.902885	5.965082	<b>0.003665</b>
res3_3	0.615928	1.481266	1.443983	<b>0.002998</b>
res4_5	1.160176	2.663172	1.76238	<b>0.020648</b>
res5_2	0.878996	2.366584	1.085149	<b>0.012676</b>

Table 66. Dataset: CARLA-VK, Label: car, Bin: 1

Layer	MMD mean			
	f2f	f2b	b2f	b2b
res2_2	<b>1.929408</b>	75.95716	39.86969	5.954215
res3_3	<b>0.784393</b>	9.541647	12.91833	7.142425
res4_5	<b>0.931707</b>	9.65685	10.33697	5.973624
res5_2	<b>1.354234</b>	11.40708	16.86537	9.518532

Table 61. Dataset: CS-CSFV(0.01), Label: car, Bin: 9

Layer	MMD mean			
	f2f	f2b	b2f	b2b
res2_2	<b>1.701219</b>	30.11269	61.23091	20.14374
res3_3	<b>2.898878</b>	9.565176	17.82692	9.921293
res4_5	<b>3.847768</b>	18.5432	15.08211	10.13089
res5_2	<b>3.891656</b>	17.04114	27.30131	16.7562

Table 63. Dataset: KS-VK, Label: car, Bin: 9

Layer	MMD mean			
	f2f	f2b	b2f	b2b
res2_2	<b>3.183262</b>	69.27134	44.71856	18.60363
res3_3	<b>3.062511</b>	16.40809	23.81949	16.98051
res4_5	<b>3.930751</b>	18.59529	25.63895	22.29927
res5_2	<b>3.950112</b>	30.34706	42.61812	33.30783

Table 65. Dataset: CARLA-KS, Label: car, Bin: 9

Layer	MMD mean			
	f2f	f2b	b2f	b2b
res2_2	<b>4.07898</b>	38.00771	44.54776	14.14914
res3_3	<b>3.656437</b>	9.317527	25.74601	18.75477
res4_5	<b>4.998009</b>	18.28671	33.85126	29.11955
res5_2	<b>5.166857</b>	18.48426	54.46207	41.99809

Table 67. Dataset: CARLA-VK, Label: car, Bin: 9

Table 68. “Car” label MMD across other datasets. The lowest values are highlighted in bold.

Layer	MMD mean			
	f2f	f2b	b2f	b2b
res2_2	<b>0.002588</b>	0.005147	0.010467	0.012556
res3_3	0.000992	0.005338	0.006035	<b>0.000693</b>
res4_5	<b>0.008631</b>	0.012306	0.025341	0.008826
res5_2	<b>0.004781</b>	0.01386	0.016515	0.004828

Table 69. Dataset: CS-CSV, Label: Person, Bin: 1

Layer	MMD mean			
	f2f	f2b	b2f	b2b
res2_2	<b>0.007112</b>	43.16728	33.35849	1.326029
res3_3	<b>0.015106</b>	5.815366	3.460745	0.492159
res4_5	<b>0.004296</b>	3.961384	3.551943	0.224099
res5_2	<b>0.012289</b>	4.934453	5.327017	0.322196

Table 70. Dataset: CS-CSV, Label: Person, Bin: 9

Layer	MMD mean			
	f2f	f2b	b2f	b2b
res2_2	0.020487	0.006696	0.027399	<b>0.004261</b>
res3_3	0.001779	0.003611	0.006618	<b>0.001257</b>
res4_5	0.005283	0.017598	0.016919	<b>0.002194</b>
res5_2	0.008838	0.016117	0.015965	<b>0.004058</b>

Table 71. Dataset: CS-CSV, Label: Bicycle, Bin: 1

Layer	MMD mean			
	f2f	f2b	b2f	b2b
res2_2	<b>0.034208</b>	37.02699	27.83576	0.850653
res3_3	<b>0.012528</b>	4.389391	3.770594	0.149715
res4_5	<b>0.004156</b>	3.142533	3.765164	0.219377
res5_2	<b>0.005631</b>	3.758185	4.059784	0.164122

Table 72. Dataset: CS-CSV, Label: Bicycle, Bin: 9

Layer	MMD mean			
	f2f	f2b	b2f	b2b
res2_2	0.002653	0.002351	0.001569	<b>0.00188</b>
res3_3	<b>0.000731</b>	0.001856	0.001826	0.000775
res4_5	<b>0.002486</b>	0.008231	0.007975	0.004156
res5_2	0.003608	0.006807	0.007905	<b>0.00264</b>

Table 73. Dataset: CS-CSV, Label: Rider, Bin: 1

Layer	MMD mean			
	f2f	f2b	b2f	b2b
res2_2	<b>0.012084</b>	31.35223	32.10123	0.232441
res3_3	<b>0.001812</b>	3.521889	3.420648	0.106992
res4_5	<b>0.003306</b>	4.706572	2.788121	0.587758
res5_2	<b>0.003795</b>	3.965521	3.294167	0.305498

Table 74. Dataset: CS-CSV, Label: Rider, Bin: 9

Table 75. MMD for non-car labels between Cityscapes and Cityscapes validation.

Layer	MMD mean			
	f2f	f2b	b2f	b2b
res2_2	0.012706	0.02892	0.011056	<b>0.002405</b>
res3_3	0.009049	0.011817	0.01295	<b>0.004601</b>
res4_5	0.008535	0.01387	0.015293	<b>0.00595</b>
res5_2	0.033776	0.018467	0.050713	<b>0.009092</b>

Table 76. Dataset: CS-CSFV(0.01), Label: Person, Bin: 1

Layer	MMD mean			
	f2f	f2b	b2f	b2b
res2_2	<b>0.022442</b>	43.01485	37.45594	1.370968
res3_3	<b>0.020119</b>	4.622701	3.734675	1.755346
res4_5	<b>0.011593</b>	3.842468	3.364573	1.326394
res5_2	<b>0.024133</b>	6.014653	5.61746	2.983906

Table 77. Dataset: CS-CSFV(0.01), Label: Person, Bin: 9

Layer	MMD mean			
	f2f	f2b	b2f	b2b
res2_2	<b>0.079213</b>	47.07988	41.98639	1.40932
res3_3	<b>0.006467</b>	4.824563	4.173671	1.93347
res4_5	<b>0.01469</b>	3.879474	3.593062	1.470991
res5_2	<b>0.048684</b>	5.987271	4.586958	2.817607

Table 78. Dataset: CS-CSFV(0.01), Label: Bicycle, Bin: 1

Layer	MMD mean			
	f2f	f2b	b2f	b2b
res2_2	<b>0.001002</b>	29.86252	18.17271	2.760283
res3_3	<b>0.000388</b>	2.548376	2.227595	1.074819
res4_5	<b>0.000858</b>	3.606037	2.066544	1.463306
res5_2	<b>0.000741</b>	6.765415	3.495808	2.904991

Table 80. Dataset: CS-CSFV(0.01), Label: Rider, Bin: 1

Table 81. Dataset: CS-CSFV(0.01), Label: Rider, Bin: 9

Table 82. MMD for non-car labels between Cityscapes and Cityscapes foggy 0.01.

Layer	MMD mean			
	f2f	f2b	b2f	b2b
res2_2	0.041437	0.012486	0.066193	<b>0.007482</b>
res3_3	0.014406	0.011046	0.021534	<b>0.008058</b>
res4_5	0.014034	0.022386	0.027688	<b>0.008207</b>
res5_2	0.021939	0.027792	0.020891	<b>0.006338</b>

Table 83. Dataset: CS-CSFV(0.02), Label: Person, Bin: 1

Layer	MMD mean			
	f2f	f2b	b2f	b2b
res2_2	<b>0.028824</b>	57.38695	36.7982	4.730632
res3_3	<b>0.016363</b>	5.833781	4.020378	2.590734
res4_5	<b>0.010052</b>	4.37115	3.505711	1.842766
res5_2	<b>0.030776</b>	8.124074	4.471739	3.923804

Table 84. Dataset: CS-CSFV(0.02), Label: Person, Bin: 9

Layer	MMD mean			
	f2f	f2b	b2f	b2b
res2_2	0.069257	0.018532	0.080604	<b>0.011693</b>
res3_3	0.008585	0.008696	0.008337	<b>0.004168</b>
res4_5	0.017052	0.02381	0.03436	<b>0.007328</b>
res5_2	0.02084	0.01877	0.028686	<b>0.008349</b>

Table 85. Dataset: CS-CSFV(0.02), Label: Bicycle, Bin: 1

Layer	MMD mean			
	f2f	f2b	b2f	b2b
res2_2	<b>0.217501</b>	57.61874	30.51592	7.320393
res3_3	<b>0.036501</b>	5.757158	5.640691	3.037142
res4_5	<b>0.023576</b>	4.001144	3.928058	1.982261
res5_2	<b>0.032258</b>	6.698612	3.487616	3.109783

Table 86. Dataset: CS-CSFV(0.02), Label: Bicycle, Bin: 9

Table 87. MMD for non-car labels between Cityscapes and Cityscapes foggy 0.02.

Layer	MVD mean			
	f2f	f2b	b2f	b2b
res2_2	1.859608	1.942252	2.138036	1.954259
res3_3	1.940999	2.190022	2.181403	2.125913
res4_5	1.866465	2.523028	2.373373	1.999623
res5_2	1.952171	2.624203	2.58357	2.456547

Table 88. Dataset: CS-CSV, Label: car, Bin: 1

Layer	MVD mean			
	f2f	f2b	b2f	b2b
res2_2	1.779225	2.391159	2.297817	2.017024
res3_3	2.069057	2.331817	2.625383	2.074096
res4_5	2.216897	2.763882	2.686462	2.42473
res5_2	2.212517	2.989791	2.954901	2.349637

Table 89. Dataset: CS-CSV, Label: car, Bin: 9

Layer	MVD mean			
	f2f	f2b	b2f	b2b
res2_2	2.15856	2.190183	2.074836	2.034821
res3_3	2.367371	2.450545	2.27529	2.351622
res4_5	2.653691	3.03468	2.548423	2.859754
res5_2	3.130844	3.103544	3.366491	2.490507

Table 90. Dataset: CS-CSFV(0.01), Label: car, Bin: 1

Layer	MVD mean			
	f2f	f2b	b2f	b2b
res2_2	2.494561	2.705416	2.8487	2.833095
res3_3	2.941381	2.967594	2.98456	2.996845
res4_5	3.145998	3.242336	2.898611	3.033752
res5_2	3.00029	3.085102	2.819701	2.865075

Table 91. Dataset: CS-CSFV(0.01), Label: car, Bin: 9

Layer	MVD mean			
	f2f	f2b	b2f	b2b
es2_2	2.632104	2.661585	2.611281	2.612724
res3_3	2.485537	2.654727	2.224296	2.383249
res4_5	2.727908	3.146172	2.648995	2.978889
res5_2	2.966326	2.762088	3.055754	2.363898

Table 92. Dataset: CS-CSFV(0.02), Label: car, Bin: 1

Layer	MVD mean			
	f2f	f2b	b2f	b2b
res2_2	2.026214	1.97831	1.888203	1.8471
res3_3	1.879495	1.93231	2.005498	2.038926
res4_5	1.913738	1.942838	1.984738	2.007567
res5_2	2.088159	2.181628	2.237213	2.166204

Table 94. Dataset: CS-CARLA, Label: car, Bin: 1

Layer	MVD mean			
	f2f	f2b	b2f	b2b
res2_2	3.141126	3.132896	3.053914	3.047343
res3_3	3.047711	3.138398	3.051047	3.146816
res4_5	3.405747	3.560306	3.312046	3.446573
res5_2	3.899754	3.783358	3.548343	3.419083

Table 96. Dataset: CS-KS, Label: car, Bin: 1

Layer	MVD mean			
	f2f	f2b	b2f	b2b
res2_2	3.12196	3.124747	2.963401	2.971671
res3_3	2.71388	3.25211	2.601027	3.130624
res4_5	3.036489	3.443498	3.249636	3.613924
res5_2	3.365768	3.809035	3.905568	3.924799

Table 98. Dataset: CS-VK, Label: car, Bin: 1

Layer	MVD mean			
	f2f	f2b	b2f	b2b
res2_2	3.134635	3.170769	3.511757	3.559752
res3_3	3.487185	3.640578	3.473435	3.643497
res4_5	3.454606	3.59765	3.163142	3.313437
res5_2	4.074189	3.814336	3.960457	3.723863

Table 99. Dataset: CS-VK, Label: car, Bin: 9

Table 100. MVD for the “Car” label .

Layer	MVD mean			
	f2f	f2b	b2f	b2b
res2_2	3.0403	3.257182	2.966835	3.200019
res3_3	3.487007	3.659496	3.198339	3.365955
res4_5	3.461587	3.589998	3.44037	3.523223
res5_2	3.668298	4.402051	3.661002	3.658707

Table 101. Dataset: KS-VK, Label: car, Bin: 1

Layer	MVD mean			
	f2f	f2b	b2f	b2b
res2_2	3.507414	3.514249	3.520947	3.533183
res3_3	3.522346	3.425131	3.500015	3.398116
res4_5	3.134606	3.721532	3.046122	3.623823
res5_2	3.868461	3.875345	3.962465	3.89308

Table 103. Dataset: CARLA-KS, Label: car, Bin: 1

Layer	MVD mean			
	f2f	f2b	b2f	b2b
res2_2	3.454729	3.781761	3.236546	3.556824
res3_3	3.621748	3.465997	3.199012	3.197285
res4_5	3.920673	3.812993	3.799213	3.693012
res5_2	4.192141	4.380007	3.829396	3.916404

Table 105. Dataset: CARLA-VK, Label: car, Bin: 1

Layer	MVD mean			
	f2f	f2b	b2f	b2b
res2_2	3.461544	3.649635	3.48551	3.650191
res3_3	3.389041	3.510327	3.432087	3.544008
res4_5	3.686021	3.632678	3.58373	3.671303
res5_2	3.698969	3.541205	3.814748	3.669518

Table 102. Dataset: KS-VK, Label: car, Bin: 9

Layer	MVD mean			
	f2f	f2b	b2f	b2b
res2_2	3.555406	3.300934	3.764535	3.515109
res3_3	3.664688	4.024245	3.658104	4.019631
res4_5	3.814338	3.796126	3.644634	3.64071
res5_2	3.8482	3.789979	3.928309	3.856924

Table 104. Dataset: CARLA-KS, Label: car, Bin: 9

Layer	MVD mean			
	f2f	f2b	b2f	b2b
res2_2	3.539233	3.843425	3.823467	4.128982
res3_3	3.808752	3.700677	3.808876	3.707256
res4_5	3.67969	3.95423	3.824463	4.085565
res5_2	3.787977	3.547388	3.901427	3.631283

Table 106. Dataset: CARLA-VK, Label: car, Bin: 9

Table 107. MVD for the "Car" label, excluding Cityscapes.

Layer	MVD mean			
	f2f	f2b	b2f	b2b
res2_2	1.90107	2.017769	2.194028	1.817359
res3_3	1.963989	2.232561	2.4385	1.997064
res4_5	2.151321	2.526028	2.610607	2.247859
res5_2	2.091379	2.417881	2.283058	1.922043

Table 108. Dataset: CS-CSV, Label: Person, Bin: 1

Layer	MVD mean			
	f2f	f2b	b2f	b2b
res2_2	2.196452	2.178004	2.406967	2.082812
res3_3	1.893176	2.151503	2.024893	1.804592
res4_5	2.522766	2.745728	2.502865	2.455195
res5_2	2.345473	2.538796	2.222222	2.148248

Table 110. Dataset: CS-CSV, Label: Bicycle, Bin: 1

Layer	MVD mean			
	f2f	f2b	b2f	b2b
res2_2	1.91087	2.360122	2.232521	2.203551
res3_3	2.466574	2.746785	2.682585	2.485354
res4_5	2.488866	2.824601	2.959751	2.64936
res5_2	2.159035	2.543545	2.623156	2.330251

Table 112. Dataset: CS-CSV, Label: Rider, Bin: 1

Layer	MVD mean			
	f2f	f2b	b2f	b2b
res2_2	2.186056	2.693957	2.535597	2.215452
res3_3	1.895071	2.485922	2.530775	2.090305
res4_5	2.130127	2.679075	2.804662	2.191113
res5_2	1.789653	2.642629	2.288085	2.042702

Table 111. Dataset: CS-CSV, Label: Bicycle, Bin: 9

Layer	MVD mean			
	f2f	f2b	b2f	b2b
res2_2	2.271712	2.855109	2.647117	2.247345
res3_3	2.502144	3.067891	3.095785	2.708157
res4_5	2.64991	2.99534	3.198842	2.948378
res5_2	2.650348	3.1807	3.208098	2.338952

Table 113. Dataset: CS-CSV, Label: Rider, Bin: 9

Table 114. MVD for non-car labels between Cityscapes and Cityscapes validation.

Layer	MVD mean			
	f2f	f2b	b2f	b2b
res2_2	2.533566	2.73321	2.390703	2.426263
res3_3	2.696752	2.698772	2.712317	2.722163
res4_5	2.622294	3.097147	2.268134	2.748999
res5_2	2.933978	2.900677	2.922567	2.68859

Table 115. Dataset: CS-CSFV(0.01), Label: Person, Bin: 1

Layer	MVD mean			
	f2f	f2b	b2f	b2b
res2_2	3.098768	2.959295	3.241907	3.012505
res3_3	2.878011	2.760813	2.803681	2.695595
res4_5	2.756639	2.868533	2.652746	2.728764
res5_2	2.983025	3.306338	3.109515	3.413838

Table 116. Dataset: CS-CSFV(0.01), Label: Person, Bin: 9

Layer	MVD mean			
	f2f	f2b	b2f	b2b
res2_2	2.727781	2.83114	2.52992	2.583405
res3_3	2.818721	2.756196	2.70085	2.6399
res4_5	2.5642	2.581732	2.259545	2.277248
res5_2	2.791654	2.624161	2.699361	2.453502

Table 117. Dataset: CS-CSFV(0.01), Label: Bicycle, Bin: 1

Layer	MVD mean			
	f2f	f2b	b2f	b2b
res2_2	2.882556	3.179741	3.197818	3.255915
res3_3	3.502498	3.495217	3.572915	3.527167
res4_5	3.392894	3.32361	3.329141	3.244925
res5_2	3.50345	3.782023	3.214624	3.504451

Table 118. Dataset: CS-CSFV(0.01), Label: Bicycle, Bin: 9

Layer	MVD mean			
	f2f	f2b	b2f	b2b
res2_2	3.00926	3.040015	3.064935	3.075195
res3_3	3.429043	3.47356	3.312546	3.365296
res4_5	3.005324	2.852956	3.2668	3.05431
res5_2	3.071791	3.246479	2.947047	3.006498

Table 119. Dataset: CS-CSFV(0.01), Label: Rider, Bin: 1

Layer	MVD mean			
	f2f	f2b	b2f	b2b
res2_2	3.3968	3.370571	3.59658	3.52491
res3_3	3.799668	4.047476	3.664054	3.885016
res4_5	3.304043	3.338629	3.423527	3.376016
res5_2	3.6104	3.774592	3.534143	3.568252

Table 120. Dataset: CS-CSFV(0.01), Label: Rider, Bin: 9

**Table 121. MVD for non-car labels between Cityscapes and Cityscapes foggy 0.01.**

Layer	MVD mean			
	f2f	f2b	b2f	b2b
res2_2	2.533566	2.73321	2.390703	2.426263
res3_3	2.696752	2.698772	2.712317	2.722163
res4_5	2.622294	3.097147	2.268134	2.748999
res5_2	2.933978	2.900677	2.922567	2.68859

Table 122. Dataset: CS-CSFV(0.02), Label: Person, Bin: 1

Layer	MVD mean			
	f2f	f2b	b2f	b2b
res2_2	2.837323	2.867575	2.98062	2.93537
res3_3	2.714125	2.893832	2.753119	2.937033
res4_5	3.117603	2.891447	2.947588	2.694934
res5_2	2.615213	2.597655	2.865389	2.793837

Table 123. Dataset: CS-CSFV(0.02), Label: Person, Bin: 9

Layer	MVD mean			
	f2f	f2b	b2f	b2b
res2_2	2.98205	3.045294	2.924633	2.981337
res3_3	3.266259	3.12661	3.140121	3.005347
res4_5	3.256986	3.103132	2.919774	2.744937
res5_2	2.599247	2.876435	2.602573	2.849469

Table 124. Dataset: CS-CSFV(0.02), Label: Bicycle, Bin: 1

Layer	MVD mean			
	f2f	f2b	b2f	b2b
res2_2	3.746639	3.715122	3.566788	3.546999
res3_3	3.404148	3.572299	3.375922	3.587521
res4_5	3.656142	3.349588	3.527766	3.152176
res5_2	3.141516	3.470738	3.360997	3.626434

Table 125. Dataset: CS-CSFV(0.02), Label: Bicycle, Bin: 9

**Table 126. MVD for non-car labels between Cityscapes and Cityscapes foggy 0.02.**

052    **8. MMD Plot**

053    This section presents the MMD plot, highlighting the dis-  
054    crepancy between bins 1 and 9. “small”, “medium”, and  
055    “large” means objects size.

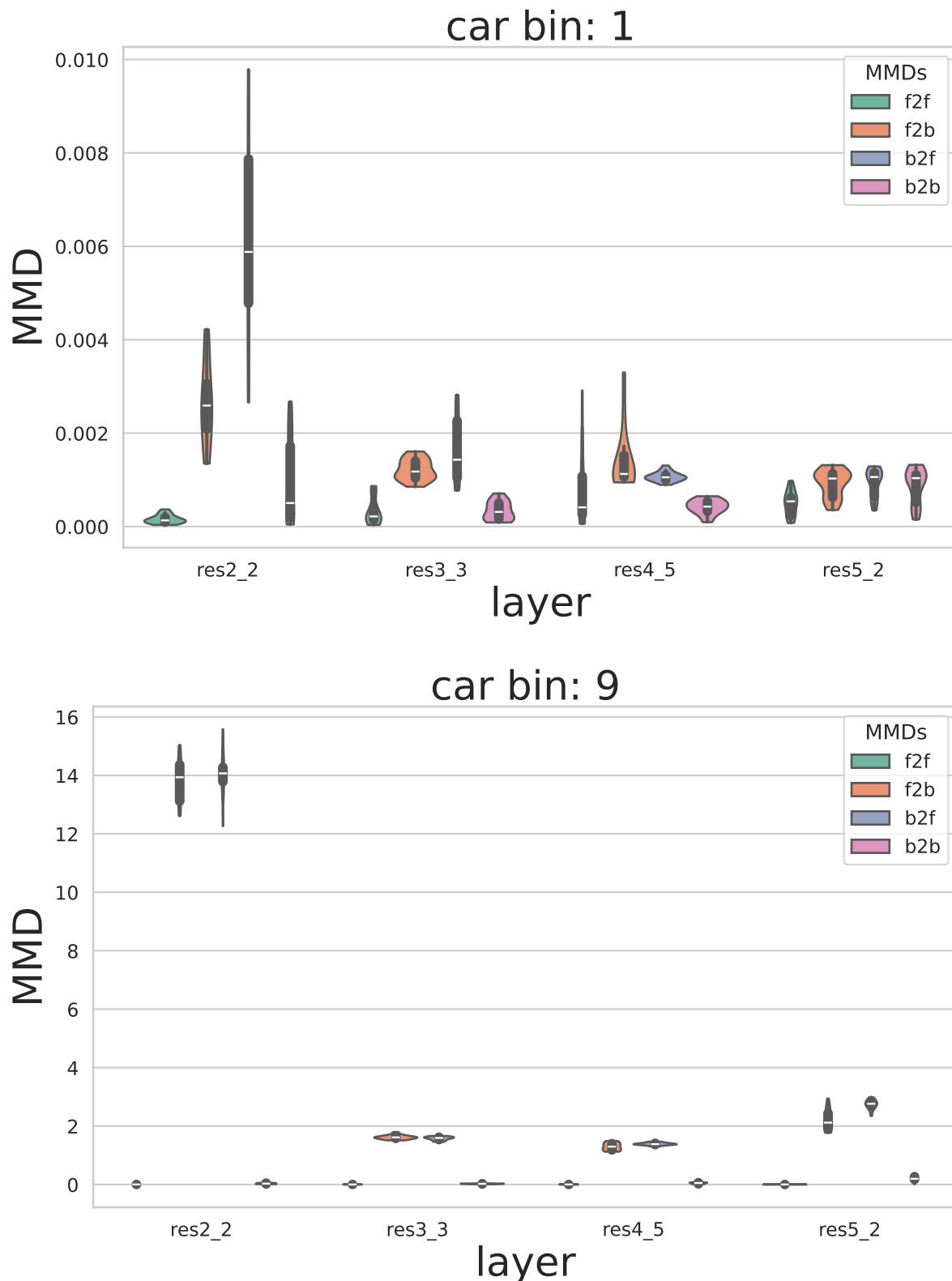


Figure 12. CS-CSV small MMD plots. Label: Car.

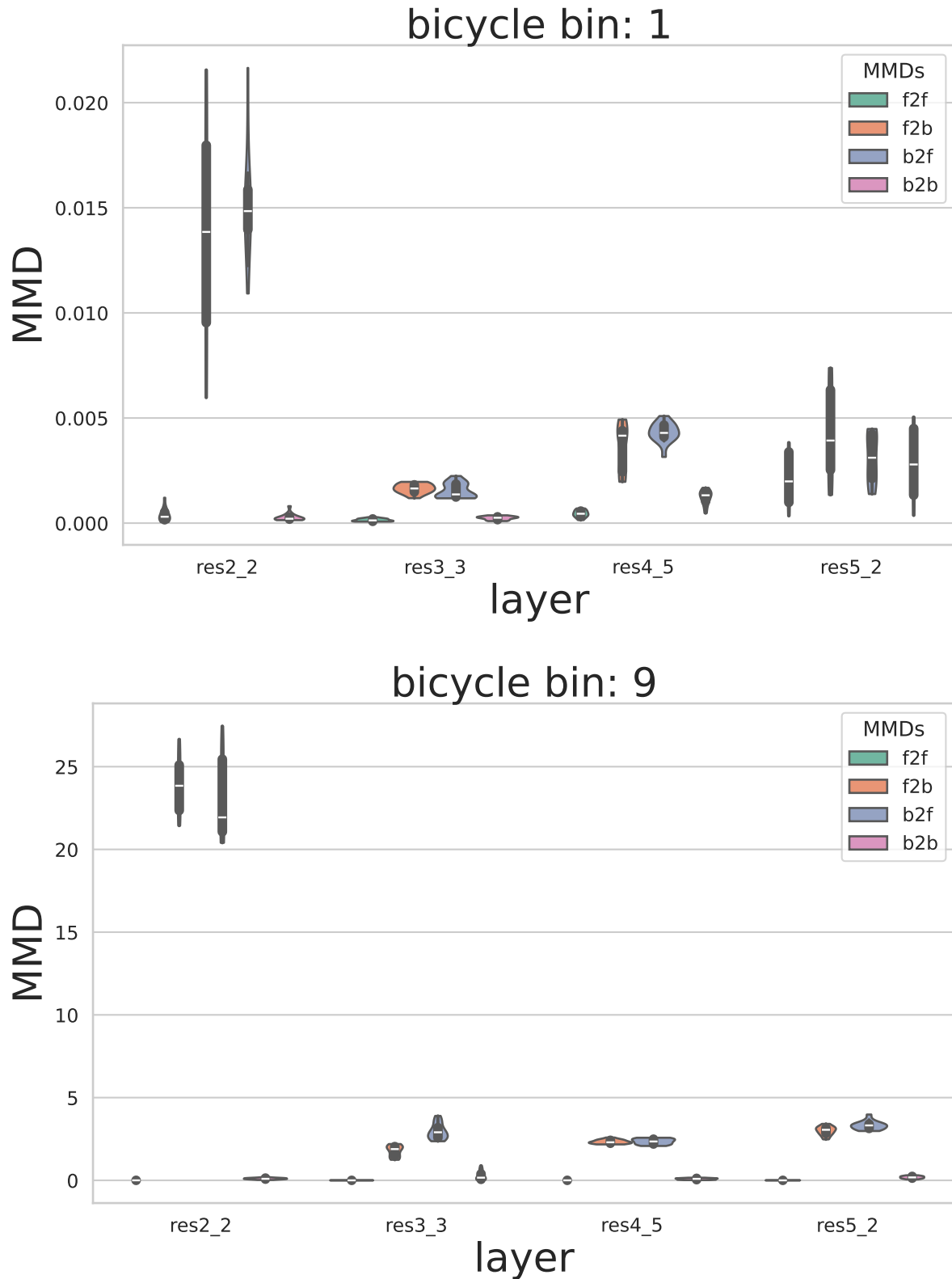


Figure 13. CS-CSV small MMD plots. Label: Bicycle.

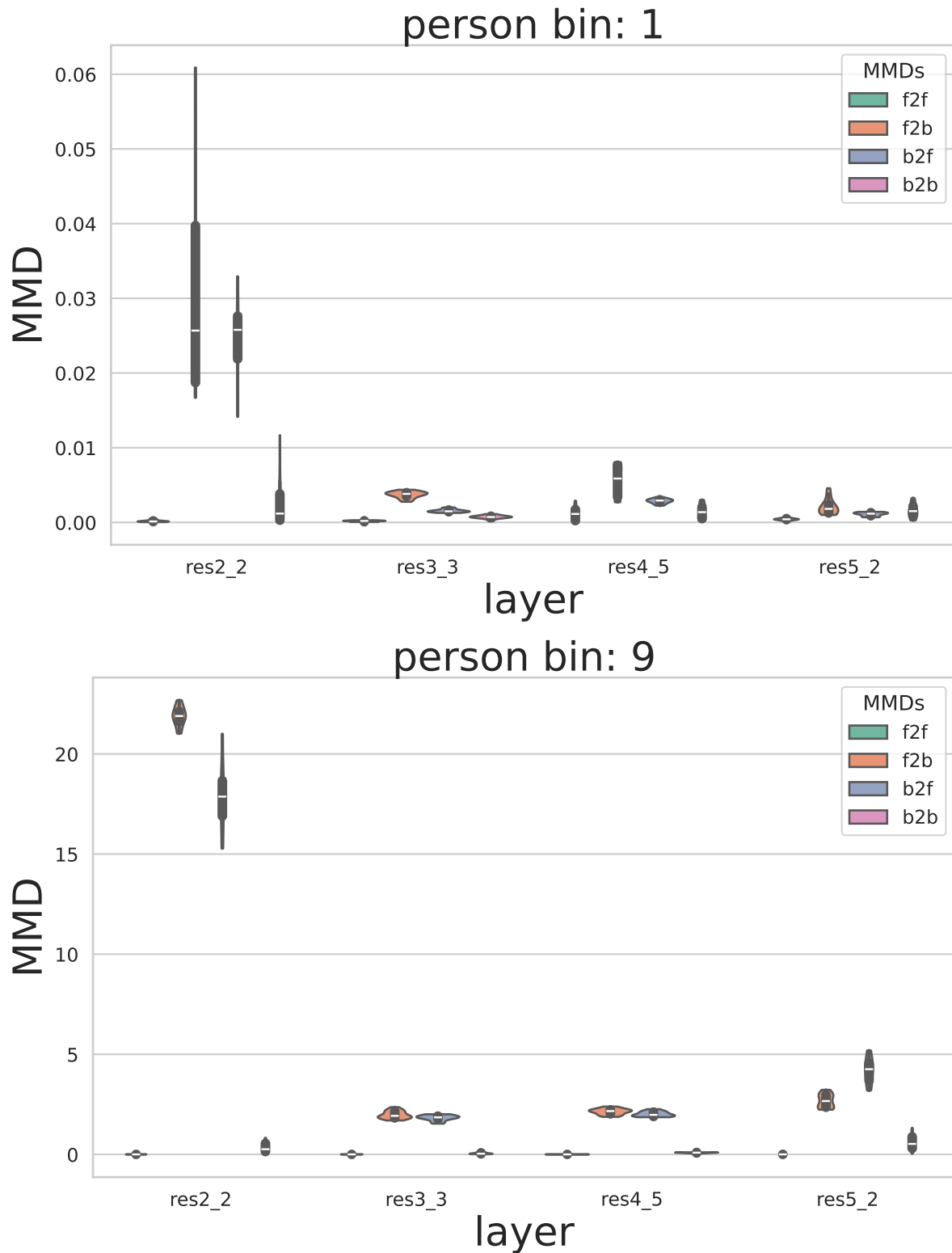


Figure 14. CS-CSV small MMD plots. Label: Person.

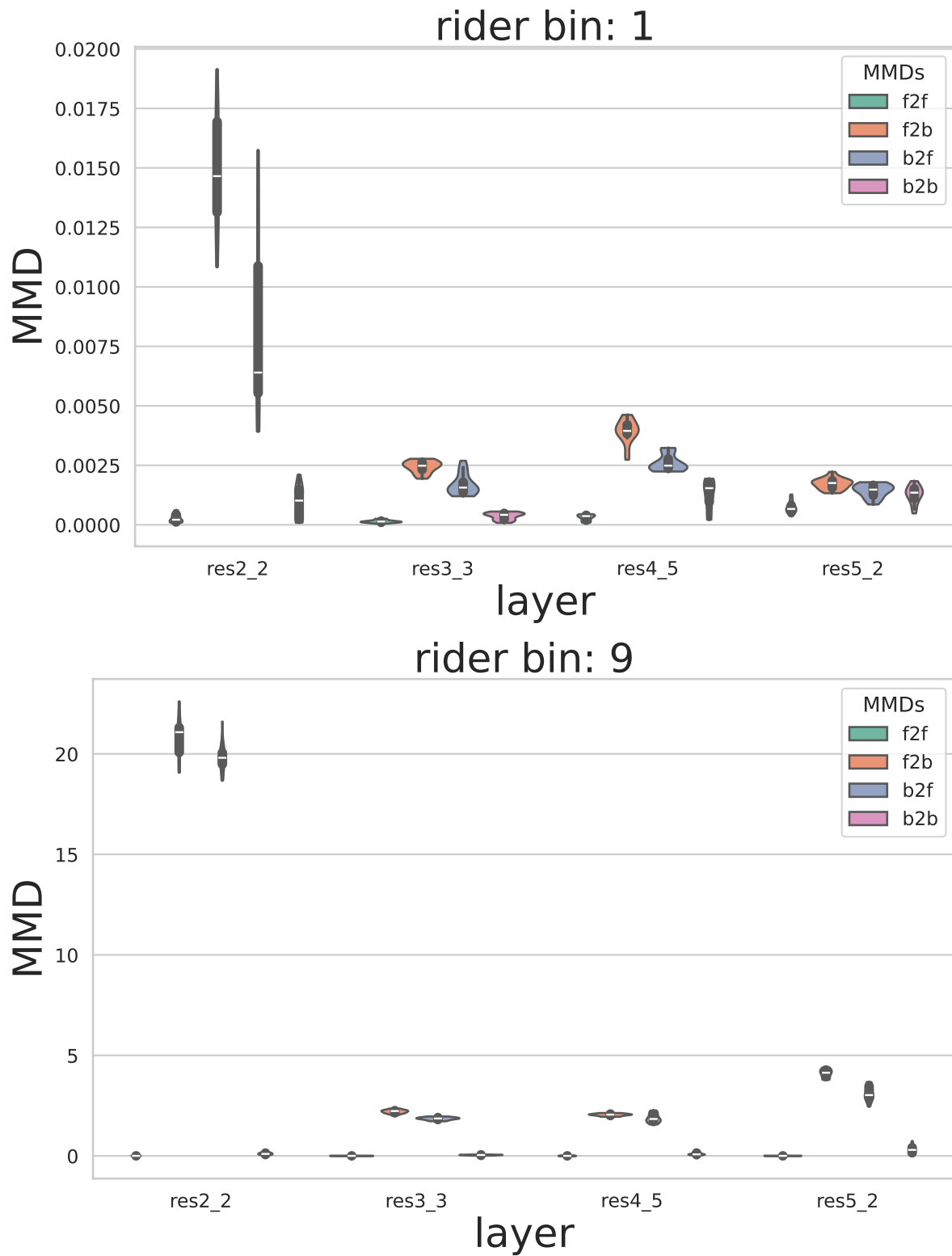


Figure 15. CS-CSV small MMD plots. Label: Rider.

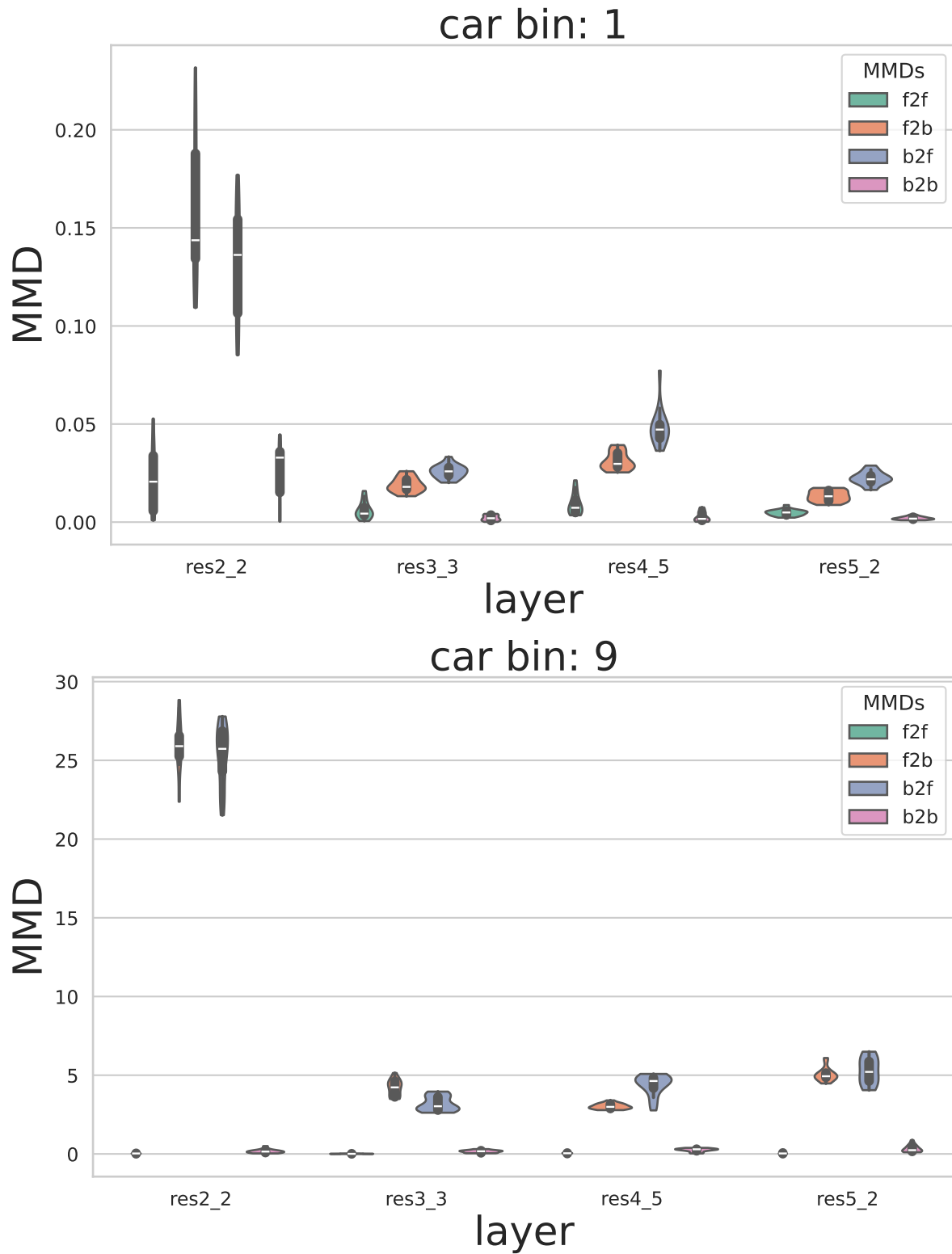


Figure 16. CS-CSV medium MMD plots. Label: Car.

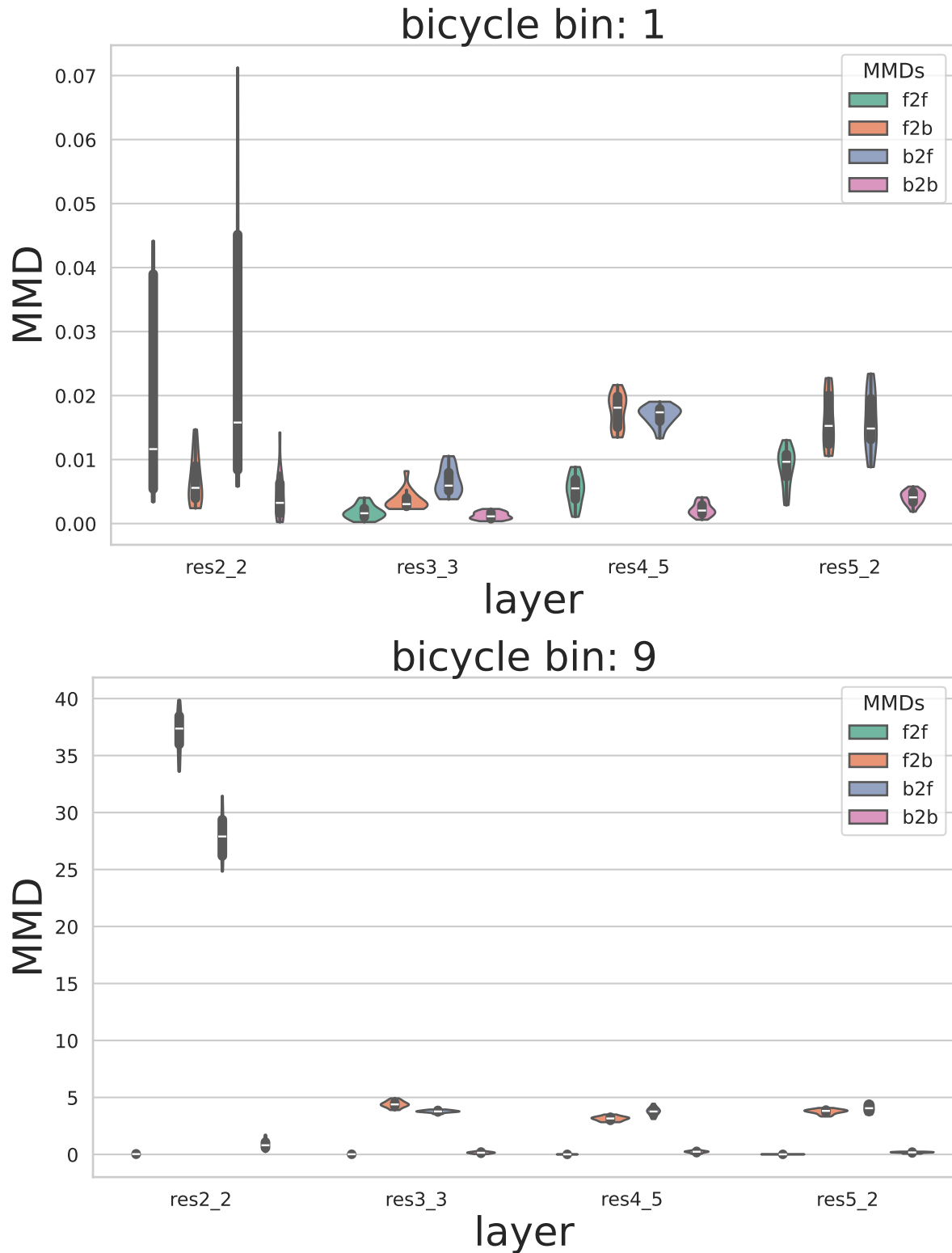


Figure 17. CS-CSV medium MMD plots. Label: Bicycle.

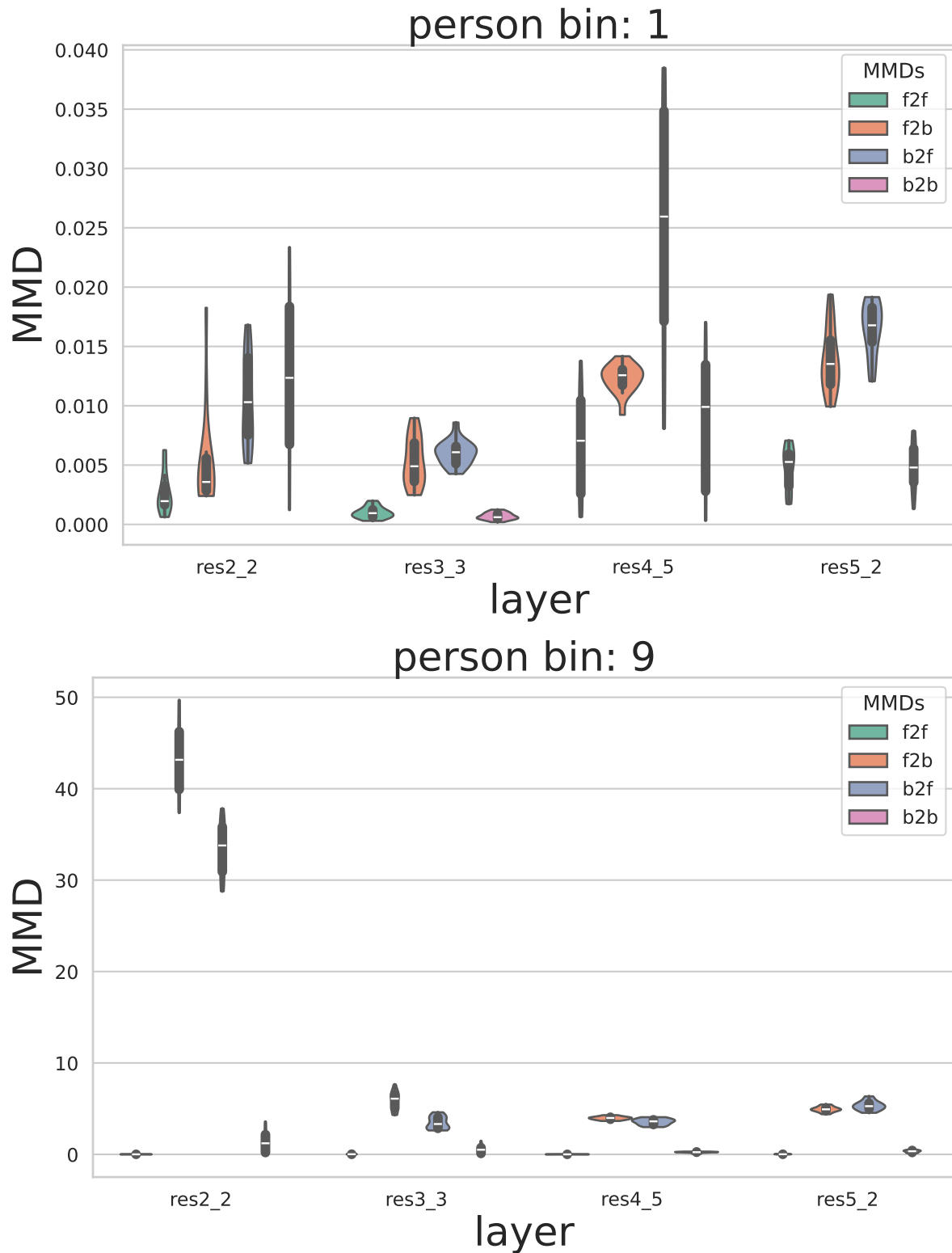


Figure 18. CS-CSV medium MMD plots. Label: Person.

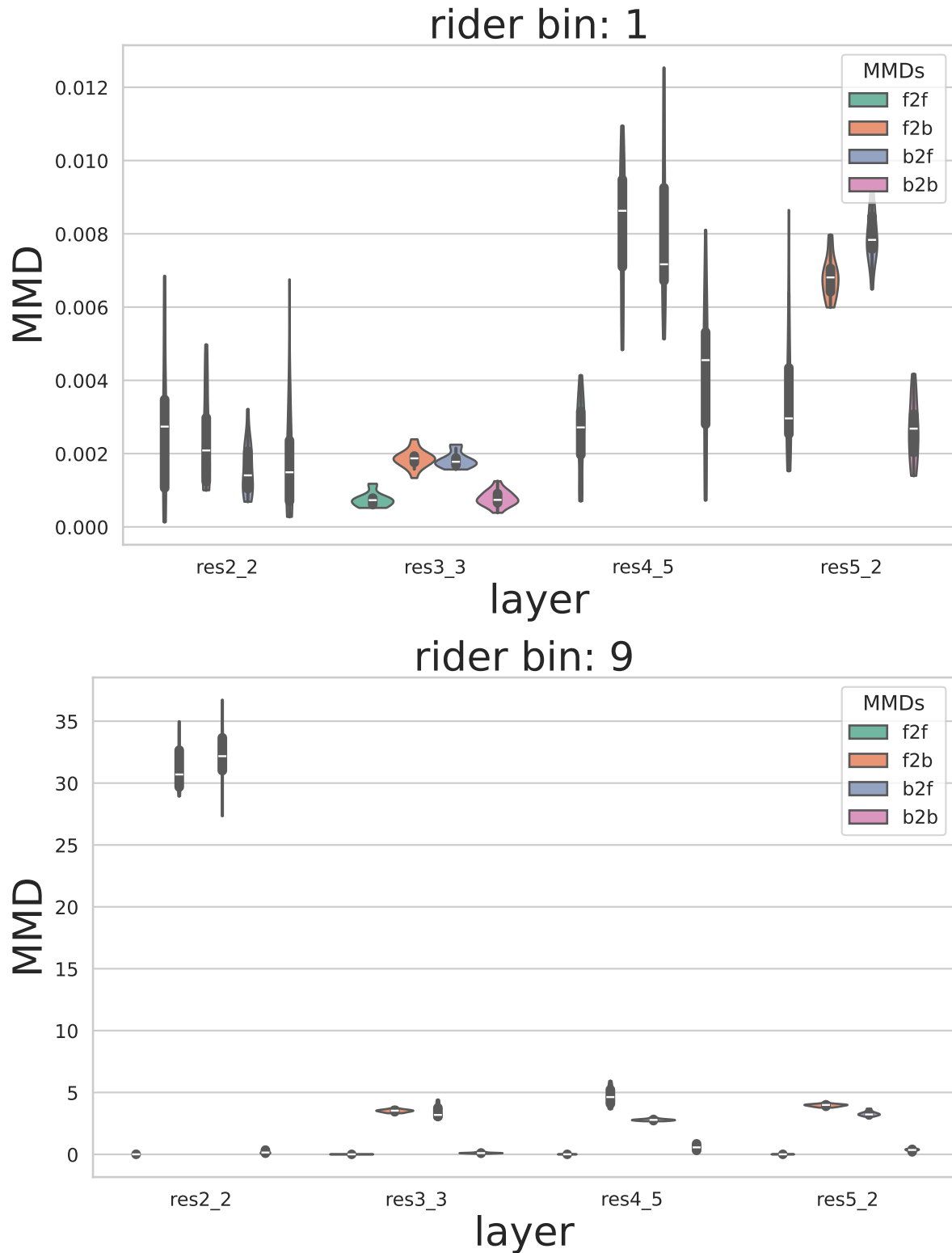


Figure 19. CS-CSV medium MMD plots. Label: Rider.

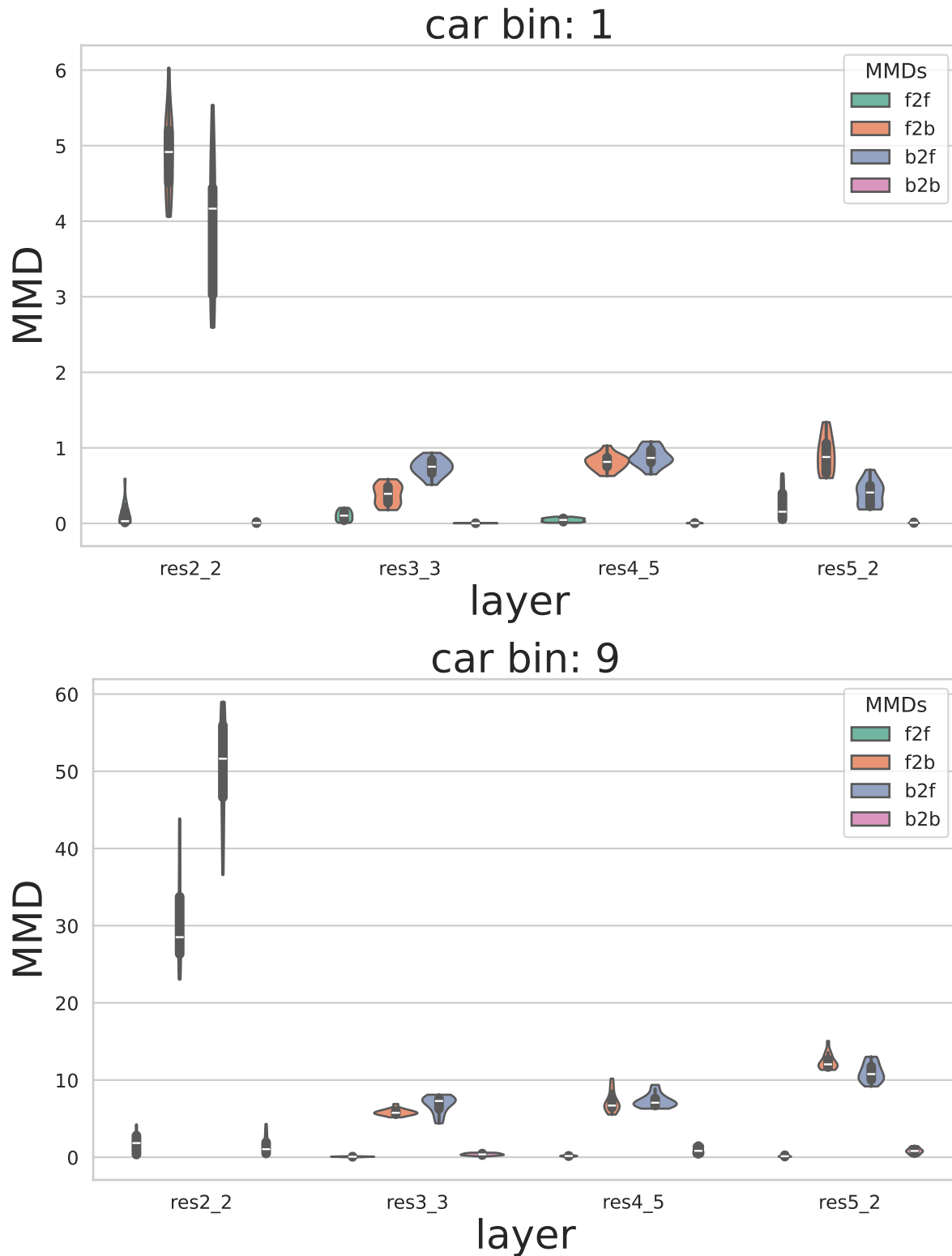


Figure 20. CS-CSV large MMD plots. Label: Car.

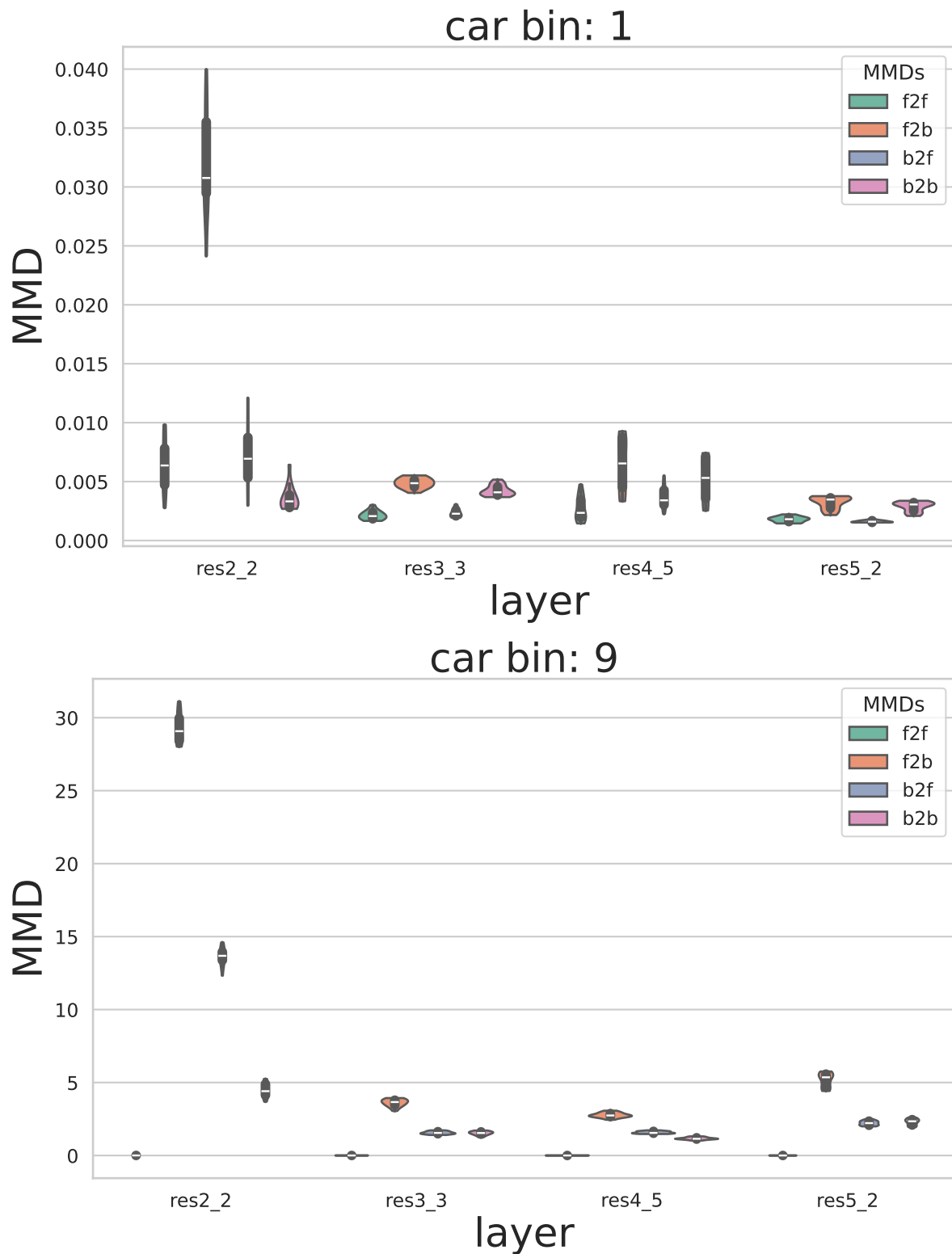


Figure 21. CS-CSFV(0.01) small MMD plots. Label: Car.

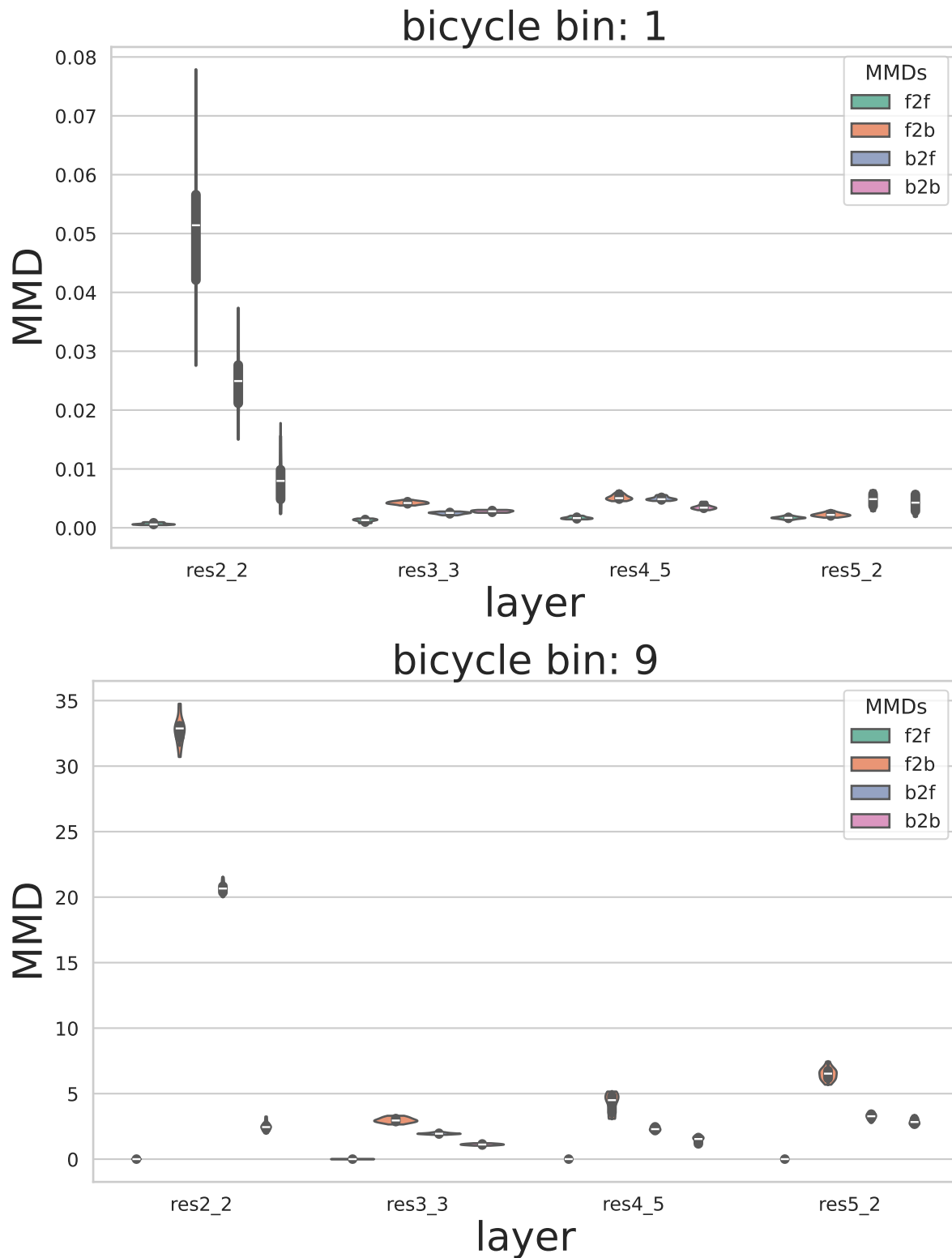


Figure 22. CS-CSFV(0.01) small MMD plots. Label: Bicycle.

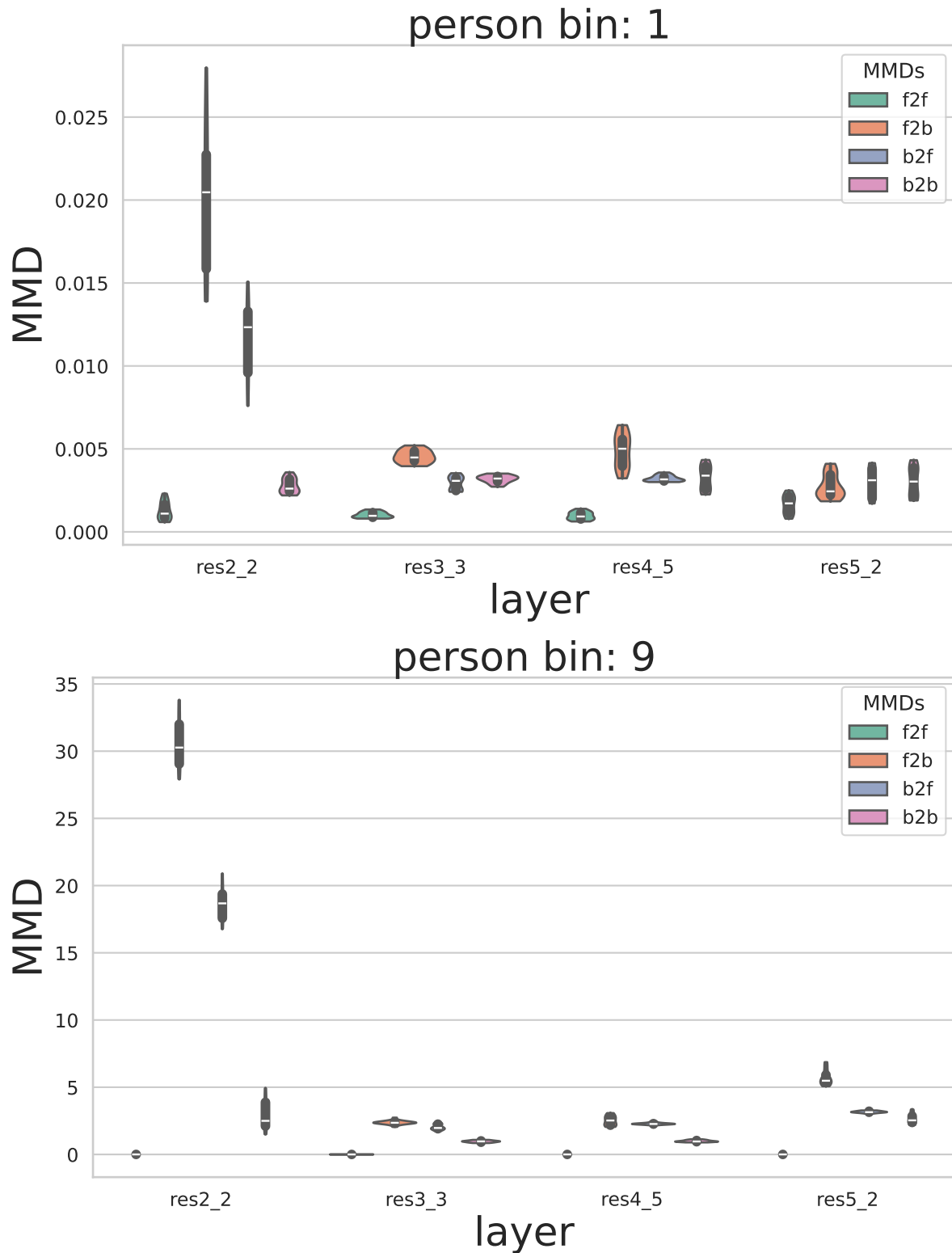


Figure 23. CS-CSFV(0.01) small MMD plots. Label: Person.

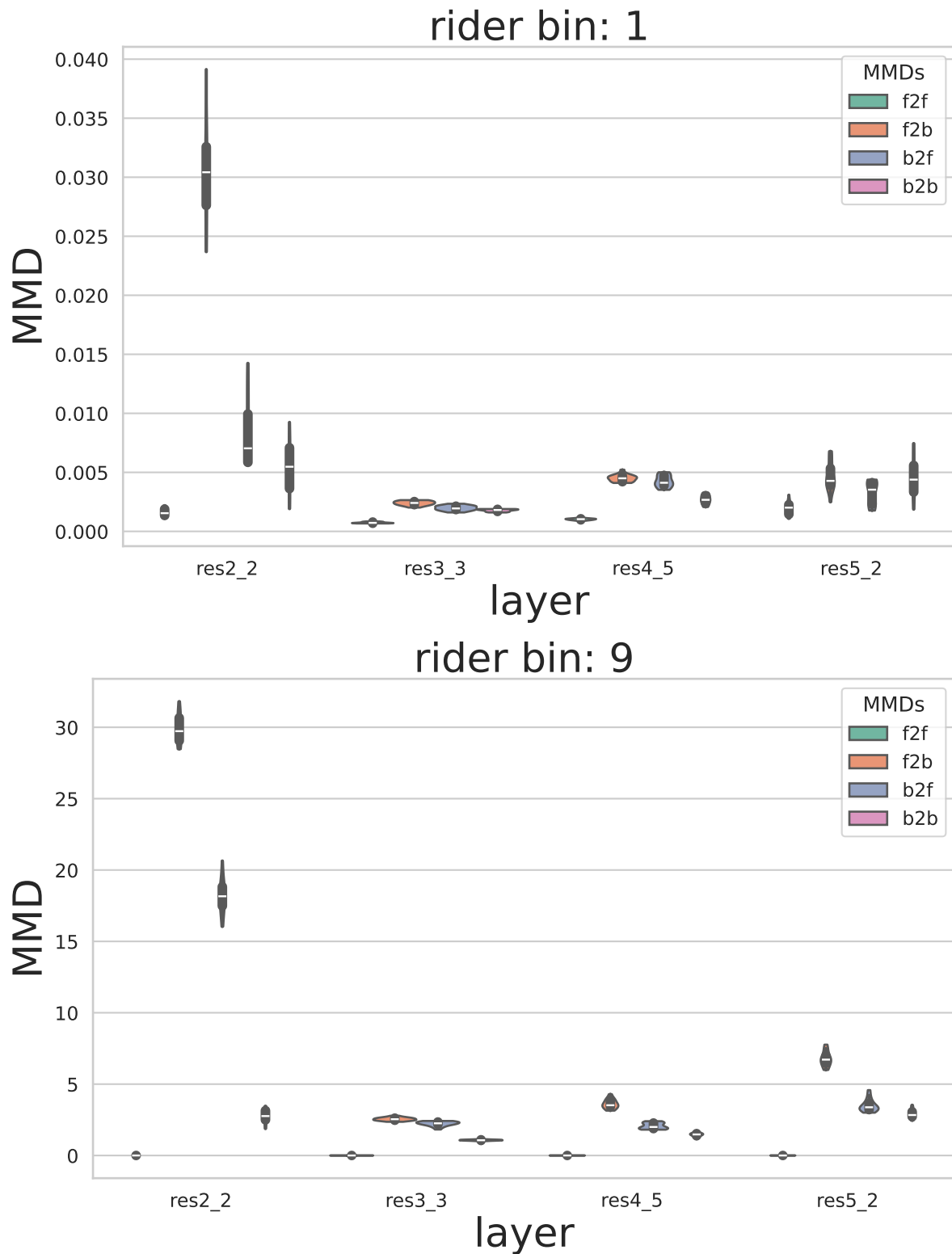


Figure 24. CS-CSFV(0.01) small MMD plots. Label: Rider.

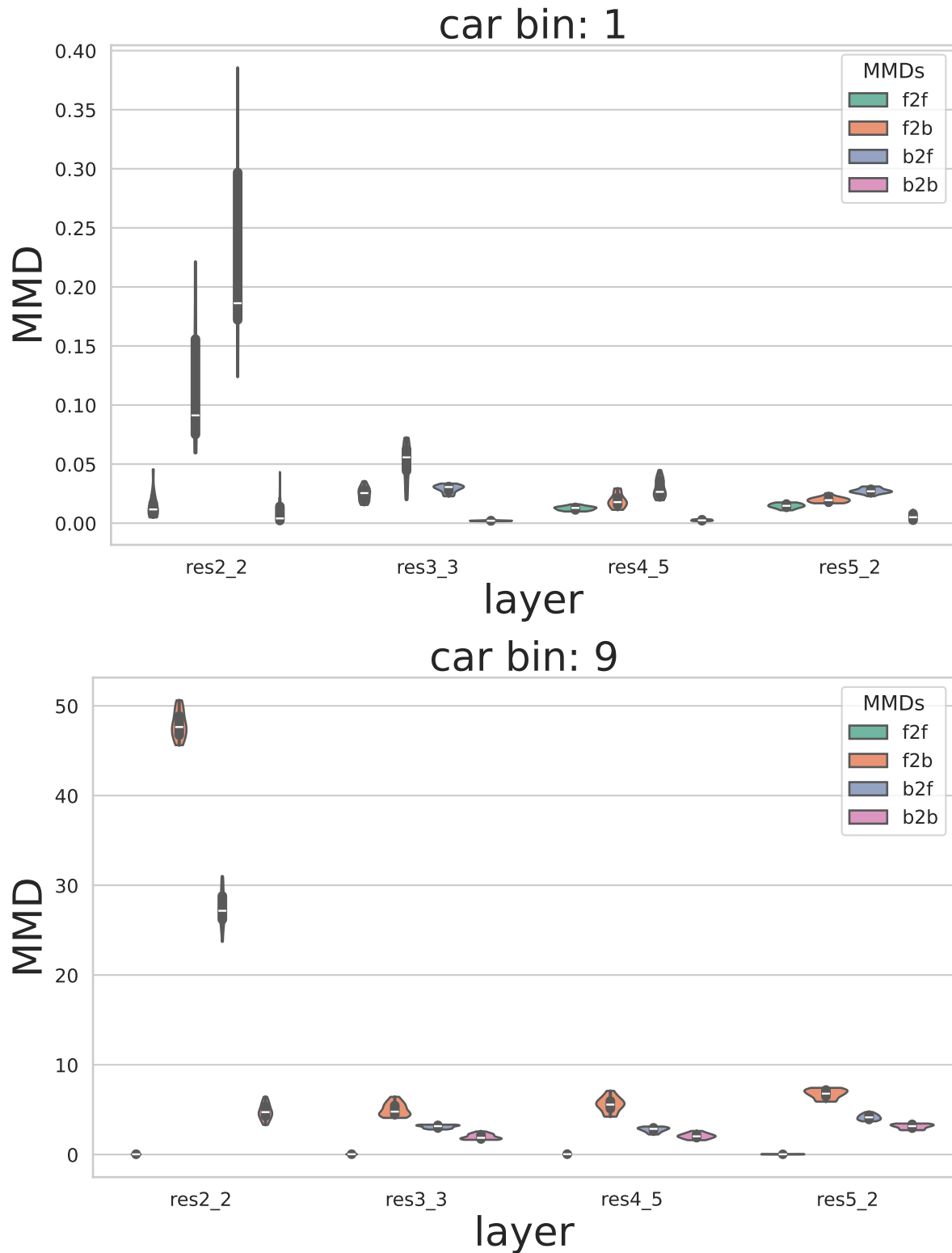


Figure 25. CS-CSFV(0.01) small MMD plots. Label: Car.

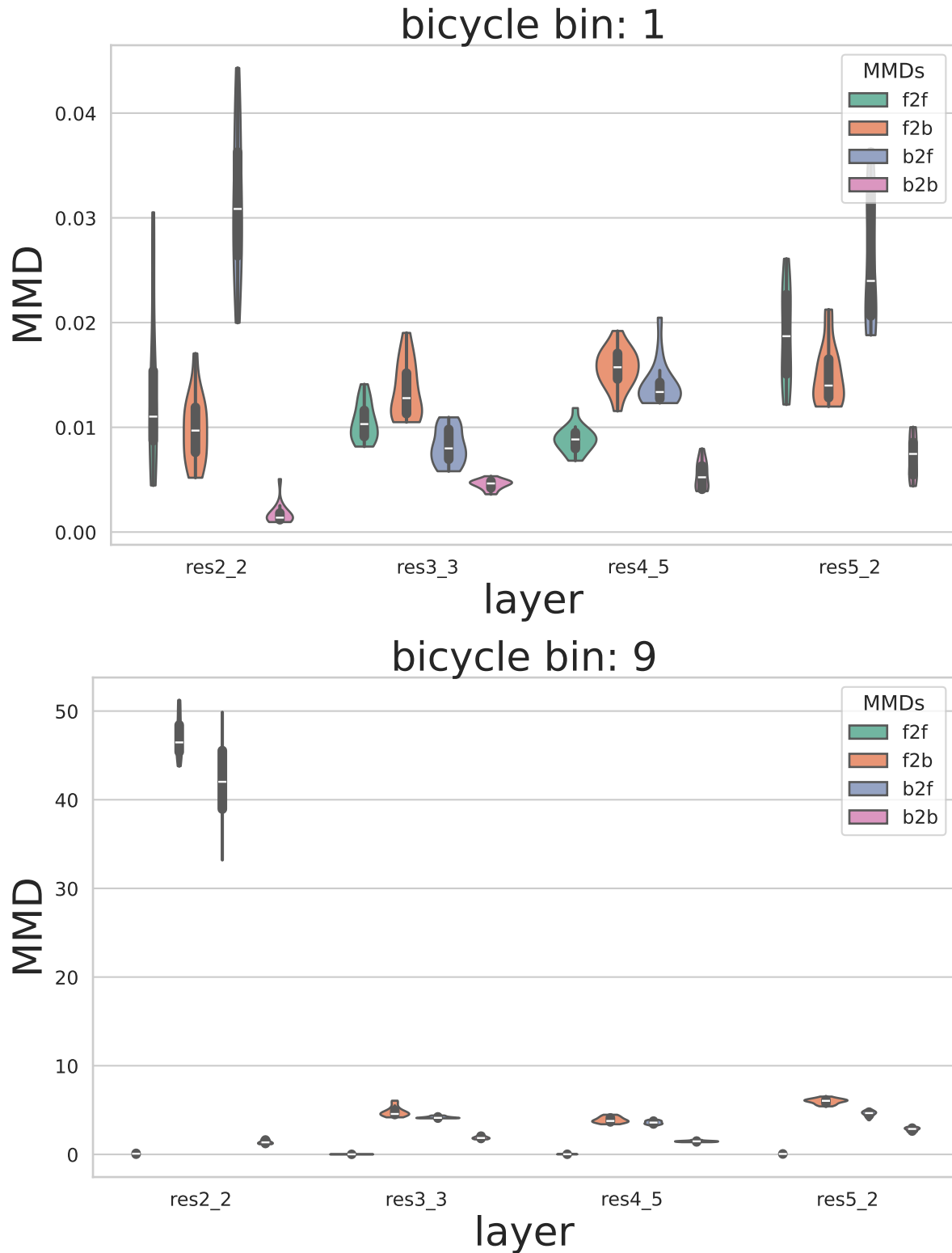


Figure 26. CS-CSFV(0.01) medium MMD plots. Label: Bicycle.

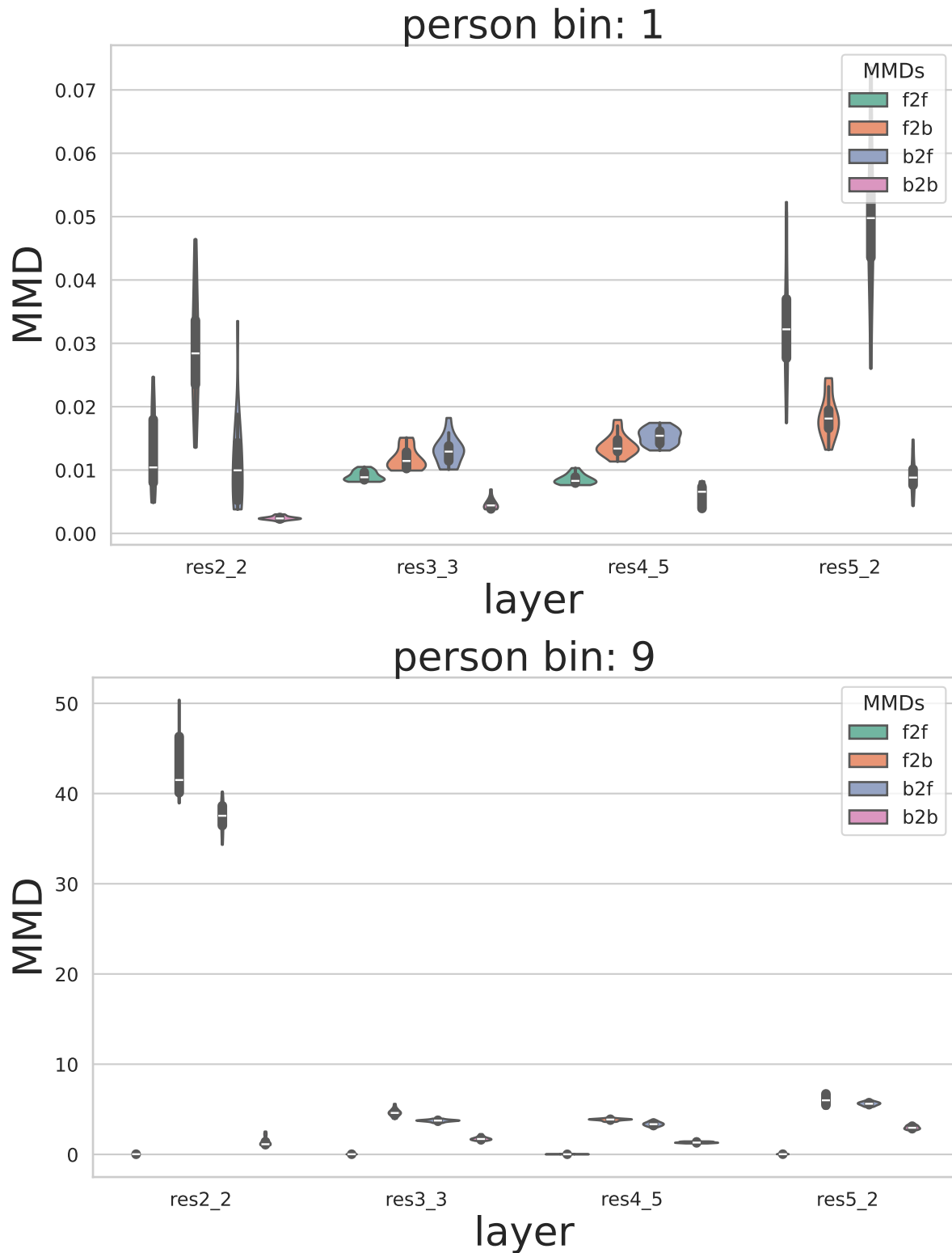


Figure 27. CS-CSFV(0.01) medium MMD plots. Label: Person.

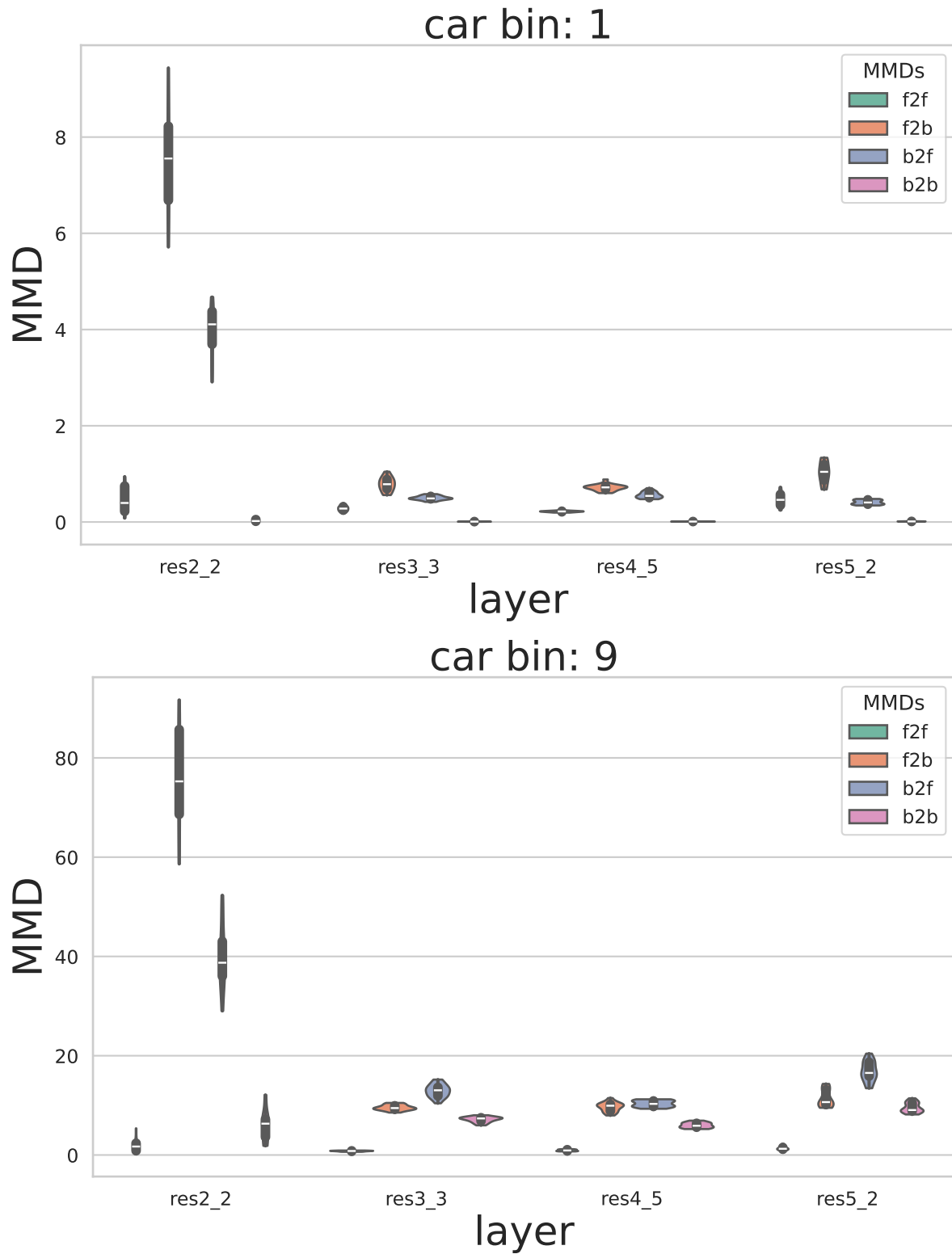


Figure 28. CS-CSFV(0.01) large MMD plots. Label: Car.

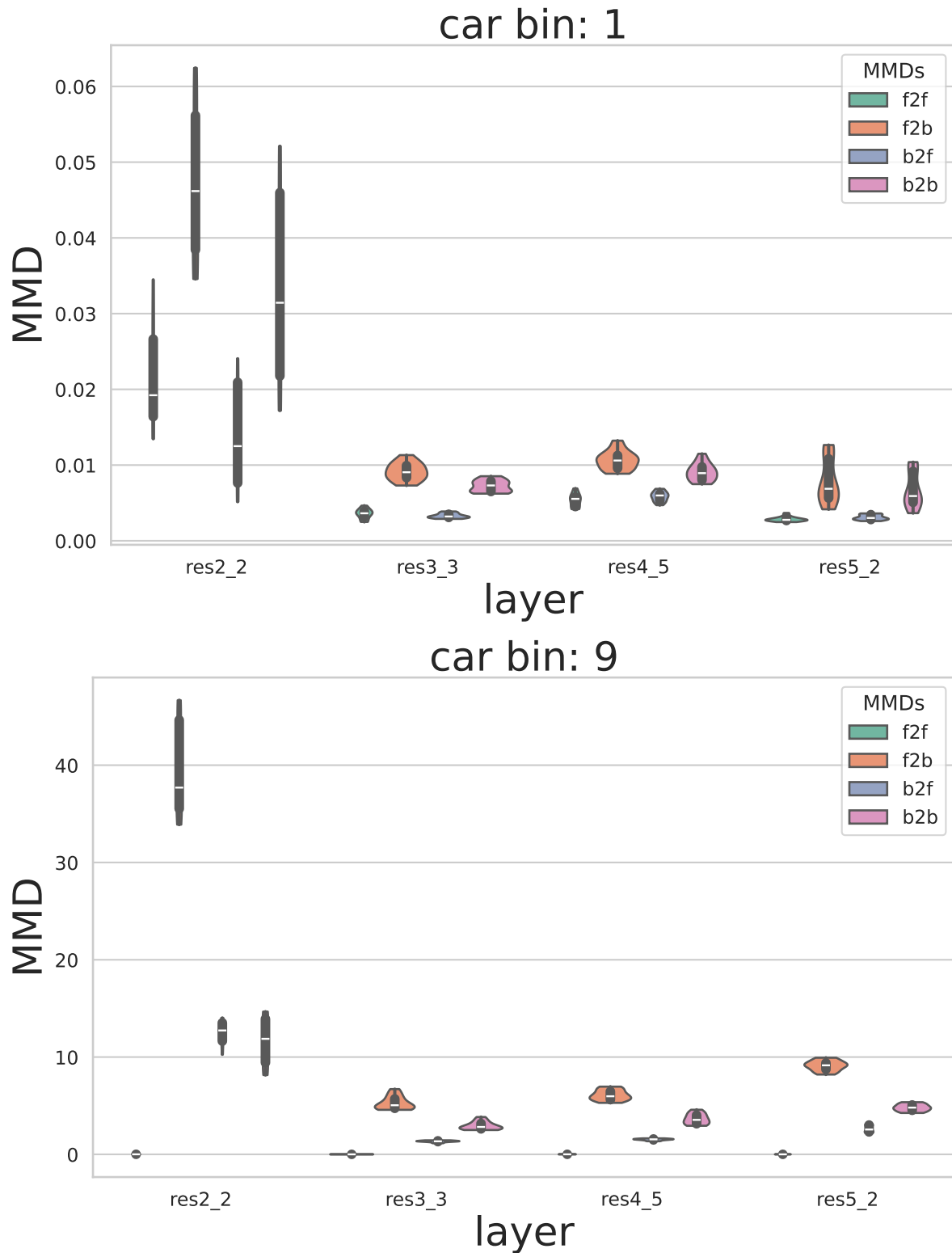


Figure 29. CS-CSFV(0.02) small MMD plots. Label: Car.

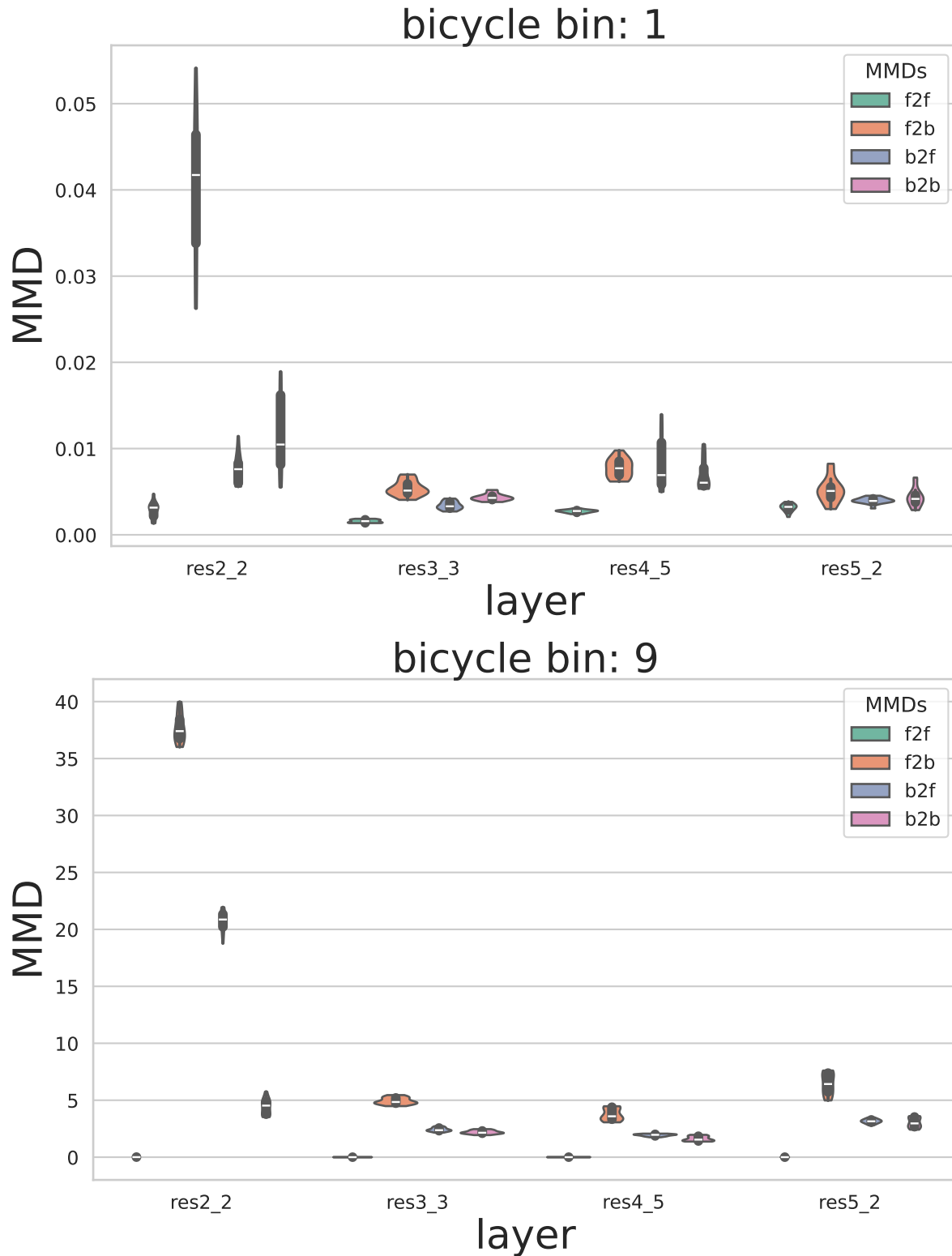


Figure 30. CS-CSFV(0.02) small MMD plots. Label: Bicycle.

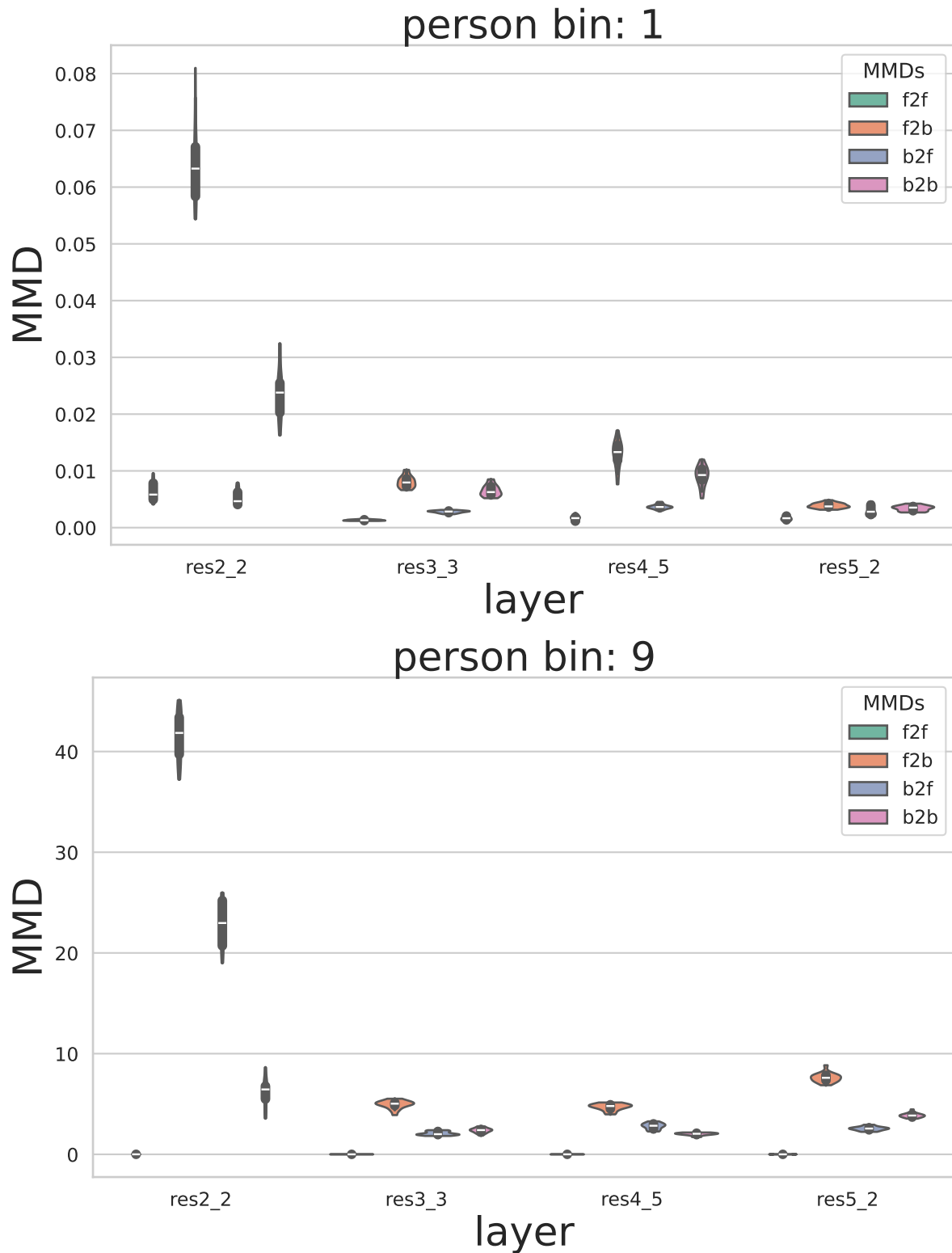


Figure 31. CS-CSFV(0.02) small MMD plots. Label: Person.

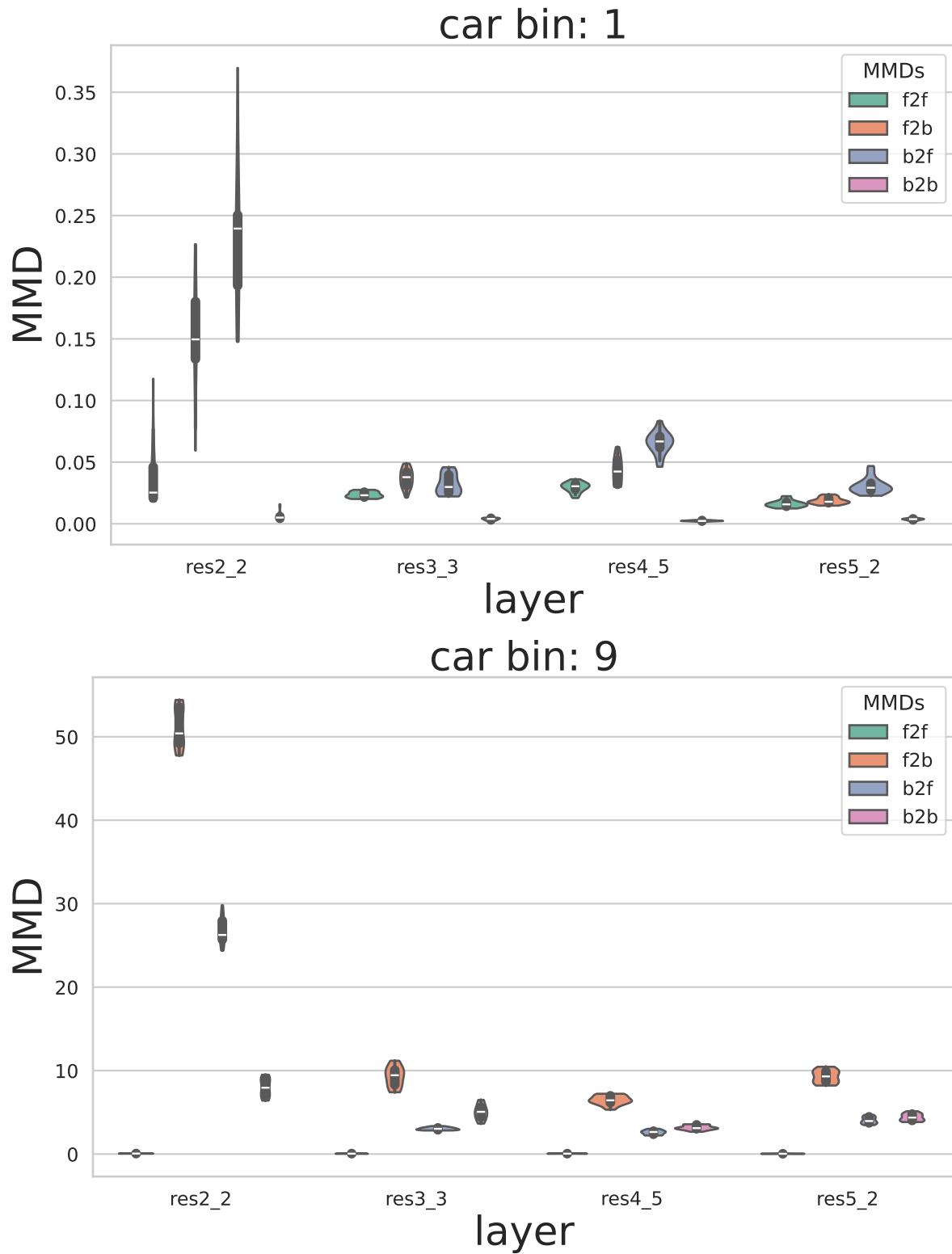


Figure 32. CS-CSFV(0.02) small MMD plots. Label: Car.

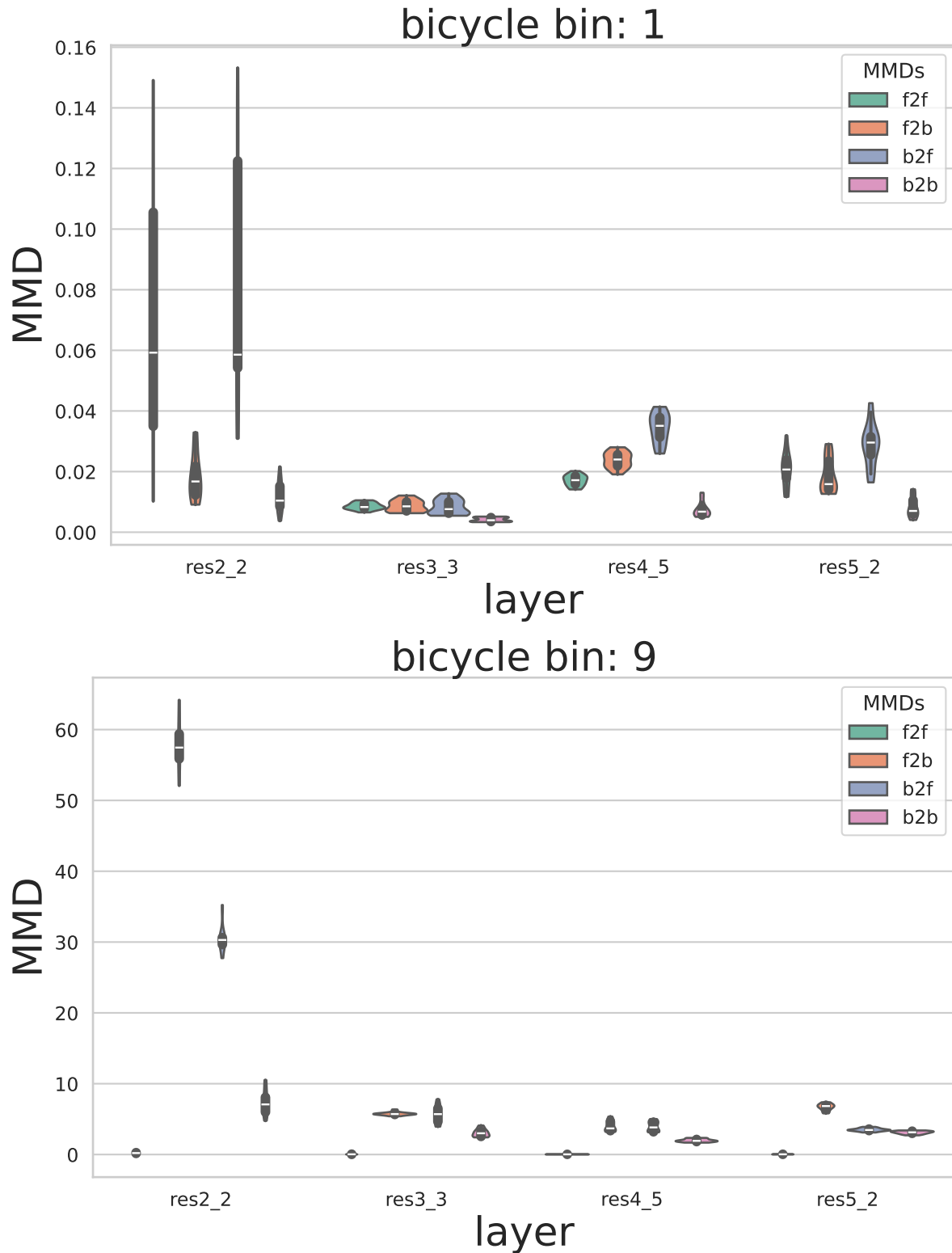


Figure 33. CS-CSFV(0.02) medium MMD plots. Label: Bicycle.

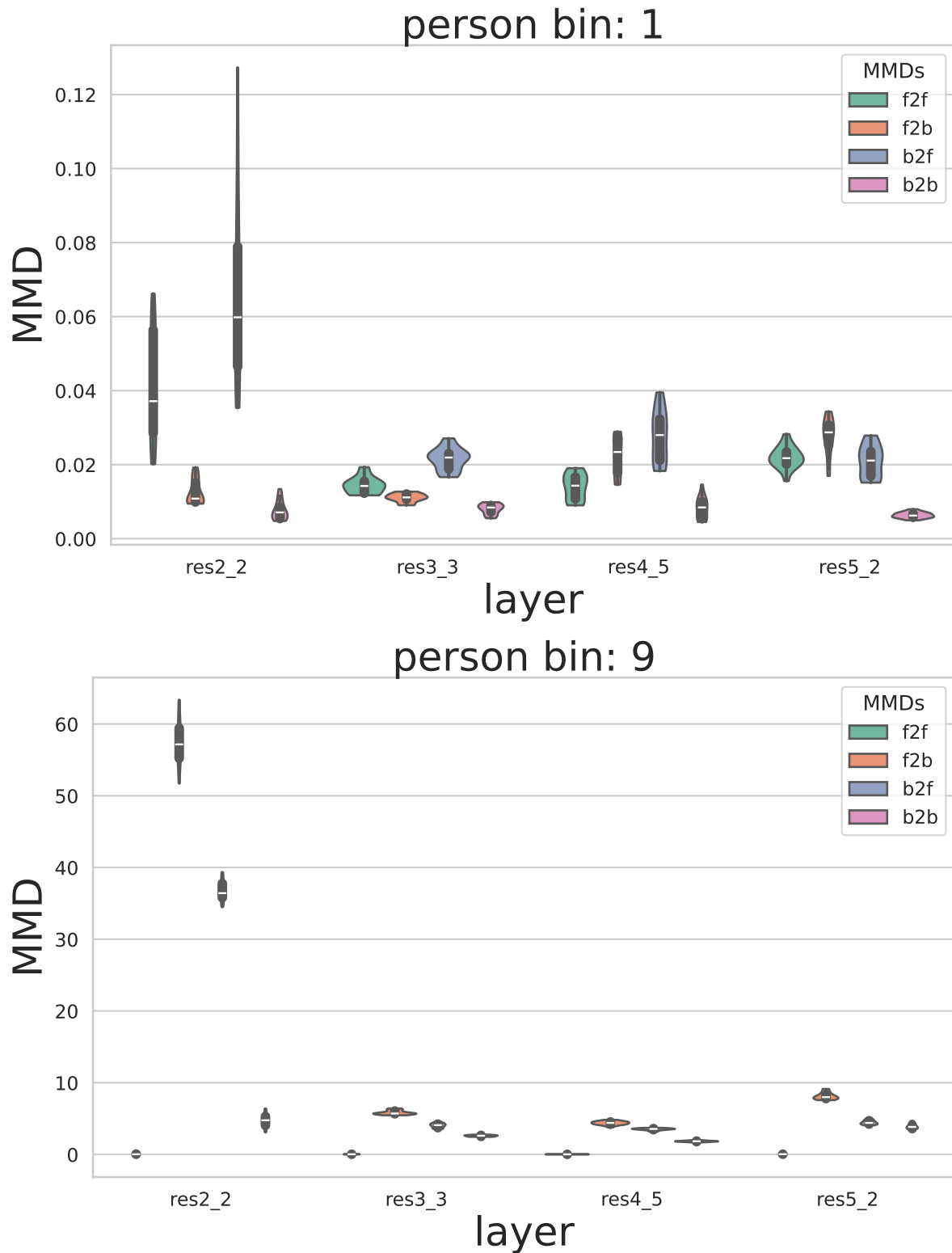


Figure 34. CS-CSFV(0.02) medium MMD plots. Label: Person.

ICCV 2025 Submission #14656. CONFIDENTIAL REVIEW COPY. DO NOT DISTRIBUTE.

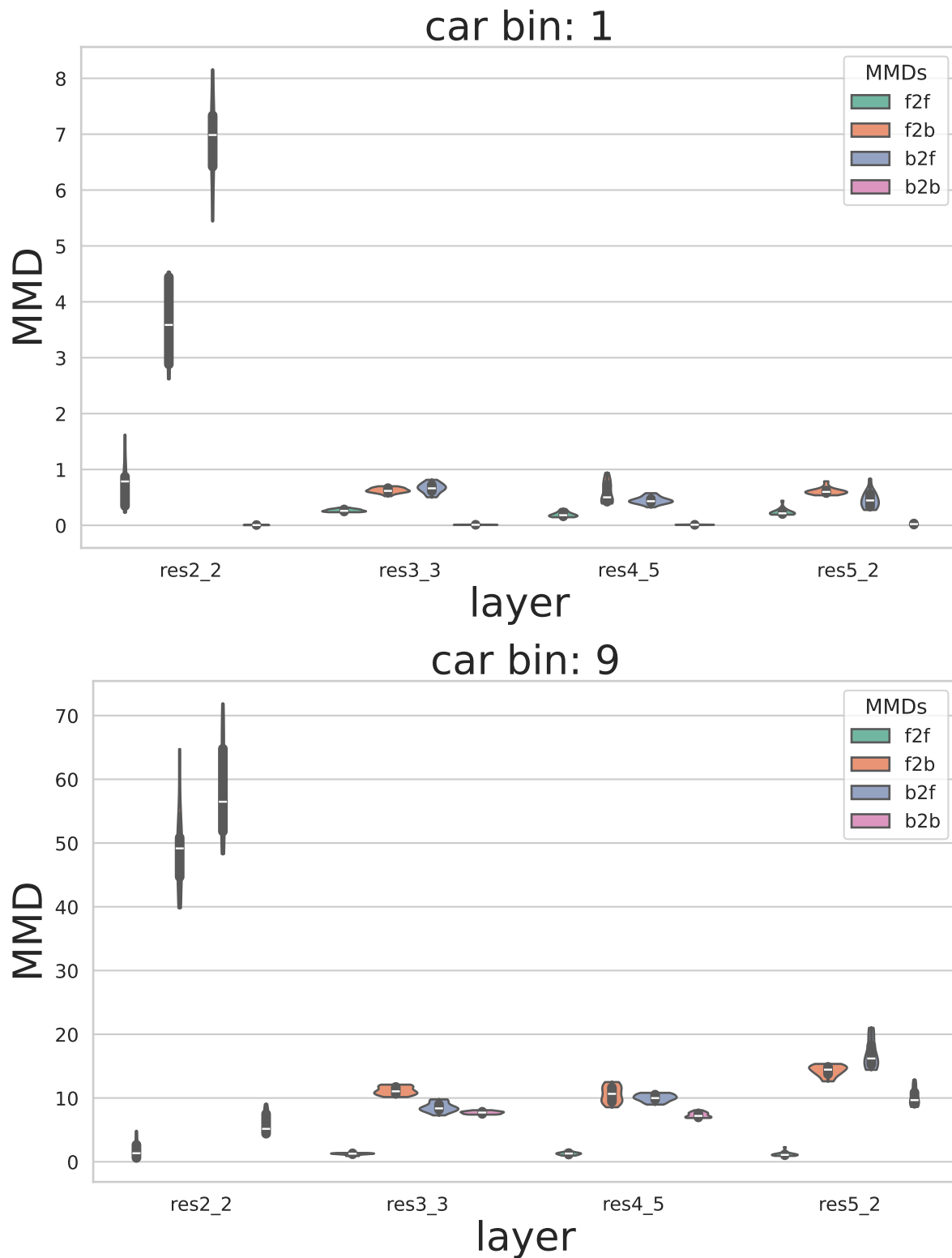


Figure 35. CS-CSFV(0.02) large MMD plots. Label: Car.

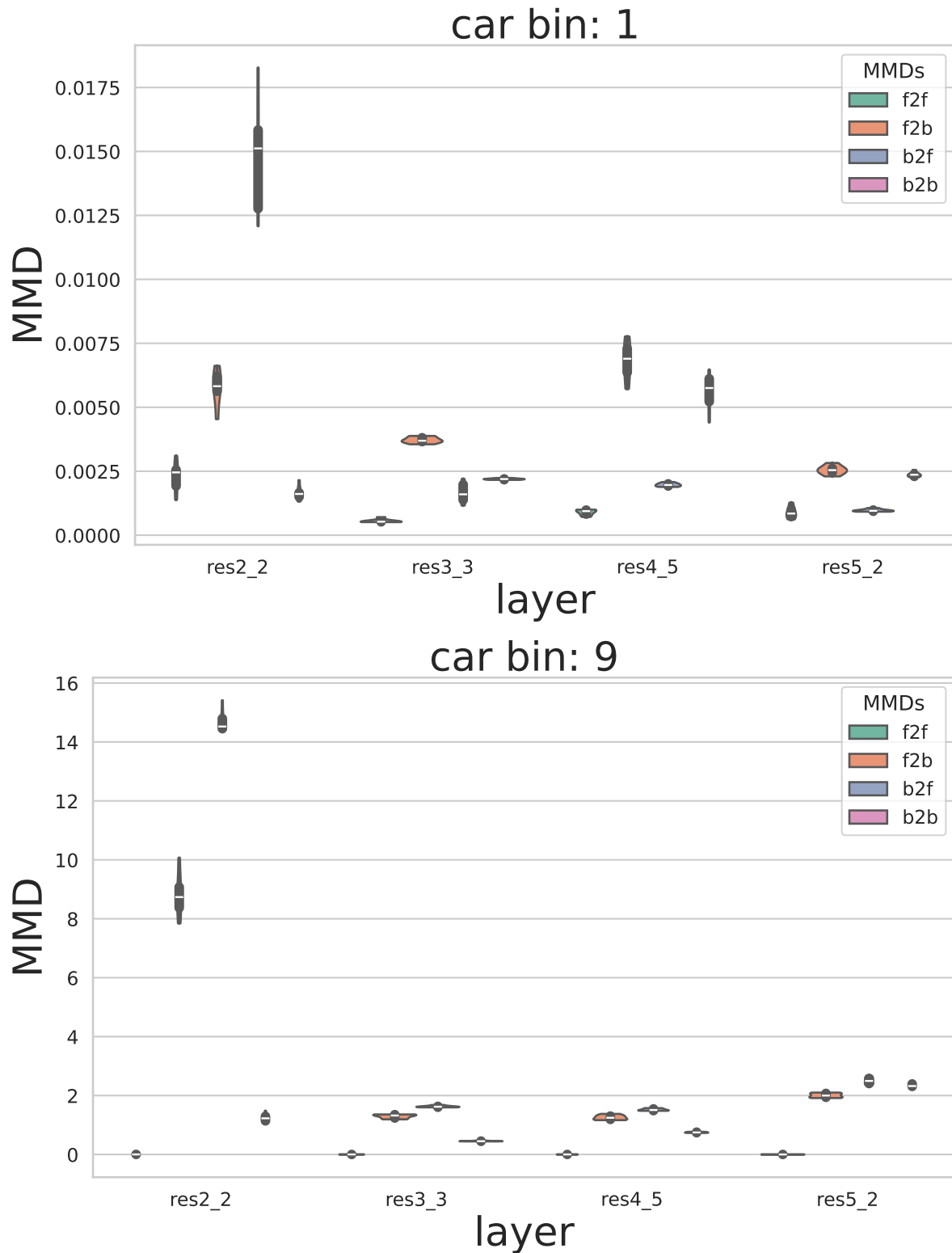


Figure 36. CS-CARLA small MMD plots. Label: Car.

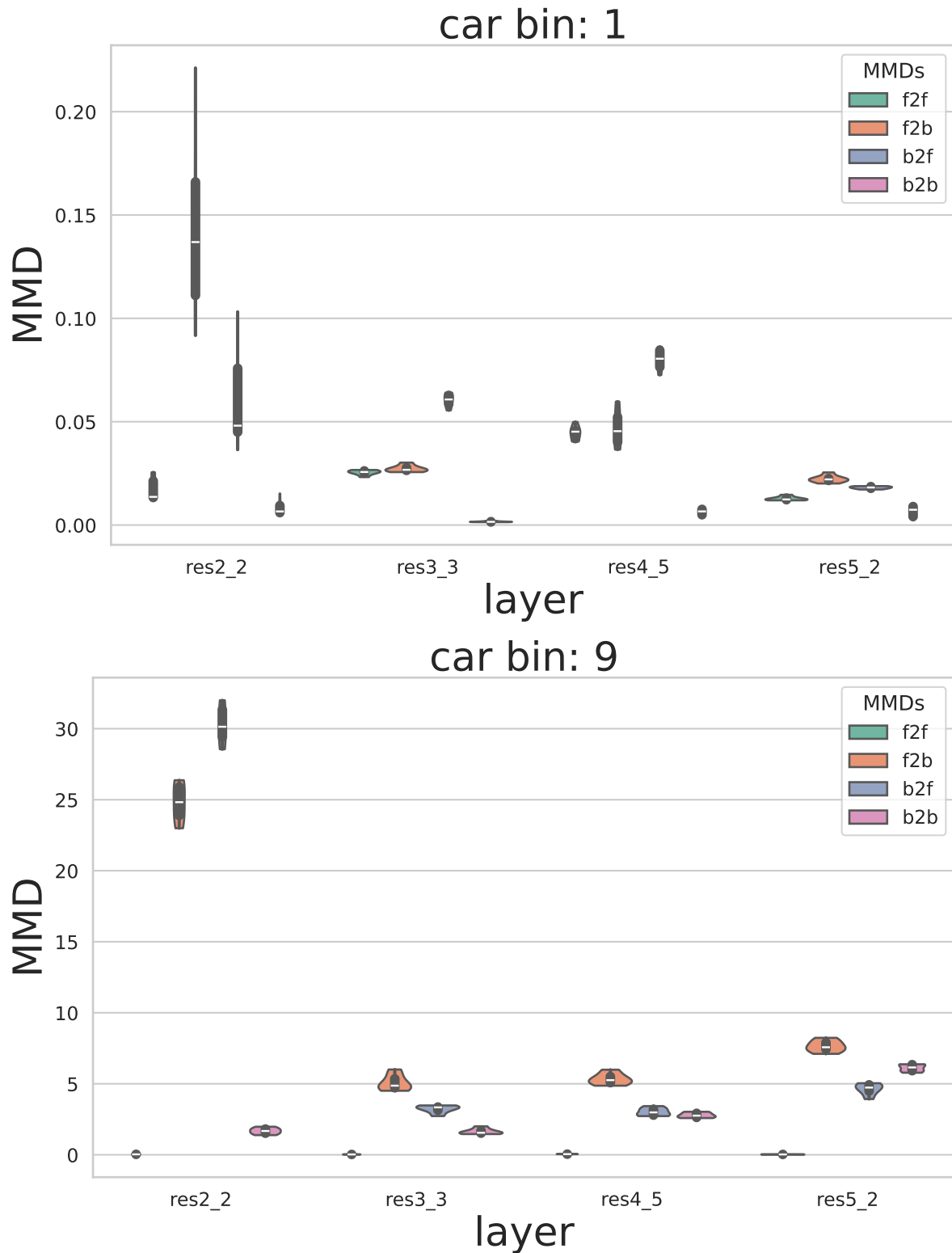


Figure 37. CS-CARLA medium MMD plots. Label: Car.

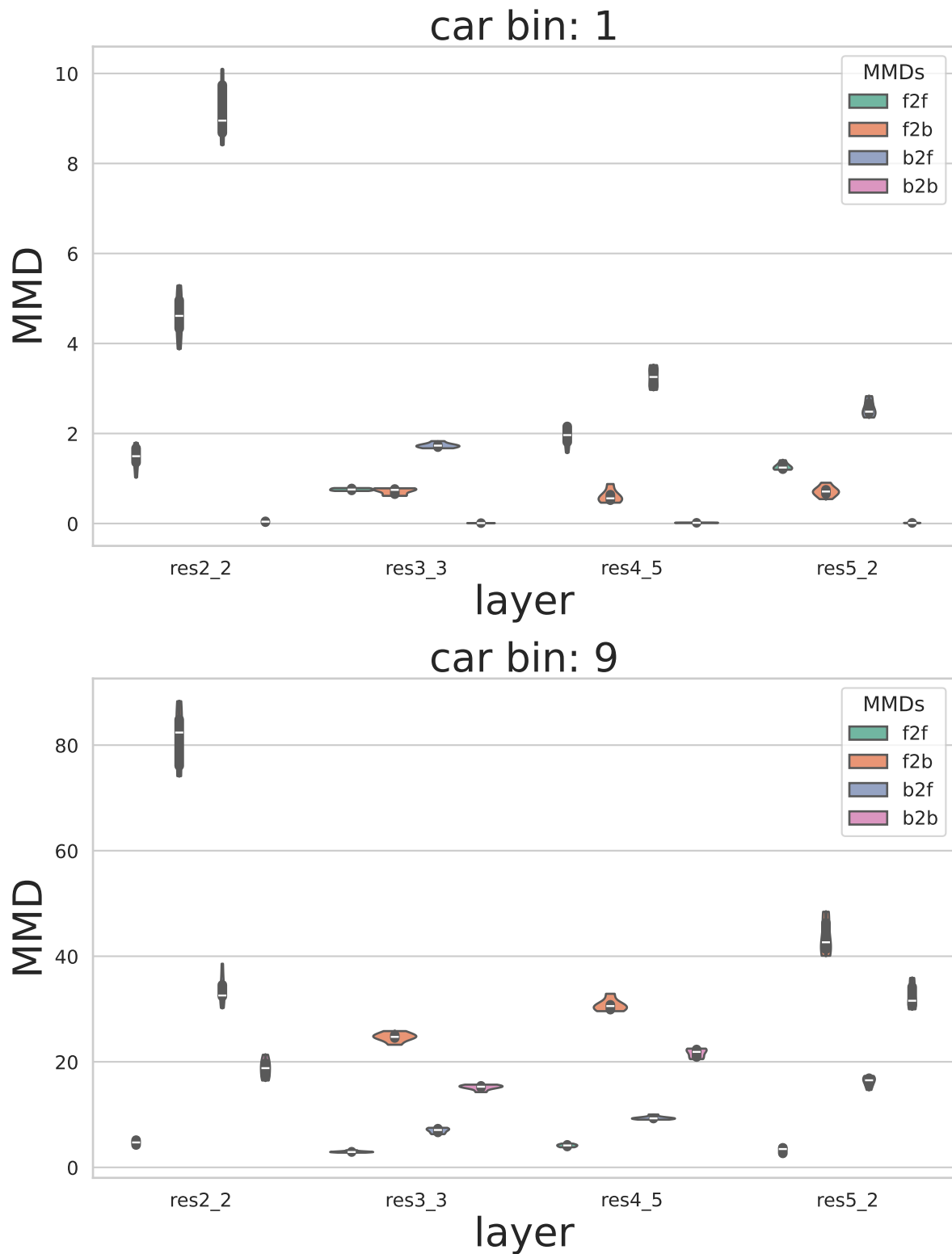


Figure 38. CS-CARLA large MMD plots. Label: Car.

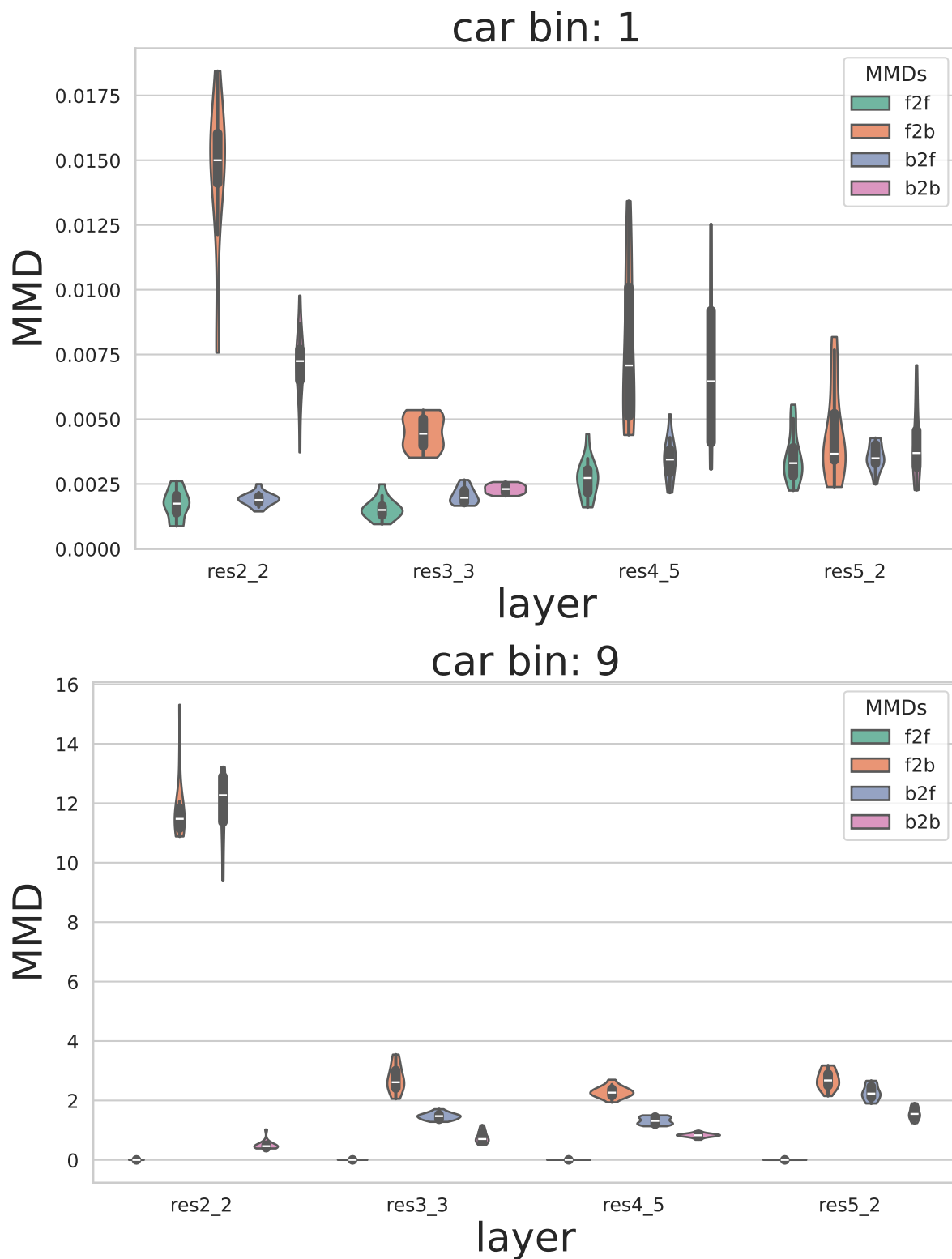


Figure 39. CS-VK small MMD plots. Label: Car.

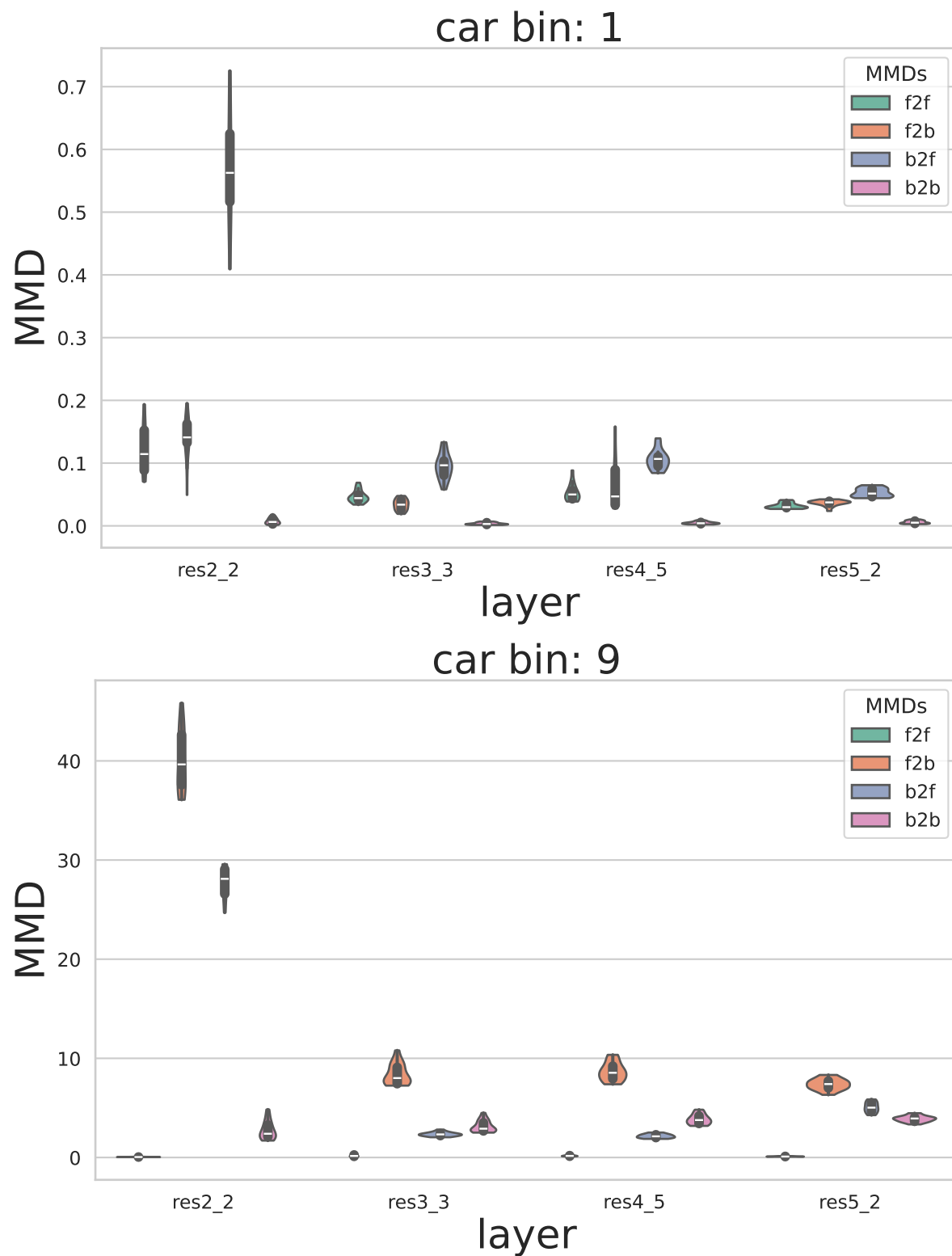


Figure 40. CS-VK medium MMD plots. Label: Car.

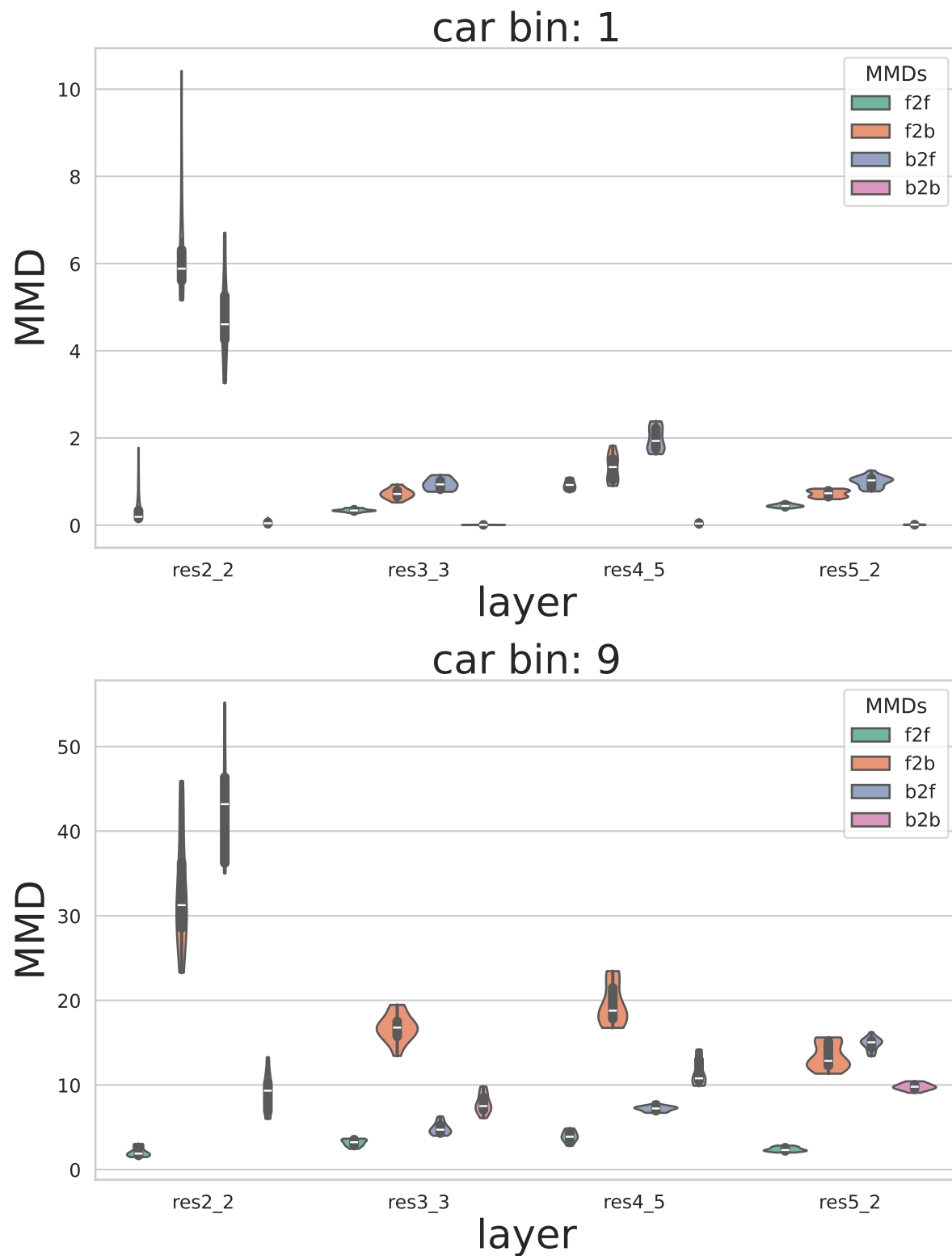


Figure 41. CS-VK large MMD plots. Label: Car.

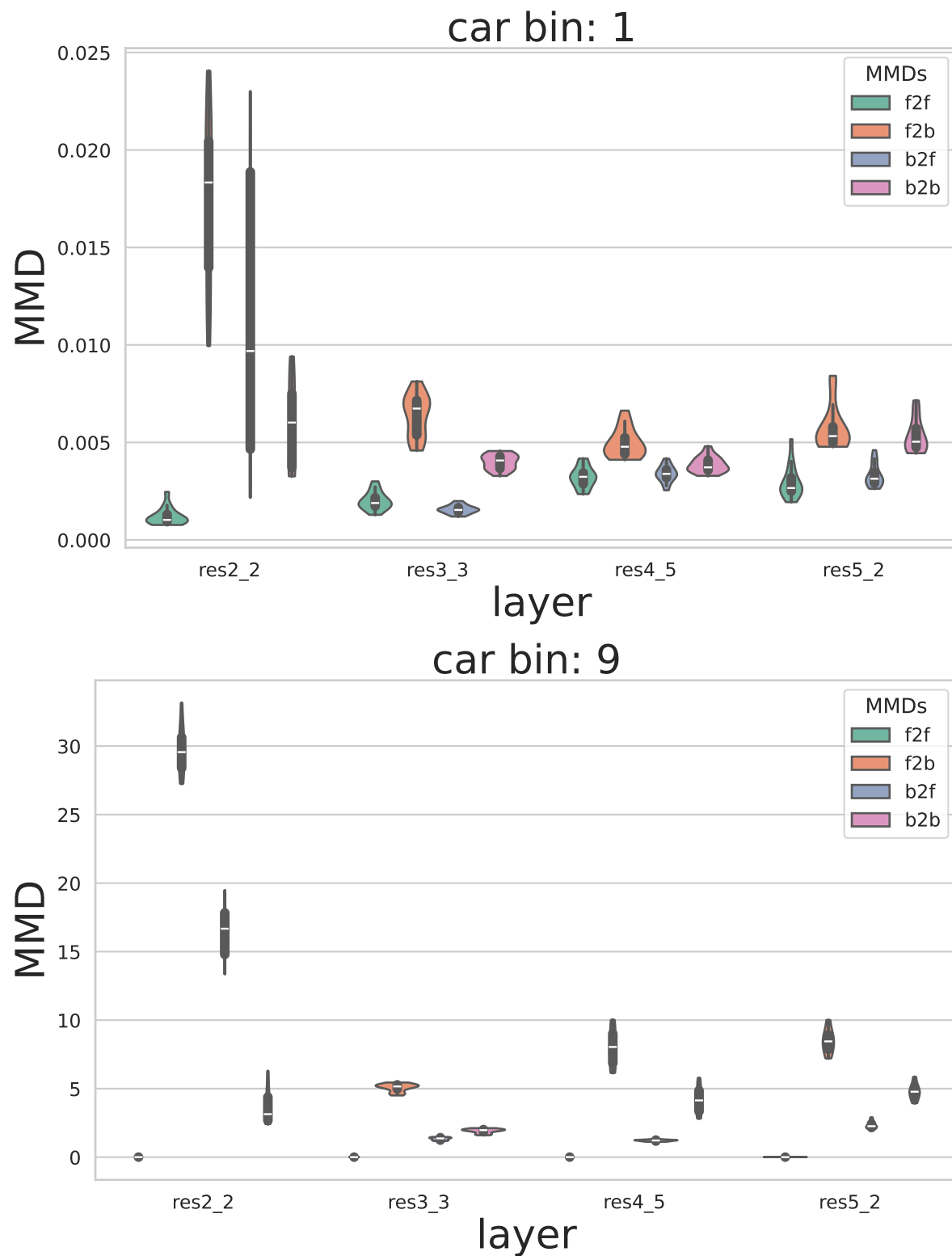


Figure 42. CS-KS small MMD plots. Label: Car.

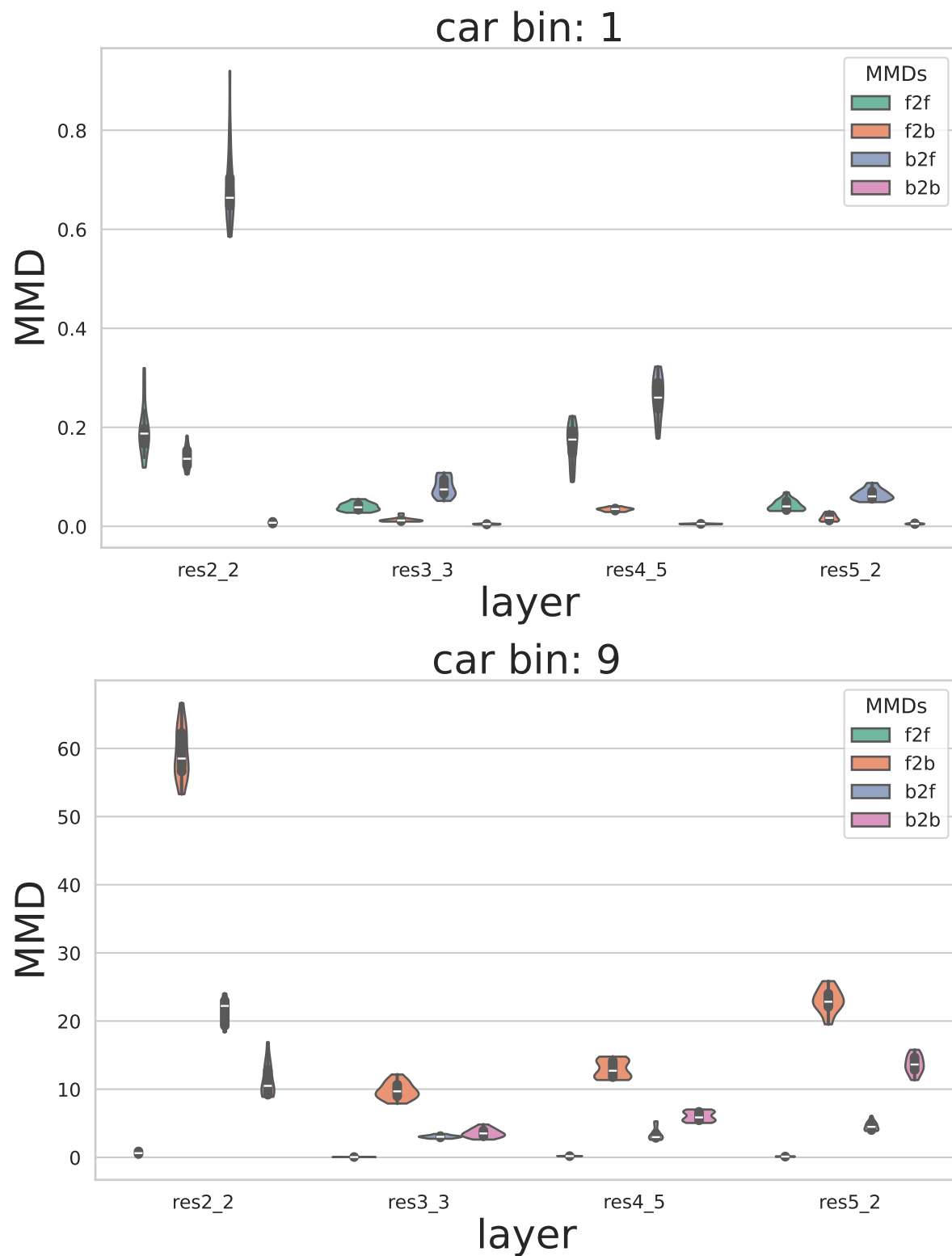


Figure 43. CS-KS medium MMD plots. Label: Car.

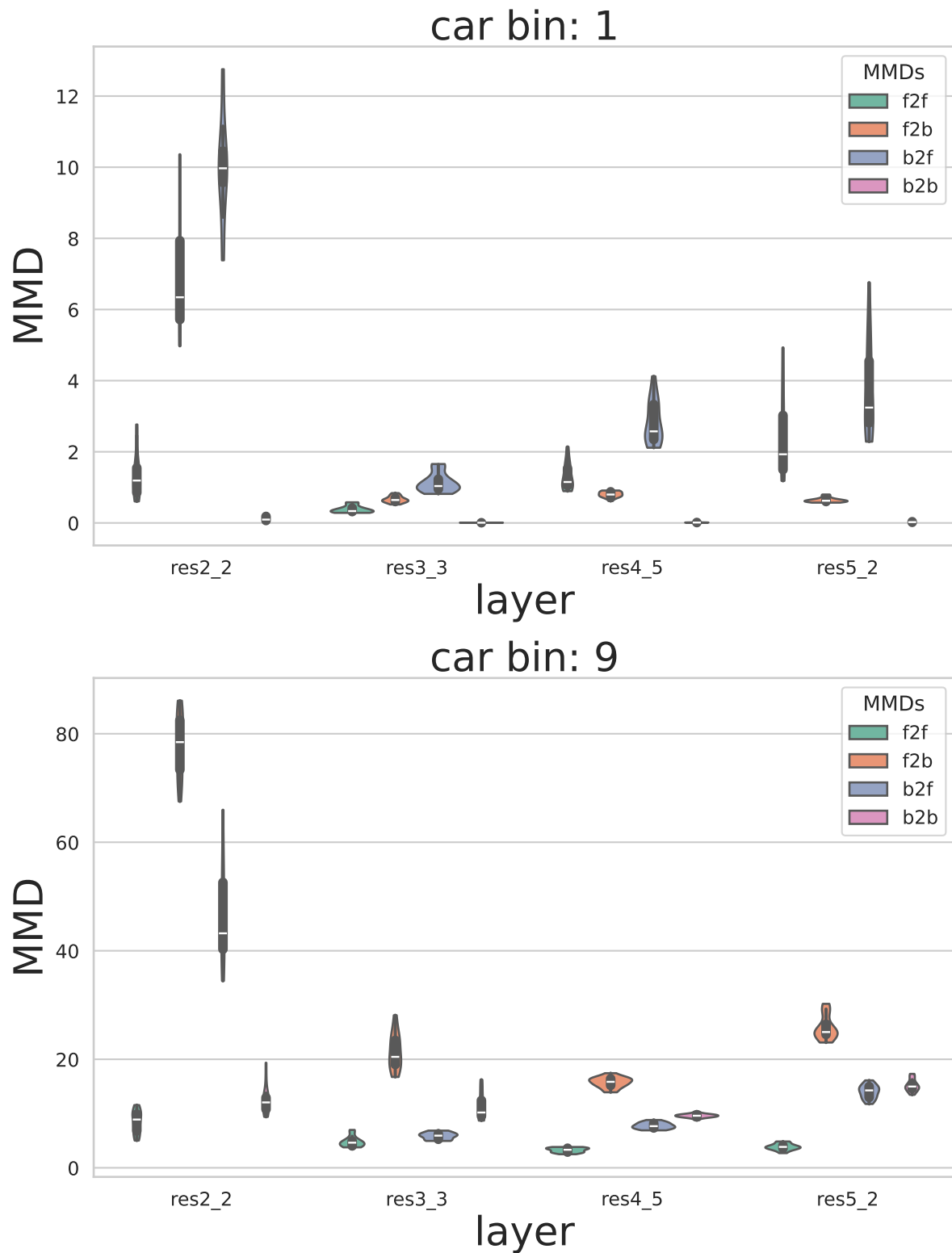


Figure 44. CS-KS large MMD plots. Label: Car.

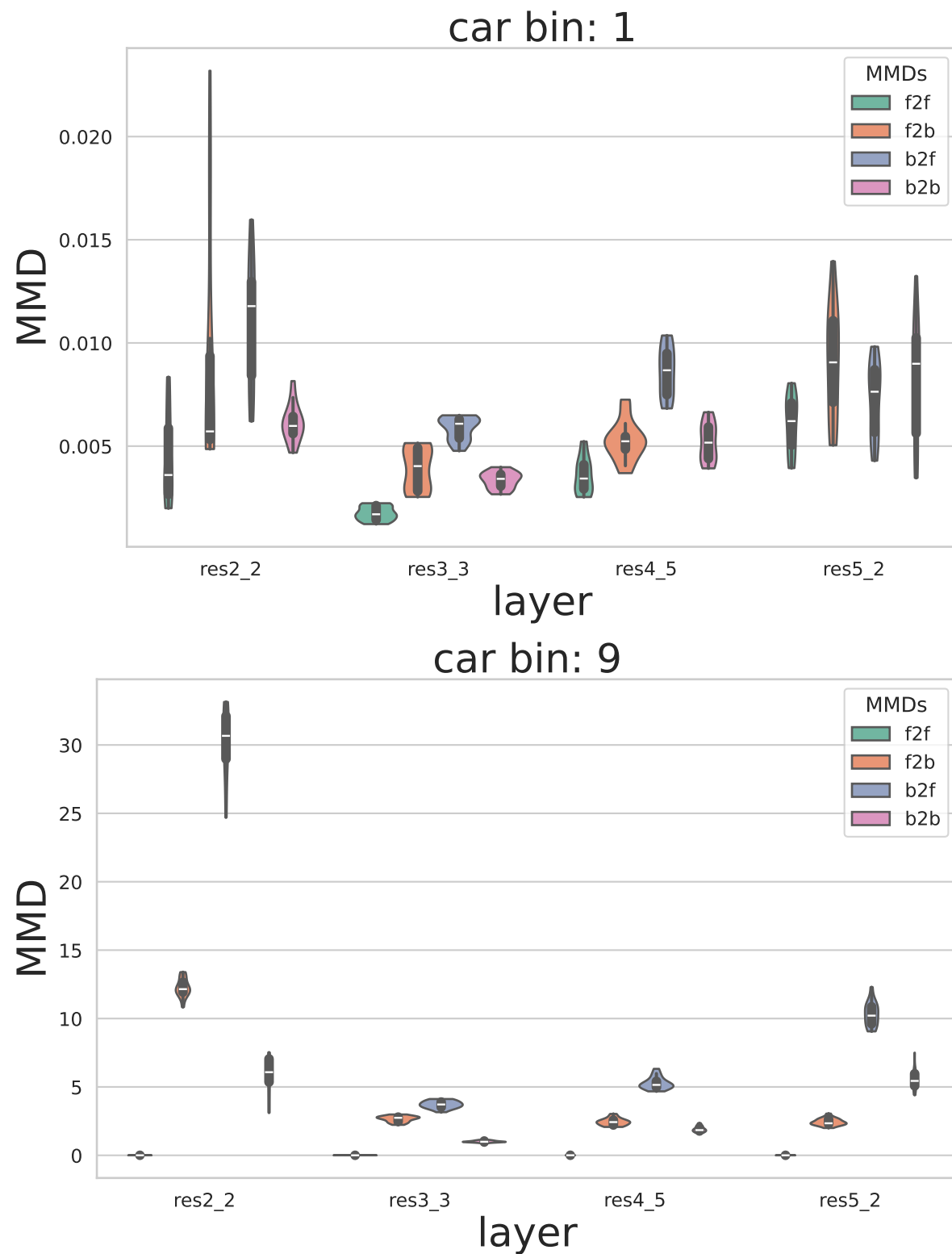


Figure 45. KS-VK small MMD plots. Label: Car.

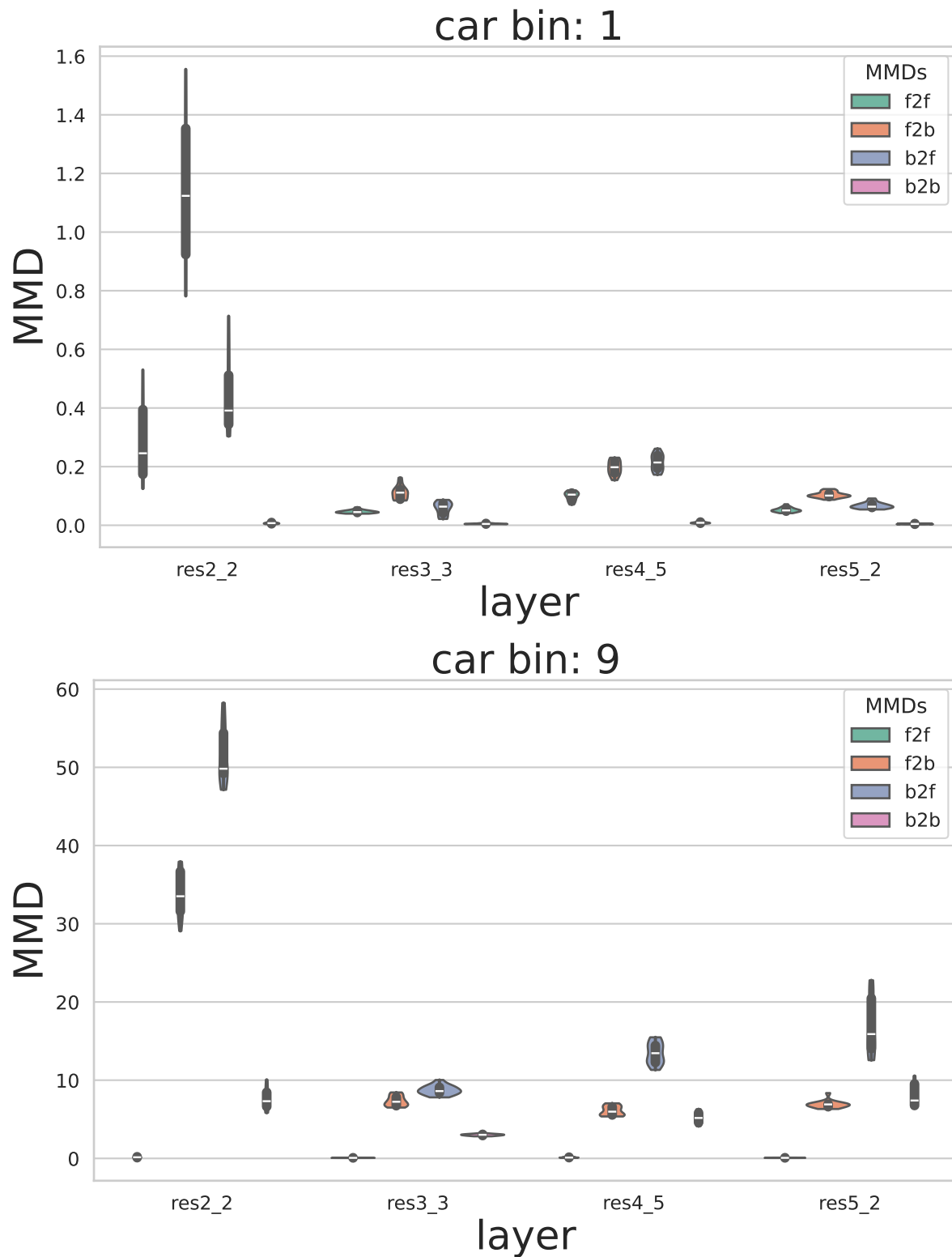


Figure 46. KS-VK medium MMD plots. Label: Car.

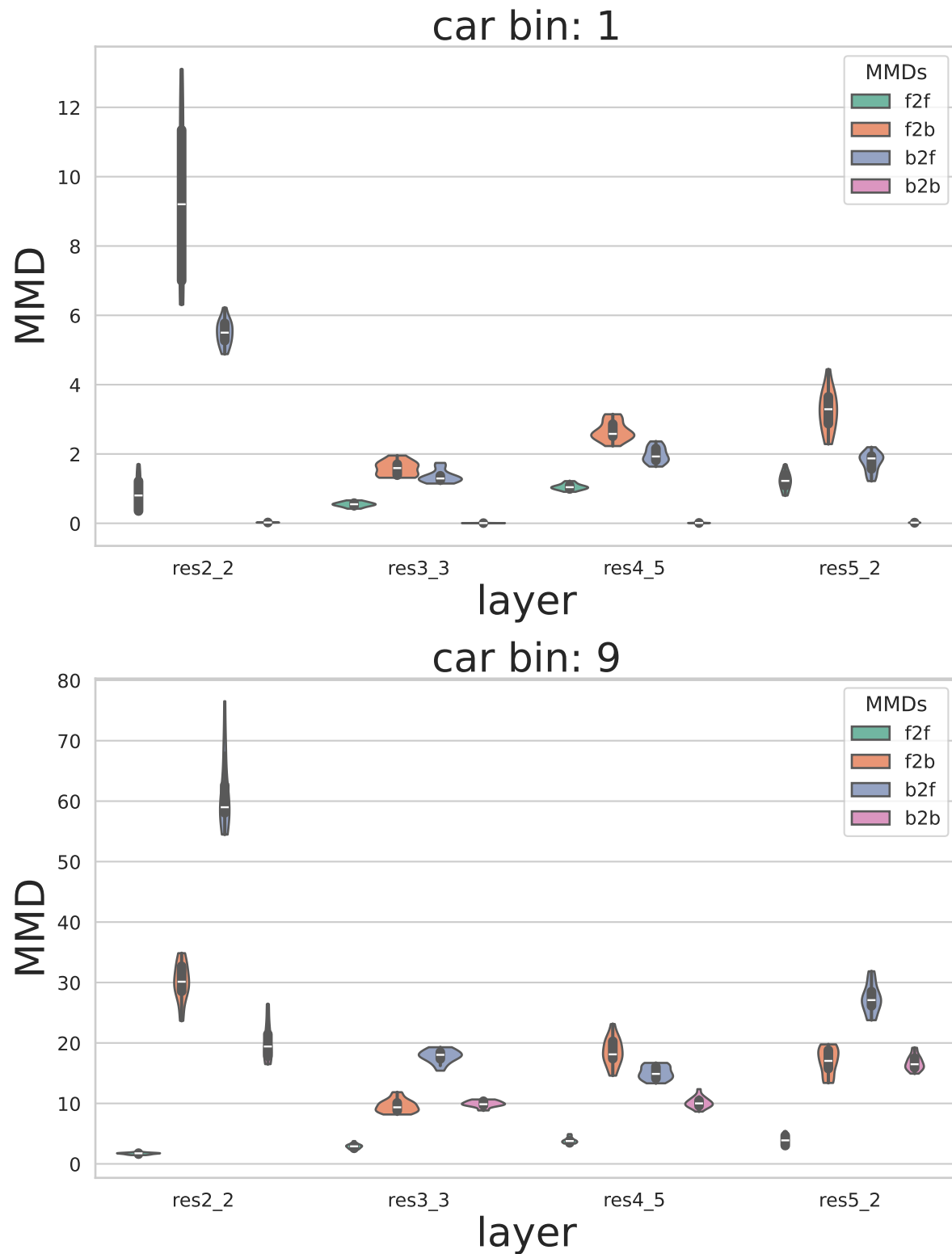


Figure 47. KS-VK large MMD plots. Label: Car.

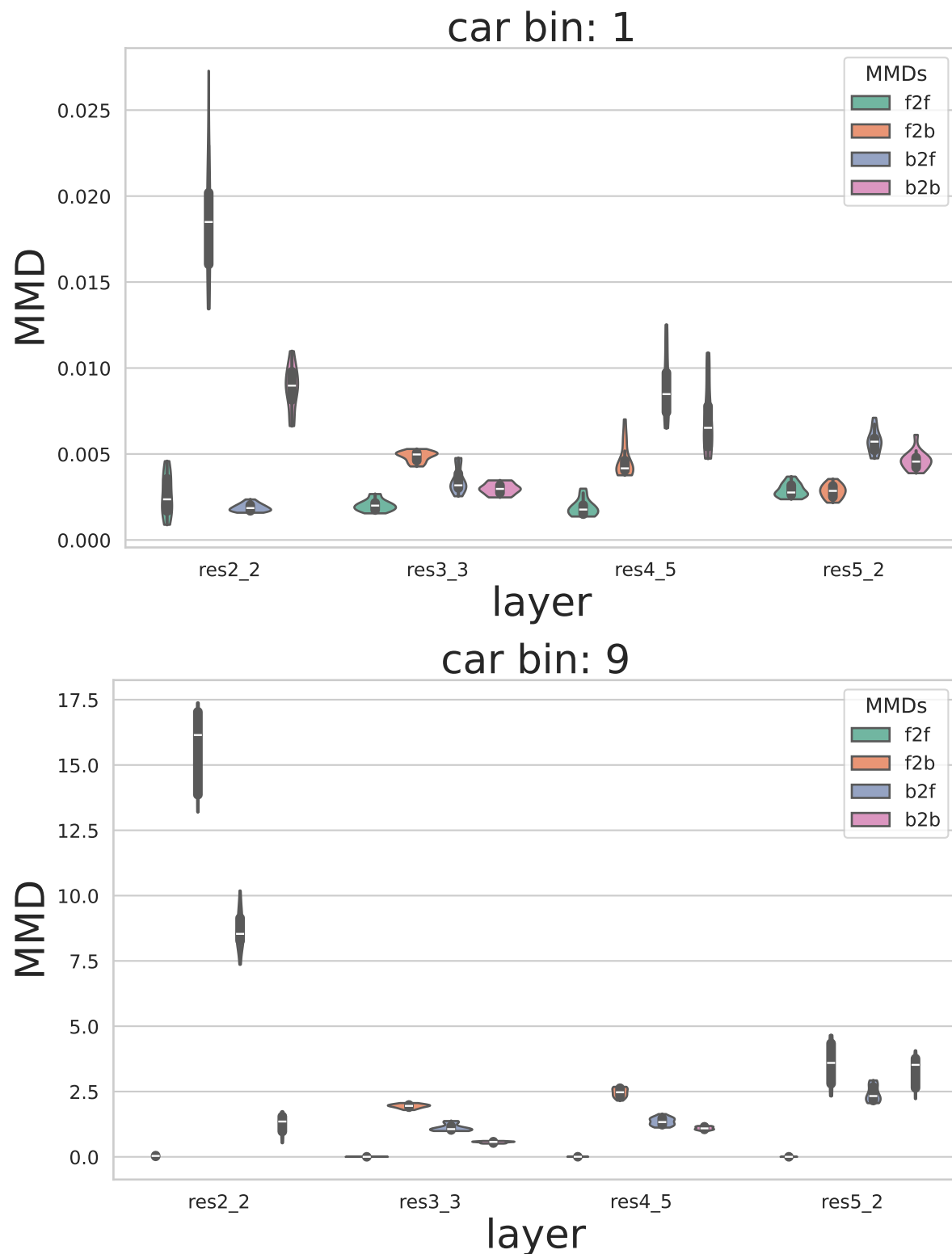


Figure 48. CARLA-VK small MMD plots. Label: Car.

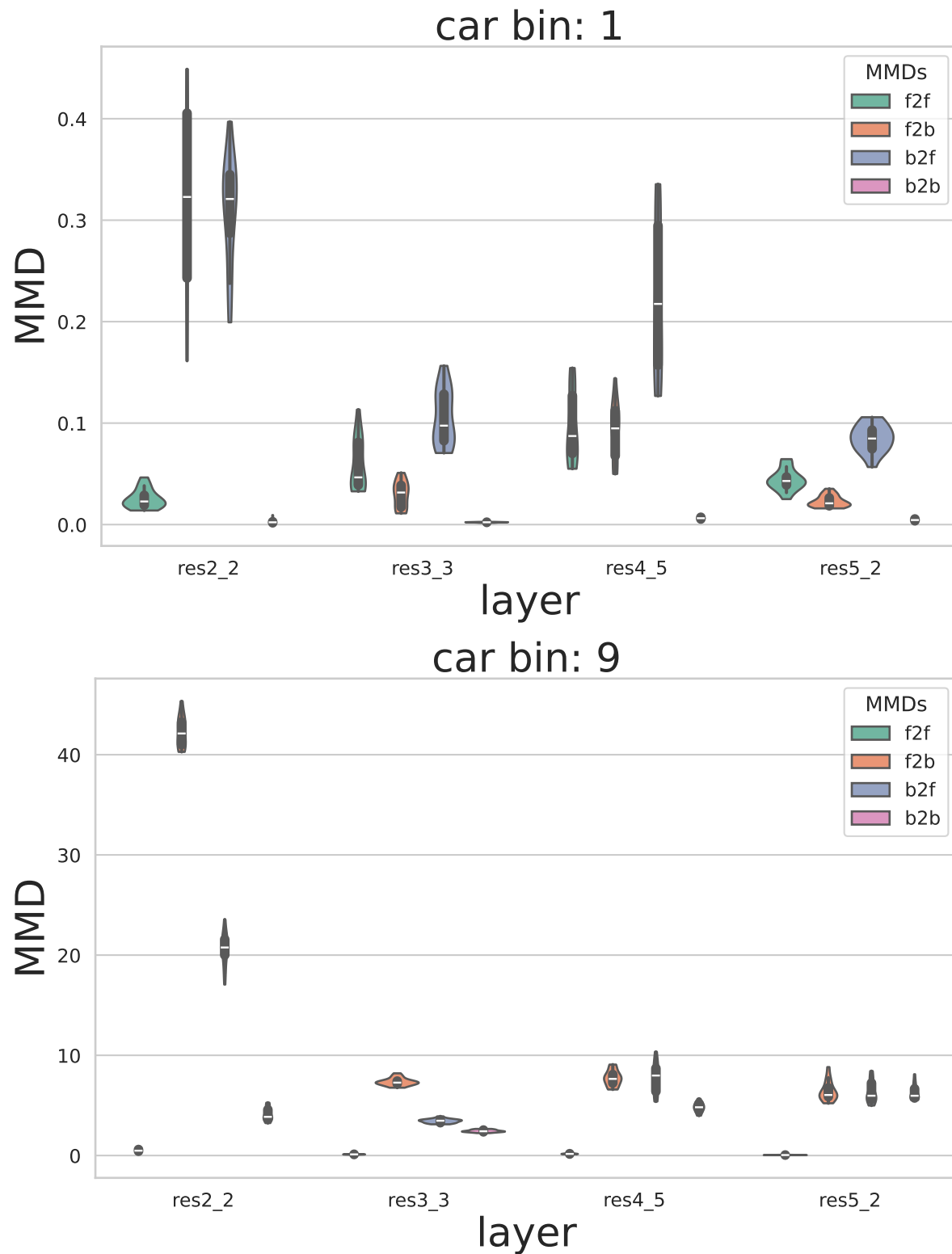


Figure 49. CARLA-VK medium MMD plots. Label: Car.

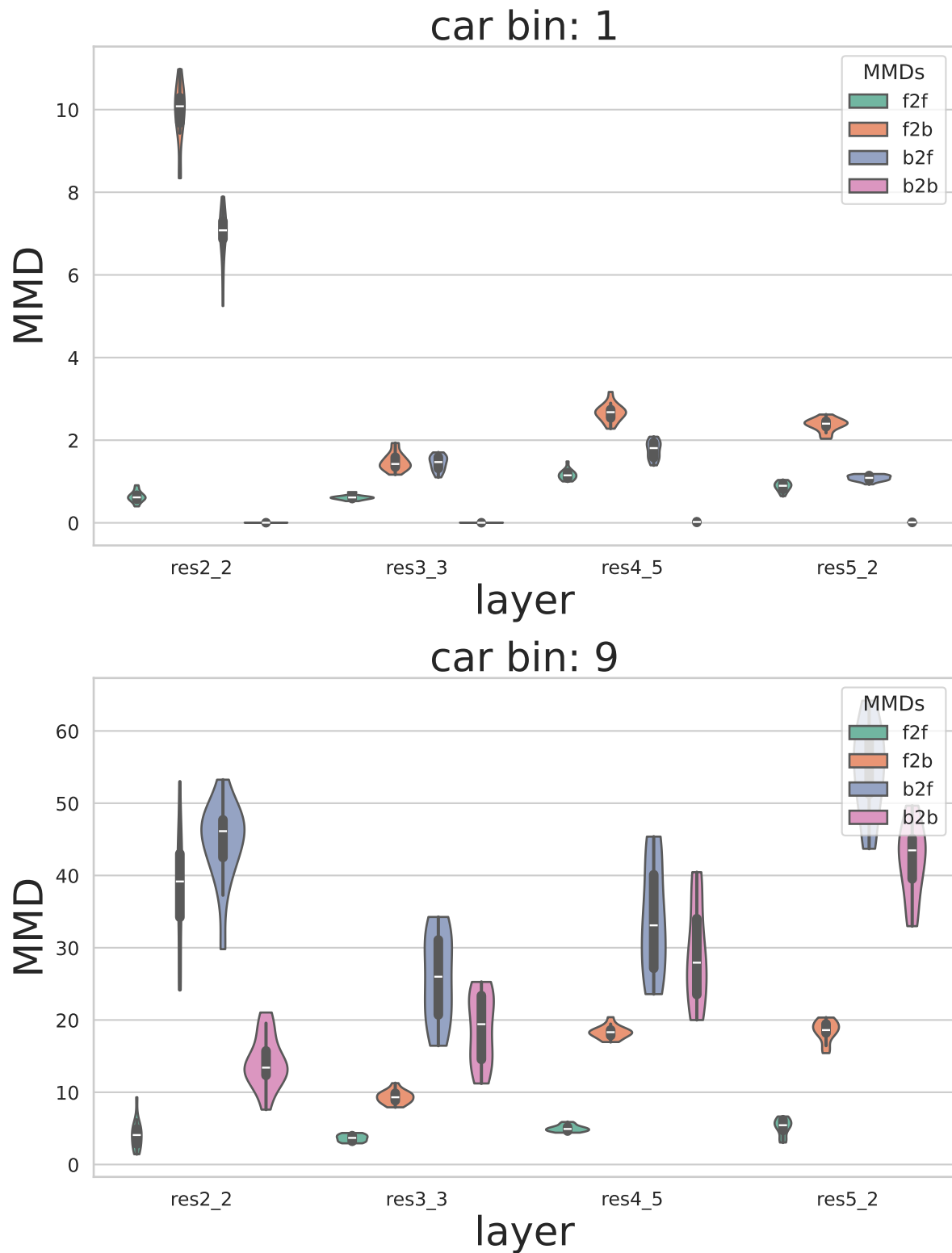


Figure 50. CARLA-VK large MMD plots. Label: Car.

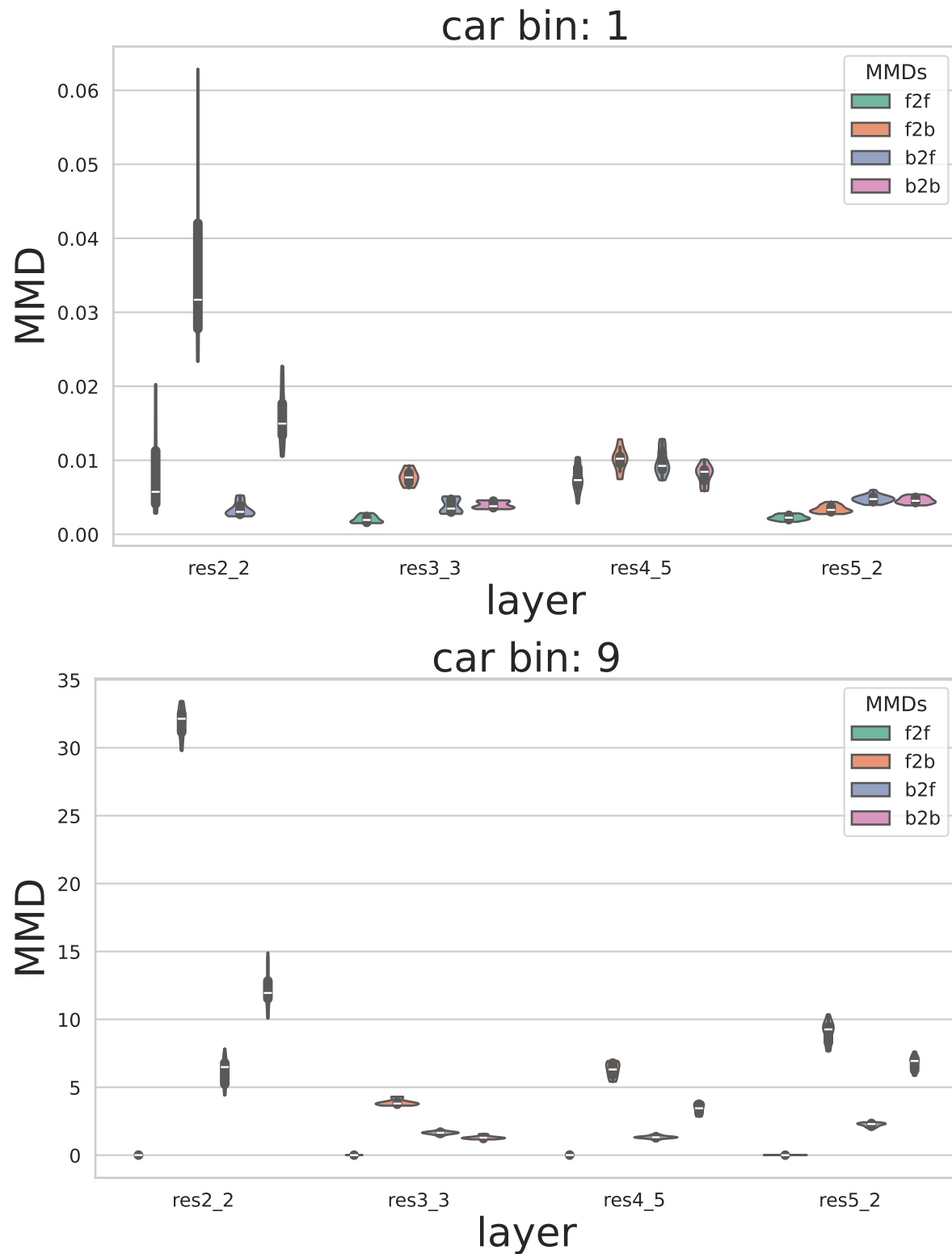


Figure 51. CARLA-KS small MMD plots. Label: Car.

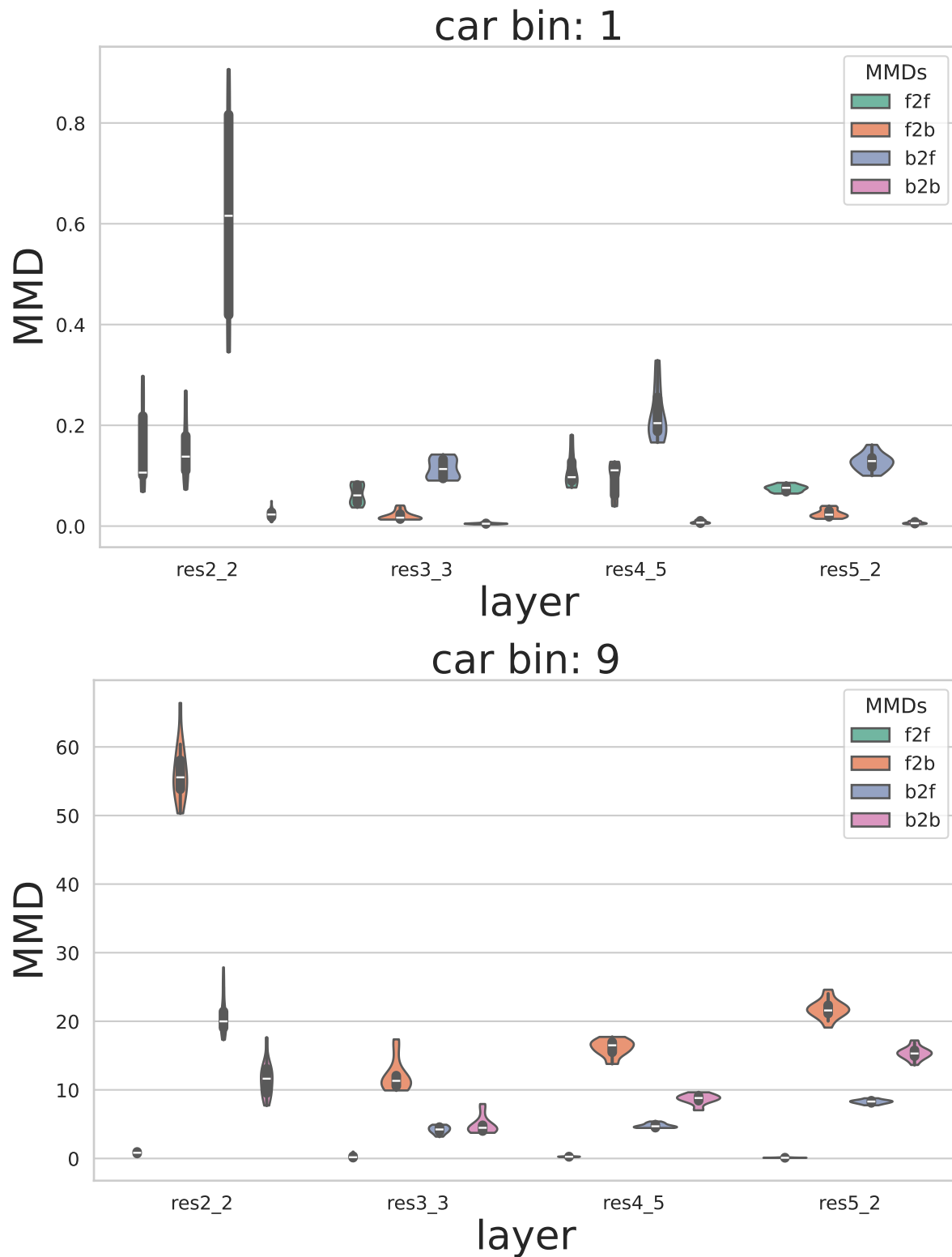


Figure 52. CARLA-ks medium MMD plots. Label: Car.

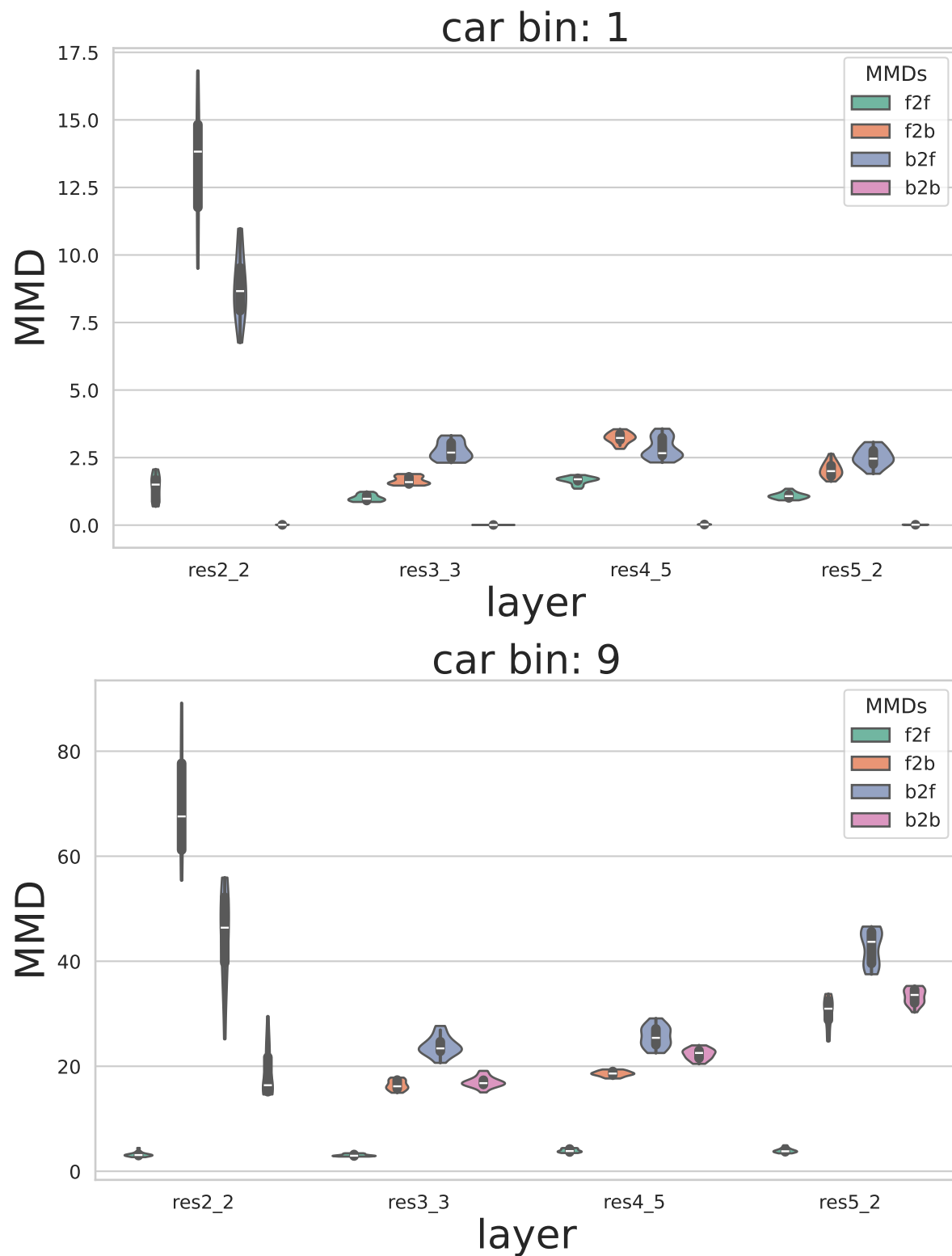
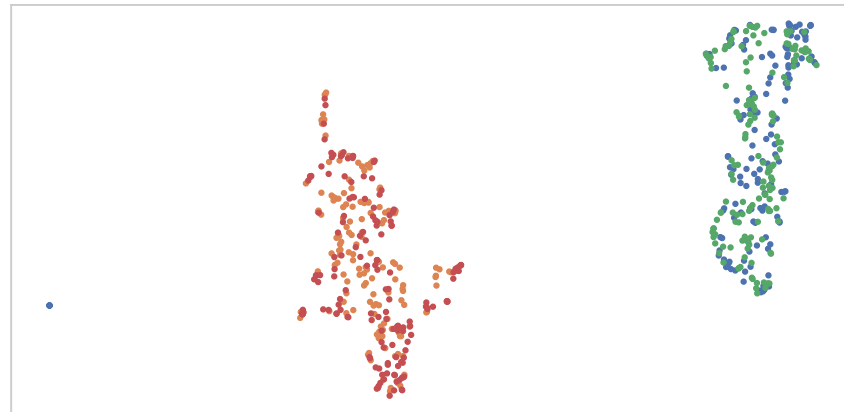


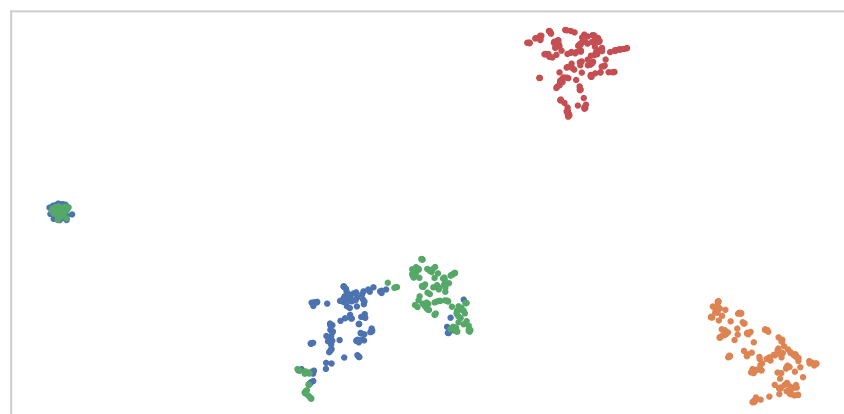
Figure 53. CARLA-KS large MMD plots. Label: Car.

056    **9. UMAP embedding**

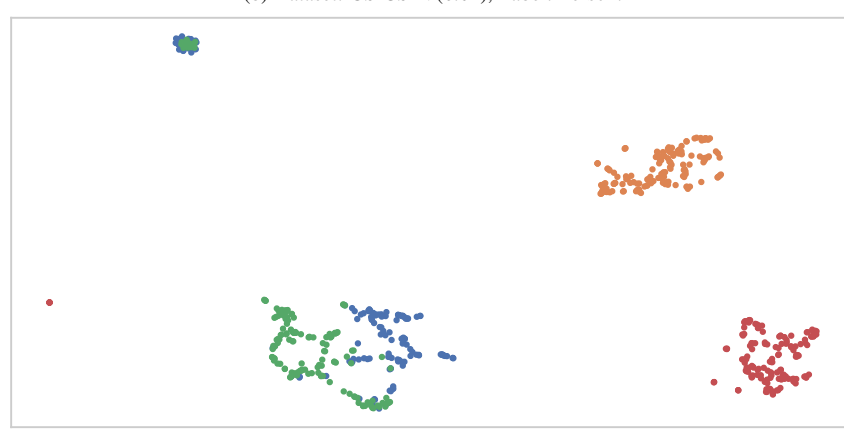
057    This section provides 2D embedding results of non-car la-  
058    bels.



(a) Dataset: CS-CSV, Label: Person.

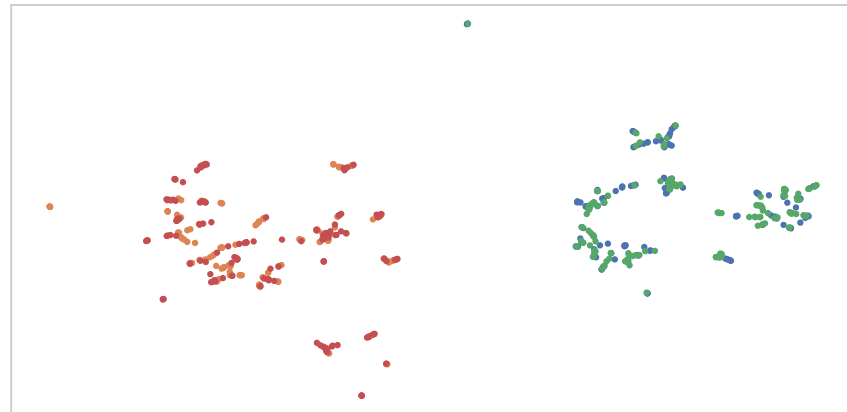


(b) Dataset: CS-CSFV(0.01), Label: Person.

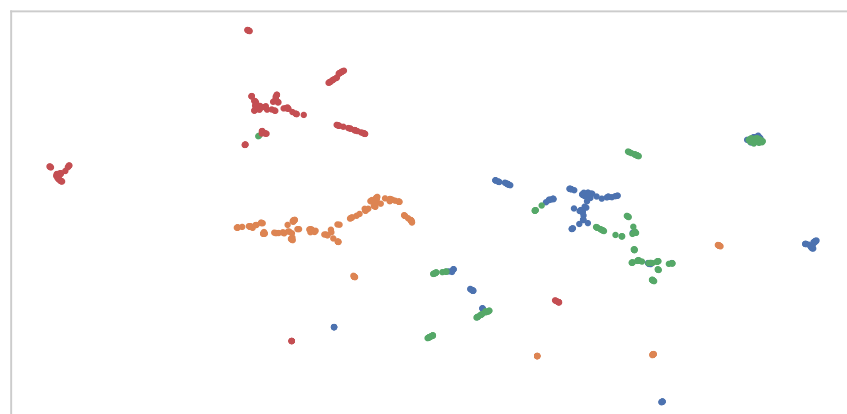


(c) Dataset: CS-CSFV(0.02), Label: Person.

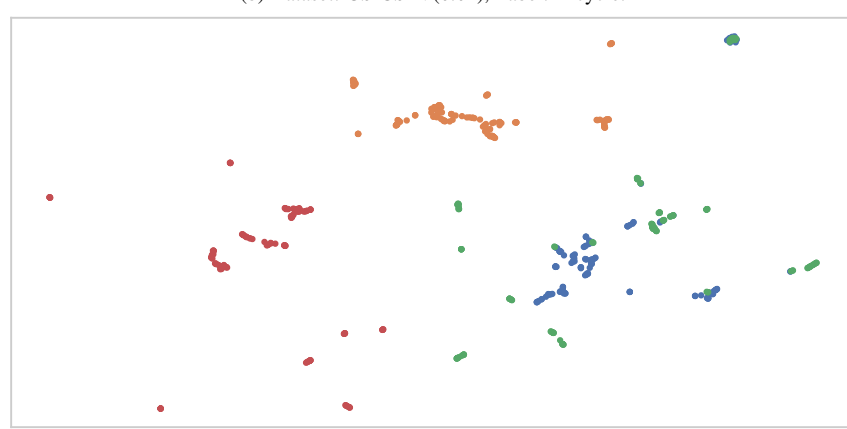
Figure 54. Person 2D embedding using features extracted by Detectron2.



(a) Dataset: CS-CSV, Label: Bicycle.

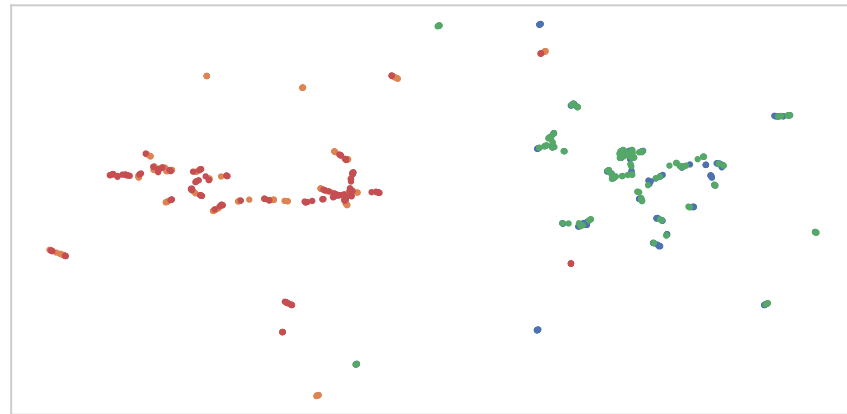


(b) Dataset: CS-CSFV(0.01), Label: Bicycle.

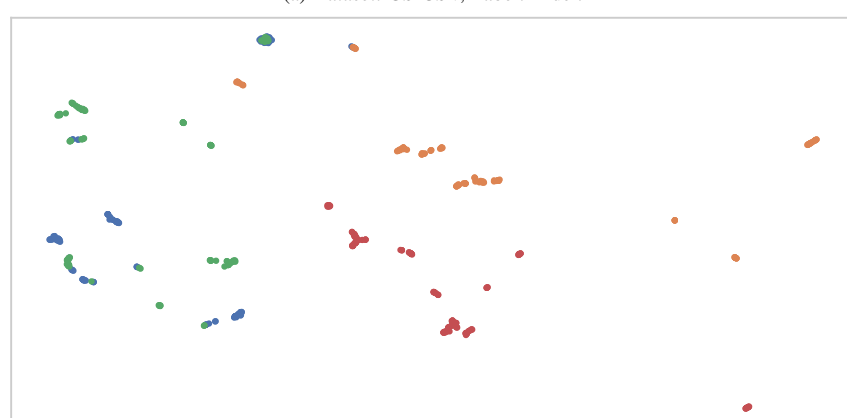


(c) Dataset: CS-CSFV(0.02), Label: Bicycle

Figure 55. **Bicycle 2d embedding using features extracted by Detectron2.**



(a) Dataset: CS-CSV, Label: Rider.



(b) Dataset: CS-CSFV(0.01), Label: Rider.

Figure 56. Rider 2d embedding using features extracted by Detectron2.

059    **10. Pixel distribution of dataset**

060    This section presents the pixel distribution for each dataset.

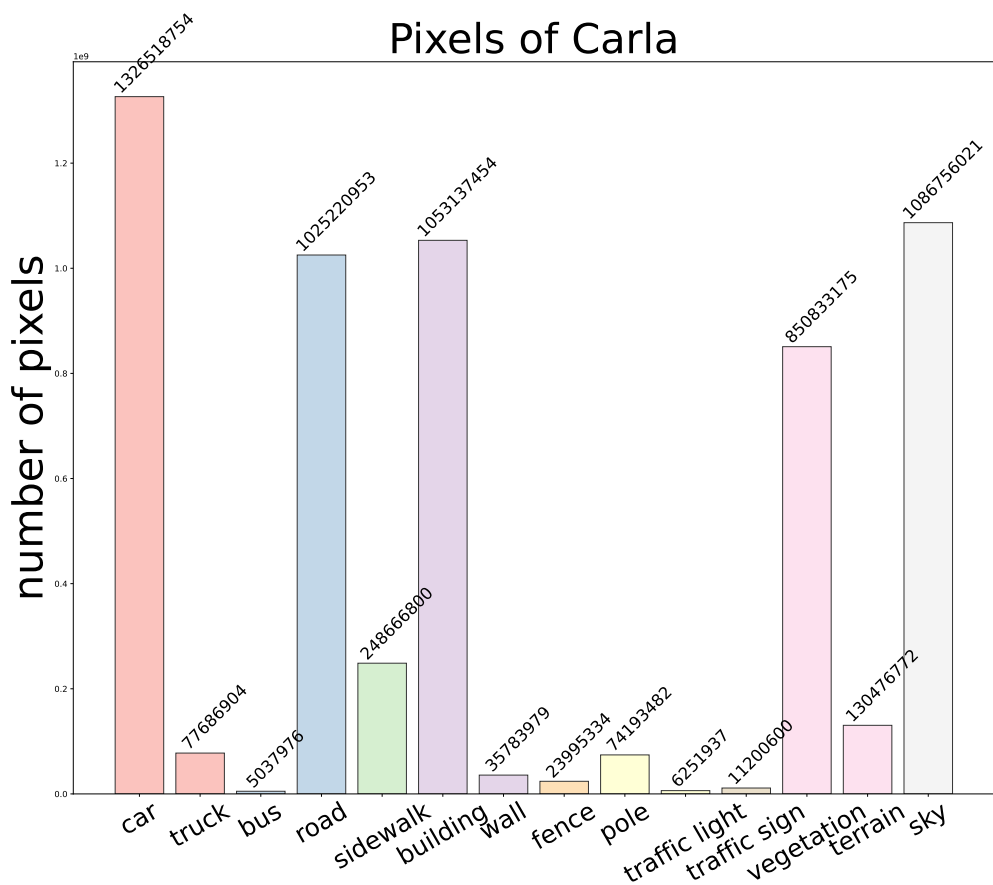


Figure 57. Pixel distribution of CARLA.

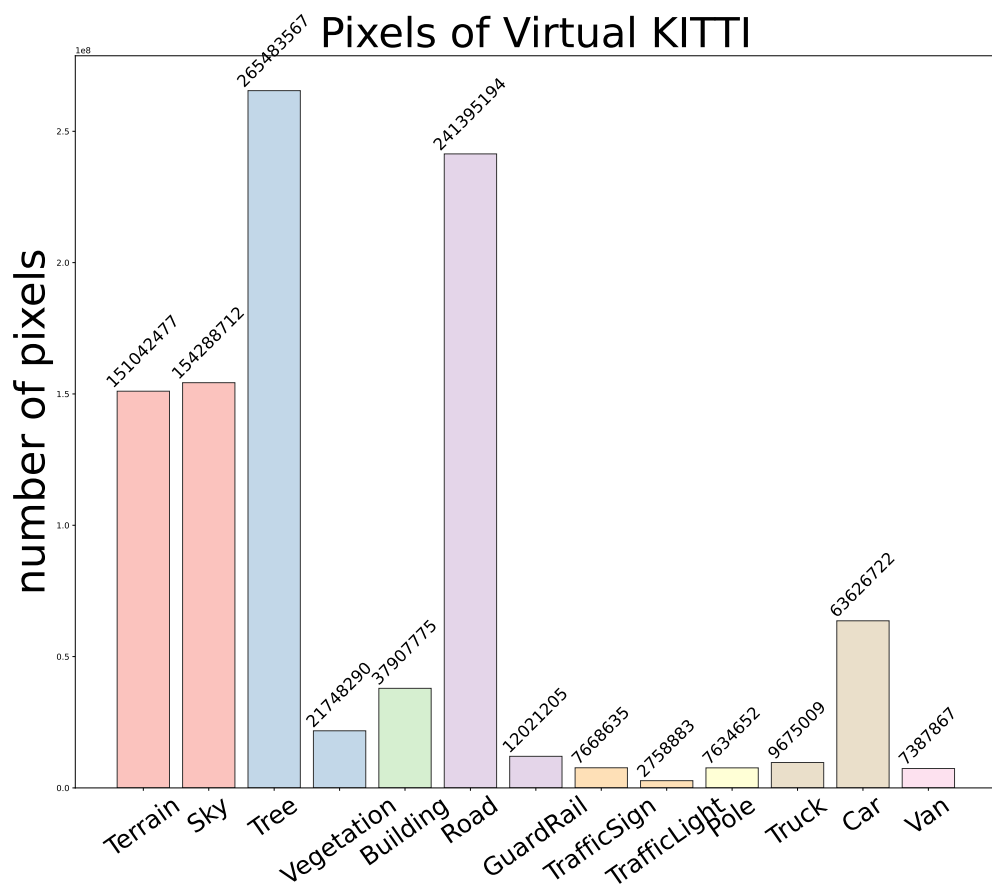


Figure 58. Pixel distribution of Virtual KITTI.

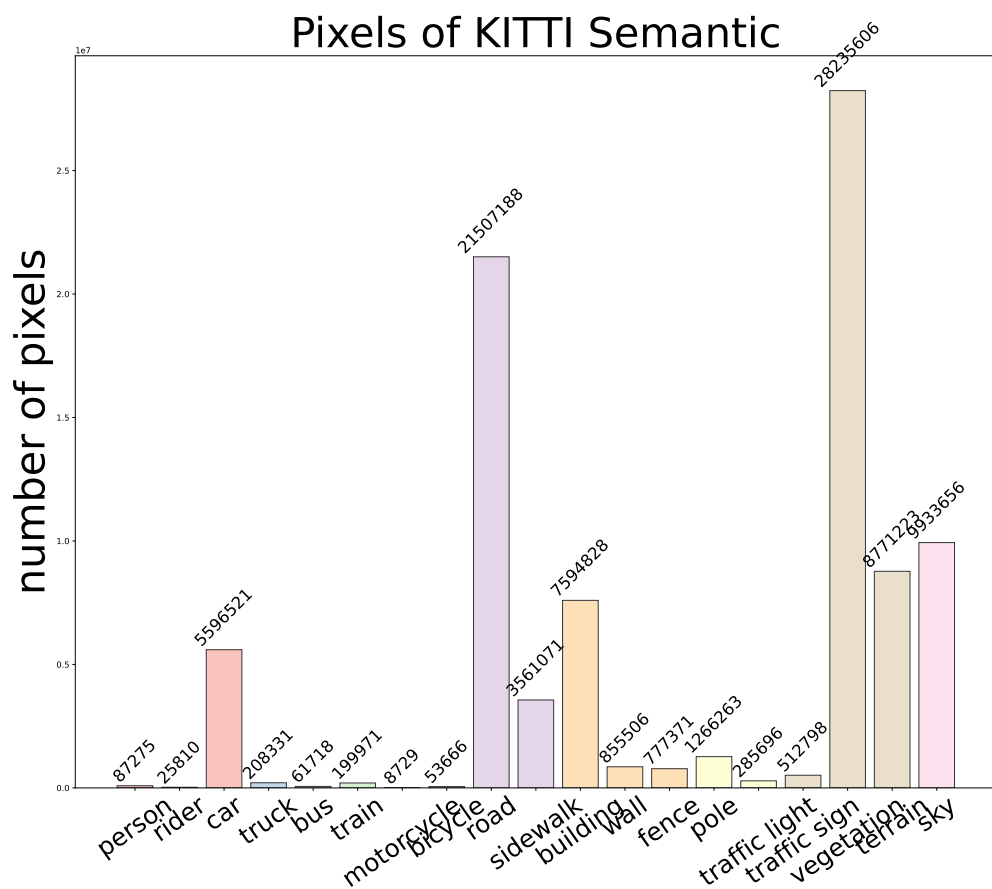


Figure 59. Pixel distribution of KITTI semantic.

061    **11. 3D embedding with image patch**

062    This section contains 3D embedding result of CS-CARLA  
063    with image patches at each aggregated location.

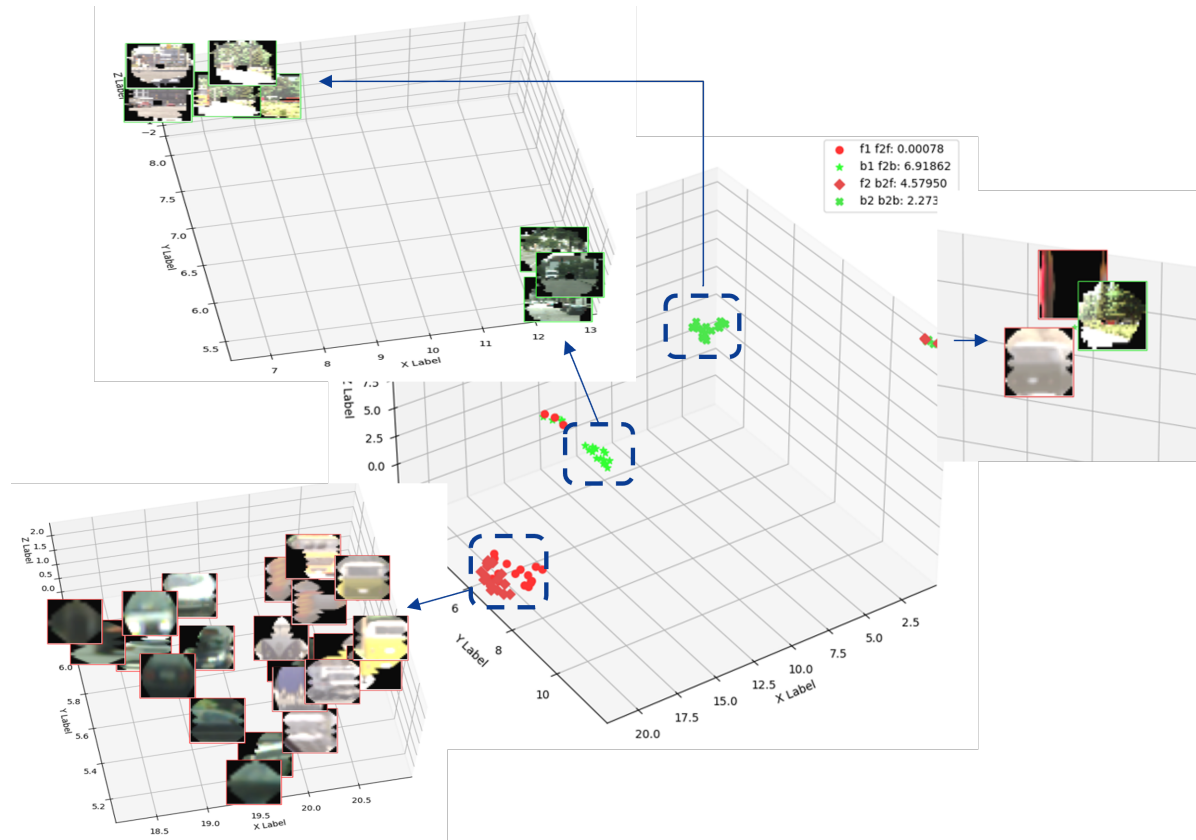


Figure 60. The 3D feature embedding results for CS-CARLA with image patches

**064 12. Quantification results with YOLOv11**

065 This section includes analysis results using YOLOv11.

Category	AP50	AP
person	-	39.136
truck	-	37.566
motorcycle	-	23.498
rider	-	39.701
bus	-	56.698
bicycle	-	28.720
car	-	60.100
train	-	27.338
<b>total</b>	<b>59.467</b>	39.095

Table 127. Training: Cityscapes. Validation: Cityscapes validation.

Category	AP50	AP
person	-	36.297
truck	-	26.304
motorcycle	-	19.945
rider	-	39.297
bus	-	43.760
bicycle	-	26.299
car	-	53.323
train	-	17.353
<b>total</b>	<b>49.502</b>	32.83

Table 128. Training: Cityscapes. Validation: Cityscapes Foggy validation all.

Layer	MMD mean			
	f2f	f2b	b2f	b2b
16	<b>0.062982</b>	46.527572	44.755515	0.739028
19	<b>0.021485</b>	33.528399	34.313704	0.385100
22	<b>0.063939</b>	49.361399	48.647746	1.886446

Table 129. Dataset: CS-CSV, Label: Car, Bin: 9

Layer	MVD mean			
	f2f	f2b	b2f	b2b
16	2.082891	2.768664	2.600703	2.235739
19	2.023870	2.480386	2.500061	2.051497
22	1.991999	2.581061	2.531971	1.971515

Table 130. Dataset: CS-CSV, Label: Car, Bin: 9

Layer	MMD mean			
	f2f	f2b	b2f	b2b
16	<b>0.001082</b>	48.304126	47.271472	0.316746
19	<b>0.000422</b>	43.704660	41.628886	1.214850
22	<b>0.006436</b>	55.798843	52.155659	2.215627

Table 131. Dataset: CS-CSV, Label: Person, Bin: 9

Layer	MVD mean			
	f2f	f2b	b2f	b2b
16	1.960343	2.573416	2.491306	2.023483
19	1.592186	2.651211	2.217081	2.216614
22	1.492126	3.311943	3.513309	1.975400

Table 132. Dataset: CS-CSV, Label: Person, Bin: 9

Layer	MMD mean			
	f2f	f2b	b2f	b2b
16	<b>0.003022</b>	49.215211	48.900521	0.359209
19	<b>0.001321</b>	40.103845	39.512206	0.694770
22	<b>0.039864</b>	56.192046	54.442013	1.584969

Table 133. Dataset: CS-CSV, Label: Bicycle, Bin: 9

Layer	MVD mean			
	f2f	f2b	b2f	b2b
16	2.230733	2.766177	2.818898	2.372704
19	2.171476	2.606431	2.676396	2.305838
22	3.153666	3.673676	3.407658	2.721582

Table 134. Dataset: CS-CSV, Label: Bicycle, Bin: 9

Layer	MMD mean			
	f2f	f2b	b2f	b2b
16	<b>0.000341</b>	48.350617	48.650631	0.234731
19	<b>0.006494</b>	39.833535	41.351455	0.646978
22	<b>0.002645</b>	55.750656	53.629656	1.461994

Table 135. Dataset: CS-CSV, Label: Rider, Bin: 9

Table 136. Dataset: CS-CSV, Label: Rider, Bin: 9

Table 137. MMD and MVD between Cityscapes and Cityscapes validation with YOLOv11.

Layer	MMD mean			
	f2f	f2b	b2f	b2b
16	<b>0.052369</b>	44.463880	44.449926	0.496768
19	<b>0.034595</b>	35.741977	34.263380	0.524899
22	<b>0.070419</b>	52.808069	47.863179	2.858149

Table 138. Dataset: CS-CSFV(0.01), Label: Car, Bin: 9

Layer	MVD mean			
	f2f	f2b	b2f	b2b
16	2.065351	2.728877	2.837551	2.233894
19	2.258033	2.975489	2.913789	2.448860
22	2.160244	3.065206	2.820929	2.627436

Table 139. Dataset: CS-CSFV(0.01), Label: Car, Bin: 9

Layer	MMD mean			
	f2f	f2b	b2f	b2b
16	<b>0.003848</b>	48.176220	48.276418	1.381587
19	<b>0.001514</b>	37.780063	43.631943	3.893865
22	<b>0.017657</b>	51.606834	55.297625	2.041304

Table 140. Dataset: CS-CSFV(0.01), Label: Person, Bin: 9

Layer	MVD mean			
	f2f	f2b	b2f	b2b
16	2.441030	3.065571	2.879739	2.834703
19	2.221090	2.844073	2.893038	2.923079
22	3.137492	3.757901	3.885831	2.926269

Table 141. Dataset: CS-CSFV(0.01), Label: Person, Bin: 9

Table 142. MMD and MVD between Cityscapes and Cityscapes foggy 0.01 with YOLOv11.

Layer	MMD mean			
	f2f	f2b	b2f	b2b
16	<b>0.002802</b>	48.780400	47.002906	1.857787
19	<b>0.006408</b>	38.230902	38.861622	2.255664
22	<b>0.017192</b>	55.024863	54.564572	2.540956

Table 143. Dataset: CS-CSFV(0.02), Label: Car, Bin: 9

Layer	MVD mean			
	f2f	f2b	b2f	b2b
16	2.138397	3.275905	2.848661	3.096649
19	2.196083	3.340245	2.868632	3.118983
22	3.123307	3.920284	3.048506	3.102361

Table 144. Dataset: CS-CSFV(0.02), Label: Car, Bin: 9

Layer	MMD mean			
	f2f	f2b	b2f	b2b
16	<b>0.000121</b>	49.264899	48.531709	1.154784
19	<b>0.000268</b>	38.410784	41.683570	4.211147
22	<b>0.001235</b>	57.679659	56.073639	6.379770

Table 145. Dataset: CS-CSFV(0.02), Label: Person, Bin: 9

Layer	MVD mean			
	f2f	f2b	b2f	b2b
16	2.350183	3.540801	2.983840	3.531022
19	3.238921	4.310045	3.734321	3.406865
22	0.442293	2.938622	2.451624	3.720328

Table 146. Dataset: CS-CSFV(0.02), Label: Person, Bin: 9

Table 147. MMD and MVD between Cityscapes and Cityscapes foggy 0.02 with YOLOv11.

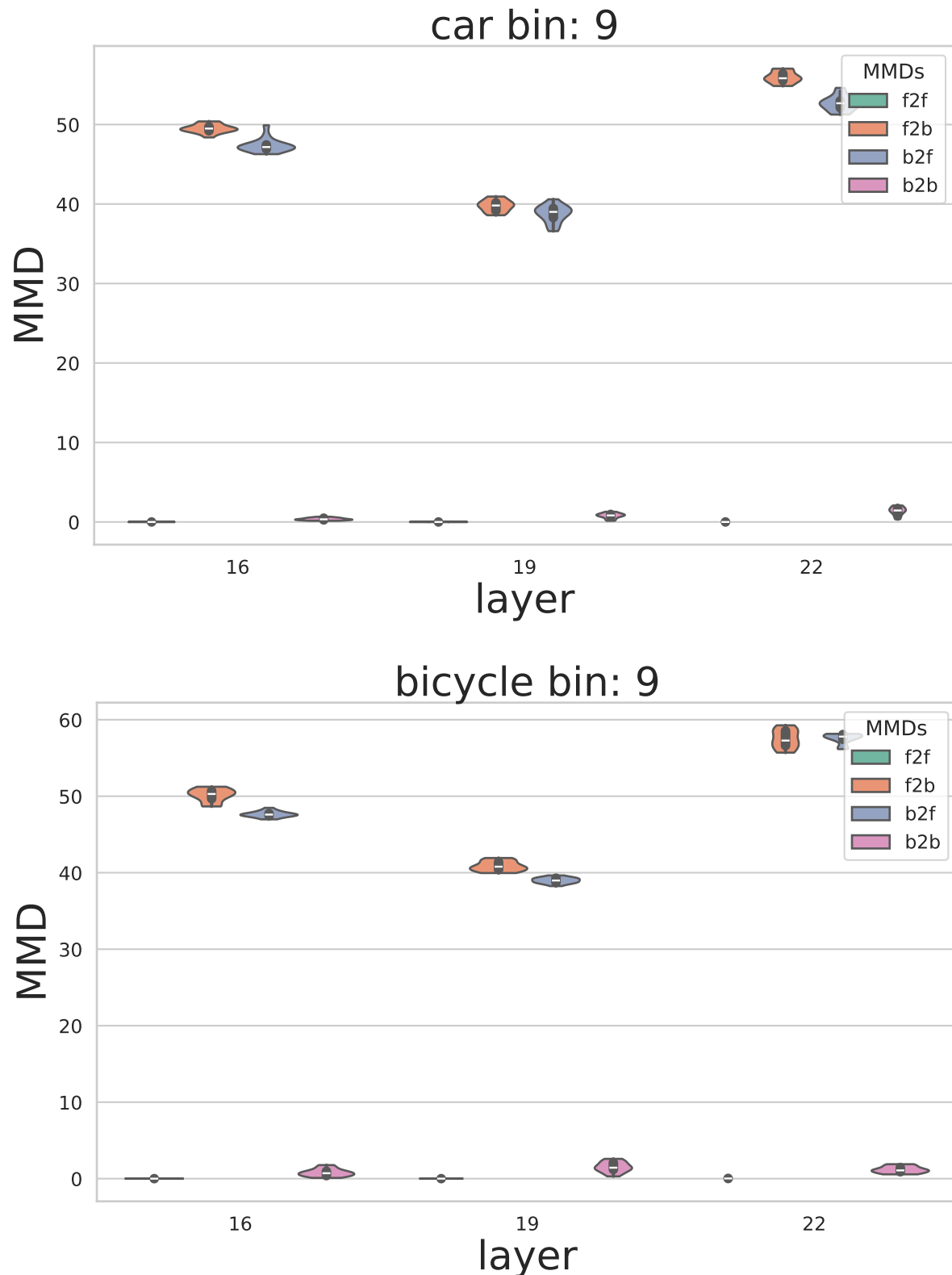


Figure 61. CS-CSV MMD plots YOLOv11.

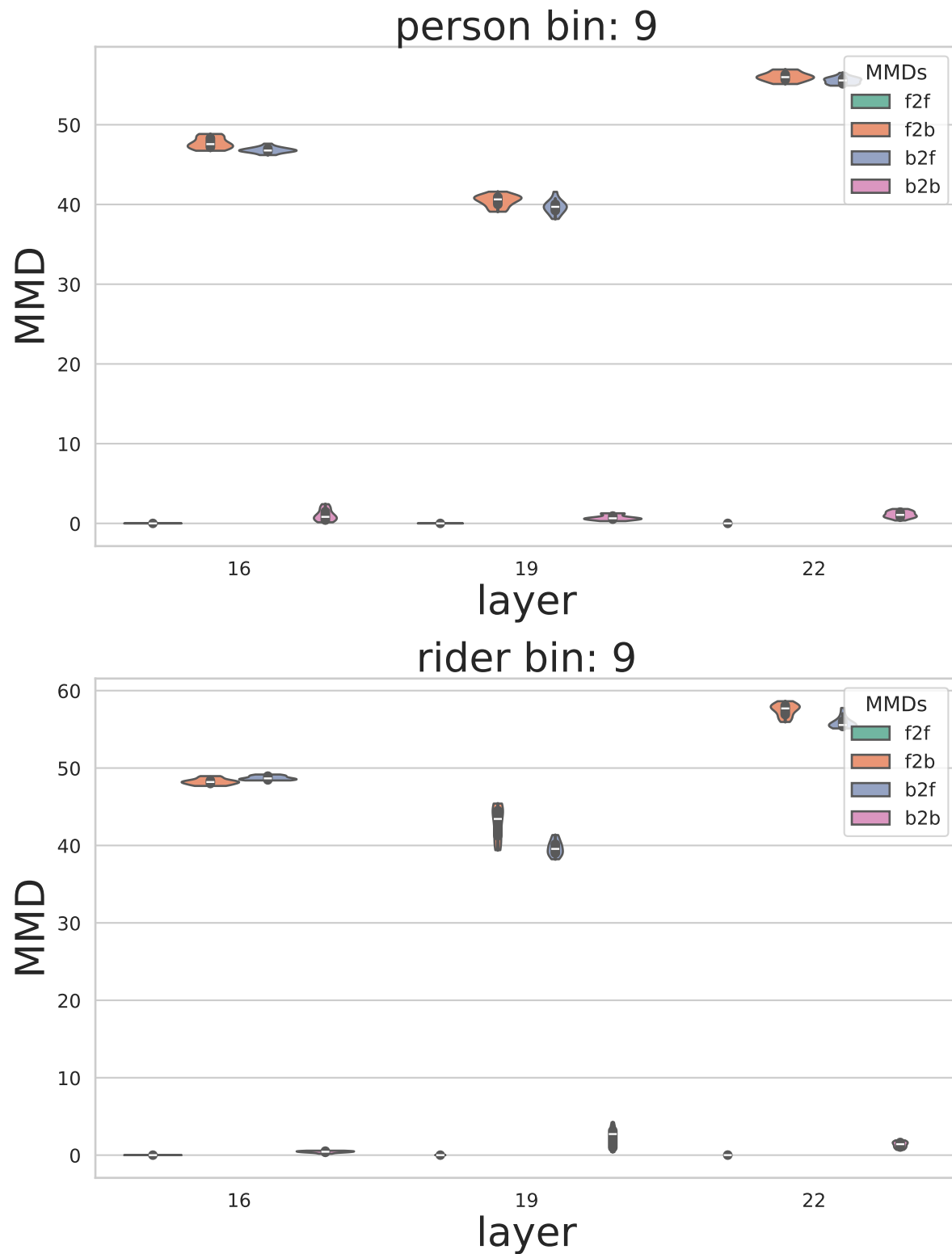


Figure 62. CS-CSV MMD plots YOLOv11.

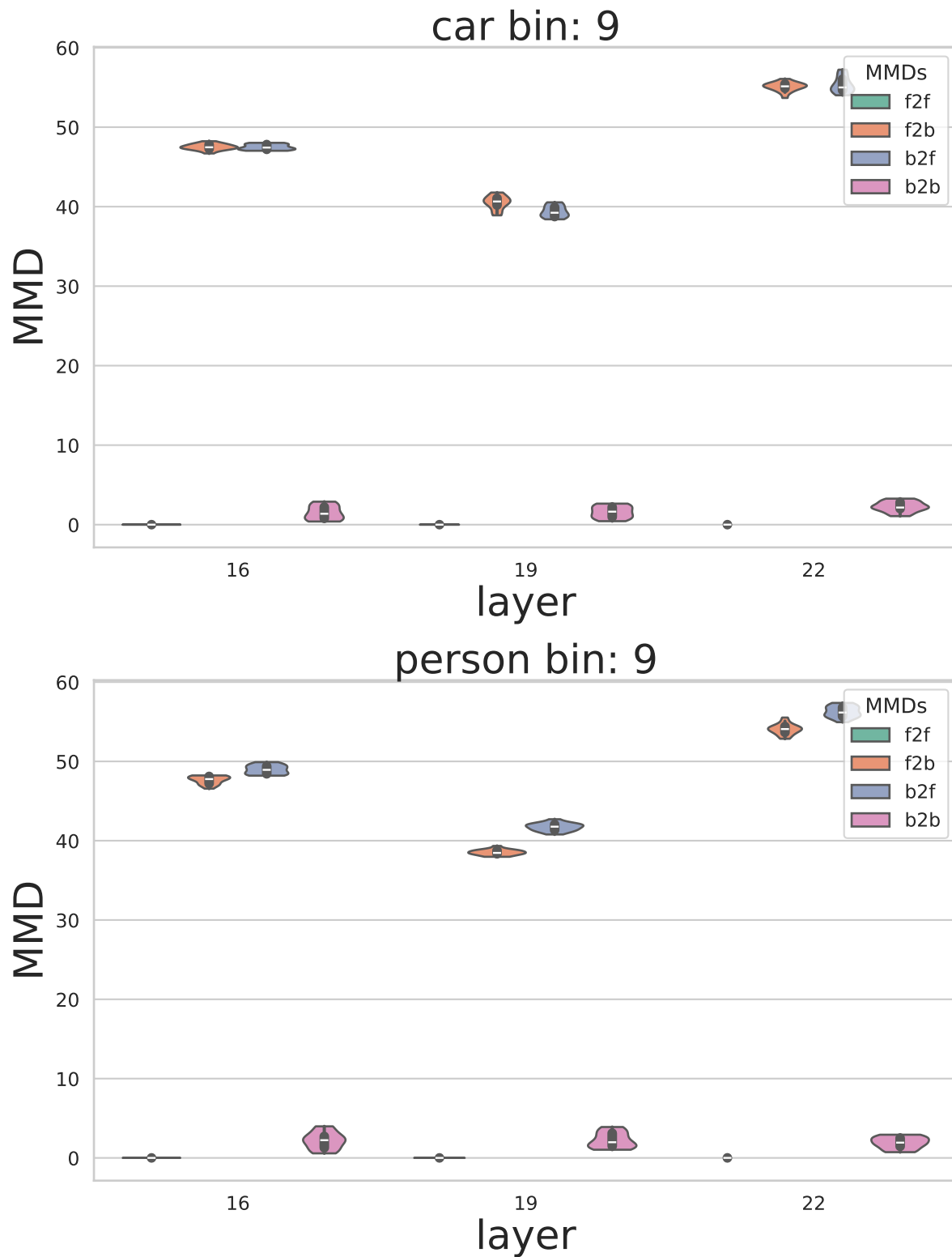


Figure 63. CS-CSFV(0.01) MMD plots YOLOv11.

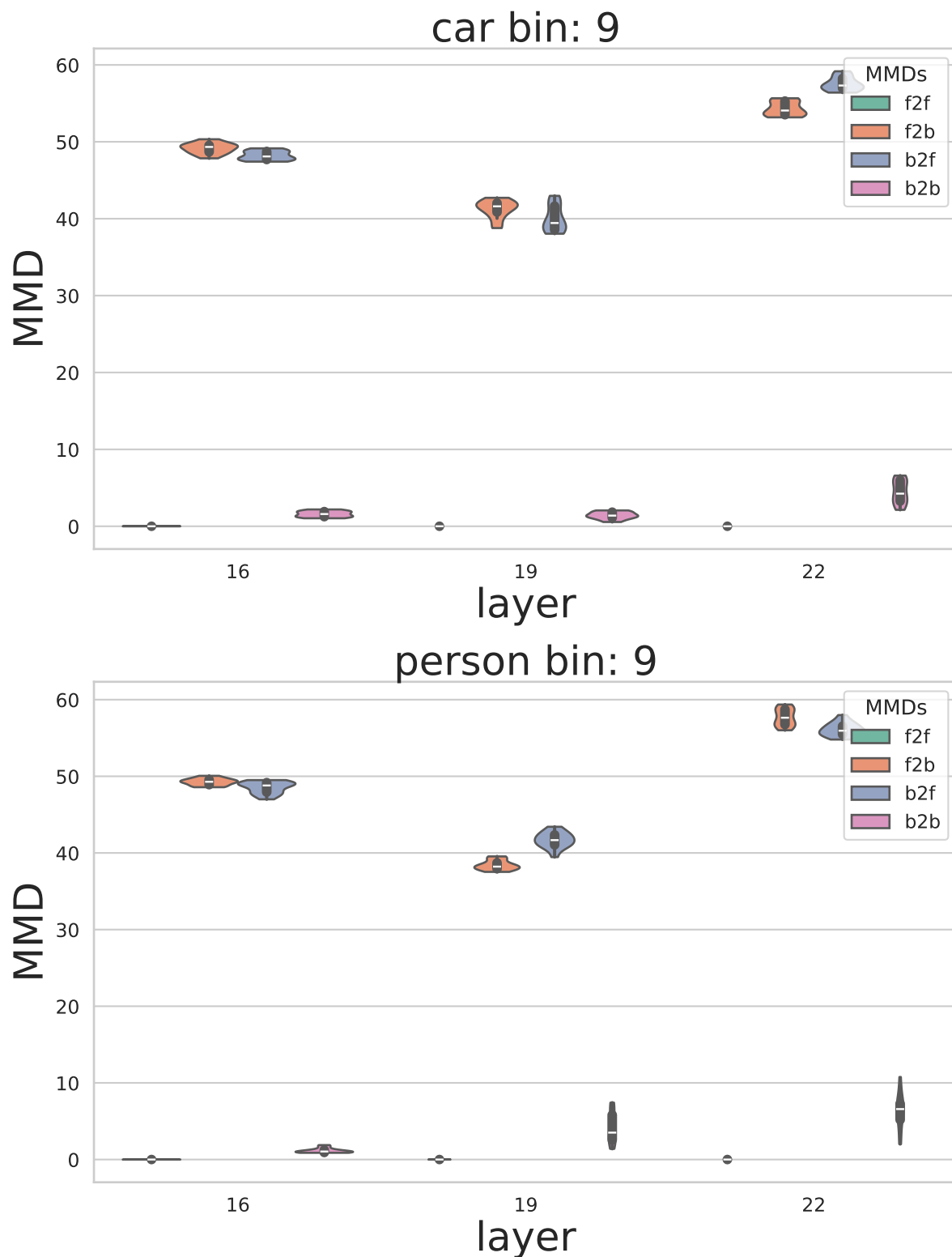
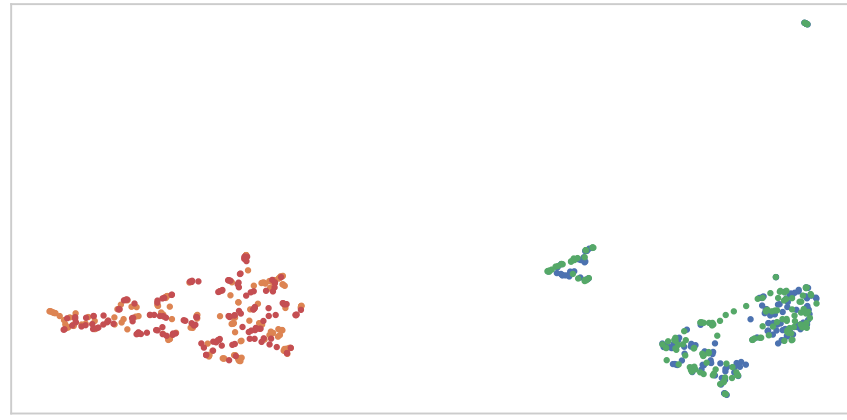
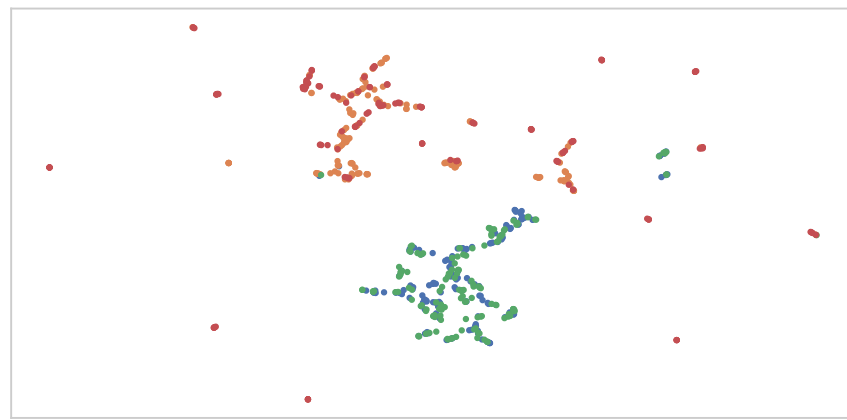


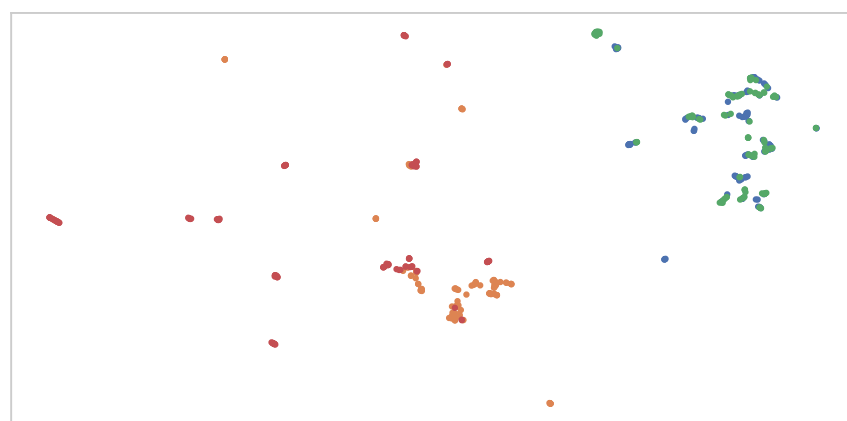
Figure 64. CS-CSFV(0.01) MMD plots YOLOv11.



(a) Dataset: CS-CSV, Label: Car

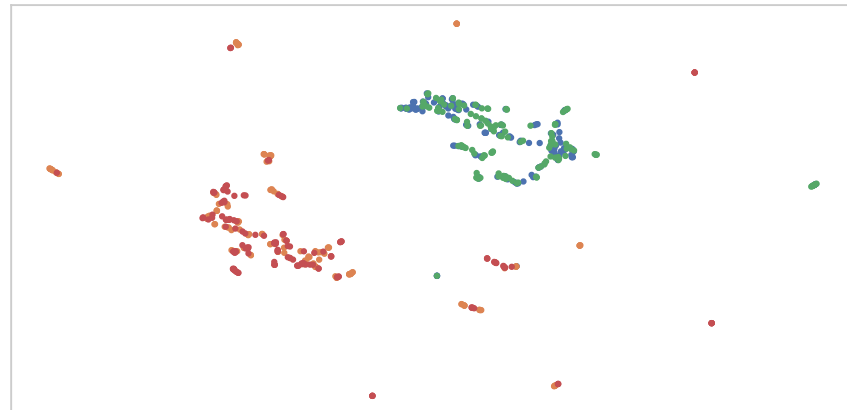


(b) Dataset: CS-CSFV(0.01), Label: Car

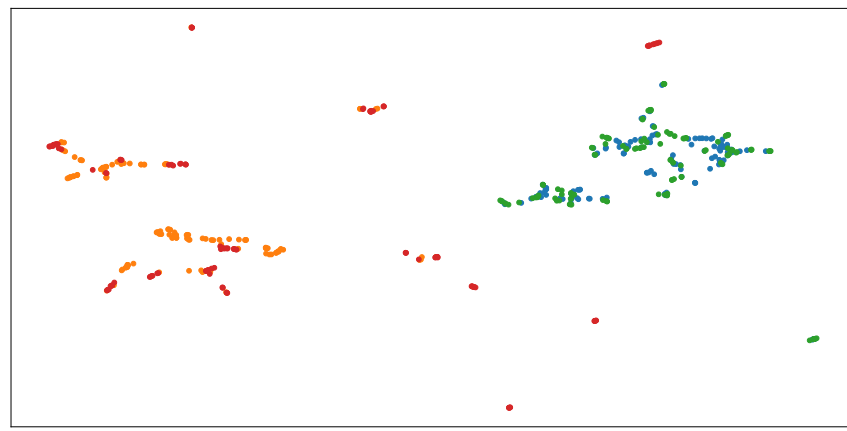


(c) Dataset: CS-CSFV(0.02), Label: Car

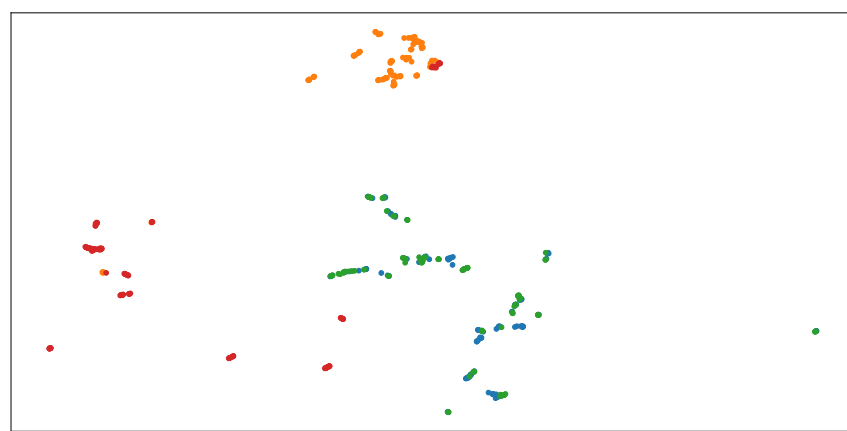
Figure 65. Car 2D embedding YOLOv11.



(a) Dataset: CS-CSV, Label: Person

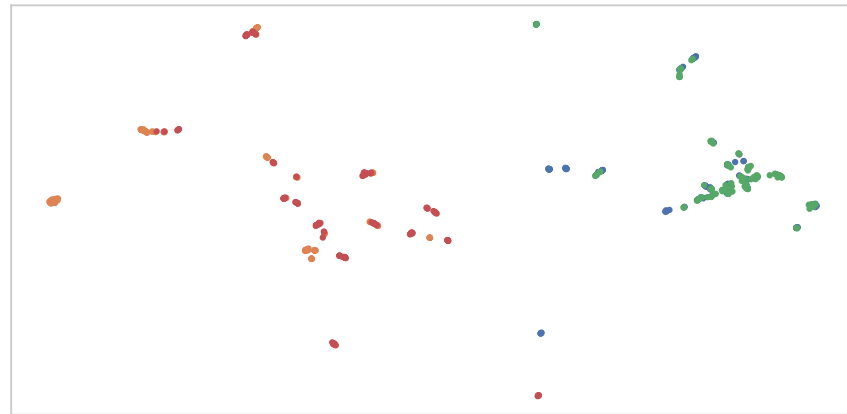


(b) Dataset: CS-CSFV(0.01), Label: Person

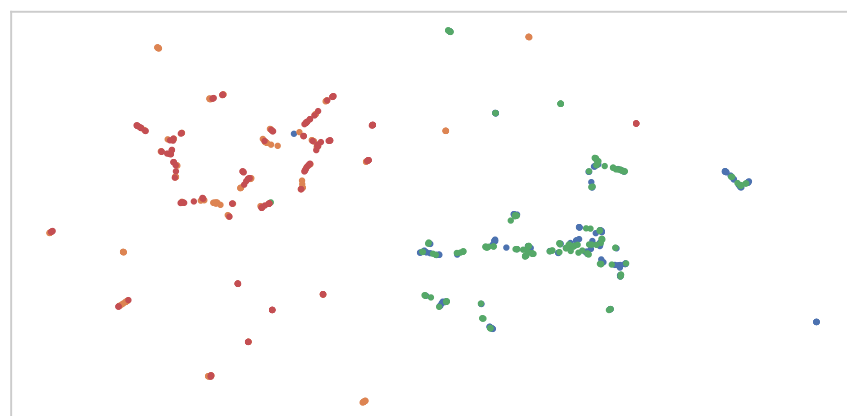


(c) Dataset: CS-CSFV(0.02), Label: Person

Figure 66. Person 2D embedding YOLOv11.



(a) Dataset: CS-CSV, Label: Rider



(b) Dataset: CS-CSV, Label: Bicycle

Figure 67. Rider and Bicycle CS-CSV 2D embedding YOLOv11